The Contribution of the RNA Dependent RNA Polymerase to Genetic Recombination in Enteroviruses

Andrew Woodman

A thesis submitted for the degree of Doctor of Philosophy

University of Warwick

School of Life Sciences

April 2015

Table of Contents

List of Tables

List of Figures

List of Appendices

Acknowledgements

This work was funded by a Biotechnology and Biological Sciences Research Council (BBSRC) studentship, for which I am extremely grateful.

I would like to thank my supervisor Professor David J. Evans for taking a gamble and supporting my application for funding. The consistent support, encouragement and general enthusiasm for this project have made the last 3 years the most rewarding and enjoyable of my working life. It has become very clear to me that not all students have the same support as I have enjoyed during my time at Warwick University.

Thanks go to the members of the Evan's lab past and present that have helped create a special atmosphere to work in. A special thanks to Fadi Alnaji, a close working colleague and friend - I'll miss our chats over coffee!

During the course of this investigation I was privileged to spend some time in the laboratory of Professor Craig Cameron at the Pennsylvania State University, U.S.A. Thanks must go to David who funded the trip, and also to the members of the Cameron lab who were so helpful during my time there - especially Jamie Arnold.

Thanks to Mum, Dad and my sister Karen, always supportive and proud of what I was doing. Your encouragement was always appreciated.

Finally, I would like to acknowledge the unwavering support of my wife, Kate. You really are amazing and have been that shoulder to lean on during the stressful times. We've been through a lot, and I wouldn't change a single thing. I must also mention my two children, Alice and Zara. You two are always smiling and are so full of love. Cheers.

Declaration

This work was completed at the University of Warwick and at the University of Pennsylvania State, USA between April 2012 and April 2015 and has not been submitted for another degree. The work is original and unless otherwise stated in the text, has been completed by the author.

Signed

Date

Summary

Positive-sense single stranded RNA viruses, like those found within the *Enterovirus* genus, have error prone polymerases, short replication cycles and high yields that together generate genetic diversity. These advantageous evolutionary mechanisms enable the virus population to survive in changing environments. However, the majority of mutations that are introduced are lethal or deleterious. RNA recombination provides a mechanism that can remove a deleterious mutation and also provides an opportunity to break the link between mutations that are lethal and those that are beneficial in the same genome.

The objectives of this investigation were to identify characteristics of the virus that were important in recombination. As genetic exchange in enteroviruses was postulated to be a replicative process, the role of the RNA dependent RNA polymerase (RdRp) was reasoned to be important. This study has benefited from utilising a novel reverse genetics *in vitro* cell based assay known as CRE-REP. The assay allowed selection and isolation of viable recombinant virus as near to the recombination event as temporally possible. Results indicated that 'copy choice' replicative recombination is a biphasic process with distinct template-exchange and resolution events. Manipulating known RNA elements within the viral genome expanded the cell-based assay further. Notably, this investigation suggested that fidelity of the RNA dependent RNA polymerase (RdRp) is a major determinant of recombination frequency.

To further validate the cell-based approach, a defined biochemical assay that allowed quantification of the template transfer event was developed in collaboration with Professor Craig Cameron. The results confirmed that the RdRp alone was sufficient for recombination and that fidelity was a major contributing factor to efficiency. The characterised high fidelity RdRp variants (*e.g.* K359R, G64S) reduced template transfer up to 25-fold. The biochemical assay was extended to investigate the sequence identity required for the template transfer event. These studies form the basis for the further biophysical dissection of a key evolutionary process present in many positive-strand RNA viruses.

Abbreviations

bp(s)	base pair(s)
CD	cluster of differentiation
cDNA	complementary DNA
CNS	Central nervous system
CO_2	carbon dioxide
CPE	cytopathic effect
CRE	cis-acting replication element
cVDPV	circulating vaccine-derived poliovirus
D	redundant nucleotide for adenine, guanine, or thymine
DAF	Decay accelerating factor
DAPI	4',6-diamidino-2-phenylindole
dH_2O	distilled water
DI	defective interfering
DMEM	Dulbecco's modified Eagle's medium
DNA	deoxyribonucleic acid
DNase	deoxyribonuclease
ds	double stranded
DTT	dithiothreitol
dNTP	deoxyribonucleotide triphosphate
E. coli	Escherichia coli
EDTA	ethylenediaminetetraacetic acid
EMEM	minimum essential medium with Earle's salts
ER	Endoplasmic reticulum
FISH	Fluorescent in situ hybridisation
FBS	foetal bovine serum
FLC	full-length clone
g	gram
GFP	green fluorescent protein
GI	gastrointestinal
GMEM	Glasgow minimum essential medium
GuHCl	guanidine hydrochloride
HeLa	human cervical cancer cell line
HI	heat inactivated
hr	hour
ICAM-1	intracellular adhesion molecule type - 1
IF	immunofluorescence
IMPDH	Inosine monophosphate dehdrogenase
IPV	inactivated poliovirus vaccine
IRES	internal ribosome entry site
K	redundant nucleotide for guanine or thymine
Kb	kilobase pair

LB	Lysogeny broth
M	redundant nucleotide for adenine or cytosine
mg	milligram
min	minute
miRNA	microRNA
ml	millilitre
mM	millimolar
MOI	multiplicity of infection
mRNA	messenger RNA
NCBI	National Center for Biotechnology Information
ng	nanogram
nm	nanometre
nt	nucleotide
NTR	Non-translated region
OPV	oral poliovirus vaccine
ORF	open reading frame
PABPI	poly(A) binding protein 1
PBS	phosphate buffered saline
PCBP2	poly(rC) binding protein 2
PCR	polymerase chain reaction
PFU	plaque forming unit
pH	power of hydrogen
PS	Penicillin and streptomycin
PVR	poliovirus type 3 receptor (CD155)
R	redundant nucleotide for adenine or guanine
RC	Replication complex
RD	rhabdomyosarcoma cells
RdRp	RNA-dependent RNA polymerase
RF	replicative form
RI	replication intermediate
RMP	Ribavirin monophosphate
RNA	ribonucleic acid
RNase	ribonuclease
rpm	revolutions per minute
RTP	Ribavirin triphosphate
RT-PCR	reverse transcription polymerase chain reaction
SDS	sodium dodecyl sulphate
s	second
shRNA	short hairpin RNA
siRNA	short interfering RNA
$TCID_{50}$	50% tissue culture infective dose
U	unit
µg	microgram
µl	microlitre
µM	micromolar

VAPP	vaccine-associated paralytic poliovirus
VDPV	vaccine-derived poliovirus
VPg	virus protein genome linked
v/v	volume per volume total
W	redundant nucleotide for adenine or thymine
w/v	weight per volume total
WHO	World Health Organisation
Y	redundant nucleotide for cytosine or thymine
°C	degrees Celsius
5-FU	5-Fluorouracil or 5-Fluoro-1H,3H-pyrimidine-2,4-dione

Virus abbreviations

BA	Baboon enterovirus (species A)
CVA	coxsackievirus A serotypes
CVB	coxsackievirus B serotypes
EVB	Enterovirus (species B)
EVC	Enterovirus (species C)
EVD	Enterovirus (species D)
EVE	Enterovirus (species E)
EVF	Enterovirus (species F)
EVG	Enterovirus (species G)
EVH	Enterovirus (species H)
EVJ	Enterovirus (species J)
E30	echovirus 30 (species B)
E6	echovirus 6 (species B)
E7	echovirus 7 (species B)
EV68	enterovirus 68 (species D)
EV71	enterovirus 71 (species A)
FMDV	foot-and-mouth disease virus
HCV	hepatitis C virus
HEV	human enterovirus
RVA	Rhinovirus species A
RVB	Rhinovirus species B
RVC	Rhinovirus species C
PV	poliovirus
PV1	poliovirus type 1 (species C)
PV2	poliovirus type 2 (species C)
PV3	poliovirus type 3 (species C)
SV	Simian enterovirus
TBSV	tomato bushy stunt virus

Protein abbreviations

VP0	precursor protein before cleavage to make VP2 and VP4
VP1	capsid protein
VP2	capsid protein
VP3	capsid protein
VP4	capsid protein
2A	virus protease
2BC	precursor protein, interacts with cellular membranes
2B	interacts with cellular proteins, induces vesicles in cells
2C	interacts with cellular proteins, induces vesicles in cells
3AB	precursor protein, binds to one or more CRE's also has chaperone activity
3A	component of virus replication complex
3B	protein VPg
3BC	precursor protein with chaperone activity
3CD	precursor protein with protease activity, binds to one or more CREs
3C	virus protease
3Dpol	RNA-dependent RNA polymerase (RdRp)
VPg	virion protein genome linked covalently to 5' NCR of virus genome
COPII	Coat protein complex II
p53	tumour suppressor protein that regulates cell cycle
PCBP2	cellular protein, promotes PV replication by binding to RNA secondary structure elements

CHAPTER ONE: Introduction

Important positive-sense single stranded RNA viruses like the human pathogens, poliovirus (PV) and rhinovirus, have a reputation of being one on nature's swiftest evolvers due to their high mutation and replication rates. This provides the basis for genetic variation amongst this group of viruses and allows rapid selection of those variants that are most suitable to the environment at any one time. RNA viruses also have the ability to exchange vast regions of genetic material, in a process known as genetic recombination, which allows for far greater variation than is possible in a single round of replication.

It has become apparent from the phylogenetic analysis of many positive sense RNA viruses that recombination has been a major driving force in their evolution. Many examples from nature and from cell based *in vitro* studies have attempted to highlight the potential mechanisms and triggers for the recombination event. However, except for an understanding of the underlying principles of recombination, very little is known about the viral and host factors that contribute to this process.

This literature review primarily concentrates on a specific group of viruses that fall within the *Picornaviridae* family, known as the genus *enterovirus.* The principles of classification, replication, evolution and recombination will be briefly considered. In the majority of cases the evidence provided is based upon the most widely studied picornavirus, poliovirus, which was also used primarily during the course of this investigation.

1.1 The Family *Picornaviridae*

The picornaviruses are small, non-enveloped RNA viruses that formally make up the family *Picornaviridae.* They are amongst the simplest of vertebrate viruses comprising a single stranded positive sense RNA genome within a $T = 1$ (quasi $T = 3$) icosahedral protein capsid of approximately 30 nm diameter (Tuthill et al., 2010, Rossmann et al., 1985). The group includes several closely related and medically important viruses such as poliovirus, rhinovirus, hepatitis A virus, coxsackievirus and echovirus. These viruses cause a wide range of acute diseases in

humans, including poliomyelitis, the common cold, liver disease, heart disease, and aseptic meningitis. Poliovirus (genus enterovirus) is the best-known and most studied member of the *Picornaviridae* family and is generally considered the prototypical picornavirus (Contreras et al., 2002). After poliomyelitis, probably the most notable disease-causing picornavirus is foot-and-mouth disease virus (FMDV; genus aphthovirus), which infects cloven-hoofed animals such as cattle and swine (Bachrach, 1968).

Taxonomy

The International Committee on Taxonomy of Viruses (ICTV) groups viruses by order, family, genus and species. A group of species will form a genera and a group of genera will form a family. Historically, classification of a virus into a family was primarily based upon virion morphology, the nature of the genomic nucleic acid, replication strategy and host species (Hyypia et al., 1997). More recently, due to the advancement in molecular sequencing technology, classification has also taken into account genomic sequence similarities. For example, the classification of enteroviruses that infect humans has been primarily based upon the sequence of the structural protein VP1 (Caro et al., 2001, Oberste et al., 2000, Oberste et al., 1999). Genetic variations within species allow them to be sub-divided into serotypes and then further into strains. This concept is especially important when considering the high mutation rates of many picornaviruses that exist not as a single genotype but as a 'quasi-species' due to the high mutation rate of the virally encoded RNA dependent RNA polymerase (RdRp) (Eigen, 1996). The classification of the family *Picornaviridae* is being continuously updated and most recently expanded to 46 species that are grouped into 26 genera (Knowles et al., Europic 2014).

Genus enterovirus

The enteroviruses are a well-characterised genus within the family *Picornaviridae* and as recently as 2009 were sub-grouped into seven species which also included the *Human Rhinovirus* (HRV) A-C groups (McIntyre et al., 2013, Arden and Mackay, 2009). In 2012 the ICTV re-named and re-classified many viruses into newly formed genera and simplified the

nomenclature to remove many host species names. For example the previous *Bovine enterovirus* species group is now known as *Enterovirus E*. The genus enterovirus now currently consists of 309 serotypes that fall within 12 species groups (Knowles *et al.,* Europic 2014) (summarised in table 1.1). The enteroviruses that infect humans are particularly well studied as they contain important pathogens responsible for acute flaccid paralysis (including poliomyelitis), myocarditis, encephalitis and a variety of other ailments (Grist et al., 1978). They are currently divided into four phylogenetically distinct species known as Enterovirus A – D, with the prototype poliovirus serotypes belonging to group C (Knowles et al., 2012).

Transmission and medically important enteroviruses

In biology and medicine the prefix term entero- refers to the intestinal region. Enteroviruses primarily infect the cells of the intestine and are transmitted by the faecal-oral and oral-oral route by contact with water, food and ground contaminated with infected faeces. Additionally, transmission can occur through direct contact with secretions from ophthalmic and dermal lesions (Rajtar et al., 2008). Enteroviruses that are transmitted by the faecal-oral route are very resilient to the extreme environmental conditions of the gastrointestinal tract (GI), virions remain stable at pH 3–5 for 1–3 hours, are not susceptible to proteolytic enzymes nor to bile salts and replicate efficiently at 37 °C (Rajtar et al., 2008). Rhinoviruses in contrast to the other members of the *enterovirus* genus are primarily transmitted from person to person via aerosol or contact (either direct or through fomites). Infection is efficiently initiated by intranasal inoculation where replication of the virus primarily occurs within the respiratory tract at temperatures of 33 °C (Jacobs et al., 2013). Enteroviruses that affect humans usually lead to infections that are asymptomatic or cause only mild illness. However, outbreaks of severe disease can be associated following enterovirus infection. For example, EV71, a member of the Enterovirus A species group can cause epidemics of hand, foot and mouth disease in young children that can also be associated with neurological symptoms (McMinn et al., 2001).

Table 1.1: Classification of the genus *enterovirus*

Species group	Example Serotypes
Enterovirus A	CVA2-8, EV71, 76, 89-92, SV19, 43, BA13
Enterovirus B	CVB1-6, E1-9, 11-21, 24-33, EVB73-88
Enterovirus C	PV1-3, CVA1, 11, 13, 17, 19-22, EVC95, 96
Enterovirus D	EVD68, 70, 94, 111, 120
Enterovirus E	EVE1-4
Enterovirus F	EVF1-6
Enterovirus G	EVG1-11
Enterovirus H	EVH1
Enterovirus J	SV6, EVJ103, 108, 112, 115, 121
Rhinovirus A	RVA1, 2, 8-13, 18-25, 28-34, 38-41, 49-68, 100-109
Rhinovirus B	RVB3-6, 99-106
Rhinovirus C	RVC1-54

Abbreviations on pg 14

Respiratory illnesses like bronchiolitis and pneumonia have been associated following EV68 infection, a member of the Enterovirus D species group (Oberste et al., 2004b). Echoviruses (species B), that were originally isolated from the faeces of asymptomatic patients have now been associated with aseptic meningitis, particularly in infants and young children (Rhoades et al., 2011, Leitch et al., 2009).

Poliovirus infection: Poliomyelitis and related illnesses

The causative agent of poliomyelitis is the Enterovirus C member poliovirus (PV), which was first discovered in 1908 by Landsteiner and Popper who demonstrated bacterially sterile transmission of the disease from human to rhesus monkeys by injection of spinal fluid from a symptomatic child into the peritoneum of a monkey (Eggers, 2002). The host receptor, CD155, is only expressed in primate cells, meaning PV has no other vectors of transmission (Mendelsohn et al., 1989). PV is spread through faecal-oral transmission, the virus initially infects and replicates in the oropharynx and gut of the host, which commonly leads to the virus entering the bloodstream. In the majority of infections no clinical signs are shown (Nathanson and Kew, 2010). The most severe outcome occurs if the virus crosses the blood-brain barrier and invades the central nervous system (CNS) where it can destroy motor neurons in the grey matter of the spinal cord, causing muscular paralysis known as poliomyelitis, as the name suggests (polio = grey, *myelitis/myelo* = marrow). The incubation period for poliomyelitis is about 10 days and occurs in 1 out of 150 PV infections (Nathanson and Kew, 2010). In around 10% of PV infected individuals, a secondary illness called abortive poliomyelitis can occur. This form of infection can lead to a variety of clinical phenotypes, such as upper respiratory tract infection, gastrointestinal illness, and influenza like infections (Kroon et al., 1995).

Polio eradication strategy

In 1988 the World Health Organization (WHO) launched the first campaign for the eradication of poliovirus with the goal of eradicating polio by the year 2000. Since that time the world has seen a 99% decrease in polio cases. However, there are a few areas of the world where PV

remains endemic in the human population, including Nigeria and the border between Afghanistan and Pakistan (www.polioeradication.org). The availability of a vaccine, a single host and good diagnostic tools were all key factors that suggested that poliovirus could be eradicated.

Three antigenically distinct serotypes of poliovirus exist (1, 2 and 3) and infection with one serotype does not convey protection against the others (Herremans et al., 2000). The oral poliovirus vaccine (OPV), licensed and introduced by Albert Sabin in 1963, contains three attenuated strains of poliovirus that induce strong immunity against infection (Eggers, 2002). The OPV was developed by continuously passaging each of the three parental strains at suboptimal temperatures in simian cells and tissues. Each of the three serotypes have been extensively studied with the critical point mutations characterised (Kew et al., 2005). The human immune response is generally able to recognise and destroy the attenuated virus before it causes significant disease. Unfortunately, the rapid evolution of the virus in the short time that it is replicating (~2 weeks) in the vaccinated host, has led to some of the attenuated vaccine strains reverting back to wild-type poliovirus which are subsequently shed as virulent virus (Dunn et al., 1990). If immunization coverage is low, the newly shed virulent virus may cause an outbreak of vaccine-associated paralytic poliomyelitis (VAPP) among non-immune individuals, thus remaining a significant threat in some areas of the world. The formalin inactivated virus vaccine (IPV), developed by Dr. Jonas Salk and licensed in 1953, and used in the developed world circumvents this problem, but it is too expensive for the global eradication campaign (Salk, 1954, Nathanson and Fine, 2002). Vaccine-derived polioviruses (VDPVs) also contribute to minor outbreaks of poliomyelitis. These outbreaks are linked to recombination events between circulating vaccine-derived polioviruses (cVDPVs) and fellow members of the enterovirus C group, in particular coxsackie A viruses (Kew et al., 2002, Combelas et al., 2011). Taken together, the failure to eradicate polio completely may call for the development of antivirals and attenuated vaccine strains that are non-recombinogenic.

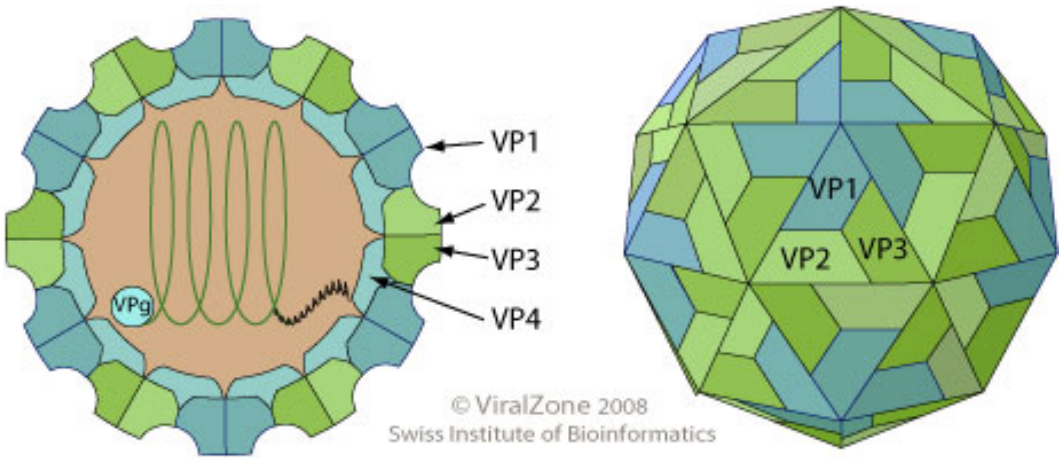

Figure 1.1: Enterovirus capsid morphology

Non-enveloped, spherical, around 30 nm in diameter, icosahedral capsid surrounding the naked RNA genome. The capsid consists of a icosahedral arrangement of 60 protomers, each consisting of 4 polypeptides, VP1, VP2, VP3 and VP4. VP4 is located on the internal side of the capsid. Source: http://viralzone.expasy.org/all_by_species/97.html.

Capsid morphology

All enteroviruses share a similar morphology with virus proteins 1-3 (VP1-3) together forming the icosahedral shell of the virion with VP4 distributed on the inner surface of the virus particle. Prior to proteolytic processing the capsid proteins are considered the protomer (Hogle et al., 1985) (figure 1.1). VP1–3 each has a similar basic structure consisting of an eight-stranded anti-parallel β- barrel. Proteolytically processed monomers assemble into pentameric subunits, 12 of which go on to form the complete icosahedral shell of the virus. Enteroviruses have a deep depression encircling the fivefold axis below VP1 (Tuthill et al., 2010). This region is known as a 'canyon' and in many cases is the site of interaction with cellular receptors (Colonno et al., 1988, Bernhardt et al., 1994).

Cellular receptors and tropism

Receptors upon the surface of host cells play a fundamental role in the entry of most viruses. In the case of enteroviruses they are involved in cell attachment, signalling and endocytosis (Tuthill et al., 2010). Many of the important virus-receptor interactions have been extensively characterised for the *enterovirus* genus with many of the host receptors falling within the immunoglobin superfamily of receptors (table 1.2). Intercellular adhesion molecule-1 (ICAM-1) is the receptor for many of the rhinoviruses and some coxsackie viruses (Greve et al., 1989, Evans and Almond, 1998). The receptor for poliovirus is cluster of differentiation 155 (CD155), also known as PVR. This receptor is only found upon cells of primates, suggesting that this virus did not emerge from any animal reservoir (Mendelsohn et al., 1989). For the remaining coxsackie group of viruses, the primary receptor is the Coxsackie and adenovirus receptor (CAR) which is a component of the tight junction between cells in intact epithelium (Coyne and Bergelson, 2005). The use of Decay accelerating factor (DAF) as a receptor by separate enterovirus species groups, for example group B echovirus members to group C coxsackie, implies that there is a distinct selective advantage in its use (Evans and Almond, 1998).

Table 1.2: Example enteroviruses and their receptors

Serotype	Receptor
Poliovirus 1-3	CD155 (PVR)
Rhinovirus (major group)	ICAM-1
Coxsackie A13, A18, A21	ICAM-1
Coxsackie B1, B3, B5	DAF
Coxsackie B1-6	CAR
Echovirus 3, 6, 7, 11-13, 20, 21, 24, 29, 33	DAF
Echovirus 22	$\alpha_v\beta_3$ Vitronectin receptor
Enterovirus 71	SCARB2, PSGL-1[(i)]

Abbreviations: CAR, coxsackievirus–adenovirus receptor; DAF, decay-accelerating factor; ICAM-1, intracellular adhesion molecule type 1; PVR, poliovirus receptor; SCARB2, scavenger receptor class B member 2; PSGL-1, human P-selectin glycoprotein ligand-1. Adapted from (Evans and Almond, 1998). [(i)](Nishimura and Shimizu, 2009).

1.2 Poliovirus life-cycle

Poliovirus, as previously stated is the prototypical picornavirus, and has been the most widely studied. Therefore, the following section upon the virus life cycle of a member of the *enterovirus* genus is based solely upon poliovirus.

Attachment and entry

The primary site of receptor interaction (CD155) upon the virus capsid is within a hydrophobic pocket that lies at the base of the 'canyon' found around the five-fold axis. The binding of the receptor to the virus acts as a trigger for the initiation of capsid structural transitions that lead to the ejection of all of the internal VP4 protein and exposure of the N terminus of VP1 (Fricks and Hogle, 1990). Isolation of virus that has gone through this transition has showed that the particles are no longer infectious when external to the cellular environment. These intermediate particles sediment more slowly on sucrose gradients than mature particles and are know as 'A' particles, or 135S particles (Fricks and Hogle, 1990). The binding and transition of the mature particle to the intermediate 'A' particle leads to internalisation by endocytosis. Discovery of empty particles (80S) that have shed their genomic load has shown that there is a second transition that accounts for the delivery of genomic RNA into the host cell (Tuthill et al., 2010). The externalized VP4 and N-terminus of VP1 are believed to form pores in the host membrane that leads to viral RNA being translocated through the vesicle membrane into the cytoplasm of the host cell (Levy et al., 2010).

Genome and translation

Every member of the *enterovirus* genus, including poliovirus, has a non-segmented single-stranded positive-sense RNA genome that is ~7.5 kb in length which encodes a single polyprotein from a lengthy open reading frame (ORF) that makes up around 90% of the genome. The genome is covalently linked to a 22 amino acid peptide found at its 5' end, termed virion genome linked protein (VPg) (Pathak et al., 2007). The ORF itself is flanked at either end by a non-translated region (NTR). The 5' NTR is approximately 750 nt in length with the 3' NTR

being shorter at 50 - 90 nt in length and followed by a poly(A) tract (figure 1.2A)(Mellits et al., 1998, Racaniello and Baltimore, 1981, Rohll et al., 1995). Following delivery of the viral RNA into the cytoplasm of the host the VPg linked protein is cleaved from the RNA by an unknown cellular enzyme, which allows translation of the viral genome to proceed (Ambros et al., 1978). An Important *cis* - acting RNA element that is required for translation is found in the 5'NTR and is formally known as the internal ribosomal entry sequence (IRES). It consists of a series of highly structured stem loops, which recruit the host ribosomal machinery and initiate translation of the virus polyprotein in a cap-independent manner (Pelletier et al., 1988, Pelletier and Sonenberg, 1988, Sonenberg and Pelletier, 1989).

Polyprotein processing

The polyprotein can be divided into three functional regions: P1, P2 and P3, and are cleaved co- and post-translationally by viral 2A and 3C/3CD protease activities. The 2A protease is involved in a single processing event where it catalyzes cleavage at the VP1/2A boundary *in cis* at a Tyr/Gly amino acid pair to release the P1 region from the rest of the polyprotein (Krausslich et al., 1989). The 3C-dependent protease activity of 3CD, and perhaps other 3C- containing precursors, is responsible for the remaining polyprotein cleavage events that occur *in trans*, with all 3C protease mediated cleavage occurring at Gln/Gly amino acid pairs (Cameron et al., 2010, Semler et al., 1981a, Semler et al., 1981b). The processing of P3 proteins is via two separate pathways. In the major pathway processing between 3B and 3C yields the precursor proteins 3AB and 3CD, with the minor pathway producing 3A and 3BCD proteins. The 3BCD protein can be further cleaved to produce 3BC and 3Dpol; 3BC can be cleaved further to produce 3B and 3C (figure 1.2B) (Lawson and Semler, 1992, Pathak et al., 2008). The temporal cascade of slow and fast proteolytic events that occurs throughout the polyprotein ensures the availability of the necessary proteins and precursors to disrupt host functioning and allow virus replication. P1 proteins are the capsid proteins. Four capsid proteins exist: VP1–4. VP1 and VP3 are produced via 3C mediated protease cleavage. VP2 and VP4 are produced in assembled virus particles that contain genomic RNA by autocatalytic cleavage of the precursor VP0 protein (Cameron et al., 2010). The protease activities of 2A and 3C proteins are not exclusively

A

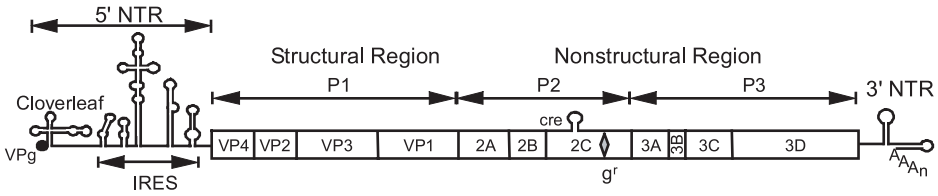

B

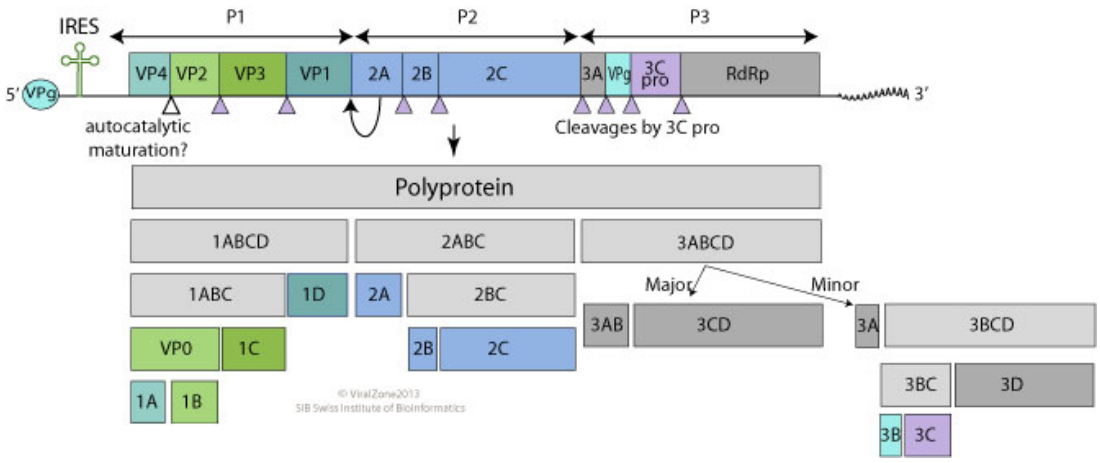

Figure 1.2: Poliovirus genome layout

(A) The 5'end is VPg linked. The 5' NTR contains the cloverleaf and IRES. The polyprotein ORF consists of viral proteins P1, P2, and P3. P1 proteins make up the structural capsid proteins. The P2 and P3 proteins include all non-structural proteins involved in formation of replication complexes and RNA replication. After the polyprotein is the 3' NTR containing stems X + Y followed by a poly(A) tail. The 2C CRE is shown as a stem loop. Source: (Jiang et al., 2007) **(B)** Genome structure and cleavage products of poliovirus coding sequence. The arrow beneath 2A indicates cleavage performed by 2A *in cis*; the purple triangles indicate 3C mediated cleavage sites that occur *in trans*; the white triangle indicates a postulated autocatalytic cleavage event. Source: http://viralzone.expasy.org/all_by_species/97.html.

directed to the viral polypeptide. For example, cleavage of eIF-4G by the 2A protease disrupts the host translation machinery, inhibiting cap-dependent translation. Additionally, the cleavage products enhance IRES driven translation. This ensures that the host cannot translate cellular mRNA and allows viral protein production to increase significantly (Ventoso et al., 1998, Etchison et al., 1982). Similarly, the activity of the 3C protease has been shown to disrupt host cellular processes. An important host cell-cycle regulatory protein, p53, is cleaved by the 3C protease with the aid of other host proteins (Weidman et al., 2001)

RNA replication - replication complex

All of the non-structural proteins encoded in the P2 and P3 regions are involved in replication of the viral RNA. The P2 proteins - 2B, 2C and 2BC have been shown to interact with host membranes and induce their rearrangements to form rosette-like structures know as replication complexes (RC) (Rust et al., 2001). The membrane bound organelle is primarily found upon the peri-nuclear endoplasmic reticulum and its formation has been shown to occur as early as 2 hrs post infection (Egger et al., 2002, Belov and Ehrenfeld, 2007). This unique virally induced super-structure is considered a closed-off entity that ensures the concentration of factors that are involved in replication whilst also protecting the viral RNA from host factors (Egger et al., 2000). The origins of the membranes that form the replication complexes are not completely known, but evidence exists for hijacking of COPII covered membranes that participate in the endoplasmic reticulum (ER)-to-Golgi trafficking (Belov and Ehrenfeld, 2007, Belov et al., 2008, Belov et al., 2012). The P3 proteins - 3A, 3B (VPg), 3C and 3Dpol (RdRp) are all involved in RNA replication and it has been shown that binding of the viral RNA to the membrane occurs during replication, via an interaction with the 2C and 3AB protein (Semler et al., 1982). Indeed, the 3AB protein has been shown to have hydrophobic domains that are consistent with an integral membrane protein whilst also exhibiting RNA chaperone activity (Towner et al., 1996, Gangaramani et al., 2010) (figure 1.3A).

RNA Replication - negative sense intermediate

To produce a genome of positive polarity, replication of the viral RNA occurs via a negative sense intermediate, with *cis*-acting RNA elements found in the 5' and 3' NTRs of the positive strand genome playing a key role. The first 88 nt of the poliovirus 5′ NTR forms a 'cloverleaf' structure that binds viral polypeptides 3C (or the 3CD precursor protein), as well as a host protein PCBP2 (poly[rC]-binding protein) to form a ribonucleoprotein complex (Andino et al., 1990). The binding of 3CD to the cloverleaf structure specifically inhibits binding of the host translational machinery and thus ensures a transition from translation to replication. This important regulatory step ensures that there is no ribosome - RdRp collisions (Gamarnik and Andino, 1998). The genome is then circularized by the interaction of the poly(A) binding protein (PABP1), which is bound to the poly(rA) tail, to the 5'NTR ribonucleoprotein structure (Wang et al., 1999). Additionally, it has been shown that 3AB and 3CD also bind to *cis*-acting elements in the 3'NTR known as stems X + Y and this interaction aids genome circularisation (Mellits et al., 1998) (figure 1.3A). Importantly, another *cis*-acting replication element within the 2C region of the poliovirus genome is also critical in RNA replication. The 61-nt stem loop structure with a terminal loop consisting of an AAACA motif is highly conserved in enteroviruses and is formally known as the CRE (Goodfellow et al., 2000). The CRE stem loop structure binds 3D, 3CD and 3B (VPg) in which the latter protein acts as primer for elongation by the 3Dpol (RdRp). The primer VPg, is firstly modified by the addition of two covalently linked uridine nt to a tyrosine residue found at the 3rd position of the protein with the template for the uridylylation process believed to be the poly(rA) tail (Paul et al., 1998, Steil and Barton, 2009). This protein-protein bridge interaction, that is reliant upon the *cis*-acting RNA elements described, brings 3CD into the proximity to the 3' end of the genome so that when 3CD is proteolytically processed the 3Dpol (RdRp) can interact with VPg-pU-pU stimulating synthesis of the negative sense RNA (figure 1.3B) (Andino et al., 1990, Herold and Andino, 2001). The enzymatic activity of the RdRp itself is reliant upon higher order structures formed between RdRp monomers. Substitutions of residues at the two known RdRp interfaces involved in the higher order lattice-like structures can be lethal (Tellez et al., 2011, Hobson et al., 2001).

A

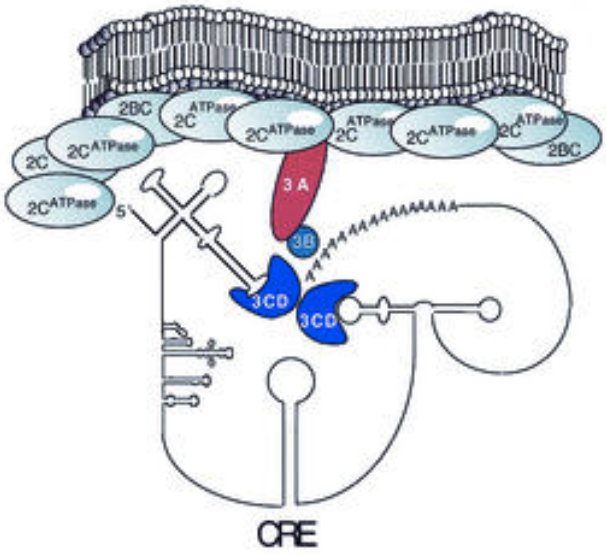

B

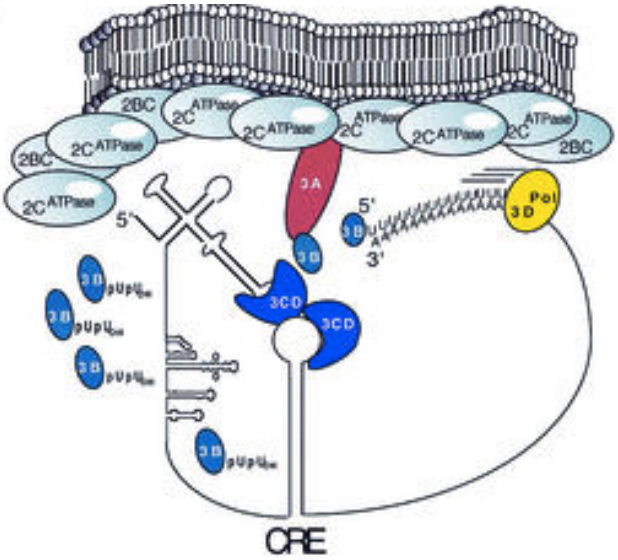

Figure 1.3: Replication complex formation and negative sense RNA initiation

(A) Formation of the replication complex. PV RNA replication occurs in large ER membrane associated complexes. Viral P2 proteins, 2C and 2BC, sequester host cell membranes. Depicted is the genome circularization event mediated by 3CD that stimulates negative sense RNA synthesis. Host proteins are not shown **(B)** Representation of negative-strand synthesis by 3Dpol. P3 proteins (3A, 3B [VPg], 3CD and 3Dpol) are responsible for RNA replication. The CRE within 2C (*cis*-acting replication element) aids the interaction of the elongation complex to the 3' end of the genome. Adapted from (Murray and Barton, 2003).

The outcome of this stage of RNA replication is a double stranded replicative form (RF) where both positive and negative genomes are present. The peak of antisense RNA synthesis occurs at 4 hrs post infection, where antisense strands are found at a ratio of 40:1 to 70:1 when compared to the positive strand genome (Novak and Kirkegaard, 1991).

RNA Replication - Positive sense genome

The newly synthesized negative sense RNA is anchored to the replication complex via interaction with the 2C protein. This interaction has been shown to occur because negative strand replication initiation can be inhibited by a chemical called guanidine hydrochloride and mutants that are resistant to this chemical can be mapped to the 2C region (Barton and Flanegan, 1997). The synthesis of positive strand genomic RNA is again initiated from a VPg-pU-pU modified primer. However, the modification of the VPg primer for positive sense RNA production is dependent upon the terminal AAACA of the 2C CRE, with the first 'A' nt serving as the templating base (Goodfellow et al., 2003a, Paul et al., 2000). Indeed, cell free *in vitro* translation and replication assays have shown that the synthesis of antisense RNA is not inhibited by mutation of the 2C CRE sequence whereas positive strand synthesis is (Goodfellow et al., 2003b, Murray and Barton, 2003). Upon initiation of positive strand RNA synthesis, the double stranded RF is melted and multiple copies of positive sense RNA are produced by elongation of the VPg-pU-pU primer from the 3' end of the antisense template. At this stage the antisense RNA acts as replicative intermediate where multiple copies of positive sense RNA are produced from a single template (figure 1.4) (Barton and Flanegan, 1997).

Packaging and release

Following multiple rounds of RNA replication. Positive strand genome is packaged into newly formed capsid structures in a process called encapsidation. Unlike the well-characterised steps of RNA replication, this step is poorly understood. Early encapsidation studies suggested that the VPg protein acted as a signal (Nomoto et al., 1977). However, this cannot be the sole determinant as both positive and negative sense RNA has VPg covalently attached.

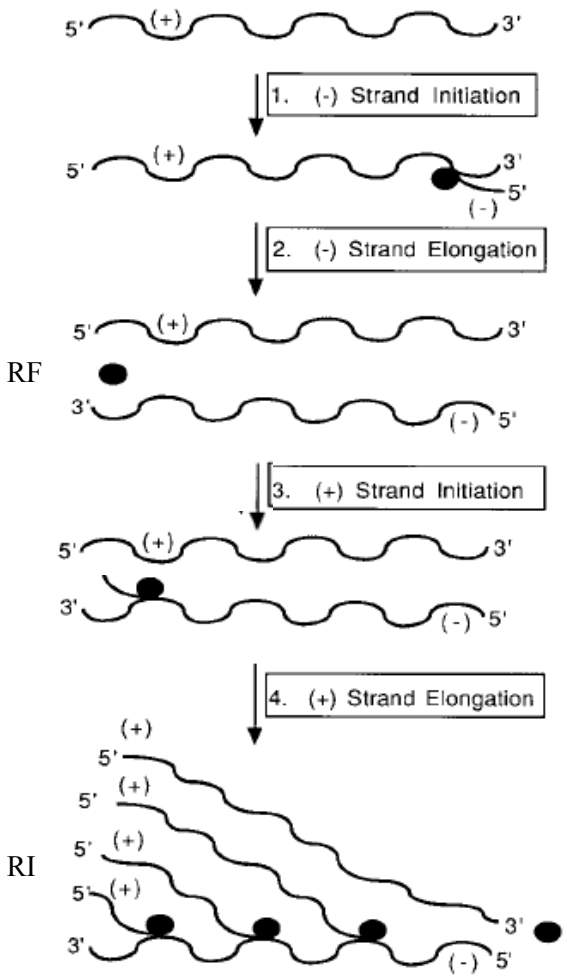

Figure 1.4: Negative strand and Positive strand synthesis

(1) Initiation of negative-strand RNA synthesis from the positive-strand genome leads to the formation of the (2) double stranded replicative form (RF). (3) Positive-strand initiation from the negative-strand RNA template. (4) The negative strand replicative intermediate (RI) RNA, initiation of multiple positive-strands from a single negative-strand RNA. Black circle represents the RdRp. Adapted from (Barton and Flanegan, 1997).

A recent study has suggested that the 3AB and 3CD proteins aid movement of newly synthesized viral RNA to capsid particles (Oh et al., 2009). Another study has shown that a specific interaction between 2C and VP3 is required to thread viral RNA into the capsid particle (Liu et al., 2010). Release of poliovirus, like most picornaviruses, is primarily due to lysis of the host cell. There is some evidence however that release of virus can occur prior to lysis via components of the autophagy pathway (Bird et al., 2014).

1.3 Evolution

Distinct characteristics of RNA virus replication aid their constant evolution and ensure their survival. These include: high mutation rates due to the error-prone nature of the viral RdRp, high yields of virus, and short replication times. As a consequence, RNA viruses like poliovirus replicate as complex and dynamic mutant swarms, called viral quasi-species (Domingo and Holland, 1997). The quasi-species theory provides a population-based framework that allows analysis of RNA virus evolution. Quasi-species exist as a cloud of diverse variants continuously generated from a related RNA sequence due to mutation and the ensuing population heterogeneity is the primary reason that new strains continuously emerge following selection pressures of the host, or from antiviral treatment (Lauring and Andino, 2010).

Error-prone nature of the RNA dependent RNA polymerase (RdRp)

An interesting characteristic of many viral RdRp's is that they generally have relatively low fidelity, meaning they have a greater frequency of misincorporated nucleotides compared to DNA polymerases. The fidelity difference can be largely attributed to the lack of 'proof-reading' capability of the RdRp. In contrast, DNA polymerases exhibit 3'-exonucleolytic activity that aids correct nucleotide incorporation (Arnold et al., 1999). The poliovirus RdRp has an estimated misinsertion error rate ranging from 1.2×10^{-4} to 1×10^{-6} nt for transition mutations and 3.2×10^{-5} to 4.3×10^{-7} nt for transversion mutations (Freistadt et al., 2007). This rate of mutation is very high when compared to DNA polymerases with exonuclease activity (typically 10^{-9} misincorporations per nucleotide copied) (Domingo et al., 2002). The low fidelity characteristic

typically means that the poliovirus RdRp inserts around two wrong bases per genome copied. This enables the virus to form sub-populations, or quasi-species, that differ from the parental virus by only one or more nucleotides (Vignuzzi et al., 2006). When fidelity and high population yields are taken together, the potential to select variants in the population that escape host or antiviral pressures becomes apparent. The selection of the three attenuated poliovirus serotypes that make up the oral polio vaccine (OPV) is a good example. All three were serially passaged in monkey cells, which eventually selected variants with multiple point mutations that were no longer able to replicate efficiently in human motor neuron cells and cause poliomyelitis. The attenuated viruses were still able to infect the gut cells, the site of natural infection, eliciting the desired immune response (Kew et al., 2005). Reversion of the attenuating phenotype by a point mutation (uracil-to-cytosine) at position 472 of PV3 Sabin OPV within the 5′ NTR and its IRES has been associated with vaccine-associated paralytic poliomyelitis (VAPP) (Gnanashanmugam et al., 2007). There is also a fine line between low fidelity and the ability of the virus to propagate successfully, and this can be used as a mechanism to attenuate a virus population. Many RNA viruses like poliovirus have an RdRp that exists on the edge of 'error catastrophe' (Crotty and Andino, 2002) with the majority of mutations encoded being lethal or deleterious (Stern et al., 2014, Acevedo et al., 2014). Any further decrease in polymerase fidelity may be lethal to the virus population. For example, as previously stated, the average misincorporation of nucleotide per genome copied in poliovirus is two. If this were to increase to four or above then the virus may be unable to propagate (Crotty and Andino, 2002). Current antiviral efforts have focused on modifying the fidelity of the viral polymerase. Firstly, decreasing fidelity by use of nucleotide analogous like ribavirin that induces lethal mutagenesis of a viral population (Crotty et al., 2000, Crotty et al., 2001, Crotty and Andino, 2002, Vignuzzi et al., 2005). Indeed, the antiviral ribavirin alongside pegylated interferon alpha is used in the treatment of those suffering chronic Hepatitis C infection (Deterding et al., 2013). Or secondly, by introduction of specific, well-characterised point mutations that increase polymerase fidelity to reduce the adaptability of the virus population to the selection pressures of the host (Vignuzzi et al., 2006, Weeks et al., 2012).

By understanding polymerase fidelity and the quasi-species theory in positive strand RNA viruses allows a certain amount of prediction in virus evolution. For example extensive sequence analysis has highlighted that selection pressure differs depending upon the area of the genome you look at, with the capsid region being the most variable (Hyypia et al., 1997). However, the fidelity of the RdRp cannot solely account for variability and evolutionary rates in viruses like polio (Freistadt et al., 2007). Another key mechanism, genetic recombination, plays a vital role in the evolution of RNA viruses.

Genetic Recombination

The process of recombination that takes place in RNA viruses results in the formation of hybrid RNA molecules from parental genomes of mixed origin. This process can occur within a single genomic segment, termed RNA recombination. For those viruses that possess segmented genomes, an exchange of entire genomic segments between viruses can occur and this exchange is usually termed reassortment. Although RNA recombination and reassortment are mechanistically very different, both require that two or more viruses infect the same host cell (Simon-Loriere and Holmes, 2011). Unlike 'genetic drift' that is associated with the gradual accumulation of mutations, genetic recombination can lead to dramatic changes to significant parts of the genome. The ability to exchange vast regions of genetic information, in a process akin to sexual reproduction, not only aids rapid evolution it also frees advantageous mutations from deleterious genomic baggage (Simon-Loriere and Holmes, 2011). Recombination therefore provides a mechanism that ensures the mutational robustness of a viral population. The mechanisms of recombination in single stranded RNA viruses will now be considered.

Replicative 'RdRp' dependent recombination - 'copy-choice'

The most widely accepted model of RNA recombination is 'copy choice'. In this process, the RdRp switches from one RNA molecule (the donor template) to another (the acceptor template) during synthesis of the negative sense RNA strand while remaining bound to the nascent

nucleic acid chain. The product of this switch is a negative sense RNA molecule carrying sequence derived from both parental templates (figure 1.5A) (Lai, 1992a, Lai, 1992b). The newly formed chimeric negative sense strand is then subsequently used as a template to produce positive sense RNA. Early experimental evidence strongly supports the notion that template exchange, or 'copy-choice' recombination occurs during negative strand synthesis (Kirkegaard and Baltimore, 1986b). The Kirkegaard and Baltimore study used an approach involving a pair of poliovirus mutants whose RNA replication could be suppressed by incubations at either a restrictive temperature or in the presence of guanidine hydrochloride (a potent inhibitor on antisense RNA synthesis). The conditions restrictive for one or the other of the partners could be predicted to differently affect the frequency of recombination. The experimental findings were strongly in favour of the 'copy-choice' model (Kirkegaard and Baltimore, 1986b). Two additional factors may also account for the preferred occurrence of recombination during negative strand synthesis. Firstly, the availability of acceptor template is presumed to have a direct impact upon recombination frequency (Jarvis and Kirkegaard, 1992). During an infection, positive sense strands are far more abundant than negative sense templates. Secondly, the synthesis of the negative sense strand leads to the formation of a double stranded replicative form (RF). The availability of the negative strand template for any recombination event will therefore be limited (Agol, 1997).

It is logical to assume that for replicative recombination to occur parental RNA will need to be in close proximity, i.e. inside the same replication complex. Recombination has been shown to occur *in vitro* between two different poliovirus serotypes as early as 2.5 hrs post infection (Egger and Bienz, 2002). A fluorescent *in situ* hybridisation (FISH) technique that used type specific riboprobes showed that replication of the two serotypes initiated at distinct sites that later overlapped at specific peri-nuclear locations, providing a clear opportunity for recombination to occur. Subsequent RT-PCR analysis confirmed recombination between the PV1 (Mahoney) and PV2 (Sabin) serotypes (Egger and Bienz, 2002).

Template switching that occurs at regions of sequence similarity between the nascent and the acceptor nucleic acid molecules, is deemed 'precise' or 'homologous' because no additional sequences are generally present (Lai, 1992b). 'Imprecise recombination' may also occur. Sequence similarity between the two parental sequences may be close to, although not necessarily at, the crossover site. This can produce a genome where additional sequence, deletions or nucleotide mismatches may be present (Nagy and Simon, 1997, Agol, 1997). Under these circumstances the genome may still be functional providing a full complement of viral protein encoding genes are present. The role of deletion via 'imprecise recombination' can account for the formation of defective interfering particles (DI). Following extensive passaging, poliovirus species lacking >10% of their genome have been isolated (Cole et al., 1971). In these examples deletions were in frame and found within the capsid-coding region of the genome. The encapsidation of the defective genomes was only possible due to the presence of a helper virus that could produce the required intact capsid proteins (Agol, 1997). Analysis of other serotypes of PV that produced (DI) particles showed no specificity to location of deletion, and ruled out the potential for cryptic ribozyme or host endonuclease activity. This indicated a random template switch during replication rather than any other non-replicative mechanism (Kuge et al., 1986). Genetic exchange between different, and genetically dissimilar, genomic regions or between non-related RNA molecules, can lead to 'non-homologous' recombination. As non-homologous RNA recombination involves regions with little sequence similarity, it will often produce non-functional genotypes (figure 1.5B) (Simon-Loriere and Holmes, 2011).

'Forced copy-choice' and non-replicative recombination

Unlike 'copy-choice' where the donor template is intact a process termed 'forced copy-choice' can account for genetic recombination. Early work with retroviruses has shown that the template-switching event occurs when there is a break in the donor template that forces the reverse transcriptase (RT) to seek an alternate functional template. In this process sequence homology of the nascent strand may dictate where the polymerase anneals upon the acceptor template (Coffin, 1979). Additionally, chimeric RNA molecules can be formed in a non-replicative way that does not involve any polymerase activity. Studies involving non-replicative

truncated PV partners and bacteriophage Qβ suggested that a trans-esterification reaction involving both templates occurred that produced a fully functional genome (Gmyl et al., 1999, Gmyl et al., 2003, Chetverin et al., 1997). Alternatively, studies involving pestiviruses and Hepatitis C virus have postulated the involvement of cellular exonucleases and RNA ligases in the process of recombination (Scheel et al., 2013, Galli and Bukh, 2014, Gallei et al., 2004).

Examples of recombination in enteroviruses

Genetic evidence for recombination between viral RNAs was first reported in the early 1960s. Mixed infections of two strains of poliovirus where each exhibited a characteristic phenotype (e.g. resistance to guanidine hydrochloride or resistance to inhibitors found in bovine sera) resulted in the appearance of variants expressing the two markers simultaneously (Hirst, 1962, Ledinko, 1963). In recipients of the live attenuated poliovirus vaccine recombinants are excreted within 7 days (Cammack et al., 1988, Guillot et al., 2000, Cuervo et al., 2001). Indeed, recombination between the Sabin vaccine strains and co-circulating enteroviruses contribute to minor outbreaks of poliomyelitis in areas of low vaccination coverage (Kew et al., 2002). Three groups of rhinoviruses (A-C) currently fall within the enterovirus genus and there is evidence for frequent recombination between group A and group C that involves the adjacent 5'NTR and VP2/VP4 genome regions (Lukashev, 2010). Genetic drift is reliant upon random mutation. Sequence analysis of six coxsackie B viruses (CVB - species B) serotypes over a 26-year period showed that all clinical isolates over this period were recombinant relative to the prototype strain of the same serotype (Oberste et al., 2004a). Furthermore, studies have indicated that recombinant forms of particular human enterovirus serotypes appear in a population, are successful in certain geographical regions and then are rapidly replaced in a predictable manner with characteristic half-lives (Leitch et al., 2009, McWilliam Leitch et al., 2012). The advancement in phylogenetic analysis clearly shows that recombination that leads to 'genetic shift' in areas outside of the capsid-coding region is a major mechanism used by this group of viruses to continuously evolve.

A

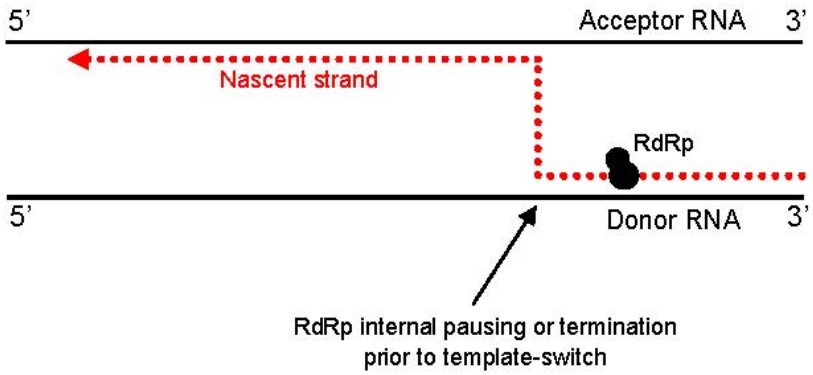

B

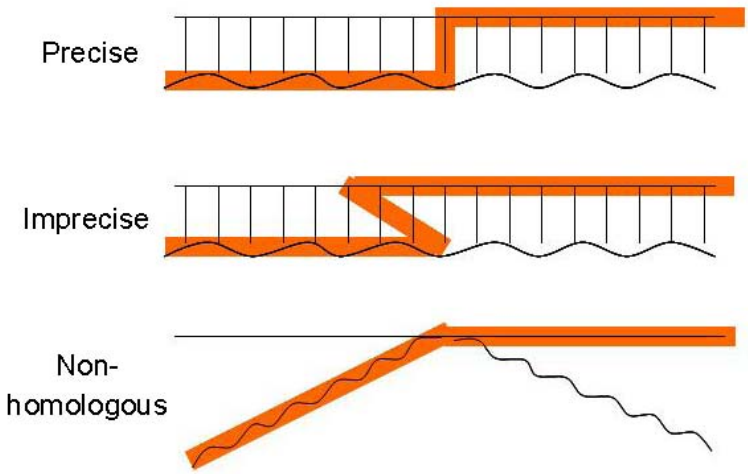

Figure 1.5: Replicative 'copy-choice' models of RNA recombination

(A) The RdRp exchanges templates from donor to acceptor during replication of a negative sense strand. Reasons for pausing or termination by the RdRp are discussed in the text **(B)** Precise and imprecise recombination is depicted. Non-homologous recombination is also shown. Source (Lai, 1992b).

Factors influencing recombination

The result of many separate recombination events have been observed and characterized in nature, with attempts made to relate recombination junctions to particular sequences and secondary structures within the virus genome. At present, it is suggested that the RdRp pauses or terminates at certain RNA sequence motifs (Nagy and Bujarski, 1997). Sequence signals include: A/U – rich and U – rich sequences, which may promote polymerase slippage (King, 1988a). Other factors that are thought to play a role in recombination junctions are the ability of the parental RNA strands to form stable heteroduplexes near or at the recombination junctions (Romanova et al., 1986). Additionally, long hairpin structures within one/both parental strand at the recombination junction are linked to an advanced opportunity to recombine (Tolskaya et al., 1987, Dedepsidis et al., 2010). Indeed, a recent study on intratypic recombination involving PV1 tagged with synonymous mutations showed that sequence composition and RNA structure correlated with, in a predictable and modifiable manner, recombination hotspots (Runckel et al., 2013). Alongside this, nucleotide mismatches have also been linked to replicase stalling and template exchange during RNA replication (Agol, 1997).

It could be fair to say that our understanding of the mechanisms and factors that contribute to replicative recombination in enteroviruses have not advanced that much from the initial findings of the mid 1980's. Only indirect discussion can be formed due to the methodology previously employed. There is potential to suggest that the historical isolates that have been characterised may not accurately represent the initial product of recombination. The majority of recombinant sequences analysed thus far in previous studies have been gained either from highly selected field isolates, or from *in vitro* studies that have used permissive and susceptible cell lines like HeLa. There is a risk that selection pressure in this highly dynamic environment has allowed the characterisation of only those recombinants that are 'fit' enough to compete. Additionally, experimental data is limited as there is currently no efficient cell-free system that recapitulates the recombination event.

1.4 Aims

Recombination clearly plays a significant role in the evolution of RNA viruses including enteroviruses. The triggers and the specific mechanisms of recombination in enteroviruses remains poorly understood with no consensus on sequence motifs or location. The aim of this study was to build on an *in vitro* experimental system developed by a previous student, Kym Lowry. The elegant cell based assay allows the isolation and subsequent characterisation of intertypic and intratypic poliovirus recombinants in the absence of parental genomes. Importantly, competition and selection pressures are minimised as much as possible.

Specific aims

- To quantify relative recombination frequency between intratypic and intertypic poliovirus partners
- To identify differences in early recombinants to those following serial passage / selection
- To determine if recombination is primarily a replicative or non-replicative process
- To determine the characteristics of the RNA dependent RNA polymerase that are important in template switching
- To expand the original Lowry *in vitro* cell based recombination assay
- To develop a cell-free biochemical assay to characterise the template switching event
- To investigate if RNA sequence or structure influences recombination frequency and, or location
- To develop a reproducible fluorescent *in situ* hybridisation (FISH) approach that would allow observation of RNA location during a co-infection

CHAPTER 2: Materials and Methods

2.1 Cell Culture and Virological Methods

2.1.1 Cell maintenance

Human cervical (HeLa), human embryonic rhabdomyosarcoma (RD), human embryonic kidney (HEK293T), and murine fibroblast (L929) cells were grown as monolayers in Dulbecco's Modified Eagle's Medium (DMEM) supplemented with 100 µg/ml of streptomycin, 100 U/ml of penicillin, 2 mM L-glutamine, and 10% heat inactivated (HI)-foetal bovine serum (FBS). Baby hamster kidney cells stably transfected with a T7 RNA polymerase expression plasmid (BsrT7) were maintained in Glasgow Minimum Essential Medium (GMEM) supplemented with 100 µg/ml of streptomycin, 100 U/ml of penicillin, 2 mM L-glutamine, and 10% HI-FBS. Antibiotic G418 was also added to BsrT7 cell medium to select cells containing the T7 RNA polymerase gene under control of the cytomegalovirus (CMV) promoter and the neomycin resistance gene (Buchholz et al., 1999). All cells were passaged using trypsin- ethylenediaminetetracetic acid (EDTA).

2.1.2 RNA transfection of mammalian cell lines

Purified RNA (amounts as specified elsewhere) in H_2O was made up to 100 µl in serum and antibiotic free medium and mixed with an equal volume solution of Lipofectamine 2000 (3:1 Lipofectamine 2000 to µg RNA), (Invitrogen) in similar medium. The mixture was incubated according to the manufacturer's instructions and added to cell monolayers in either 6 or 12-well tissue culture plates.

2.1.3 Luciferase assay

Supernatant was removed from transfected cell monolayers, cells were briefly washed with PBS and lysed using 200 µl 1 x Glo Lysis Buffer (Promega®) per well in a 12- well plate. The oxidation reaction was catalysed by the addition of 50 µl cell lysate (luciferase enzyme) to 50 µl room temperature *Bright-Glo*™ Luciferase Assay System (Promega®) substrate and shielded from the light for 5 mins. Luciferase activity was measured using a luminometer (Turner

Biosystems) with values normalised to mock transfection controls.

2.1.4 Isolation of media from transfected cells

Media from individually or co-transfected cells was isolated at 48-72 hrs post transfection. Any cellular debris was pelleted by centrifugation, with media being placed into new 1.5 ml microfuge tubes. Plaque assays were then carried out to detect virus.

2.1.5 Tissue culture infectious dose$_{50}$ (TCID$_{50}$)

Recombinant virus from co-transfections was titred by $TCID_{50}$ which measures the quantity of virus required to infect 50% of inoculated microplate wells per sample (Minor, 1985). Each well of 96-well plates was seeded with 2.5 x 10^4 HeLa cells, allowing for four replicates of titration per sample. In a separate 96-well round-bottomed plate, a serial 10-fold dilution of sample with DMEM/10% FBS/penicillin- streptomycin (PS) from 10^{-1} to 10^{-12} was performed. Media was removed from confluent cells, 100 µl of the appropriate virus dilution was added to each well, (including 100 µl DMEM/10% FBS/PS to control wells) and incubated for 1 hour at 37°C/5% CO_2. An extra 100 µl DMEM/10% FBS/PS was added per well and plates were incubated for four days. Plates were stained with crystal violet for one hour and rinsed with tap water before drying upside down on paper towel. Virus titre was expressed as $\log_{10}$ $TCID_{50}$/ml (Reed & Muench, 1938).

2.1.6 Plaque assay

RD or HeLa cells were seeded in 6 or 12-well plates and grown to 95% confluency. Where appropriate ten-fold dilutions of virus stock were made in DMEM. Once medium was removed from seeded wells, cells were washed with sterile PBS then inoculated with 500 µl of prepared virus and incubated for 30 mins at 37°C in the presence of 5% CO_2/air to allow absorption to occur. Plaque overlay media (refer to section 2.6 for contents) was added to each well and plates were incubated inverted for two to three days at 37°C in the presence of 5% CO_2/air. Cells were stained with crystal violet solution and re-stained post-removal of the plaque overlay media. Plaques were counted and the virus titre expressed as plaque forming units per millilitre (PFU/ml).

2.1.7 Plaque purification by limiting dilution

Recombinant virus from RNA transfections was biologically cloned by limiting dilution in 96-well microtitre plates. Virus dilutions were performed using a multichannel pipette in a round bottomed 96-well microtitre plate (Sterilin) prior to transfer onto fresh cell monolayers. Fifty-five microlitres of serum-free media was added to each well prior to addition of diluted virus. Approximately 55 µl diluted virus supernatant was added to each well in the top row. After mixing by pipetting, 55 µl of solution was transferred to the next row (already containing 55 µl serum- free media). Pipette tips were discarded after the mixture was mixed in each row and these two-fold dilutions continued down the plate. Fifty microlitres was transferred from each well onto a fresh cell monolayer in flat bottomed 96-well plates seeded with 2.6 x 10^4 HeLa cells/well. The plates were left to allow for virus absorption for 30 mins at 37°C in the presence of 5% CO_2/air. An extra 200 µl serum-free media was added to each well and plates were incubated at 37°C/5% CO_2/air. After 4 days, the supernatant was transferred to a new microtitre plate and cell monolayers were stained by crystal violet for the presence of complete CPE. RNA was extracted from the highest dilution of virus supernatant per column and RT-PCR was carried out to amplify the crossover region of the recombinant virus.

2.1.8 Virus infections

Cell monolayers (RD or HeLa) were inoculated with virus at the stated MOI. Virus was absorbed onto monolayers for 30 mins at 37°C/5% CO_2/air. Virus supernatant was removed and replaced with medium supplemented with or without 10% HI-FBS. For passaging, virus supernatant was removed 24 hours post-infection, upon completion of full cytopathic effect (CPE; appearance of cell rounding or detached cells).

2.1.9 Disruption of cellular microtubules and nocodazole treatment

Following the protocol taken from Egger & Bienz, 2005. To disrupt microtubules, cells were kept for 10 min at 0°C. Nocodazole at concentrations of 5 mM (Sigma) was added to prevent re-polymerization of microtubules upon rewarming to 37°C.

2.2 Molecular Genetic Techniques

2.2.1 Plasmid DNA extractions from Escherichia coli using commercial kits

Overnight cultures (5 ml and 100 ml) of transformed *E. coli* in Lysogeny broth (LB) broth with the appropriate antibiotic for selection were pelleted in preparation for mini-preps and midi-preps respectively. Small-scale isolations were carried out using GeneJET™ Plasmid Mini-prep Kit (Fermentas) according to the protocol provided. Plasmid DNA was eluted in 50 µl distilled H_2O. Medium scale isolations were performed according to the instructions supplied with the QIAfilter™ Plasmid Midi Kit (Qiagen) and DNA was re-suspended in 200 µl dH_2O. A list of plasmids/replicons used during this project is outlined in table 2.1 at the end of this chapter.

2.2.2 Virus RNA extractions from cell culture supernatant

RNeasy Mini Kit (Qiagen) was used for RNA extraction from supernatant recovered from virus infections or transfections according to the manufacturer's instructions. RNA was stored at -80°C and was thawed in an ice bath when required.

2.2.3 PCR product column clean up

QIAquickPCR® Purification Kit (Qiagen) was used for purification of DNA from PCR reactions according to the manufacturer's instructions. DNA was stored at -20°C until required.

2.2.4 Extraction of DNA from agarose gel

Deoxyribonucleic acid fragments were extracted from agarose gel using the DNA Extraction Kit (Qiagen) according to the manufacturer's instructions. The DNA was eluted in 20 - 40 µl dH_2O and quantitated by spectrophotometry and then used for all down-stream activities.

2.2.5 Transformation of E. coli with plasmid DNA

Around 3 µl ligation mixture (or 1 µl plasmid DNA where appropriate) was added to 50 µl ice-thawed α-Select Chemically Competent *Escherichia coli* (Bioline) and stored in an ice bath for 20 mins. The mix was placed in a 42°C waterbath for 35 seconds before being returned to ice for 2 mins. Five hundred microlitres of SOC medium (Sambrook and Russell, 2001) was added before

incubating the tube in a 37°C shaker (225 rpm) for 1 hour. One hundred and seventy-five microlitres of cells were plated onto LB agar plates supplemented with appropriate antibiotic selection and incubated overnight at 37°C.

2.2.6 Ligation of DNA fragments

Digested DNA fragments or PCR products were ligated into vectors at a molar ratio of 3:1 (insert:vector) in a 20 µl reaction containing 1 x Ligation Buffer (400 mM Tris- HCl, 100 mM $MgCl_2$, 100 mM dithiothreitol (DTT), 5 mM adenosine trisphosphate (ATP) (pH 7.8 at 25°C)) and 5 U T4 DNA Ligase (Fermentas). Reactions were incubated at room temperature for 2 hrs and used directly without further purification for bacterial transformations.

2.2.7 DNA sequencing

All sequencing reactions were set up in a 10 µl total volume mix using 25 pmol of appropriate primer. Plasmid sequencing required 400-500 ng, whereas PCR fragment sequencing required 100-400 ng. GATC Biotech sequenced all DNA samples.

2.2.8 Restriction enzyme digestion

Digestion of DNA was carried out using the manufacturer's recommended amount of restriction enzyme in a solution containing 1 x the specific supplied reaction buffer, and if required, with 100 µg/ml bovine serum albumin (BSA). Incubation temperature and subsequent thermal inactivation were carried out according to the manufacturer's instructions. The digestion reaction was incubated from 1 to 4 hrs before being run on a 1% weight per volume total (w/v) agarose gel for size/banding pattern analysis. The restriction sites used to linearise plasmids during this project are outlined in table 2.2 at the end of this chapter.

2.2.9 *In vitro* reverse transcription (cDNA synthesis)

Reverse transcription reactions were carried out using Superscript II Reverse Transcriptase (Invitrogen). Ten microlitres of purified RNA (at unknown concentration) was incubated in a mixture containing 100 pmol oligo dT (Invitrogen), 10 mM dNTP mix and 1.5 µl H_2O for 5 min at 65°C. Following a 2 min cool on an ice bath, 0.2 µmoles DTT, 1 x Superscript Buffer (250 mM Tris-HCl, pH 8.3 at RT, 375 mM KCl, 15 mM $MgCl_2$), and 20 U RiboLock RNase Inhibitor

(Fermentas) was added and incubated for 2 mins at 42°C. Two hundred units of Superscript II were added to the reaction before a final 50 min incubation at 42°C and reaction termination at 70°C for 15 mins. The cDNA mixture was stored at -20°C while not in use.

2.2.10 Amplification of DNA fragments (up to 3kb) - PCR

A master mix was prepared containing 1 x *Taq* Buffer with $(NH_4)_2SO_4$ (750 mM Tris-HCl (pH 8.8 at 25.5°C), 200 mM $(NH_4)_2SO_4$, 0.1% Tween-20), 2.5 mM each deoxyribonucelotide triphosphate (dNTP), 30 pmoles of the relevant forward and reverse oligonucleotide, and 2.5 U *Taq* DNA Polymerase (Fermentas) in a 50 µl reaction volume.

Thermal cycling comprised 30 - 40 cycles as follows: one cycle of denaturation for 2 mins at 95°C, 29-34 cycles of denaturation for 1 min at 95°C, annealing for 30 sec at 55°C (or different according to oligonucleotide conditions) and elongation for 1 min/kilo base pairs (kps) at 72°C, and a last cycle of 5 min at 72°C. A list of oligonucleotides is recorded in section 2.9 at the end of this chapter.

2.2.11 Site-directed mutagenesis

Point mutations were introduced into cDNAs using QuikChange® II XL Site-directed Mutagenesis Kit (Stratagene). Briefly, 20 to 40-mer oligonucleotides were designed for opposite strands of the plasmid and incorporated nucleotide mutations necessary for the project. The plasmids were amplified by PCR using the mutagenic oligonucleotides in table 2.3 according to the provided protocol. Competent *E. coli* cells provided with the kit were transformed with amplified plasmid and individual clones sequenced to confirm the presence of specifically introduced mutations. The mutated regions were subsequently sub-cloned into a reliable, characterised construct to ensure no additional off target changes were incorporated and sequenced to confirm.

2.2.12 Overlap extension PCR

This method was used when multiple changes to virus cDNA was required. Polymerase chain reaction oligonucleotides that were complementary to the virus cDNA and carrying the desired mutation(s) were designed to ensure that mismatches were at least 10 base pairs (bps) from

either the 5' or 3' end of the oligonucleotide. Two DNA fragments that overlapped in the region based upon the mutagenic oligonucleotides were produced using appropriate external oligonucleotides. Oligonucleotides used to construct pRLucΔCRE_3'CRE and pPV3-LIKE are shown in tables 2.4 and 2.5 respectively. Following column purification, the two DNA fragments were then used in a linear polymerase chain reaction that lacked the external oligonucleotides. Briefly, 9 cycles of PCR consisted of:

95°C - 2 minutes

95°C - 30 seconds

56°C - 30 seconds

72°C - Variable depending on length of product (typically 1 min per Kb)

Followed by a final extension:

72°C - 5 minutes

4°C - Hold

The two external oligonucleotides were then added at standard concentrations as recommended by the manufacturers protocol. Twenty-nine cycles of PCR were then used at standard conditions, using annealing temperatures best suited for the two external oligonucleotides being used. Extension time was also based upon the size of the desired product.

2.2.13 Construction of pSL3Δ, ΔpT7Rep3-L and ΔpRLucWT

pT7Rep3-L and pRLucWT were digested with *PmlI* and *PacI* and re-ligated following Klenow fragment treatment to produce suitable blunt ends. This effectively removed the entire IRES and the majority of the luciferase coding region. Similarly, pT7FLC/SL3 was digested with *XhoI* and *SalI* and re-ligated, removing the polymerase-coding region. No Klenow fragment treatment was required given the complementarity in sticky-ends.

2.2.14 *In vitro* transcription

Linearised plasmid for RNA transcription was first prepared by column purification using the QIAquickPCR® Purification Kit (Qiagen) and re-suspended in RNase-free water. T7 MEGAscript Kit® (Ambion) was used for *in vitro* transcription following the manufacturers protocol.

Between 1.5 and 2 µL of RNA was confirmed on a 1% agarose gel before column purification using RNeasy Mini Kit (Qiagen) and quantification on a spectrophotometer.

2.3 Biochemical assay Sym-subU and denaturing PAGE analysis

2.3.1 Symmetrical - Substrate 'U' biochemical assay

Following the protocol taken from Arnold & Cameron, 1999. An initial assay mix comprising of 50 mM HEPES pH 7.5, 5 mM $MgCl_2$, 10 mM *Beta*-mercaptoethanol (BME), 60 µM $ZnCl_2$, 1 µM symmetrical substrate 'U' (annealed labelled primer-template described fully in chapter six) and 500 µM ATP were warmed in a water bath at 30°C. Following 5 min incubation, purified poliovirus RNA dependent RNA polymerase (RdRp) and variants (see text for description) was added at a concentration of 5 µM (see Gohara et al., 1999 for purification of polio RdRp protocol). An additional 5 mins incubation period followed that allowed stable elongation complexes to form and the incorporation of the first nucleotide. A second assay mix was then rapidly added that comprised 500 µM CTP, GTP and UTP, 60 µM RNA acceptor template (variations described in text) and 1 mM $MgCl_2$. Samples were quenched (EDTA) for polymerase activity at timed intervals (described in text) with products analysed by 7M urea denaturing polyacrylamide gel electrophoresis (PAGE).

2.3.2 Denaturing PAGE and phosphorimaging

An equal volume of loading buffer, 10 µl (90% formamide, 0.025% bromophenol blue, and 0.025% xylene cyanol), was added to 10 µl of the quenched reaction mixtures and heated to 70°C for 2–5 min prior to loading 5 µl on a 20% denaturing polyacrylamide containing 1x TBE and 7M urea. Electrophoresis was performed in 1x TBE at 75 watts. Gels were visualized by using a PhosphorImager and quantitated by using the ImageQuant software (Molecular Dynamics).

2.3.3 Quantification of total RNA product and % of template transfer

ImageQuant software (Molecular Dynamics) was used to quantify total RNA. Four regions were selected: - 10mer (Sym-subU), 11mer (Sym-subU + ATP), n>1 (Extended Sym-subU) and the product of template switching. Addition of these gave total RNA values. Percentage of transfer product was calculated as follows: - Transfer product reads / Total reads x 100.

2.4 Fluorescent *in situ* hybridisation (FISH) (Appendix only)

2.4.1 Stellaris probe storage

Sets of Stellaris probes were manufactured and shipped by Biosearch Technologies™. The dry mixes of probes were dissolved in 200 µL of nuclease-free TE (10 mM Tris-HCl, 1 mM sodium EDTA, pH 8.0) to give a stock solution of 25 µM mixed oligonucleotides. Aliquots of probe (10 µl) were stored at -20°C and thawed in an ice bucket when required. Each aliquot was used a maximum of three times.

2.4.2 Cell seeding and virus infection

HeLa cells were seeded upon sterile 1 mm coverslips in 12-well plates. Required density at time of infection was 80%. Cell monolayers were gently washed twice in 1x PBS prior to virus inoculation. All cells were singularly or dual infected at an M.O.I of 10. Virus was absorbed onto monolayers for 30 mins at 37°C/5% CO_2/air. Virus supernatant was then removed and cell monolayers were then gently washed twice in 1x PBS before addition of new media to each well.

2.4.3 Cell fixation

HeLa cell monolayers were fixed at 4 hrs post infection. Media supernatant was removed from each well and each monolayer was gently washed twice in 1x PBS. Cell monolayers were then covered in ice cold 100% ethanol and fixed for 20 minutes at -20°C. Cell monolayers were then gently washed twice in 1x PBS.

2.4.4 Sample denaturing

Cell monolayers were thermally denatured in order to probe for the anti-sense viral RNA. Briefly, following fixation cell monolayers were incubated in 95% formamide, 0.1% SSC (saline sodium citrate) at 65°C for 10 minutes. Cells were then washed twice in 0.1% SSC in preparation for probe hybridisation.

2.4.5 Stellaris probe hybridisation

One microliter of the re-suspended Stellaris probe were added to the hybridisation buffer (section 2.6) to give a final volume of 20 µl. The washed coverslip was then placed on top of the probe mix face down (cell monolayer in contact with probe). Samples were then stored in a humidified chamber at 37°C overnight.

2.4.6 Slide preparation

Following overnight probe hybridisation coverslips were washed in the recommended wash solution (section 2.6) twice for 30 minutes at 37°C. Wash solution was removed and coverslips were then washed twice in 2x SSC. Coverslips were then mounted face down in Vectashield mounting medium containing 4',6-diamidino-2-phenylindole (DAPI) on to glass slides (Menzel-Glaser) and stored in the dark at 4°C for future fluorescence microscopy.

2.5 Poliovirus recombinant nomenclature

The reference sequences of poliovirus type 3 Leon (Genbank #X00925), type 1 Mahoney (Genbank #V01149) or the type 1 Mahoney-derived luciferase-encoding sub-genomic replicon (pRLucWT) was used to number the recombinant genomes in this study. To facilitate definition of junctions defined in clonal groups of recombinant virus genomes a standardised naming scheme was used; the 5' components were numbered from the first to last nucleotide derived from the acceptor (pT7FLC/SL3). The remaining 3' nomenclature indicates the first to last nucleotide derived from the donor template (poliovirus type 3 or the type 1 derived sub-genomic replicon). For example #105B = [PV3 (1- 3491) Luc (137) - PV1 - A Tail], 1-3491 relates to sequence from acceptor template (pT7FLC/SL3), Luc (137) - PV1 - A Tail indicates the final 137-nt from the luciferase coding gene followed by the remaining P2 and P3 regions from the PV1 sub-genomic replicon. Where recombination has occurred downstream of the

luciferase coding region defined numbering based upon the PV1 or PV3 reference sequences are provided. All recombinant viral sequences were aligned to the parental PV3 = Leon strain and PV1 = Mahoney strain reference sequences (if applicable). All sequence differences to the acceptor (pT7FLC/SL3) template are indicated.

2.6 Stock Solutions and Buffers

Crystal violet

0.5 g crystal violet powder in 20 ml 100% ethanol, 880 ml dH_2O containing 0.9 g NaCl and 100 ml 40% formaldehyde.

6 x DNA agarose gel loading buffer

25 mg bromophenol blue to 3 ml 100% glycerol. Make up to 10 ml with dH_2O. Store at RT.

Guanidine hydrochloride

Guanidine hydrochloride powder dissolved in H_2O at 200mM.

Plaque overlay medium

10% v/v Minimum Essential Medium (EMEM) with Earle's salts (10x), 1% v/v L- glutamine, 3% v/v 7.5% sodium bicarbonate, 2% v/v FCS, 1% v/v PS, and 30% v/v 2% agar.

Agar for plaque overlay medium

2% w/v bacto-agar (Dibco) in distilled water. Microwaved to dissolve powder, autoclaved and stored at RT.

Penicillin/streptomycin

Filter sterilised 10000 U/ml of penicillin and 10000 µg/ml streptomycin in distilled water.

DMEM, GMEM/G418, 10 x EMEM, trypsin/EDTA, and sterile PBS

Supplied by the Media Preparation facility in School of Life Sciences, University of Warwick.

Stellaris probe hybridisation buffer

1 g dextran sulfate, 1 ml 20x SSC, 1 ml deionized formamide. Nuclease free water to 10 ml final volume (all supplied by Sigma)

Stellaris probe wash solution

5 ml 20x SSC, 5 ml deionized formamide. Nuclease free water to 50 ml final volume.

2.7 List of DNA plasmids

Table 2.1: List of sub-genomic replicons and full-length clones used in this study

Plasmid name	Description	Reference
pE7Luc	E7 Replicon with capsid replaced by luciferase, derived from pT7E7	Chris Bull and Minghui Ao (in house)
pT7E7ΔCRE	pT7E7 with mutated CRE, unable to synthesise positive-sense RNA	Kym Lowry (in house)
pRLucWT	PV1 replicon with capsid replaced with luciferase	Andino et al., 1993
pRLuc-G64S	pRLucWT with G64S substitution within the 3Dpol region	Vignuzzi et al., 2006
pRLuc-D79H	pRLucWT with D79H substitution within the 3Dpol region	This project
pRLuc-Y275H	pRLucWT with Y275H substitution within the 3Dpol region	This project
pRLuc-D79H-Y275H	pRLucWT with D79H and Y275H substitutions within the 3Dpol region	This project
pRLuc-K359R	pRLucWT with K359R substitution within the 3Dpol region	Weeks et al., 2012
pRLucΔCRE	pRLucWT with mutated CRE, unable to synthesise positive- sense RNA	This project
pRLucΔCRE_3'CRE	pRLucWT with mutated native CRE, carrying a synthetic CRE in its 3'NTR	This project
pRLucΔCRE_3'CRE-K359R	pRLucΔCRE_3'CRE with a K359R substitution within the 3Dpol region	This project
pT7Rep3-L	PV3 replicon with capsid replaced by luciferase derived from pT7FLC	Barclay et al., 1998
pT7Rep3-L-G64S	pT7rep3-L with a G64S substitution within the 3Dpol region	This project
pT7rep3-L-Y275H	pT7rep3-L with a Y275H substitution within the 3Dpol region	This project
pT7FLC	Full-length PV3 Leon P3/Leon/37 infectious clone	Goodfellow et al., 2000
pT7FLC/SL3	pT7FLC with mutated CRE, unable to synthesise positive-sense RNA	Goodfellow et al., 2000
pT7FLC/SL3-G64S	pT7FLC/SL3 with a G64S substitution in the 3Dpol region	This project
pT7FLC/SL3-K359R	pT7FLC/SL3 with a K359R substitution in the 3Dpol region	This project
pT7FLC/SL3-Y275H	pT7FLC/SL3 with a Y275H substitution in the 3Dpol region	This project
pT7FLC/SL3-D79H-Y275H	pT7FLC/SL3 with a D79H and Y275H substitution in the 3Dpol region	This project
pPV1FLC	Full-length PV1 Mahoney infectious clone	This project
pPV1FLCΔCRE	PV1FLC with mutated CRE unable to synthesise positive-sense RNA	This project

pFLCΔCRE_3'CRE	PV1FLC with mutated native CRE, carrying a synthetic CRE in its 3'NTR	This project
pSL3Δ	pT7FLC/SL3 with the 3Dpol coding region removed	This project
ΔpT7Rep3-L	pT7Rep3-L with the 5'NTR removed	This project
ΔpT7Rep3-L-G64S	pT7Rep3-L with 5'NTR removed carrying a G64S substitution in the 3Dpol region	This Project
ΔpRLucWT	pRLucWT with the 5'NTR removed	This project
pJC105B	Molecular clone of an imprecise PV3/1 recombinant	This project

2.8 Restriction enzymes to linearise plasmids

Table 2.2: Restriction enzymes used to linearise plasmids for RNA transcription

Plasmid name	Restricton enzyme	Linearised size (bp)
pE7Luc	*XhoI*	9726
pT7E7ΔCRE	*NotI*	10328
pRLucWT	*ApaI*	~10500
pRLuc-G64S	*ApaI*	~10500
pRLuc-D79H	*ApaI*	~10500
pRLuc-Y275H	*ApaI*	~10500
pRLuc-D79H-Y275H	*ApaI*	~10500
pRLuc-K359R	*ApaI*	~10500
pRLucΔCRE	*ApaI*	~10500
pRLucΔCRE_3'CRE	*ApaI*	~10500
pRLucΔCRE_3'CRE-K359R	*ApaI*	~10500
pT7Rep3-L	*SalI*	10231
pT7Rep3-L-G64S	*SalI*	10231
pT7rep3-L-Y275H	*SalI*	10231
pT7FLC	*SalI*	11128
pT7FLC/SL3	*SalI*	11128
pT7FLC/SL3-G64S	*SalI*	11128
pT7FLC/SL3-K359R	*SalI*	11128
pT7FLC/SL3-Y275H	*SalI*	11128
pT7FLC/SL3-D79H-Y275H	*SalI*	11128
pPV1FLC	*ApaI*	~11400
pPV1FLCΔCRE	*ApaI*	~11400
pFLCΔCRE_3'CRE	*ApaI*	~11400
pSL3Δ	*NruI*	9716
ΔpT7Rep3-L	*SalI*	8201
ΔpT7Rep3-L-G64S	*SalI*	8201
ΔpRLucWT	*ApaI*	~8500
pJC105B	*ApaI*	11267

2.9 List of oligonucleotides

Table 2.3: Mutagenic oligonucleotides used throughout the study

Mutagenic primer	Sequence
PV1-G64S-F	CTCCAAGTACGTGTCTAACAAAATTACTGAAGTGGATGAG
PV1-G64S-R	CTCATCCACTTCAGTAATTTTGTTAGACACGTACTTGGAG
PV1-K359R-F	CTAACTATGACTCCAGCTGACCGATCAGCTACATTTG
PV1-K359R-R	CAAATGTAGCTGATCGGTCAGCTGGAGTCATAGTTA
PV1-D79H-F	GTACATGAAAGAGGCAGTACATCACTATGCTGGCCAGC
PV1-D79H-R	GACATGAGCTGGCCAGCATAGTGATGTACTGCCTCTTTCATGTAC
PV1-Y275H-F	CTAAACCACTCACACCACCTGCATAAGAATAAAACATACTGTGTCAAGG
PV1-Y275H-R	CCTTGACACAGTATGTTTTATTCTTATGCAGGTGGTGTGAGTGGTTTAG
PV3-G64S-F	CAATCTTCTCTAAGTATGTATCGAACAAGATCACTGAGGTGG
PV3-G64S-R	CCACCTCAGTGATCTTGTTCGATACATACTTAGAGAAGATTG
PV3-K359R-F	CATGACTCCGGCAGATAGGTCTGCCACTTTTGAGAC
PV3-K359R-R	GTCTCAAAAGTGGCAGACCTATCTGCCGGAGTCATG
PV3-D79H-F	GATGAGTACATGAAAGAGGCAGTGCATCATTATGCTGGACAACTTATG
PV3-D79H-R	CATAAGTTGTCCAGCATAATGATGCACTGCCTCTTTCATGTACTCATC
PV3-Y275H-F	CTTAACCATTCACACCACTTGCATAAAAACAAGATATATTGTGTT
PV3-Y275H-R	AACACAATATATCTTGTTTTTATGCAAGTGGTGTGAATGGTTAAG

Table 2.4: Oligonucleotides used to construct pRLuc_ΔCRE_3'CRE

Name	Sequence
CRE_MUT-F	CAACTATATCCAATTTAAATCCAAACACCGTATCGAACCAG
CRE_MUT-R	CTGGTTCGATACGGTGTTTGGATTTAAATTGGATATAGTTG
BSSHII-F	CATTTTAGGCGCGCTAACCCTACCTCAGTCGAATTGG
BSSHII-R	GGTTAGCGCGCCTAAAATGAGTCAAGCCAACGGCGGTAC
SYNTH_CRE-F	CGCGCCCGGGTAAGAGCAAACACCGTATTACCCGGG
SYNTH_CRE-R	CGCGCCCGGGTAATACGGTGTTTGCTCTTACCCGGG

Table 2.5: Oligonucleotides used to construct pPV3-LIKE

Name	Sequence
PV3-LIKE-F	GGAAATACTACCCAGTATCCTTTGTGGGACCCACCTTC
PV3-LIKE-R	CTAAGCCACTGCCATGGTGAAGCATCACACCCAAGAAGAA
pRLuc_5'-F	GACATAGCTTACTGGGACG
pRLuc_5'-R	GATACTGGGTAGTATTTCCT
pRLuc_3'-F	CACCATGGCAGTGGCTTAG
pRLuc_3'-R	CCACTGTTGATACCATCT

Table 2.6: Additional oligonucleotides used throughout this study

Name	Sequence
GEN-4615R	RTADCCRTCRAAGTGWKMYGG
PV1/3-3280F	AACACRTMMGWGTCTGGTGC
PV1-3004F	GCAAACCTCATCAAATCCATCA
PV1-3679R	GAGCATATGGGACTGGTA
PV1-5594F	GAAGTGGAGATCTTGGATGCC
PV1-5440R	TCCTTGTACCTTTGCTGTCCG
PV3-2995F	GCAAACATCTTCCAACCCGTCC
PV3-3249F	CGCATTTACATGAAACCC
PV3-5191-R	GGAGTCAACTGCTTGAAGCAGA
PV3-5587F	GAGGTTGAAATCCTAGACGCT
PV3-7390R	CCGAATTAAAGAAAAATTTACCCCTAC
EV7-6F	CAGATCATGTACATACC
EV7-5247R	GACACGAATGTGGTTAGTGC
Oligo dT	TTTTTTTTTTTTTTT

CHAPTER THREE: The Biphasic Nature of Enterovirus Recombination

3.1 Introduction

Many recombinant enteroviruses have been isolated and characterised from field samples following outbreaks of infection (Kew et al., 2002, Zhang et al., 2010, Oberste et al., 2004a). Early studies have highlighted potential triggers found in the RNA sequence and RNA secondary structure that provides preferential sites for recombination (section 1.3). However, the mechanisms of recombination still remain poorly understood. The field isolates studied in all examples have been exposed to a highly selective and dynamic environment, and may not necessarily represent the initial recombinant molecules produced. Characterising the mechanisms that drive recombination will help us understand a basic evolutionary mechanism. Additionally, potential strategies to limit the occurrences of such events can be developed. This would be helpful in the fight to eradicate poliovirus for example; production of a live attenuated vaccine strain that doesn't recombine would be very beneficial to this process.

Recombination is a rare event, with intertypic recombinants estimated to have frequencies of $1x\ 10^{-6}$ (Kirkegaard and Baltimore, 1986b, Jiang et al., 2007). Identification of recombinant genomes in a population that is predominately made up of parental viruses has therefore been an issue in all cell based studies. Early *in vitro* approaches have largely relied upon crossing parental genomes carrying different selectable markers. Those that 'escape' the selection process will have inherited the mutations from the two parental strains and would be recombinant viruses (Kirkegaard and Baltimore, 1986a). There is no doubt that such studies have provided some interesting observations, most notably the 'copy-choice' model of recombination (section 1.3). Although, identification of the recombinant viruses isolated under such selective pressures was limited to only a small region of the genome as defined by the selectable markers and may again not have represented the initial recombination event. An additional risk of reversion is also a possibility in such approaches, with a point mutation reverting a genome back to wild type around 10-100 fold more likely that an intertypic recombination event (Crotty et al., 2001). To overcome such issues, a novel *in vitro* assay has

been developed by a previous student (Kym Lowry) that uses two defective parental genomes that are each unable to generate infectious virus. Only a recombination event can produce a genome that can be potentially infectious.

Methodology

The first parental RNA is a sub-genomic replicon that has a large deletion of the virus genome. The capsid region (P1) was replaced with a reporter gene; in this study it is a firefly luciferase gene. This type of genome can translate and replicate successfully as it contains the key *cis*-acting elements and is a well established approach used to study polioviruses (Barclay et al., 1998, Percy et al., 1992). The lack of a capsid region ensures no virus particles are produced when transfected into permissive cells alone. In any recombination assay this genome would provide the non-structural P2 and P3 regions, and is therefore considered the 'donor'. The second genome (the acceptor in a recombination event) would be required to produce the capsid-coding region, but carry a defect in the non-structural region preventing production of a viable virus upon transfection. A suitable candidate is the well characterised genome that carries eight synonymous mutations in the highly conserved 2C CRE that disrupts positive strand RNA synthesis (Goodfellow et al., 2003a). This genome can produce negative strand RNA so is considered suitable for a replicative recombination assay, as it is believed recombination occurs during negative strand synthesis (Kirkegaard and Baltimore, 1986b). This approach relies upon delivering both RNA templates into cells, via transfection, where subsequent recombination and genomic re-arrangements can occur. Donation of a capsid from one parental genome and a functional CRE from the other parental genome would in principle produce a viable virus, and is termed the CRE-REP assay (figure 3.1). In principle, this provides a region of 1.058 Kb, between the end of VP1 and the 2C CRE, where recombination can occur. Importantly, the use of rodent cell lines like the murine L929 or baby hamster BsrT7 cells allows minimal selection of recombinant virus as is possible. Both cell types lack the poliovirus receptor CD155, but can support RNA replication. They are therefore deemed permissive but not susceptible to infection. Any recombinant virus produced and released from the cell into the media supernatant cannot re-infect neighbouring cells. This ensures that the recombinant virus is

isolated and characterised as near to the recombination event as possible. Additionally, by minimising selection, this approach allows isolation of a range of recombinant regardless of growth advantages. This is in contrast to previous *in vitro* cell based approaches that have largely used HeLa cells that are susceptible to re-infection due to the availability of receptor. This may have biased the identification of recombinant viruses to the ones that had a growth advantage over others. Quantification of any recombinant virus is by plaque assay, media supernatant is isolated from transfected rodent cells following an incubation period and subsequently used with permissive and susceptible cell lines like HeLa (section 2.1 for full description).

The CRE-REP has allowed various combinations of enterovirus partners to be used previously (Lowry et al., 2014). The primary enterovirus serotypes studied in this investigation were poliovirus type 1 (Mahoney) and type 3 (Leon). This was due to the availability of cDNA, the subsequent re-producibility of the CRE-REP assay when using these partners (outlined in text later), and the vast amount of past research into the life cycle of this virus.

Aims

The aim was to build upon the findings of a previous student, Kym Lowry. These included: comparing intratypic and intertypic poliovirus recombination frequencies, characterisation of early intratypic and intertypic recombinant isolates, cell specificity and characterisation of early intertypic recombinants to those following serial passage. In addition, it was felt important to develop a non-replicative recombination assay that would contrast the CRE-REP assay, which was presumed to be replicative i.e. recombinant virus genome produced during replication of the parental RNA. This would determine if the recombinant progeny was produced via a replicative mechanism like 'copy-choice', whilst also highlighting the relative contribution of non-replicative recombination to the overall yield of virus. The results in this chapter have contributed to the manuscript Lowry et al., 2014.

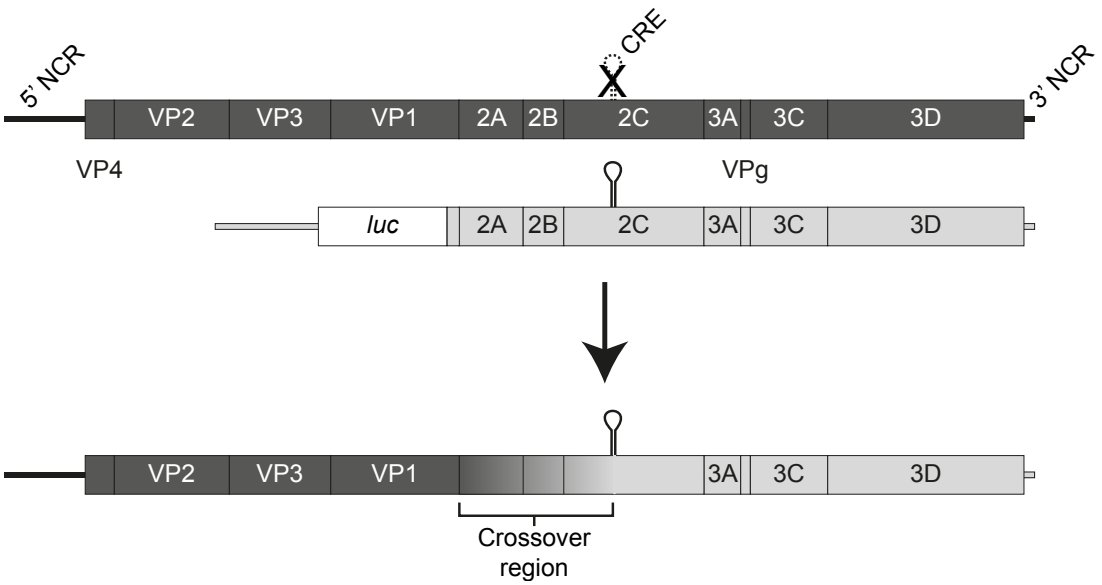

Figure 3.1: Overview of the CRE-REP assay

Two genomes, upper [dark shading] bears a defective CRE indicated as a broken line with a superimposed X in the 2C-coding region. Lower genome is a luciferase-encoding sub-genomic replicon (light shading). Following co-transfection into permissive cells (indicated by an arrow), a recombinant replication competent genome may be recovered of the generic structure shown, consisting of the 5' part of the genome derived from the CRE-defective parent (the recipient) and the 3' part of the genome from the luciferase-encoding replicon (the donor). The graduated shading between the 3' end of the VP1-coding region and the 2C CRE indicates the area within which recombination must occur to produce a functional genome.

3.2 Intraserotypic and interserotypic recombination ratio

Sequence similarity between parental genomes may provide a limitation to recombination frequency. It has been postulated that intertypic recombination frequency may be as much as 100-fold lower than intratypic recombination (King, 1988b, Tolskaya et al., 1983). This has been further supported by the work of Kirkegaard & Baltimore who found a similar phenomenon when using two parental genomes that carried resistance markers (Kirkegaard and Baltimore, 1986a). The CRE-REP assay has been previously used successfully to isolate intratypic and intertypic recombinant polioviruses (Lowry et al., 2014). By combining parental partners known to recombine these studies were extended to allow the relative frequencies to be ascertained. Both the PV3 sub-genomic replicon pT7Rep-3L and the PV3 CRE mutant pT7FLC/SL3 were linearised with *Sal*I. The PV1 replicon pRLucWT was linearised with *Apa*I. All three templates were used to transcribe RNA *in vitro* using T7 polymerase. Intratypic recombination frequency was measured using the PV3/3 partners (SL3 and Rep3-L). Comparative intertypic recombination frequency was measured using the PV3/1 partners (SL3 and RLucWT). In a standardised protocol, two micrograms of RNA were co-transfected into L929 cell monolayers in 6-well plates using Lipofectamine 2000 at a ratio of 1:1 (replicon: CRE mutant genome) in three separate experiments. Additional single transfection controls were also carried out. Cells were incubated for 48 hrs to allow a suitable time for recombination to occur. At this point media supernatant (containing potential recombinants) was harvested and 500 µl was used diluted or undiluted (as indicated) to inoculate monolayers of HeLa cells in 6-well plates for plaque assays. Plates were incubated for 60 hrs, stained with crystal violet, and photographed (figure 3.2). The null hypothesis would be that the observed frequency of recombinants in the PV3/PV3 experiments is equal to the observed frequency of recombinants in the PV3/PV1 experiments.

When RLucWT or SL3 were transfected into L929 cells alone no virus was detected. Viable intertypic recombinant virus was detected in all three co-transfections as observed by plaque formation. Yields of PV3/1 recombinant virus averaged at 115 pfu/ml. Similarly, viable PV3/3

A

Negative **RLucWT** **SL3**

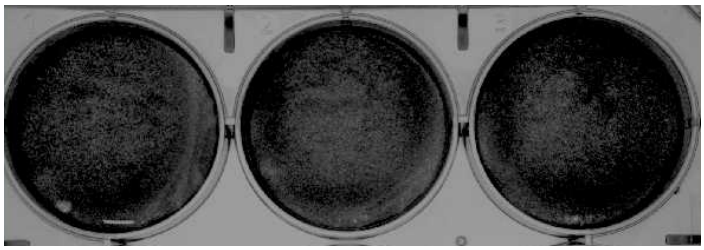

RLucWT + SL3

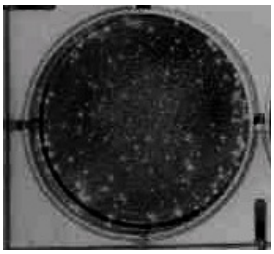

B

Rep3-L + SL3 **10^{-1}** **10^{-2}**

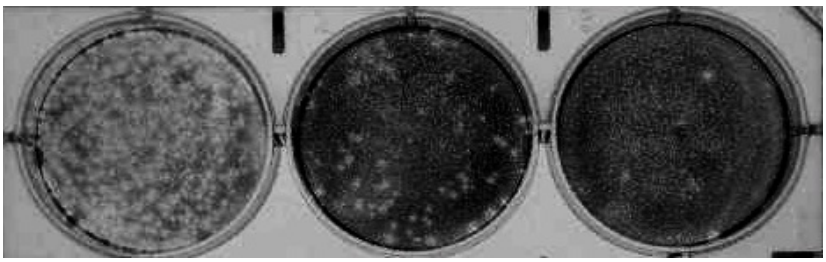

C

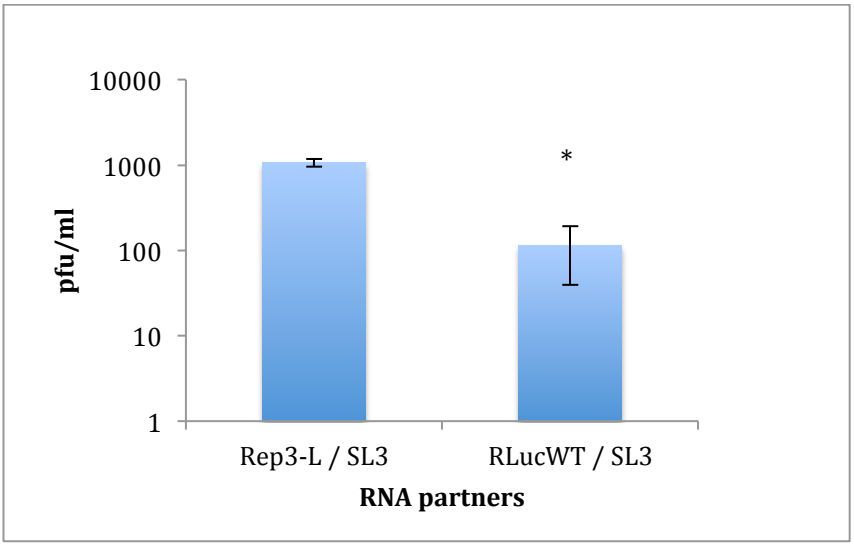

Figure 3.2: Virus recovered from L929 murine cells co-transfected with intertypic and intratypic poliovirus partners.

(A) Representative crystal violet stained HeLa cells inoculated with undiluted transfection supernatant and overlayed with plaque assay overlay medium. Control wells containing only one RNA partner were free of plaques. Viable virus was produced, as indicated by plaque formation, when intertypic RNA partners were co-transfected. RNA as indicated **(B)** Representative crystal violet stained Hela cells inoculated with dilutions of transfection supernatant. Viable virus was produced when intratypic partners were used. Similar controls to (A) were performed (data not shown). RNA as indicated **(C)** Comparative frequency of intratypic and intertypic recombination. The data represents the mean from three separate experiments. Error bars indicate standard deviation. Asterisk; $P < 0.01$ by Chi square test with PV3/PV3 values used as the expected and PV3/PV1 as the observed.

recombinants were produced from the co-transfected cells. Individual transfections produced no virus (data not shown). In contrast to PV3/1 recombination, yields of PV3/3 virus was significantly higher (as determined by chi-square test) and averaged at 1.1 x 10^3 pfu/ml.

3.3 Precise and imprecise recombination

The type of recombinant produced from intratypic and intertypic partners may provide insight into the mechanism of template switching. The CRE-REP assay has previously been used to characterise the recombination junctions of over 100 intertypic PV3/1 recombinant isolates (Lowry et al., 2014). The in-depth study on recombinants isolated from a co-transfection using RNA generated from pRLucWT and pT7FLC/SL3 cDNA showed that additional sequence is typically found at the recombination junction (hereafter termed 'imprecise' recombinants). Indeed, the largest insert identified was 321 nt. All isolates were in-frame, maintaining the open reading frame (ORF) and further extensive analysis could find no obvious link between RNA sequence to sites of recombination (figure 3.3). Of the 136 genomes in which the sequence could be unambiguously identified, 95 (70%) contained additional sequences, forming 17/20 (85%) distinct sequence junctions analysed. A striking feature of the imprecise recombinants recovered was their clustering in regions encoding the amino and carboxyl termini of 2A, termed cluster 1 and cluster 2 respectively. The consequences of this clustering were that the majority (94/95 individual sequences in 16/17 groups) of imprecise recombinants retained the ability to encode non-chimeric versions of the 2A and 2B proteins. The only isolate that encoded a chimeric protein had a recombination junction adjacent to the 2A / 2B boundary. This isolate only had one amino acid within the 2B gene that was not coded from the donor template, and this amino acid was the same between each parent. This means that the 2B protein translated was the same amino acid sequence as the PV1 replicon.

In contrast, a small amount of characterised isolates obtained using the intratypic partners, Rep3-L and SL3, have generally been shown to have no additional sequence at the recombination junction (hereafter termed 'precise' recombinants). Unlike their intertypic

counterparts the junctions of the 'precise' intratypic recombinants could not be identified due to the sequence identity between the two parental genomes. In this current study twenty PV3/3 recombinant isolates were biologically cloned using a limiting dilution approach (section 2.1.7). RNA was extracted from biologically cloned virus and reverse transcribed to produce cDNA (section 2.2.9). The specific region of recombination between the end of VP1 and the 2C CRE was amplified using the primers PV3-2995F and PV3-5191R. Additionally, a number of PV3/1 recombinant isolates were also amplified using a similar approach for comparison (RT-PCR). The zone of recombination for these biologically cloned isolates was amplified using the primers PV1/3-3280F and GEN-4615R. The majority of the PV3/1 recombinants amplified by RT-PCR looked to contain additional sequence within the amplified region when compared to a PCR product from a wild-type genome length control (figure 3.4A), a result that supports previous observations (Lowry et al., 2014). These were not sequenced. In contrast, only three of the twenty PV3/3 isolates looked to have additional sequence, as shown by a larger PCR product when compared to a wild-type length genome control (figure 3.4B). All twenty PCR products were sequenced using the same primers that were used to amplify from the cDNA (Figure 3.4C). The first 'imprecise' clone PV3 (1-3451/3) PV3 (3356/8 - A tail) has an additional 96 nt in viral sequence 2A (section 2.5 for recombinant nomenclature scheme). The second clone, PV3 (1-3393/4) PV3 (3355/6 - A tail) has an additional 39 nt also inserted in the 2A sequence. Finally, the third clone PV3 (1-3453) Luc (63) PV3 (3292 - A tail) has the largest insert of 222 nt. In this example the recombinant genome also includes 63 nt of the C-terminus of the firefly luciferase gene. In all three isolates the ORF is maintained and the full complement of viral proteins are present. They have all inherited the capsid-coding region from the SL3 template and inherited the majority of the non-structural P2 and P3 regions from the Rep3-L. Crossover positions were determined from full-length PV3 sequence strain Leon (GenBank accession number X00925).

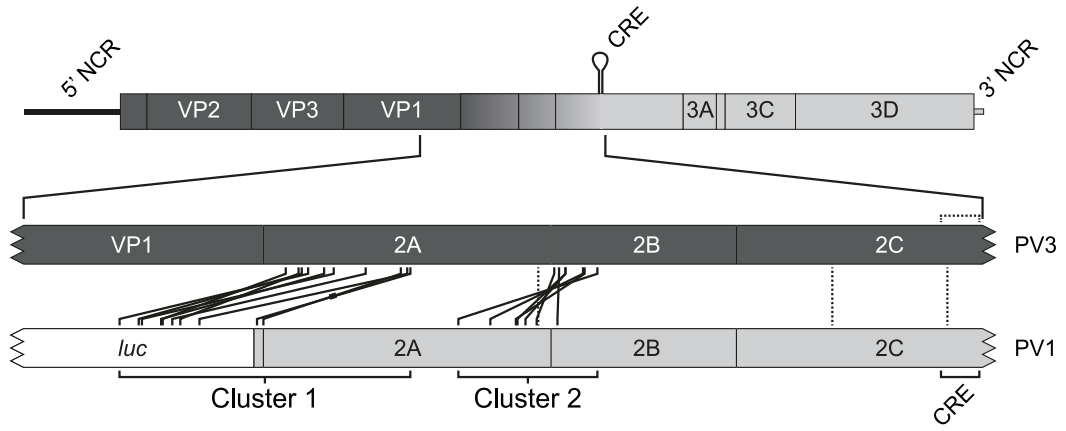

Figure 3.3: Twenty distinct recombination junctions identified from 136 cloned PV3/1 recombinants

Schematic diagram showing the location of recombinant junctions characterised following co-transfection of murine L929 cells with CRE-defective type 3 poliovirus genome (SL3; dark shading) and poliovirus type 1 sub-genomic replicon RNA (RLucWT; light shading). The graduated shading in the upper genome indicates the region within which recombination must have occurred to generate viable progeny virus. The expanded portion of the genomes (below) indicates the position of the junctions in the donor (RLucWT) and recipient (SL3) genomes. Solid lines indicate the groups of imprecise junctions – defined by sequence – which are grouped into two clusters spanning the P1/P2 and 2A/2B boundaries. The thickened line in one of the cluster 1 imprecise recombinants indicates the genome bearing additional sequence derived from the 5' NTR. Precise recombinants are indicated with vertical dotted lines within the 2A and 2C coding regions. Ref: (Lowry et al., 2014)

A

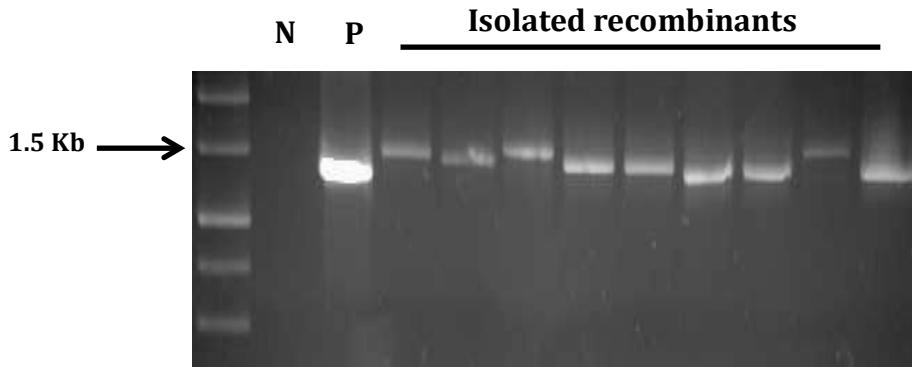
N
P
Isolated recombinants
1.5 Kb

B

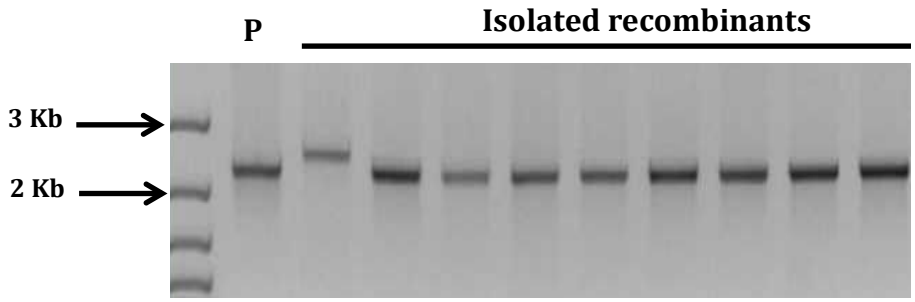
P
Isolated recombinants
3 Kb
2 Kb

C

PV3 (1-3451/3) PV3 (3356/8 - A tail)

```
PV3: GCCACTAAGGAGGATTTACAAAATGC
PV3: -A-C-CTTATCT--GAA-GGTTTGA-
REC: ----------GAA-GGTTTGA-
```

PV3 (1-3393/4) PV3 (3355/6 - A tail)

```
PV3: TGGGCATCAGAATAAAGCTGTGTACA
PV3: G-AC-CCTTATC-G-GAAA-GT-TG-
REC: ----------G-GAAA-GT-TG-
```

PV3 (1-3453) Luc (63) PV3 (3292 - A tail)

```
PV3: ACTAAGGAGGATTTACAAAATGCTGT
LUC: CCGG-AA-ACTCGACGC--GAAAAA-
REC: ----------CGACGC--GAAAAA-
```

Figure 3.4: Comparison of intratypic and intertypic Poliovirus recombinants.

(A) Representative gel electrophoresis of RT-PCR product of the PV3/1 recombination region. Ethidium bromide stained 1% agarose gels showing a heterogeneous mixture of amplified virus sequences from biologically cloned PV3/1 recombinants, N and P = negative and positive controls respectively **(B)** Representative gel electrophoresis of RT-PCR product of the PV3/3 recombination region. Ethidium bromide stained 1% agarose gels showing a general homogeneous mixture of amplified virus sequences from biologically cloned PV3/3 recombinants, P = positive control **(C)** Sites of imprecise crossover junctions in recovered PV3/PV3 recombinants. PV3 = Leon strain, GenBank accession numbers X00925. REC = indicates recombinant sequence, red boxes shows indicate sequence identity in the region of template switching. Dashes indicate nt identity with PV3, any differences in sequence are indicated.

3.4 Enterovirus species B intratypic recombination

During the initial stages of this investigation attempts to expand the CRE-REP assay into a different enterovirus species group was considered. The availability of suitable cDNA meant that echovirus 6 and 7 were chosen. These two viruses share similar genome length and layouts to poliovirus, and their CRE is located in the 2C region. This ensured a similar region of recombination was available. Additionally, sequence divergence within the potential recombination region is 20%, very similar to the PV3/1 divergence of 22%. An echovirus sub-genomic replicon (E7Luc) and a CRE defective full-length clone (E7ΔCRE) (Kym Lowry thesis) were used in a similar fashion to the species C poliovirus intratypic partners previously outlined. A total of 2 μg of RNA was co-transfected at a 1:1 ratio using Lipofectamine 2000 (replicon: CRE mutant genome) into BsrT7 baby hamster kidney cells in a 6-well plate. Media supernatant was isolated at 48 hrs post transfection and 500 μl undiluted supernatant was used to inoculate human embryonic rhabdomyosarcoma cells (RD) monolayers for plaque assays. Plates were incubated for 48 hrs, stained with crystal violet, and photographed. Individual transfection controls produced no virus, as expected. The co-transfected cells did produce recombinant virus as indicated by plaque formation (figure 3.5). The yield was calculated to be 26 pfu/ml. The recombinant virus population was subsequently biologically cloned in RD cells and the region of recombination amplified by RT-PCR using the primers EV7-6F and EV7-5247R. The homogenous population of PCR products all migrated in a similar fashion to the control. Subsequent sequence analysis indicated that all the PCR products were 2382 base pairs (bp) in length and wild-type E7, with no additional sequence present.

Importantly, the ability to isolate recombinant virus from a different species group provides further validity to the overall experimental approach. During the course of this study an E6 d'Amori strain sub-genomic replicon carrying a firefly luciferase gene in place of the P1 region was produced that would allow E7/E6 intertypic recombination to be investigated via a CRE-REP style experiment. Sequence analysis confirmed the replicons identity and luciferase assays indicated that the replicon replicated well (data not shown). However no intertypic E7/E6

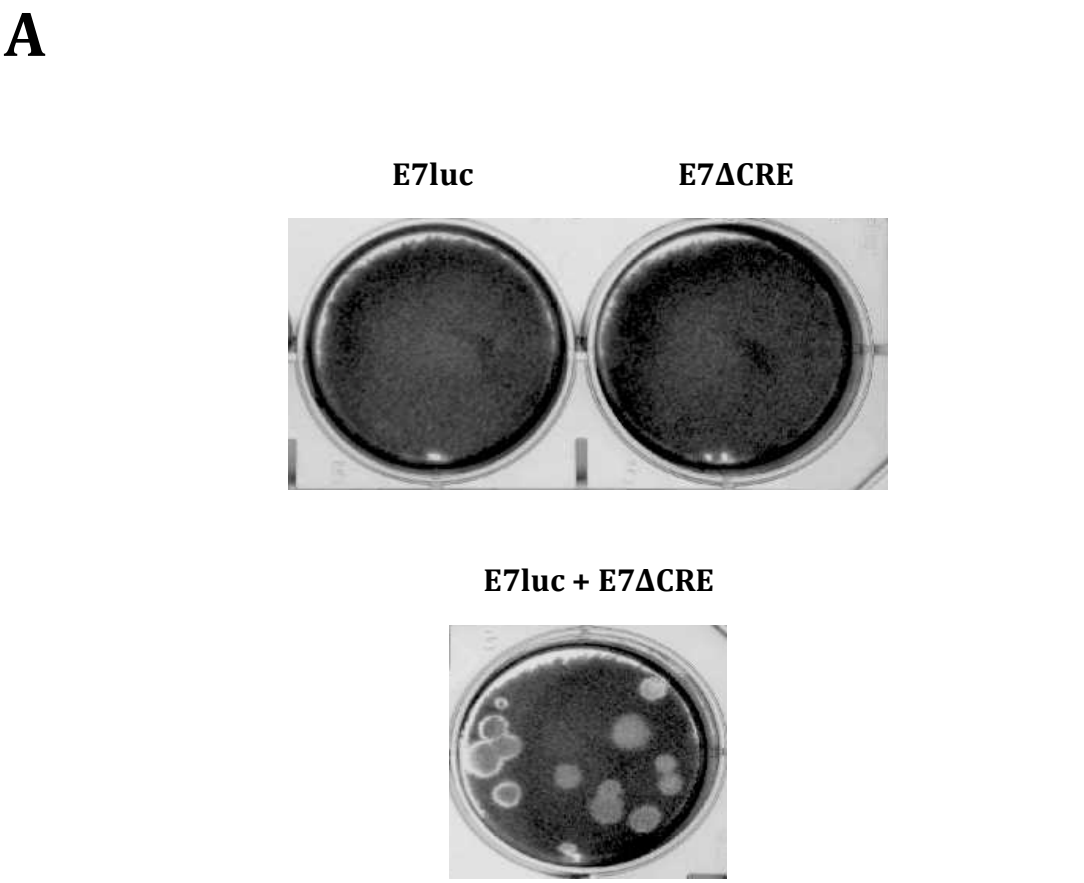

Figure 3.5: Identification and biological cloning of E7/E7 recombinant viruses.

(A) Individual transfection and co-transfection supernatant was inoculated undiluted onto a fresh RD cell monolayer and overlaid with plaque overlay medium. Cells were stained 48 hrs post-infection with crystal violet. Viable virus is evident by the presence of plaques. **(B)** Gel electrophoresis of RT-PCR product of recombination region following biological cloning of recombinant virus. Ethidium bromide stained 1% agarose gels showing a homogeneous mixture of amplified virus sequences from cloned recombinants. N = negative control, P = positive control.

recombinants were isolated. Many separate experiments were carried out that used altered donor: acceptor template ratios as well as different rodent cell lines (L929 and BsrT7). Due to the good reproducibility of the species C poliovirus CRE-REP assay a decision was made to concentrate the majority of future work on these partners.

3.5 Intertypic poliovirus recombinants isolated from HeLa cells

Previous studies and indeed the majority of the work presented in this thesis are based upon a system that uses rodent cell lines from which recombinant virus is recovered (L929 and BsrT7 respectively). The imprecise nature of many of the intertypic recombinants isolated could have been due to the host environment that is specific to rodent cell lines. The influence of host cell type and the type of recombinant produced was therefore considered. A co-transfection of HeLa cells with the intertypic partners RLucWT and SL3 was carried out using a total of 2 µg of RNA at a 1:1 ratio (replicon: CRE mutant genome) in a 6-well plate. Individual transfection controls were also done. HeLa cells are human cells that have the poliovirus receptor CD155, so are susceptible to re-infection unlike the rodent cell lines that are typically used. Additionally, HeLa cells have been widely used in the majority of studies with poliovirus so were considered the most appropriate. It was decided that harvesting of the media supernatant at 24 hrs post transfection instead of the normal 48 hr incubation would minimise any selection and allow characterisation of the early products of recombination. Following the incubation period, 500 µl of the media supernatant was used to inoculate fresh HeLa cell monolayers for plaque assays. Cells were incubated for 60 hrs and stained with crystal violet. Individual transfections of either parental genome produced no virus, as expected. Co-transfected cells produced viable recombinant virus as indicated by plaque formation and yield of PV3/1 recombinant virus was calculated to be 32 pfu/ml. Recombinant virus was biologically cloned using a limiting dilution method and the recombination region was amplified by RT-PCR using the primers PV1/3-3280F and GEN-4615R. The products of the PCR reaction indicated additional sequence when compared to the control, which was 1335 bp in length (figure 3.6). The migration of the PCR products amplified from recombinant cDNA indicated that all are imprecise in nature, similar to

A

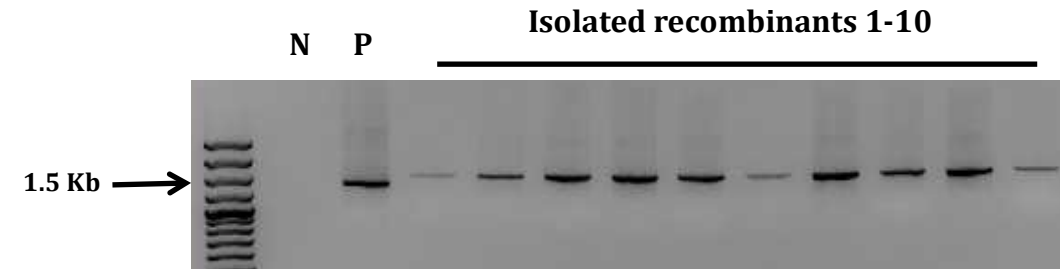

B

PV3 (1-3475/76) Luc (32/33) - PV1 - A tail

```
PV3:  ATACTGTAAGCATCATGTGGAATAGA
LUC:  GAGAGA-CCT---A-A-GCC--G-AG
REC:  --------------A-GCC--G-AG
```

Figure 3.6: Biologically cloned PV3/PV1 recombinants from a HeLa cell co-transfection.

(A) Ethidium bromide stained 1% agarose gel showing the non-uniform virus fragments from biologically cloned recombinants isolated from a HeLa cell co-transfection. N = negative control, P = positive control **(B)** Imprecise recombinant example**.** PV3 = Leon strain (GenBank accession numbers X00925), LUC = Luciferase sequence carried by the PV1 replicon and REC = recombinant sequence. Red boxes show nt identity at cross-over junctions. Dashes indicate nt identity with PV3, any differences in sequence are indicated.

the phenomenon seen in rodent cells. This indicates that the initial recombination event incorporating additional sequences at the site of recombination is not a cell specific trait. Three of the PCR products were sequenced, with all returning the same sequence PV3 (1-3475/76) Luc (32/33) - PV1 - A tail. These 'imprecise' isolates have an additional 150 nt when compared to wild-type genome length.

3.6 Resolution of imprecise intertypic recombinants

The identification of intertypic recombinants (PV3/1) carrying additional sequence at the recombination junctions in this study and the Lowry study was somewhat unexpected. Recombinant polioviruses characterised from field isolates following outbreaks of infection never carry any additional sequences (Kew et al., 2002, Zhang et al., 2010, King, 1988b). Perhaps the methodology employed in the CRE-REP assay had isolated the very early recombinant genomes that had not been exposed to any selection pressure? Indeed, passaging of imprecise intertypic recombinants has provided evidence to suggest that the primary products of recombination go through a secondary event that selects virus where all additional sequences have been lost and the genome returns to wild-type length (Lowry et al., 2014). This provides the hypothesis that recombination in enteroviruses is a biphasic event. An initial promiscuous recombination event that incorporates additional sequence is then followed by loss of the additional sequence after serial passage in permissive and susceptible cells (HeLa for example) in a process hereafter termed 'resolution'.

Serial passaging of three 'imprecise' PV3/1 recombinant viruses

Three 'imprecise' recombinant viruses that had been identified were chosen for serial passaging in HeLa cells. The first two had imprecise junctions that spanned the VP1/2A cleavage boundary (cluster 1 isolates) and had been isolated and characterised in the Lowry study. These were designated as #53A [PV3 (1-3505) Luc (168) - PV1 - A Tail], and #105B [PV3 (1- 3491) Luc (137) - PV1 - A Tail], which carry an additional 294 and 249 nt respectively. An isolate

characterised in this study known as #E1 [PV3 (1-3858/59) PV1 3774/75 - A Tail] had an imprecise junction at the C-terminus of 2A carrying an additional 75 nt (cluster 2 isolate). All were serially passaged individually in HeLa cells in T20 flasks 12 times. Virus samples were taken at various passages and subjected to RT-PCR analysis. The region of recombination from the end of VP1 to the 2C CRE was amplified using the primers PV1/3-3280F and GEN-4615R. The PCR band size of #53A (with all additional sequence) is 1629bp. By passage 5 three bands can be seen, one representing junction with insert, one intermediate and one smaller band. By passage 7 all additional sequence looks to have been lost and the PCR product has migrated as far as the wild type control (figure 3.7). The passaging of #105B and #E1 also show a similar phenomenon (figures 3.8 and 3.9 respectively). The recombinant #105B looks to have a band primarily migrating to the same position as the wild type control at passage 11. Only #E1 looks to have retained any additional sequence but there is a clear change in PCR product size following passage. In all three examples the serial passaging of 'imprecise' recombinant genomes has led to a secondary stage where additional sequence was lost. Indeed, the biologically cloned isolates from each group that were isolated and characterised by RT-PCR at passage 12 all migrated in a similar fashion to a wild type genome length PCR product. All amplified regions from the biologically cloned isolates at passage 12 were sequenced to characterise their altered recombination junctions. The eight 'resolved' #53A isolates all returned the same sequence. The #105B isolates returned two unique sequences and the #E1 isolates returned one unique sequence. In the three groups, all had lost the additional sequence and the genomes were wild type in length, or 'precise' recombinants (figure 3.10ABC). The majority of the 'imprecise' PV3/1 isolates characterised in the Lowry study provided recombination junctions that could be identified down to a single nucleotide. As previously stated no obvious link to RNA sequence could be identified at this stage, with recombination seemingly 'promiscuous'. It is interesting to note that in all the examples of 'resolved' recombination in this study, all the junctions are ambiguous i.e. we were unable to identify the exact position of recombination due to sequence identity between the parental genomes. Importantly, all of the passaged isolates had new recombination junctions that could have arisen from the initial 'imprecise' parental genome following resolution (figure 3.10D).

A

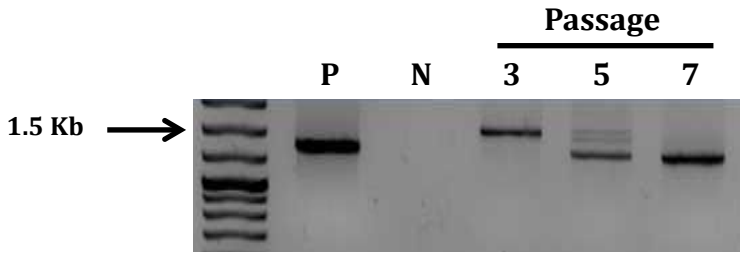

B

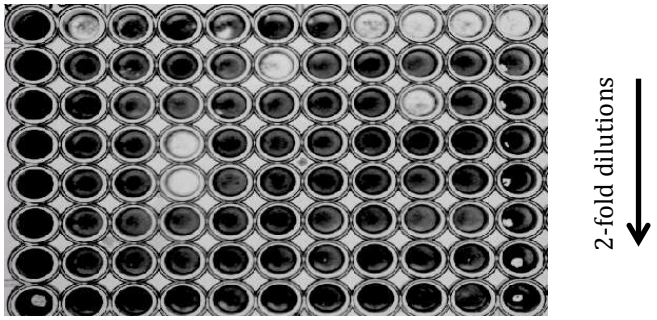

C

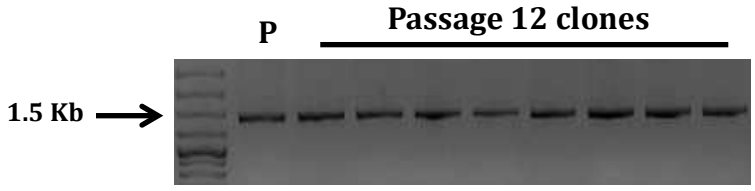

Figure 3.7: Serial passaging of PV3/1 recombinant #53A

(A) Ethidium bromide stained 1% agarose gel. (N) Indicates negative control. The positive control (P) represents a wild type genome length product from a PCR reaction using primers that amplified the specific recombination region. Products from RT-PCR can be seen from passages 3, 5, and 7 respectively. Arrows show 1.5 Kb size marker **(B)** Limiting dilution approach to biologically clone recombinant virus from passage 12. **(C)** RT-PCR derived product from 8 biologically cloned recombinant viruses from passage 12, (P) represents the wild type genome length PCR product.

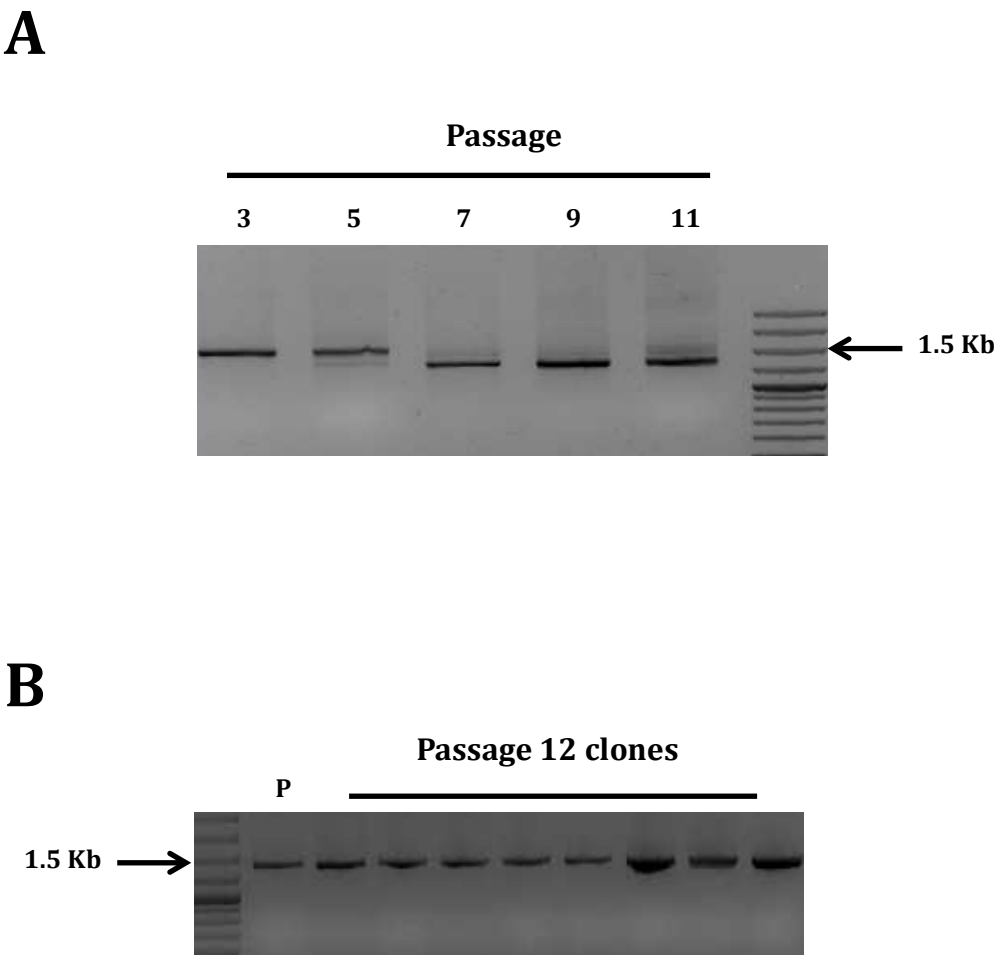

Figure 3.8: Serial passaging of PV3/1 recombinant #105B

(A) Ethidium bromide stained 1% agarose gel. Products from RT-PCR can be seen from passages 3, 5, 7, 9 and 11 respectively. Arrows show 1.5 Kb size marker **(B)** RT-PCR derived product from 8 biologically cloned recombinant viruses from passage 12, (P) represents control PCR from wild type length genome.

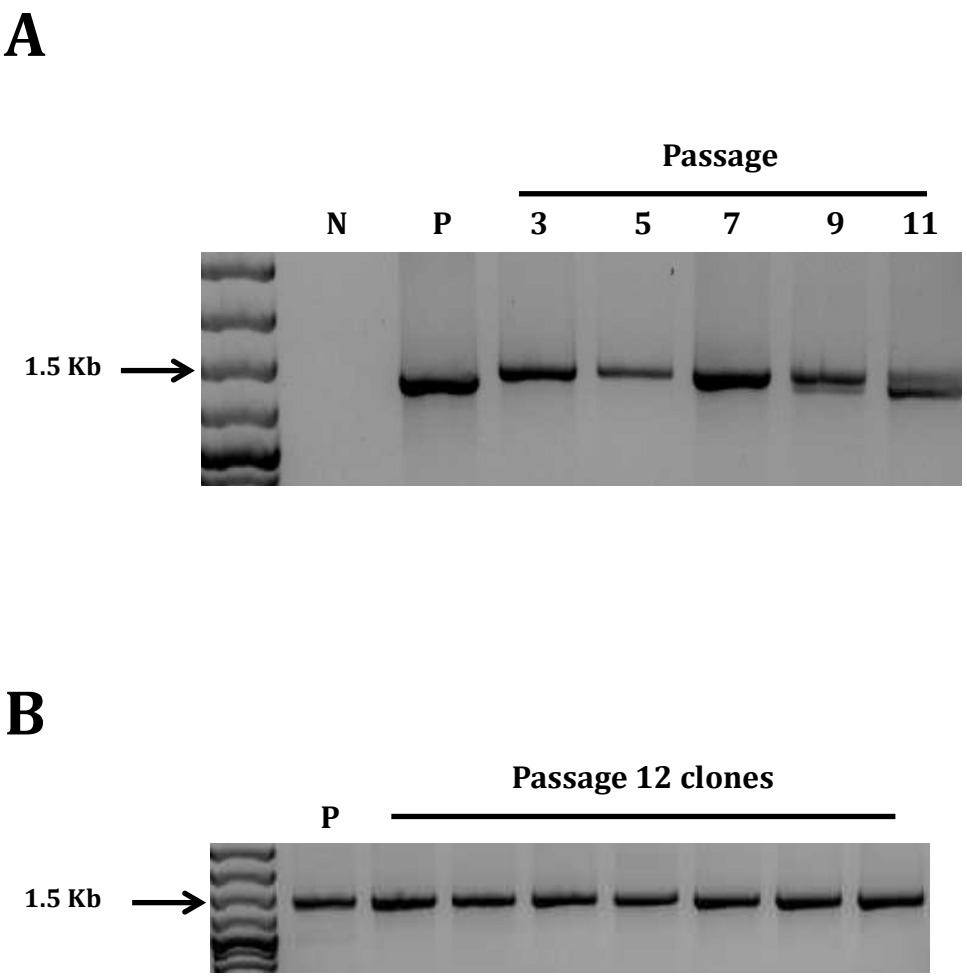

Figure 3.9: Serial passaging of PV3/1 recombinant virus #E1

(A) Ethidium bromide stained 1% agarose gel. (N) Indicates negative control. The positive control (P) represents a wild type genome length product from a PCR reaction using primers that amplified the specific recombination region. Products from RT-PCR can be seen from passages 3, 5, 7, 9 and 11 respectively. Arrows show 1.5 Kb size marker **(B)** RT-PCR derived product from 7 biologically cloned recombinant viruses from passage 12, (P) represents control PCR from wild type length genome.

A

PV3 (1-3412/3420) - PV1- A tail

```
PV3: TGTGTACACTGCTGGTTACAAGATCTGCAACTACC
PV1: G----------A--------A--T----------
REC: ----------------------A--T----------
```

B

PV3 (1-3367/3379) - PV1- A Tail

```
PV3: TGAGAAAGGTTTGACCACATATGGCTTTGGGCATC
PV1: CACC--G-A-C----------A--C--A--C-
REC: ----------------------A--C--A--C-
```

PV3 (1-3391/3) - PV1- A tail

```
PV3: ATGGCTTTGGGCATCAGAATAAAGCTGTGTACACT
PV1: ----A--C--A--C--A--C-----G---------
REC: ------------------C-----G---------
```

C

PV3 (1-3787/3798) - PV1- A tail

```
PV3: CTCTGACATAAGGGACTTGTATGCTTACGAGGAAGA
PV1: T--A-----T--A----------C-----A-----
REC: ----------------------C-----A-----
```

D

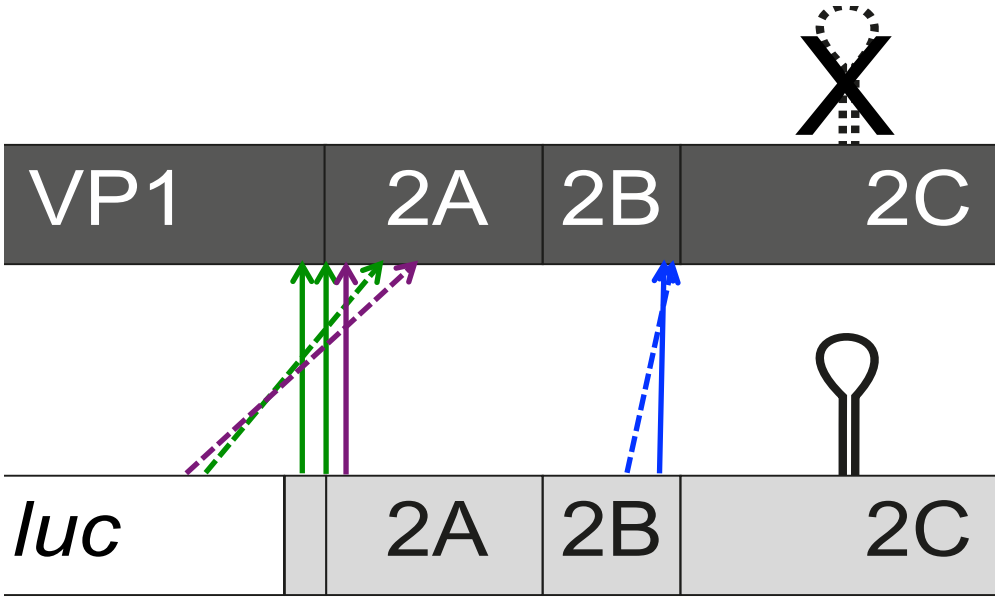

Figure 3.10: Sites of the recombination junctions in the passaged recombinants #53A, #105B and #E1.

PV3 = Leon strain, PV1 = Mahoney strain (GenBank accession numbers X00925 and V01149 respectively), REC = recombinant sequence. Red boxes indicate sequence identity at positions of template switching. Dashes indicate nt similarity with PV3, any differences in sequence are indicated **(A)** One unique crossover site from clones after recombinant #53A was serially passaged through HeLa cells **(B)** Two unique crossover sites after recombinant #105B were serially passaged through HeLa cells **(C)** One unique crossover site after recombinant #E1 was serially passaged through HeLa cells **(D)** Recombinants are colour coded as follows, **PURPLE** = #53A [PV3 (1-3505) Luc (168) - PV1 - A Tail], **GREEN** = #105B [PV3 (1- 3491) Luc (137) - PV1 - A Tail] and **BLUE** = #E1 [PV3 (1-3858/59) PV1 3774/75 - A Tail]. Dashed arrows represent the initial recombinants with insert sequence. Arrows represent biologically cloned precise recombinants derived from serial passage of the initial recombinant.

3.7 Construction of the molecular clone JC105B

The isolation of resolved recombinant viruses utilised a limiting dilution approach. One limitation of such an approach is the possibility that the population of virus may not be clonal, and could potentially contain additional recombinant virus. This seems to be evident with a result shown in the Lowry PhD thesis, where a serially passaged imprecise recombinant virus produced precise recombinant genome sequences that could not have arisen from the original biologically cloned virus. This was not observed in section 3.6 where all of the resolved recombinant genomes could have arisen from the initial 'imprecise' recombinants. However, the resolution step where additional sequence was lost could still have been due to the presence of a low level of a precise recombinant virus that out-competes the imprecise recombinant population following a suitable passage length. The resolution event needed to be unambiguously characterised.

To overcome this, a molecular clone of an imprecise recombinant that was identical in sequence to an isolate known as #105B was constructed by a two-step cloning strategy by Dr. Jonathon Cook (the construct hereafter known as JC105B is described in figure 3.11A). The decision to produce this 'imprecise' recombinant cDNA was based upon the availability of suitable restriction enzyme sites for cloning. The PCR product used in the first step of cloning was synthesised using the primers PV1/3-3280F and GEN-4615R. The entire region of cloned cDNA was sequenced to confirm its identity and RNA was transcribed using T7 polymerase. One microgram of the RNA produced was then used to transfect L929 cells in a 12-well plate. Transfection supernatant was isolated at 24 hrs post transfection and a serial dilution was used to inoculate RD cell monolayers for a plaque assay. Cells were incubated for 48 hrs, stained with crystal violet and photographed (figure 3.11B). As indicated by the plaque formation, the RNA was infectious and virus yield was calculated to be 8×10^4 pfu/ml.

A

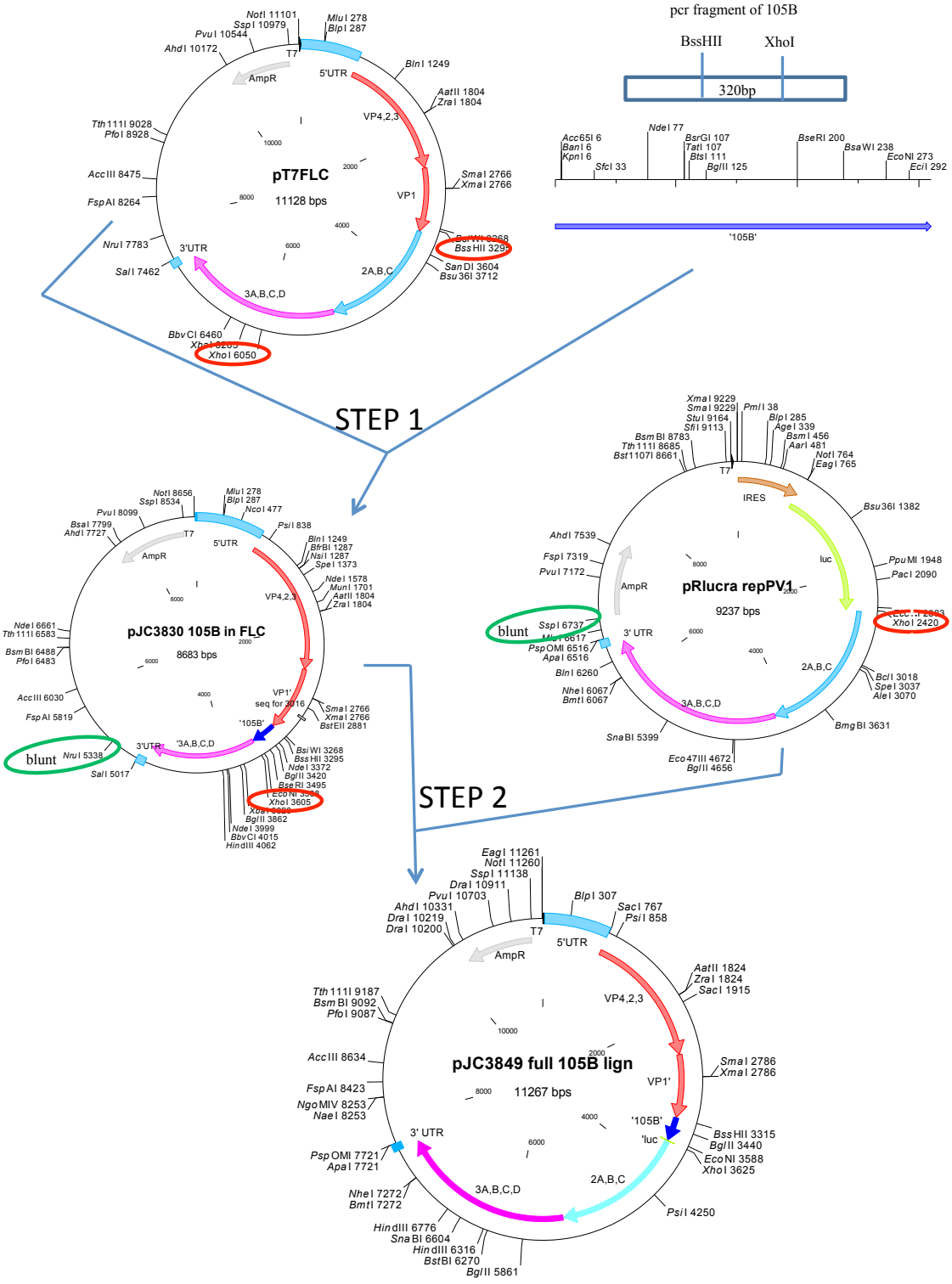
pcr fragment of 105B
BssHII
XhoI
320bp
'105B'
pT7FLC
11128 bps
T7
5'UTR
VP4,2,3
VP1
2A,B,C
3A,B,C,D
3'UTR
AmpR
STEP 1
pJC3830 105B in FLC
8683 bps
pRIucra repPV1
9237 bps
IRES
luc
blunt
STEP 2
pJC3849 full 105B lign
11267 bps
'105B'
'luc

B

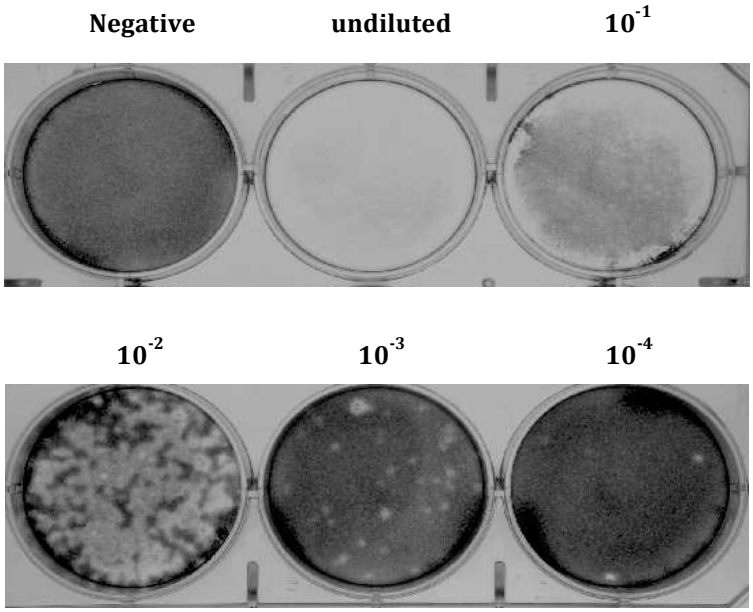

Figure 3.11: Construction of the molecular recombinant clone JC105B

(A) The construction of the intertypic recombinant JC105B occurred in a two-step process. Firstly, the amplified recombination region from the original #105B isolate was sub-cloned into the pT7FLC/SL3 plasmid using the unique restriction sites *BssHII* and *XhoI*. Secondly, the non-structural region of the PV1 replicon (pRLucWT) was sub-cloned into the intermediate plasmid (pJC3830) using the *XhoI* site along with the two unique blunt cutting sites (*NruI* and *SspI*) to produce the complete construct (pJC3849) **(B)** Crystal violet stained RD cells infected with a dilution series of transfection supernatant and overlaid with plaque overlay medium. The supernatant was obtained from a transfection of L929 cells with RNA produced from pJC3849.

3.8 Serial passage of the molecular clone JC105B

To validate the experimental evidence provided from the serial passage of three biological 'imprecise' recombinants, virus derived from JC105B was also passaged in HeLa cells. Unlike the original 12-passage regime, this virus was passaged only 7 times. It was reasoned that this would provide the best opportunity to isolate possible intermediate sized recombinant viruses that neither resembled the original nor the completely resolved genome. RNA was extracted from various passages and subjected to RT-PCR analysis. The primers used to amplify the specific region of recombination were PV1/3-3280F and GEN-4615R. Like its biological counterpart, JC105B went through a 'resolution' stage following passage (figure 3.12). At passage 4 two PCR products can be visualised that are smaller than the expected 1584 bp size of JC105B with complete insert. One of these bands migrated as far as the wild type control, suggesting a fully resolved product. The second PCR product looked intermediate in size, smaller than the 105B with insert yet larger than the wild type band. Subsequent isolation of individual clones from passage 7 material, using a limiting dilution approach, produced a heterogeneous population of PCR products. Six clones were sequenced, with one providing an identical sequence to a previously isolated precise #105B biological clone shown in figure 3.10B [PV3 (1-3367/3379) - PV1 - A tail]. A second precise junction was also identified [PV3 (1-3401/3411) - PV1 - A tail]. In both examples the exact location of the new junction cannot be determined due to sequence identity of the parental genomes from which the clone was produced (figure 3.13). The remaining four clones exhibited the same 'imprecise' junction, but this was different to the original JC105B construct. The latter retained a 57 nt insert derived from the C-terminal part of the firefly luciferase reporter gene, but had lost the remainder of the insert that was present in the JC105B construct. This was an intermediate recombinant, a phenomenon not characterised before.

Taken together, two conclusions can be drawn from this experiment. Firstly, the imprecise recombinants isolated from L929 are the likely progenitors of the precise recombinants subsequently selected by serial passage in HeLa cells. Secondly, the identification of precise and imprecise recombinant with a duplicate sequence reduced in length from the input suggests

that process of resolution may progress using a step-wise mechanism via intermediate imprecise recombinants. In principle, this event could have occurred *in cis* where the additional sequences are 'looped' out upon the same template during RNA replication. Alternatively, the resolution event could have occurred *in trans*, involving another acceptor template via a copy-choice like recombination event.

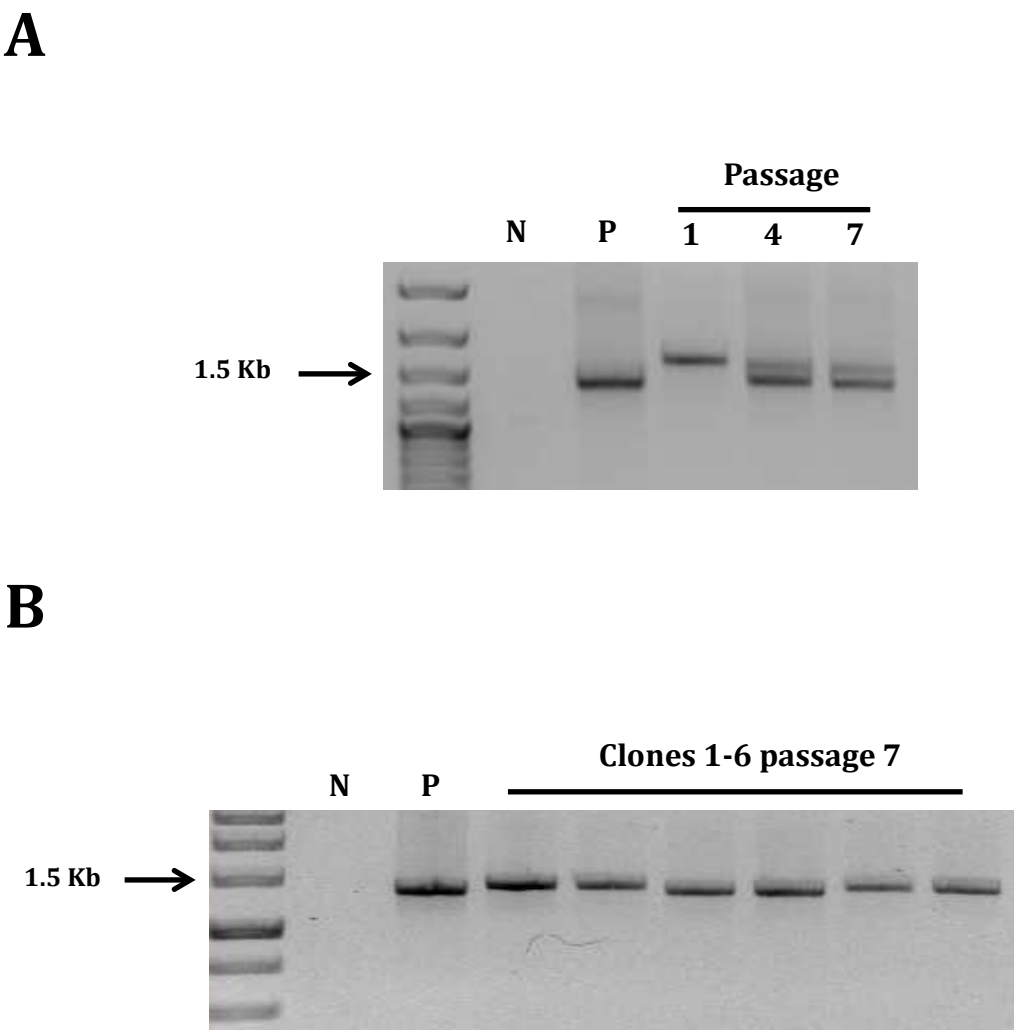

Figure 3.12: Changes in the crossover region of passaged molecular clone JC105B recombinant.

Following seven passages through HeLa cells. RT-PCR product of amplified region in the recombinant virus was run on 1% agarose gel and stained with ethidium bromide **(A)** New construct JC105B recombinant crossover region gradually reduced in size from 1584 bp (with insert) (N) indicates negative control; (P) indicates the positive control representing a wild type genome length product. Two bands can be seen from p4 onward, the smaller being 1335 bp (length of precise crossover) the larger band represented an intermediate recombinant **(B)** Ethidium bromide stained 1% agarose gel showing the non-uniform PCR products from biologically cloned recombinants isolated from p7.

A

PV3 (1-3401/3411) - PV1 - A tail

```
PV3: GAATAAAGCTGTGTACACTGCTGGTTACAAGATCT
PV1: A--C-----G----------A--------A--T-
REC: --------------------A--------A--T-
```

PV3 (1-3367/3379) - PV1 - A tail

```
PV3: TGAGAAAGGTTTGACCACATATGGCTTTGGGCATC
PV1: CACC--G-A-C----------A--C--A--C-
REC: --------------------A--C--A--C-
```

B

PV3 (1-3381/82) Luc (35/36) - PV1 - A tail

```
PV3: GTTTGACCACATATGGCTTTGGGCATCAGAATAAA
LUC: AAA-C-GAGAGATCCT-A-AAA-GCCA----GGGC
REC: ----------------AAA-GCCA----GGGC
```

Figure 3.13: Sites of the recombination junctions in the passaged JC105B

(A) Precise recombinants. PV3 = Leon strain, PV1 = Mahoney strain (GenBank accession numbers X00925 and V01149 respectively), REC = recombinant sequence. Red boxes show nt similarity at cross-over junctions. Dashes indicate nt similarity with PV3, any differences in sequence are indicated **(B)** Imprecise intermediate recombinant. LUC = Luciferase sequence carried by the PV1 replicon, the remaining nomenclature is the same as (A).

3.9 Contribution of non-replicative recombination

The development of the CRE-REP assay was based upon the assumption that recombination occurs via the 'copy-choice' mechanism. The identification of additional sequences at the recombination junctions is something that has been seen in other *in vitro* cell based assays involving other positive sense strand RNA viruses like Bovine viral diarrhea virus (BVDV), Hepatitis C and Brome mosaic virus (Scheel et al., 2013, Nagy and Bujarski, 1997, Gallei et al., 2004). The BVDV study utilised partners that were unable to replicate, indicating that the recombination process was likely via another mechanism. Additionally, as outlined in section 1.3, poliovirus recombinants have also been isolated via a non-replicative approach (Gmyl et al., 1999, Gmyl et al., 2003). Previous interpretations of the results obtained in the CRE-REP assay suggested that the recombination event is replicative. It was shown that production of recombinant progeny could be inhibited by the use of a potent inhibitor (guanidine hydrochloride) of negative RNA strand synthesis (Lowry PhD thesis). However, if recombination in the CRE-REP assay were from a non-replicative mechanism then the use of an inhibitor of replication would produce the same result. All replication of the recombinant genome would be inhibited whether it via a replicative process or non-replicative. In principle, the recombination we observed could have been entirely replication independent. If the process of recombination in the CRE-REP assay were primarily replicative we would expect far more recombinant progeny than via a non-replicative assay, which is presumably far more inefficient.

In order to investigate the contribution of non-replicative recombination in our overall assay constructs were developed that completely ablated their ability to replicate within the host cell. Firstly, the region encoding the RdRp (3D) was removed from the pT7FLC/SL3 template producing a construct known as pSL3Δ. Secondly, a region from the 5' end extending into the luciferase reporter gene was removed from both replicons pRLucWT and pT7rep3-L (section 2.2.13 for full description) producing ΔpRLucWT and ΔpT7Rep3-L respectively (figure 3.14). This would ensure that the translated product of the SL3Δ RNA template would be unable to replicate due to the lack of RdRp activity. Additionally, the sub-genomic replicons would not be translated due to the removal of the 5' NTR. These constructs mimicked the ones used by Gmyl

and colleagues when investigating non-replicative recombination in polioviruses. For any viable recombinant to be produced a non-replicative process, involving unknown step(s), would be required to modify the genomes and produce a recombinant virus capable of replication. Importantly, the region within which recombination must occur between the end on VP1 upon SL3Δ and the intact 2C CRE on the sub-genomic replicon remained the same. This ensured that comparison of recombinant yield to the replicative CRE-REP assay could be carried out.

A comparison of recombinant virus yield from replicative and non-replicative intertypic and intratypic partners was carried out. The SL3Δ cDNA was linearised with *NruI* and the ΔpRLucWT and ΔpT7Rep3-L constructs were linearised with *ApaI* and *SalI* respectively. All were used as templates to transcribe RNA using T7 polymerase. As a positive control, a CRE-REP assay was carried out alongside the non-replicative assay (hereafter termed NON-REP). This ensured that a representative comparison of both processes of recombination was done. L929 cells were seeded in a 12-well plate and were co-transfected with 0.5 μg total RNA in a 1:1 ratio (replicon: CRE mutant) in triplicate. The NON-REP assay used a similar approach, using an equimolar ratio of RNA to the CRE-REP assay in all co-transfections (190 ng ΔRLucWT or ΔRep3-L / 205 ng SL3Δ). Individual control transfections were also done. Incubations were extended post transfection to 60 hrs. It was reasoned that any non-replicative process might take longer than its replicative counterpart, so an extension in incubation would provide the best opportunity for recombination to occur. Transfection supernatant was harvested after the incubation period and used to inoculate HeLa cell monolayers. Following 60 hrs of incubation, cells were stained with crystal violet and photographed. Comparison of intertypic progeny virus yield by plaque assay indicated that recombination via a non-replicative pathway is far more inefficient than the replicative pathway (figure 3.15). Recombinant virus was produced using the PV3/1 partners in the NON-REP assay, but the yield was only 3.8% of the yield produced in the CRE-REP assay. Similarly, intratypic non-replicative partners also produced recombinant progeny (figure 3.16). The yield represented ~ 1% of the yield from the replicative intratypic partners. The use of L929 cells, that lack the poliovirus receptor, ensured that the amount of recombinant virus that was isolated from both assays was representative of the recombination

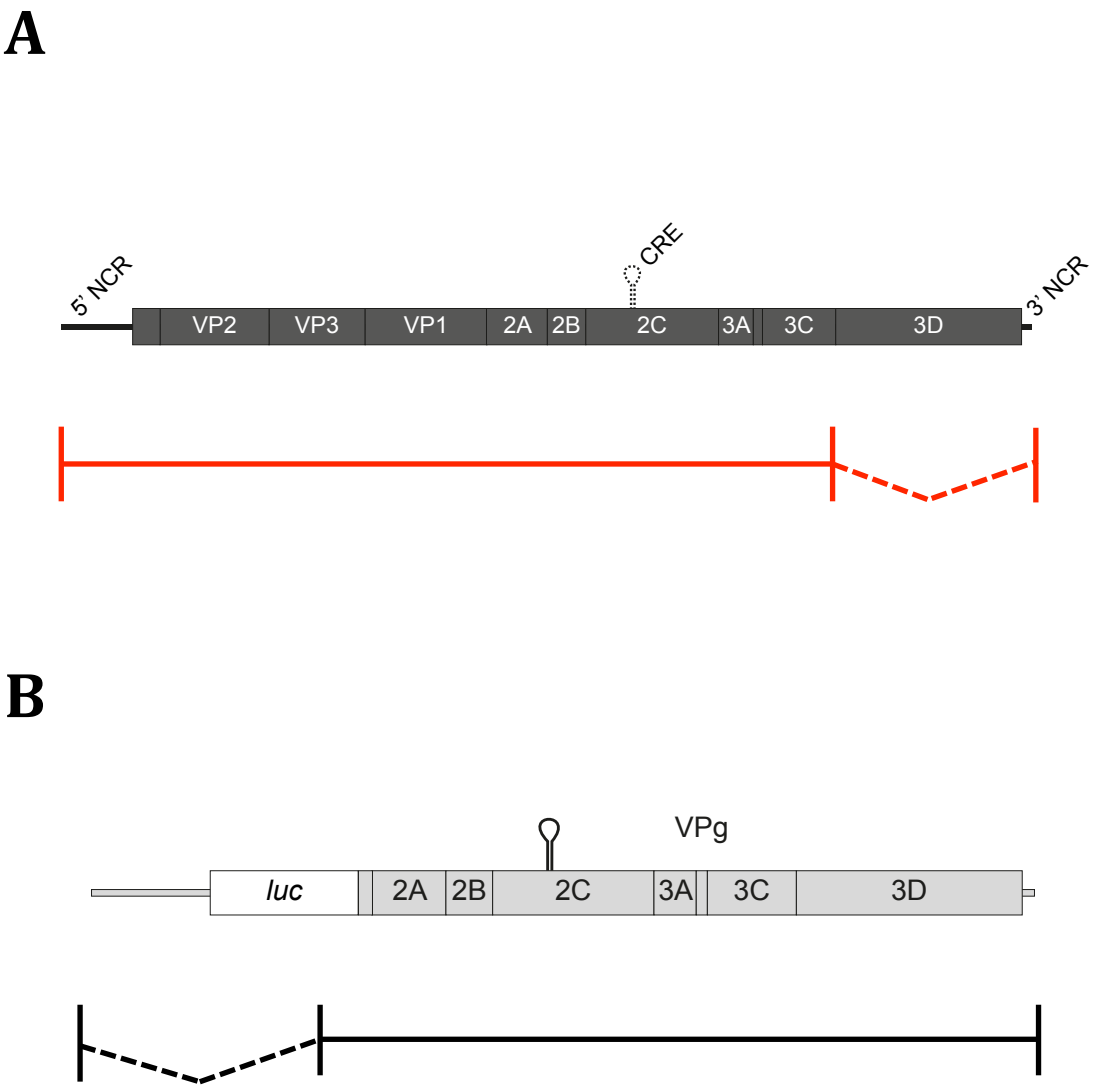

Figure 3.14: Non-replicative recombination partners

(A) SL3 construct with the 3Dpol region removed (SL3Δ), as indicated by the dashed red lines, for description see section 2.2.13 **(B)** PV1 and PV3 sub-genomic replicons with the majority of the IRES and luciferase coding gene removed (ΔpRLucWT & ΔpT7rep3-L respectively), as indicated by dashed black line.

A

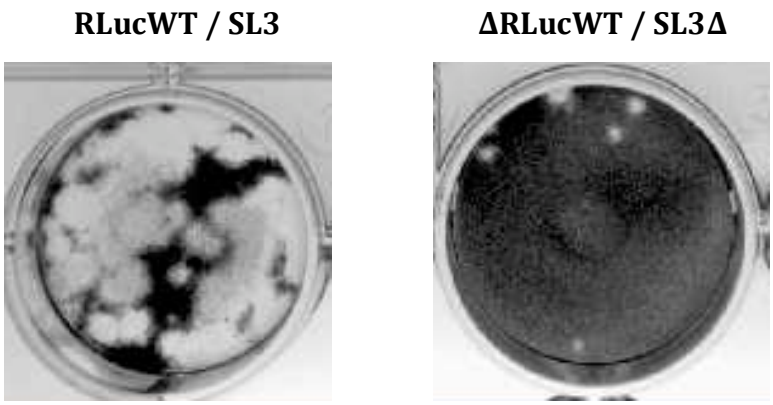

B

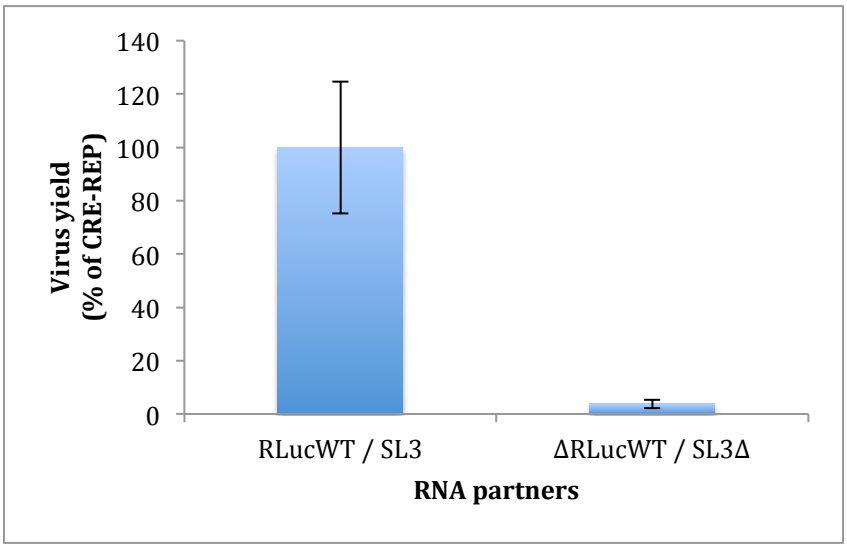

Figure 3.15: Intertypic non-replicative recombination frequency

(A) Representative crystal violet stained HeLa cells inoculated with undiluted transfection supernatant and overlayed with plaque assay overlay medium. RNA partners as indicated. Control wells containing only one RNA partner were free of plaques (data not shown) **(B)** The figures represent the mean from three independent samples comparing CRE-REP and NON-REP assays. Error bars indicate standard deviation.

A

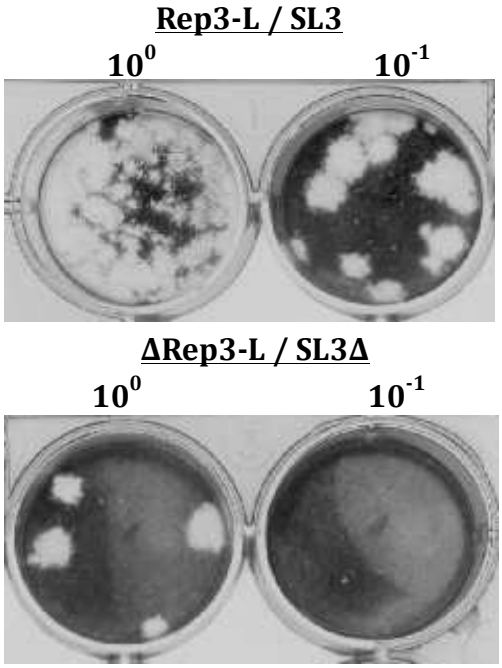

B

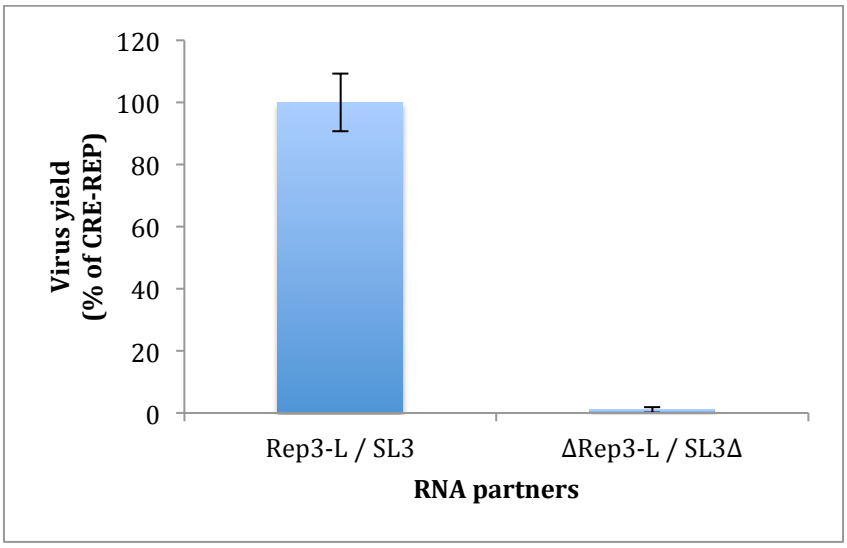

Figure 3.16: Intratypic non-replicative recombination frequency

(A) Representative crystal violet stained HeLa cells inoculated with diluted transfection supernatant (as indicated) and overlayed with plaque assay overlay medium. RNA partners as indicated. Control wells containing only one RNA partner were free of plaques (data not shown) **(B)** The figures represent the mean from three independent samples comparing replicative to non-replicative recombination. Error bars indicate standard deviation.

process in both systems. These results strongly suggest that recombination in the CRE-REP assay, regardless of parental genome, is primarily replicative.

3.10 Discussion

Recombination is a well-defined phenomenon in enteroviruses, as well as other important positive-strand RNA virus pathogens. However, the underlying mechanism(s) by which recombinants arise is relatively poorly understood. Studies on replicative recombination have suggested that the copy-choice template-switching model is additionally influenced by sequence homology between parental genomes, or by the RNA secondary structure of donor or recipient templates (section 1.3).

The analysis of historical isolates has generally implied that the selected recombinant genome contains a junction that reflects the point at which the polymerase switched from donor to recipient template. The development of a novel *in vitro* assay that generates recombinant enteroviruses in the absence of parental virus background allows the isolation of recombinants soon after they have arisen. This minimises additional selection and competition that may occur following serial passage. The experimental evidence gained has provided some interesting results to debate.

A previous study using this approach (Lowry et al., 2014) has shown that the primary progeny from intertypic recombination are largely 'imprecise' in nature, with clustering of junctions primarily found within two main gene boundaries: VP1/2A and 2A/2B. The consequences of this clustering are that the majority of imprecise recombinants retained the ability to encode non-chimeric versions of the 2A and 2B proteins. This clustering maybe a consequence of the overriding requirement for functional 2A and 2B proteins in the initial recombinant and this may not occur in a single step. Indeed, functionality at this early stage seems paramount, as an in-depth analysis of over 100 intertypic recombinant isolates could find no obvious or clear link between RNA sequence and only a limited link between RNA secondary structure and the site of

recombination (Lowry et al., 2014).

The characterisation of an imprecise intertypic recombinant virus from a co-transfection of HeLa cells indicated that the promiscuous nature of recombination was not as a result of a rodent cell specific factor. Only a minimal amount of progeny were sequenced and they could all have arisen from the same recombination event, but the principle of imprecise recombination was shown. The recombinant sequence itself, shown in figure 3.6, suggested a switch from the PV1 replicon template to the acceptor template at an 'A' triplet motif. Intertypic poliovirus recombination junctions have been linked to similar sequences in a previous study (King, 1988b).

It has been suggested that the reason why fewer intertypic and interspecies recombinants are observed in nature is due to the sequence divergence between RNA partners (Kirkegaard and Baltimore, 1986b). Using standardised conditions, the CRE-REP assay showed that intratypic recombination frequency is significantly higher than intertypic recombination (Chi square test). Indeed, approximately 10-fold more frequent, which is a figure slightly less than the 100-fold difference previously postulated (Kirkegaard and Baltimore, 1986b, King, 1988b, Tolskaya et al., 1983). Although, the amount of recombinant progeny isolated may be inherently linked to its type. Perhaps, intratypic recombinants replicate better than intertypic recombinants following the initial recombination event due to correct protein-to-protein interactions. This would affect the overall yield of virus and not necessarily represent the actual number of recombination events. The qualitative data suggested that the type of recombinant, precise or imprecise, could be directly linked to the sequence identity of the parental genomes. In section 3.3, isolation and characterisation of intratypic recombinant virus indicated that only a minor amount were imprecise with additional sequence at the recombination junction (3/20). This contrasts to the generally imprecise intertypic recombinants isolated to date. These findings suggest that sequence identity may indeed influence location of recombination. Although, section 3.6 described the secondary stage of recombination in enteroviruses, a stage we term 'resolution'.

All three imprecise intertypic recombinants lost all the additional sequence following serial passage in HeLa cells and returned to wild type length. Sequence analysis of the 'resolved' isolates indicated new recombination junctions, where the precise location of recombination could not be identified due to sequence identity of the parental genomes. This finding was further supported by the construction of a molecular clone that represented one of the passaged imprecise recombinants. Similarly, this construct went through the resolution process and produced a genome indistinguishable from wild type in length. Sequence analysis also highlighted sequence identity at the new recombination junctions and provided a junction that was exactly the same as the biological clone that carried the same imprecise sequence. This strongly suggests that the characterisation of intertypic field isolates that has proposed sequence identity at the recombination junction (King, 1988b) have missed the early events of recombination and only characterised the end product. The sequence identity found within the resolved recombination junctions may indicate that sequence does play a role, but perhaps not during the initial stage which seems a more promiscuous process that may be subjected to other primary limitations e.g. packaging restraints and protein-protein functionality. It also remains to be determined if the resolution stage of recombination is a *cis* or *trans* event that involves the viral RdRp. In principle, it could be either or even both. The fewer imprecise intratypic recombinants isolated may actually be a reflection of their ability to resolve at a faster rate than an imprecise intertypic recombinant. Potentially, the characterised intratypic recombinants in section 3.3 had already gone through the secondary resolution stage where any additional sequence is lost. Indeed, a single poliovirus genome is replicated an average of six times in a single cell (Schulte et al., 2015). Perhaps sequence identity is a key factor during subsequent rounds of replication within the same cell following the initial promiscuous recombination event? To answer this an imprecise intratypic recombinant, similar to JC105B could be produced. Serial passaging of such a recombinant, when compared to an intertypic version (JC105B) might highlight any differences in the resolution process.

The ability to extend the CRE-REP assay into a species B enterovirus group indicates that the approach may be universal to these genera of viruses. The inability to isolate intertypic

recombinant (E7/E6) was disappointing. They share similar divergent genomes as that of PV3/PV1 at ~ 20%, indicating their suitability to the assay. As stated, this study has shown that intratypic recombination frequency is 10 fold higher than intertypic, a finding broadly in line with previous studies (Kirkegaard and Baltimore, 1986b). The inability to recover E7/E6 recombinant virus is therefore not surprising given the relatively low frequency of E7/7 recombinants isolated from BsrT7 cells. Potentially the permissive cells that were being used were sub-optimal for this species of virus. Unfortunately, due to time restrictions an extended study of this group was not carried out and it was determined that all future experiments would concentrate upon the enterovirus C poliovirus.

The CRE-REP assay, in principle, could have produced the initial recombinant virus by either a non-replicative or replicative pathway. The development of the NON-REP assay that was based on previous non-replicative approaches (Gmyl et al., 1999, Gmyl et al., 2003) allowed quantification of viable recombinants within the same 1058 nt region between the 2C CRE and P1 coding region. This allowed the relative contribution of non-replicative recombination to the CRE-REP assay to be calculated. The very low yield of recombinant progeny in the NON-REP assay when compared to the postulated replicative approach strongly suggested that recombination in the CRE-REP assay was primarily replicative.

The suggestion that an imprecise replicative recombination process results in partial duplication of the virus genome also has implications for the wider understanding in the evolution of positive strand RNA viruses. There are several well-characterised evolutionary duplication events that have shaped the picornavirus genome. For example, the capsid proteins (VP1-3) share a common 'jelly roll' structure (Hogle et al., 1985) that have arisen from duplication. Another example is the tandem repeat regions that encode the three contiguous VPg proteins of foot and mouth disease virus (Forss and Schaller, 1982) and even the non-contiguous 2A and 3C proteases (Palmenberg at al., 2010). In addition, other positive strand RNA viruses exhibit genome duplications (Simon-Loriere and Holmes, 2013) such as the

multiple VPg proteins of some dicistroviruses, which can encode as many as six from one genome. It was postulated that the redundancy in VPg coding provided an advantage in overall replication rates (Nakashima and Shibuya, 2006). Additionally, the functionally distinct adjacent leader proteinases of the *Closteroviridae,* that have arisen from duplication events, provide common protease activities but also possess specialised functions in virus RNA replication, virus invasion and cell-to-cell movement (Peng et al., 2001). The type of imprecise recombination event described in section 3.3, potentially coupled with partial resolution, could account for this 'evolution by duplication'. Likewise, duplication and subsequent resolution events could explain the unique C-A-B motif arrangement in the palm domain of the polymerase reported in some Alphavirus-like insect tetraviruses (Gorbalenya et al., 2002). Other than the ancestral evolution of the capsid proteins the majority of these involve duplication of relatively short sequences, and this is presumed to reflect intrinsic constraints on genome length that may prevent their fixation (Simon-Loriere and Holmes, 2013).

In summary, recombination in enteroviruses is a biphasic process that provides an insight into the potential mechanisms of genome evolution. The observations in section 3.9 strongly suggested that the process of recombination in the CRE-REP assay was primarily replicative. The characteristics of the viral RdRp (a key factor in the copy-choice model of recombination) that determine recombination frequency were therefore considered an area of interest.

CHAPTER FOUR: Fidelity of the RNA Dependent RNA Polymerase (RdRp) Influences Replicative Recombination Frequency

4.1 Introduction

The results presented in chapter three highlighted the biphasic nature of recombination in enteroviruses. The use of an *in vitro* assay known as CRE-REP has shown that intertypic recombination is initially a promiscuous event where additional sequence can be incorporated at the recombination junction (Lowry et al., 2014). The overriding criteria for viable virus at this early stage are the ability to produce a genome that is functional. Clustering of recombination junctions to cleavage boundaries ensures progeny inherit complete protein coding regions from one or the other parent. This suggests that protein-protein interactions during the course of replication are vital, and play a role in the yield and type of recombinant isolated.

The development of a non-replicative assay (NON-REP) that had the same potential region of recombination showed that recombinants isolated from the CRE-REP assay was primarily due to a replicative mechanism. The next step in this investigation was to look at the role of the viral RNA dependent RNA polymerase (RdRp) in recombination. If the output of the CRE-REP assay were due to replicative recombination then it would be reasonable to postulate that characteristics of the RdRp are important. Positive sense strand RNA viruses have low fidelity RdRps (section 1.3). A nucleotide misincorporation event has been proposed as a trigger for template switching, and this can be directly linked to the inherent low fidelity of the RdRp (Agol, 1997). Known mutagens and well-characterised RdRp mutations have been shown to decrease and increase RdRp fidelity respectively (Crotty et al., 2000, Crotty et al., 2001, Crotty and Andino, 2002, Pfeiffer and Kirkegaard, 2003, Arnold et al., 2005, Weeks et al., 2012, Korboukh et al., 2014). By incorporating known mutagens and a high fidelity RdRp variant into both NON-REP and CRE-REP assays a correlation between fidelity and recombination may be identified.

Aims

The aim was to analyse the influence of known mutagens that decrease wild type RdRp fidelity and then contrast this to a known RdRp variant that has a higher fidelity phenotype. The role of fidelity in recombination frequency was investigated by performing NON-REP and CRE-REP assays with mutagen and then with a high fidelity RdRp variant. By using both experimental systems it was believed a clear distinction could be identified. Additional aims were to incorporate a drug known as nocodazole, a known inhibitor of replication complex coalescence (Egger and Bienz, 2005). It was reasoned that for replicative recombination to occur a key prerequisite would be co-localisation of parental RNA within the same replication complex. The influence of RNA co-localisation on both NON-REP and CRE-REP approaches was therefore examined. The results in this chapter have also contributed to the manuscript by Lowry et al., 2014.

4.2 Influence of RdRp fidelity on non-replicative recombination

Positive strand RNA virus populations are a collection of similar but genetically different viruses. They exist as a quasi species due to the high mutation rates of the low fidelity replicase (Vignuzzi et al., 2005). This is an advantageous adaptation that allows for rapid evolution in changing environments. However, any increase in mutation rate could push the viral population into 'error catastrophe', a phenomenon where the accumulation of errors becomes lethal, leading to viral extinction (Crotty and Andino, 2002). The use of mutagens that increase the error rate would, in principle, tip the virus population into 'error catastrophe'.

One such mutagen is ribavirin, a nucleoside analogue that can be incorporated by viral polymerases, causing mutations by allowing base mismatches (Pfeiffer and Kirkegaard, 2003, Crotty et al., 2000, Crotty et al., 2001, Crotty and Andino, 2002). An *in vitro* system capable of measuring the kinetics and biochemical properties of the RdRp has showed that ribavirin triphosphate (RTP) is directly incorporated into the poliovirus genome (Crotty et al., 2000). Ribavirin is templated by cytidine or uridine and incorporated in the place of GMP or AMP, leading to transition mutations (Cameron and Castro, 2001). Indeed, the rate of incorporation and binding affinity of the RdRp for RTP is similar to the incorporation kinetics of incorrect nucleotides (Cameron and Castro, 2001). It was reasoned that the incorporation (or attempted incorporation) of RTP by the viral RdRp would lead to an un-favourable thermodynamic event. This would mimic incorrect nucleotide incorporation that may lead to an increase in recombination.

In principle, the progeny produced from the NON-REP assay (section 3.9) is mediated by a currently unknown mechanism that is independent of the viral RdRp. It was therefore important to see if recombination frequency in this approach was influenced by a mutagen that is known to directly interact with the viral RdRp. A NON-REP assay was carried out using intratypic partners SL3Δ and ΔRep3-L, using similar experimental conditions described in section 3.9. One difference was the incorporation of 100 μM of ribavirin. This level of the

mutagen was determined to be the correct amount due to historical studies showing that this level is sub-lethal, but can lead to a decrease in RdRp fidelity (Vignuzzi et al., 2005). L929 murine cells were incubated with ribavirin two hours pre-transfection and the mutagen was added to the media post transfection. Transfection supernatant was harvested at 60 hrs and used undiluted to inoculate HeLa cell monolayers for plaque assays (figure 4.1). Quantification of recombinant progeny showed that the presence of ribavirin had no significant effect on the overall yield of intratypic recombinant virus in the NON-REP assay.

The passage of polio in the presence of 100 μM ribavirin selects for a glycine to serine change at position 64 of the 3D RdRp coding region (G64S) (Vignuzzi et al., 2005, Pfeiffer and Kirkegaard, 2003). This region of the RdRp lies within a small region spanning the fingers and thumb domain, an area outside the known functional domains of the viral RdRp (Arnold et al., 2005). The replacement of glycine for the bulkier serine affects a key conformational change step that precedes phosphoryl transfer during nucleotide incorporation, increasing fidelity four-fold (Arnold et al., 2005). To contrast the ribavirin experiment, this well-characterised mutation was introduced into the RdRp (3D) coding region of the ΔpT7rep3-L template (the only RdRp coding region present in the NON-REP assay due to the removal of 3D in SL3Δ). An experiment, which replaced the ΔRep3-L with the ΔRep3-L-G64S, was carried out which had similar experimental conditions to the NON-REP assay outlined in section 3.9. Quantification of recombinant progeny indicated no significant difference between the two conditions (figure 4.2). Conclusions from this area of the investigation are that polymerase fidelity does not influence the yield of recombinant progeny produced from the NON-REP recombination assay.

A

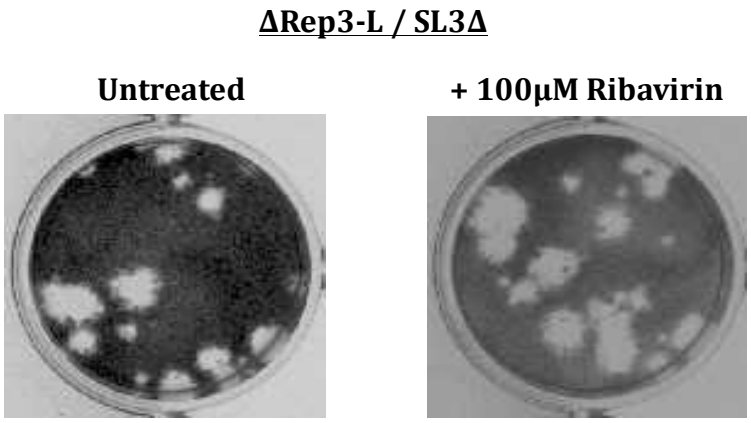

B

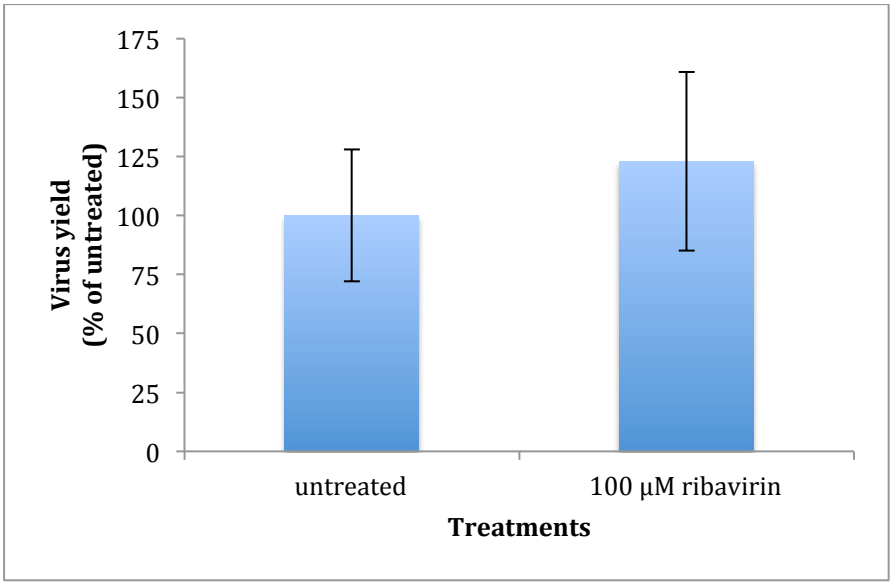

Figure 4.1: Intratypic NON-REP assay +/- 100 μM ribavirin

(A) Representative crystal violet stained HeLa cell monolayers inoculated with undiluted transfection supernatant and overlayed with plaque assay overlay medium. RNA partners ΔRep3-L and SL3Δ. Ribavirin conditions as indicated. Control wells containing only one RNA partner were free of plaques (not shown) **(B)** The figures represent the mean from three independent samples comparing non-replicative recombination +/- ribavirin . Error bars indicate standard deviation

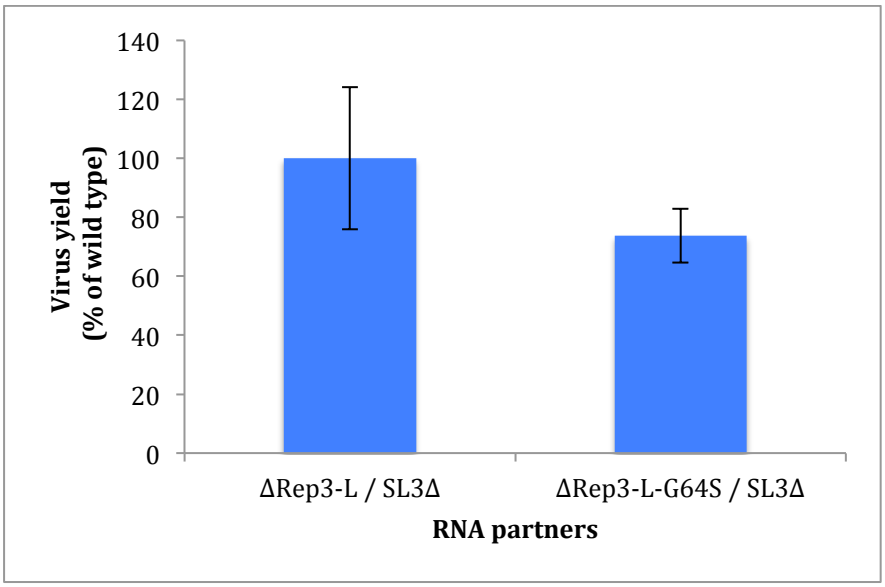

Figure 4.2: Influence of the high fidelity polymerase (G64S) upon intratypic non-replicative recombination frequency

The figures represent the mean from three independent samples. Error bars indicate standard deviation. The high fidelity G64S mutation is present in one RNA template only (ΔRep3-L-G64S). RNA partners as indicated.

4.3 Influence of RdRp fidelity on the CRE-REP assay

The influence of RdRp fidelity was investigated in the CRE-REP assay. The high fidelity mutation (G64S) was introduced into the RdRp coding region (3D) of the replicons, pRLucWT and pT7rep3-L and the potential acceptor template pT7FLC/SL3, by overlap extension PCR (section 2.2.12). It was important to know how the mutation affected the overall replication kinetics of the virus. If there was a difference in replication then this may have had an effect on overall recombinant progeny yield that would have nothing to do with fidelity.

It has been reported that this mutation has no impact upon replication when compared to wild-type (Vignuzzi et al., 2006). A similar approach used by Vignuzzi and colleagues was employed. Briefly, 250 ng of the PV1 replicon (RLucWT) or the mutant RLuc-G64S were transfected into L929 cells in duplicate with samples taken at various time-points and measured for luciferase activity (section 2.1.3) (figure 4.3A). In general, the replication kinetics, as measured by luciferase activity, was similar between the two replicons in agreement with previous findings (Vignuzzi et al., 2006). As replication kinetics between the two was similar it was decided to proceed with an intertypic CRE-REP assay that incorporated the high fidelity polymerase variant. L929 cells in a 12-well plate were co-transfected in triplicate with RLucWT and SL3 or RLuc-G64S and SL3-G64S. Total RNA was 0.5 μg in a 1:1 ratio (replicon: CRE mutant genome). Cells were incubated for 48 hrs post transfection and media supernatant was then harvested and used to inoculate HeLa cell monolayers for plaque assays. Following sixty hours incubation, cells were stained with crystal violet and plaques quantified (figure 4.3BC). Results indicated that the introduction of the high fidelity G64S mutation into the donor and acceptor templates had significantly reduced intertypic recombination frequency to 5% of partners bearing a wild type RdRp (as analysed by student T-test). A small quantity of the G64S recombinant progeny was biologically cloned and the presence of the G64S mutation confirmed by sequencing (data not shown).

A

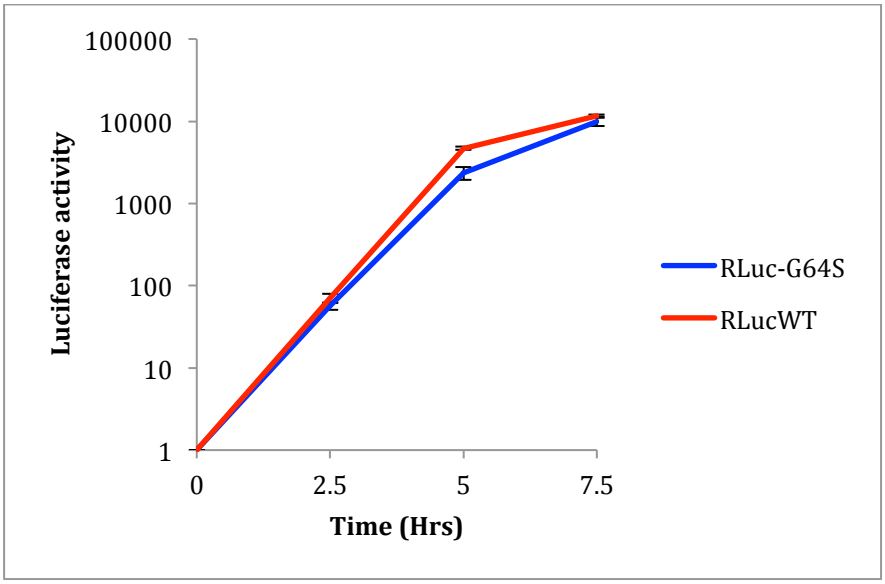
100000
10000
1000
100
10
1
Luciferase activity
0
2.5
5
7.5
Time (Hrs)
RLuc-G64S
RLucWT

B

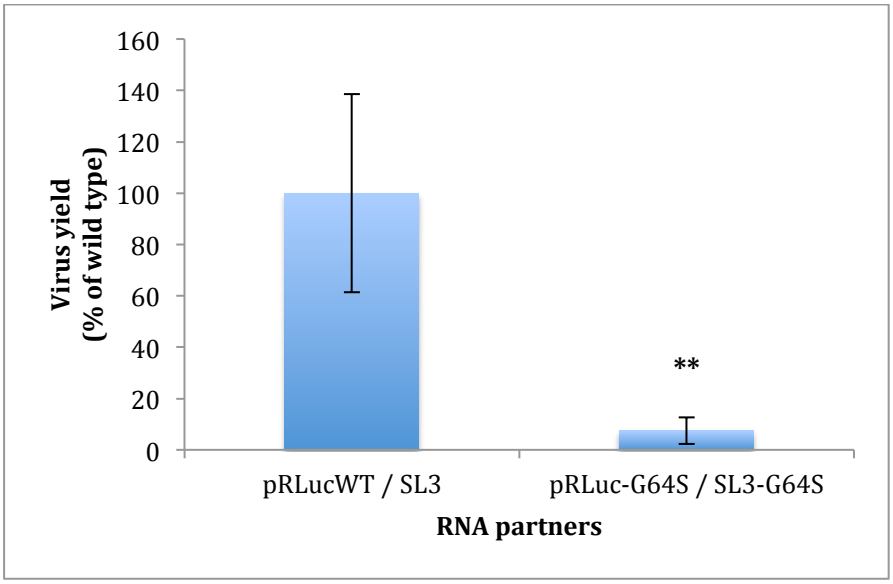
160
140
120
100
80
60
40
20
0
Virus yield
(% of wild type)
**
pRLucWT / SL3
pRLuc-G64S / SL3-G64S
RNA partners

C

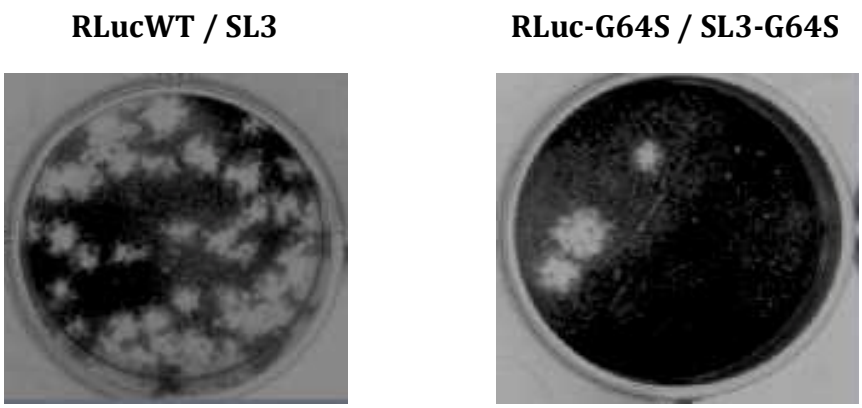

Figure 4.3: Influence of a high fidelity polymerase (G64S) upon replication and Intertypic recombination

(A) Replication kinetics of a PV1 sub-genomic replicon (RLucWT) bearing a G64S high fidelity polymerase mutation. 250 ng of RNA generated *in vitro* was transfected into L929 cells. Samples were taken at the times indicated and luciferase activity was measured in light units and normalised using a mock transfected control. Error bars indicate standard deviation of two independent samples **(B)** Influence of a high fidelity polymerase upon the frequency of intertypic recombination. RNA partners as indicated. The data represents the mean from three independent samples. Error bars indicate standard deviation. Asterisk; $P < 0.01$ by Student's T-test test **(C)** Representative crystal violet stained HeLa cell monolayers inoculated with undiluted transfection supernatant and overlayed with plaque assay over lay medium. RNA partners as indicated. Control wells containing only one RNA partner were free of plaques (not shown)

To further verify these findings a similar experimental approach was used with the CRE-REP intratypic partners, Rep3-L and SL3. A luciferase assay showed that the G64S mutation had little effect upon the replication kinetics of the sub-genomic replicon when compared to wild type, a similar finding to the PV1 replicon. A subsequent CRE-REP assay showed that intratypic recombination frequency fell to 10% of wild type when the high fidelity G64S mutation was present (figure 4.4). The results from the two experiments indicated that intertypic and intratypic recombination is adversely affected by higher than normal RdRp fidelity.

It remained to be determined if an increase in fidelity affected the type of recombinant isolated. To answer this, a number of intertypic recombinants were isolated from the high fidelity intertypic CRE-REP assay supernatant that was used previously (figure 4.3). Biological cloning was done by a limiting dilution approach, and the 1.058 Kb zone of recombination amplified by RT-PCR using the primers PV1/3-3280F and GEN-4615R. Six unique PV3/1 junctions were characterised, five had additional sequences with one being precise with no additional sequences present when compared to wild type poliovirus. A similar clustering to gene boundaries, as seen previously, was observed. Four junctions were at, or spanned the VP1/2A boundary (cluster one isolates, figure 4.5AB). The remaining two junctions were at or spanned the 2A/2B boundary (cluster two isolates, figure 4.5CD). The location of template switching with the precise recombinant junction in cluster two could not be completely identified due to limited sequence identity between parental genomes. One interesting observation in 75% of the imprecise cluster one junctions is that template switching seems to have occurred at an 'A/U' dinucleotide upon the donor template, a similar finding to that seen in a previous study (King, 1988b). Although, the King et al., study looked at precise recombinants only. The remaining isolate in this group has left the donor template just before an A-rich motif. The imprecise cluster two isolate has a sequence that also suggests that template switching has occurred at a 'U' dinucleotide.

A

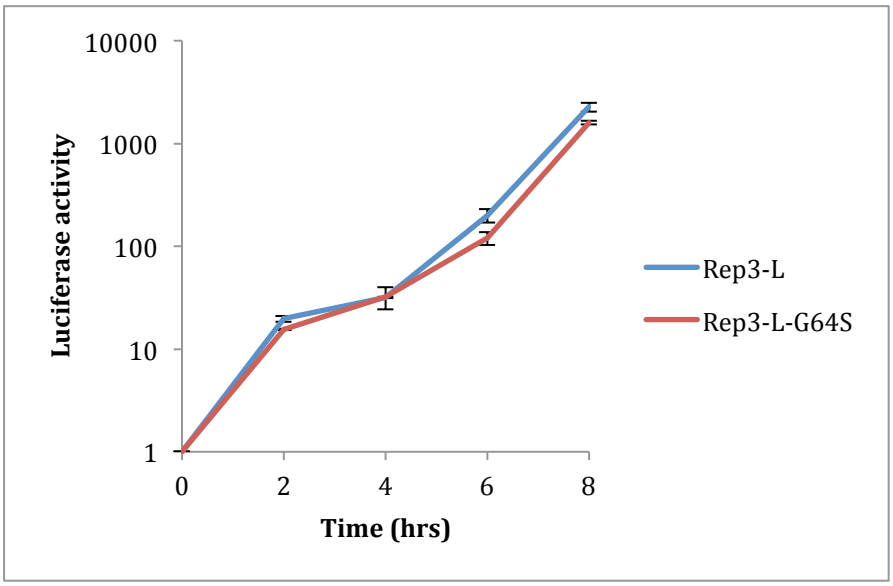
10000
1000
100
10
1
Luciferase activity
0
2
4
6
8
Time (hrs)
Rep3-L
Rep3-L-G64S

B

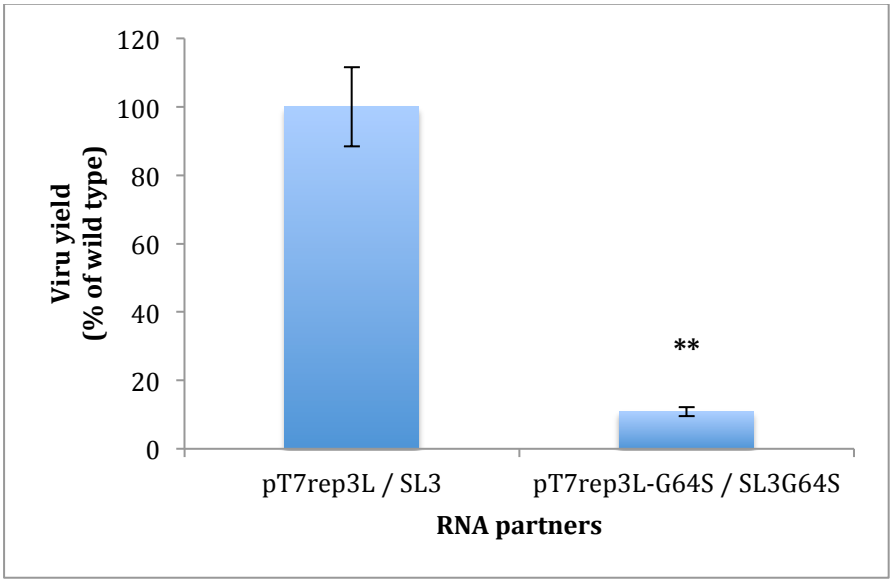
120
100
80
60
40
20
0
Viru yield
(% of wild type)
**
pT7rep3L / SL3
pT7rep3L-G64S / SL3G64S
RNA partners

C

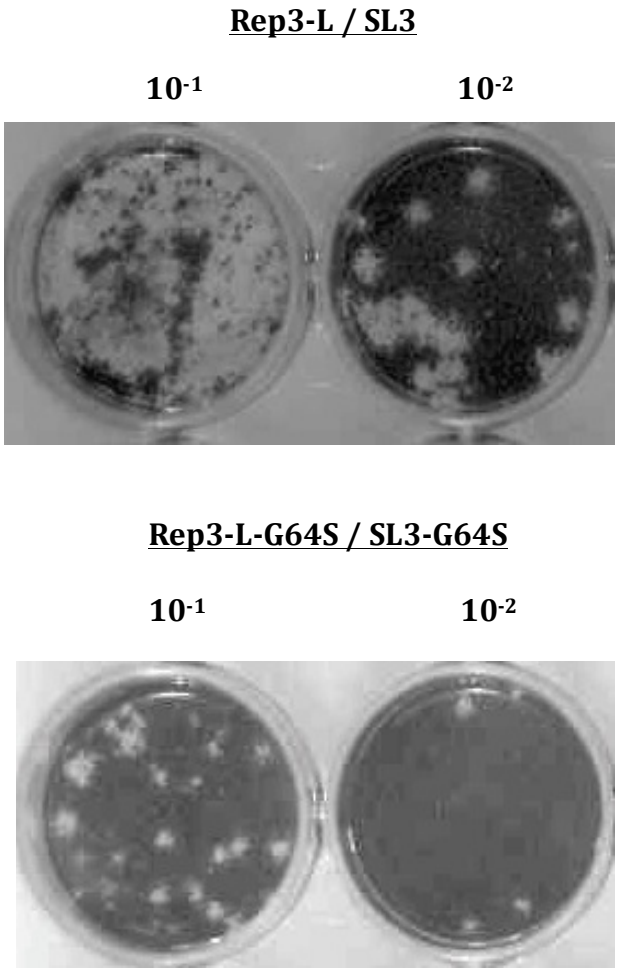

Figure 4.4: Influence of a high fidelity polymerase (G64S) upon replication and Intratypic recombination

(A) Replication kinetics of a PV3 replicon (Rep3-L) bearing a G64S high fidelity polymerase mutation. 250ng of RNA generated *in vitro* was transfected into L929 cells. Samples were taken at the times indicated and luciferase activity was measured in light units and normalised using a mock transfected control. Error bars indicate standard deviation of two independent samples **(B)** Influence of a high fidelity polymerase upon the frequency of Intratypic recombination. The data represents the mean from three independent samples. RNA partners as indicated. Error bars indicate standard deviation. Asterisk; $P < 0.01$ by Student's T-test test **(C)** Representative crystal violet stained HeLa cell monolayers inoculated with diluted transfection supernatant and overlayed in plaque assay overlay medium. Dilutions as indicated. RNA partners as indicated. Control wells containing only one RNA partner were free of plaques (data not shown)

A

PV3 (1-3407) Luc (78) PV1 - A Tail

```
PV3: ATAAAGCTGTGTACACTGCTGGTTACA
LUC: -AGT-C-GAAAGGTCT-A-C--AA-AC
REC: ---------------T-A-C--AA-AC
```

PV3 (1-3397) Luc (25) PV1 - A Tail

```
PV3: CATCAGAATAAAGCTGTGTACACTGCT
LUC: GCCA--GCC--GAAG-GCGGA-AGT-C
REC: ------------AAG-GCGGA-AGT-C
```

PV3 (1-3434) PV1 (3390 - A Tail)

```
PV3: AGATCTGCAACTACCATCTCGCCACTA
PV1: T--C-ACAT-TGGATTCGGACA-CAA-
REC: ---------------TCGGACA-CAA-
```

PV3 (1-3381) Luc (121) PV1 - A Tail

```
PV3: ACCACATATGGCTTTGGGCATCAGAAT
LUC: -A--ACCGCAAAAAGTT--GCGGAGGA
REC: --------------GTT--GCGGAGGA
```

B

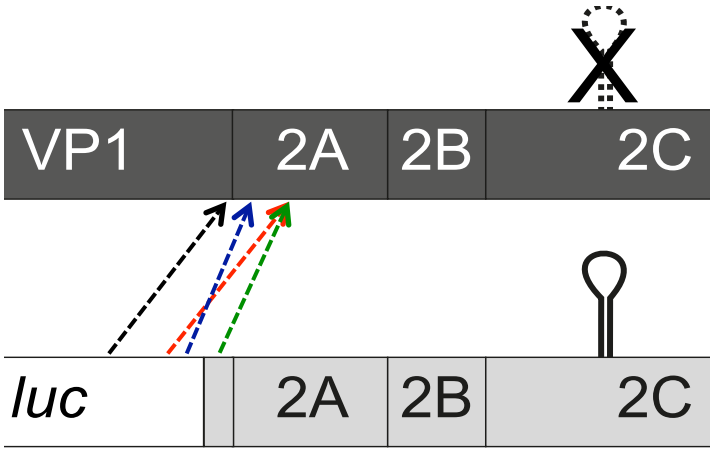

C

PV3 (1-3874/82) PV1 - A Tail

```
PV3: TGGGTTCACTCAGCAAATAGGGGATAA
PV1: ---A--T--------G--TA-C--C--
REC: ---------------G--TA-C--C--
```

PV3 (1-3829/30) PV1 (3773/74 - A Tail)

```
PV3: GGAGCAGGGATTTCAAACTATATTGAG
PV1: --T-GC-AAGGG-TGGTTGCAT--TCA
REC: ----------T-TGGTTGCAT--TCA
```

D

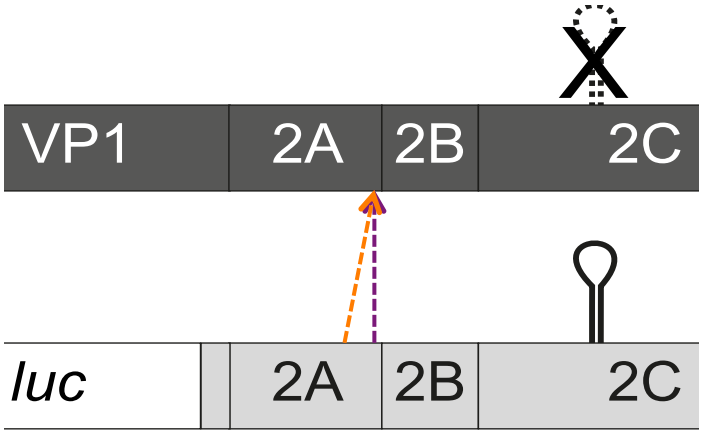

Figure 4.5: Biologically cloned PV3/1 recombinants obtained from co-transfection of RNA partners bearing the high fidelity G64S mutation

(A) Genome sequences of four biologically cloned intertypic recombinant viruses with junctions that fall within cluster one **(B)** Dashed arrows indicates points of crossover from donor (replicon) to acceptor template (CRE mutant) in the cluster one isolates. Colour codes match nomenclature in (A) **(C)** Genome sequences of two biologically cloned intertypic recombinant virus that fall within cluster two **(D)** Dashed arrows indicate points of crossover from donor (replicon) to acceptor template (CRE mutant) in the cluster two isolates. Colour codes match nomenclature in (C) PV3 = Leon strain, PV1 = Mahoney strain (GenBank accession numbers X00925 and V01149 respectively), LUC = Luciferase sequence carried by the PV1 replicon. REC = recombinant sequence. Red boxes indicate sequence identity in the region of template switching. Dashes indicate nt identity with PV3, any differences in sequence are indicated.

4.4 Influence of ribavirin on poliovirus yield

The increase in RdRp fidelity had a striking impact upon recombination frequency. It was therefore decided to contrast these observations by testing the influence of a known mutagen that decreases RdRp fidelity. The incorporation into nascent viral RNA and subsequent mutagenesis caused by the nucleoside analogue ribavirin has been outlined in section 4.2. In the context of this study, an initial experiment was set up to measure the overall reduction in virus yield following mutagen treatment. This was deemed important, as it would aid interpretations of any CRE-REP assay that included the mutagen. HeLa cells in a 6-well plate were treated with ribavirin two hours prior to infection and throughout subsequent incubation. Cells were infected with a full length PV3 at an M.O.I of 0.01 and incubated for 48 hrs. Media supernatant was then isolated and dilutions were used to inoculate HeLa cell monolayers for plaque assays. Cells were incubated for 60 hrs, stained with crystal violet and virus plaques counted with the titre converted to pfu/ml (figure 4.6). All titres were normalised as a percentage of an untreated control. The use of the mutagen led to a dramatic fall in viable virus. Ribavirin treatment levels of 100 μM and 400 μM led to a 75% and 2-$\log_{10}$ reduction in virus yield respectively, in line with previous studies (Pfeiffer and Kirkegaard, 2003, Vignuzzi et al., 2005). It was also considered important to see if ribavirin treatment had any effect on transfection efficiency of L929 cells. This was an important control that would aid interpretation of any CRE-REP assay that included the mutagen. In order to measure transfection efficiency the replicon pT7Rep3-L was linearised with the restriction enzyme *XhoI*. The unique site is located at position 6050 of the PV3 sequence, very near to the 3C/3D cleavage boundary (figure 4.7A). The cDNA was used as a template to transcribe RNA using a T7 polymerase. All RNA transcripts that were produced lacked the RdRp coding region, ensuring a translation only readout. L929 cells in a 12-well plate were treated with ribavirin 2 hours prior to transfection. Cells were transfected with 250 ng of the truncated replicon RNA, in triplicate, and luciferase activity was measured at 4 hours post transfection and normalised to a mock-transfected control (figure 4.7B). The luciferase signal measured was from translation only, as RNA replication was inhibited by the lack of RdRp coding sequence. Results showed that transfection efficiency is not affected by ribavirin treatment.

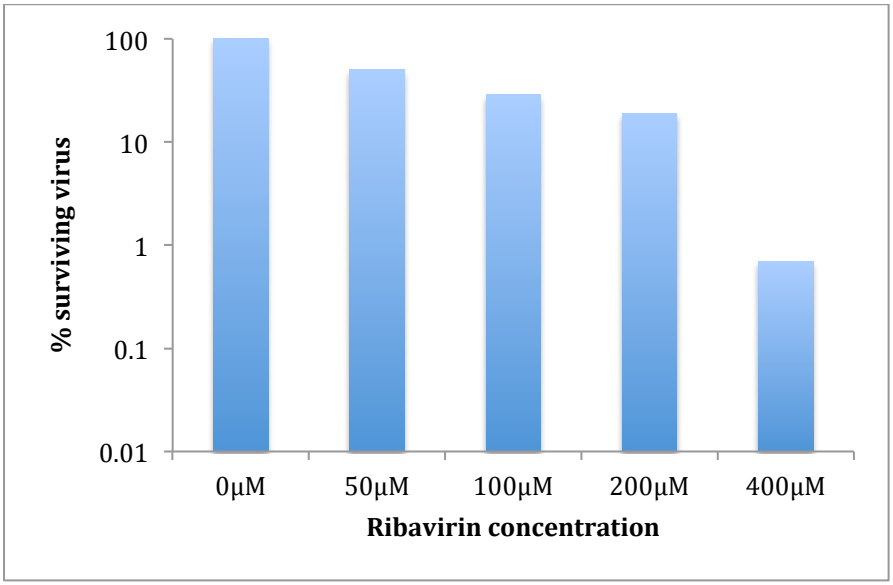

Figure 4.6: The affect of the mutagenic compound ribavirin on PV3 viability

HeLa cells were treated 2 hours prior and post infection with ribavirin (concentrations as indicated). Cells were then infected at an MOI of 0.01. Media supernatant was harvested following an incubation period of 48 hrs and a plaque assay was used to quantify viable virus. % of viable virus is shown in relation to an untreated sample.

A

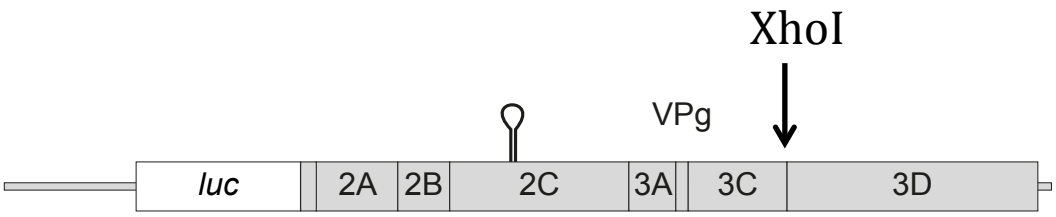

B

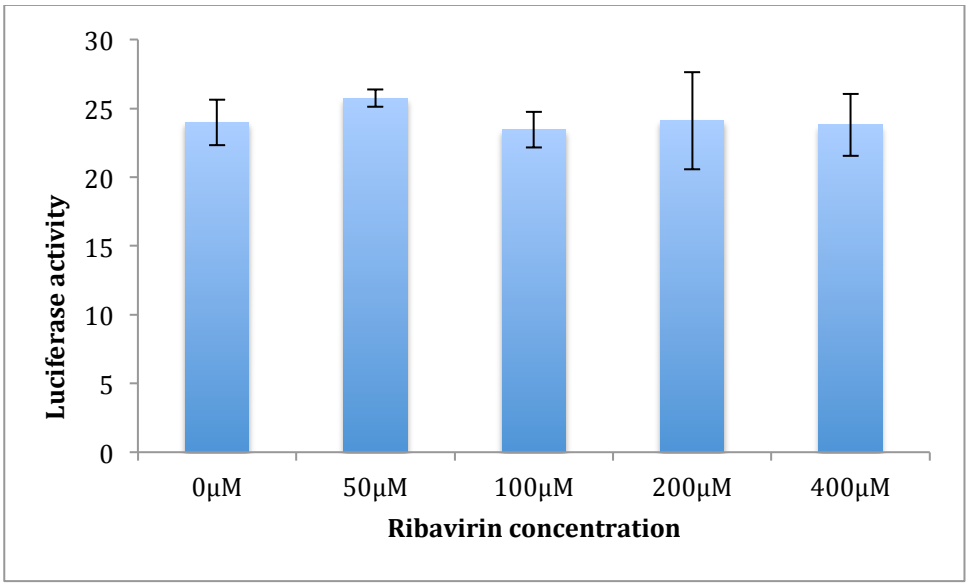

Figure 4.7: The effect of ribavirin on transfection efficiency in L929 cells

(A) The PV3 sub-genomic replicon pT7Rep3-L was linearised with XhoI (which cleaves the cDNA at nt. 6050 within the P3 coding region) and used as a template for T7 polymerase-mediated *in vitro* RNA synthesis **(B)** Ribavirin at the concentrations indicated was included in the supernatant media for two hours pre-transfection and during all subsequent analysis. 250 ng of RNA generated *in vitro* was transfected into L929 cell monolayers in a 12-well plate and luciferase activity was quantified 4 hours post-transfection after normalisation to mock transfected control. The figures plotted indicate the mean of three samples, with error bars indicating standard deviation.

4.5 The influence of ribavirin treatment on the CRE-REP assay

As ribavirin treatment seemed to be non-toxic and have little effect upon transfection efficiency it was decided to continue with a CRE-REP assay that incorporated the mutagen. L929 cells in 12-well plates were treated with various concentrations of ribavirin (as indicated) 2 hrs prior to transfection and then maintained post-transfection. Five hundred nanograms of RNA in a 1:1 ratio (RLucWT / SL3) was transfected in triplicate wells. Cells were then incubated for 48 hrs. Transfection supernatant was harvested and used to inoculate HeLa cell monolayers for plaque assays and incubated for sixty hours. Cells were then stained with crystal violet and photographed (figure 4.8). Following quantification of recombinant progeny it was obvious to note that treatment of L929 cells with 100 μM or 200 μM of ribavirin led to a significant increase in intertypic recombinant yield (as measured by Students T-test). At these same levels PV3 virus replication is inhibited by 75 % and 81 % respectively (see figure 4.6). No recombinant was isolated from ribavirin treatment at 400 μM. This is not surprising given that this level of mutagen reduced PV3 virus-yield by over 2-$\log_{10}$. In a similar approach, intratypic recombination in the presence of varying ribavirin level was also investigated. A similar phenomenon was observed (figure 4.9). Treatment of L929 cells with ribavirin led to a significant increase in recombination frequency (measured by Students T-test). However, the significant increase was limited to 50 μM levels of the mutagen, less than that observed in the intertypic experiment.

A

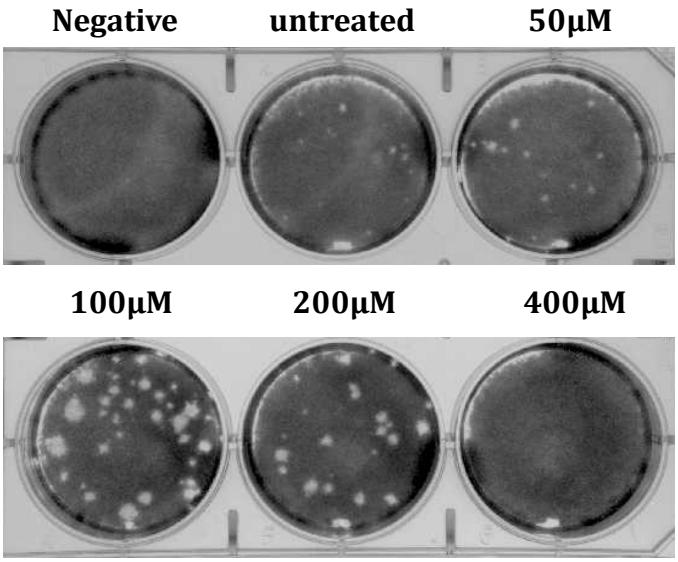

B

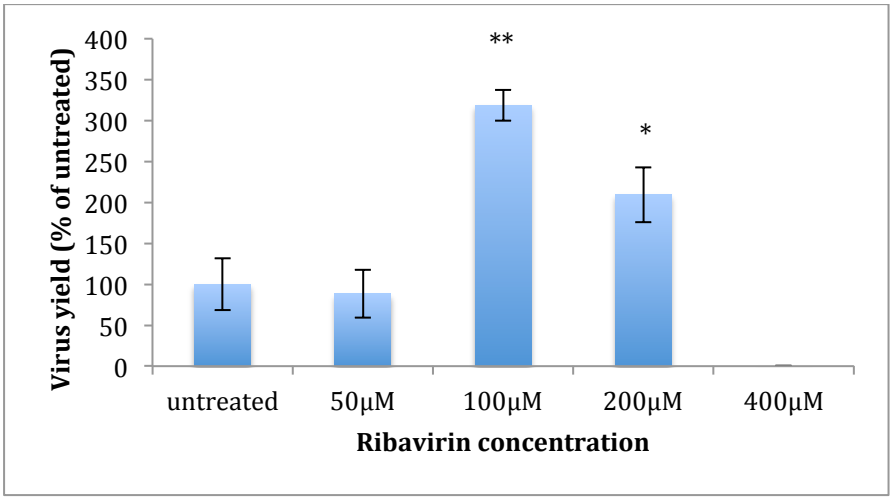

Figure 4.8: PV3/1 recombination frequency in the presence of ribavirin.

Intertypic recombinants recovered from co-transfections of RLucWT and SL3 in L929 cells seeded in the presence of varying ribavirin concentrations. **(A)** Co-transfection supernatant was used to inoculate fresh RD cell monolayers and overlaid with plaque overlay medium. Cells were stained 60 hours post-infection with crystal violet. Viable virus is evident by the presence of plaques. Concentrations of ribavirin as indicated **(B)** Figures show the effect of varying concentrations of ribavirin. The data are means from three separate experiments. Error bars indicate standard deviation. Asterisk; *$P < 0.05$, **P<0.01 by one tailed T-test with the ribavirin treated samples compared to the untreated sample.

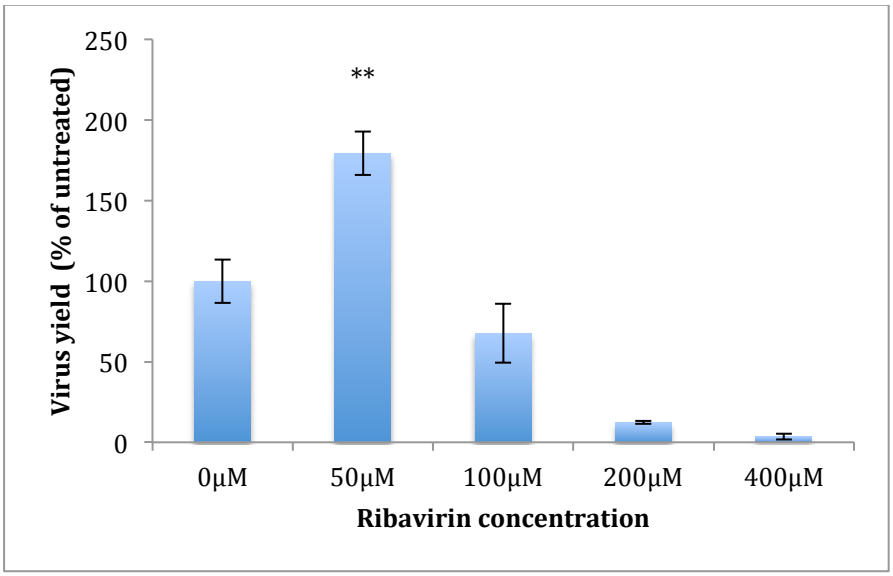

Figure 4.9: PV3/3 recombination in the presence of varying levels of ribavirin

Intratypic recombinants recovered from co-transfections of Rep3-L and SL3 in L929 cells seeded in the presence of varying ribavirin concentrations. Figures indicate the effect of varying concentrations of ribavirin (as indicated). The data are means from three independent experiments. Error bars indicate standard deviation. Asterisk; **P<0.01 by one tailed T-test with the ribavirin treated samples compared to the untreated sample.

4.6 The influence of 5-fluorouracil treatment on the CRE-REP assay

Another nucleoside analogue with a similar mode of action to ribavirin is the mutagen 5-fluorouracil (5-FU). This chemical is a pyrimidine analogue that is extensively used in cancer chemotherapy. 5-FU, like ribavirin, can also be metabolised into its triphosphate form and be used as a substrate by viral RNA dependent RNA polymerases leading to lethal mutagenesis (Agudo et al., 2009, Perales et al., 2009), and the reduction in virus yield following mutagen treatment has been well characterised (Crotty and Andino, 2002, Vignuzzi et al., 2005). The increase in recombination frequency observed in the presence of ribavirin therefore warranted the use of 5-FU.

A similar approach to that described in section 4.4 was undertaken to measure the overall reduction in PV3 yield following mutagen treatment (figure 4.10A). This was an important control that would aid in the subsequent interpretation of any CRE-REP assay carried out in the presence of the mutagen. The detrimental effect of 5-FU was apparent during the course of the experiment, concentrations above 100 μM led to toxicity and cell death prior to infection (not observed with ribavirin). This observation would have had an obvious impact on overall virus yield, something that would need to be considered in any CRE-REP assay. 5-FU levels of 100 μM, the highest non-toxic level observed, led to a 2-$\log_{10}$ fall in virus yield. A second infectivity assay involving PV3 was carried out using lower concentrations of 5-FU. This was deemed appropriate given the toxicity issues seen in the first assay. Three concentrations were used (20-40 μM) in triplicate, with HeLa cells being treated 2 hours prior to infection and then post infection with mutagen. Cells in a 6-well plate were infected at an M.O.I of 0.01 and incubated for 48 hrs. Dilutions of harvested media supernatant were then used to inoculate HeLa cell monolayers for plaque assays. Cells were incubated for 60 hrs, stained with crystal violet and virus plaques counted with titre converted to pfu/ml and normalised as a percentage of an untreated control (figure 4.10B). Results indicated that treatments of between 20-40 μM led to a maximum fall of 80% in PV3 yield, similar to the results obtained when virus yield was measured following ribavirin treatment at a concentration of 200 μM.

An intratypic CRE-REP assay was carried out using four concentrations of 5-FU that varied from 20 μM to 160 μM. L929 cells in a 12-well plate were treated with mutagen 2 hrs prior and then post transfection. A total of 0.5 μg RNA was co-transfected in triplicate wells in a 1:1 ratio (Rep3-L / SL3). Cells were incubated for 48 hrs. Dilutions of harvested media supernatant were then used to inoculate RD cell monolayers for plaque assays. Cells were incubated for 60 hrs, stained with crystal violet and photographed (figure 4.10CD). Yield of recombinant progeny indicated that treatments of 20 μM and 40 μM of 5-FU led to a significant increase in recombination frequency. This result correlates well with the results obtained in the presence of ribavirin. Under conditions where virus viability is reduced by around 80%, recombination frequency, as measured by yield from the CRE-REP assay, increases. Treatments of 80 μM and above led to a fall in recombination frequency, which can be associated to the high loss of virus viability at these levels.

A similar approach was used to look at the impact of 5-FU upon intertypic recombination frequency. All conditions were the same as the intratypic CRE-REP assay, with only the PV3 replicon (Rep3-L) being replaced with the PV1 replicon (RLucWT). Unlike the intratypic assay, only a concentration of 40 μM led to a significant increase in recombination frequency (figure 4.11). Treatments above this amount led to a fall or loss of recombinant virus, which was expected given that these doses led to a fall in infectivity of around 2 $\log_{10}$.

A

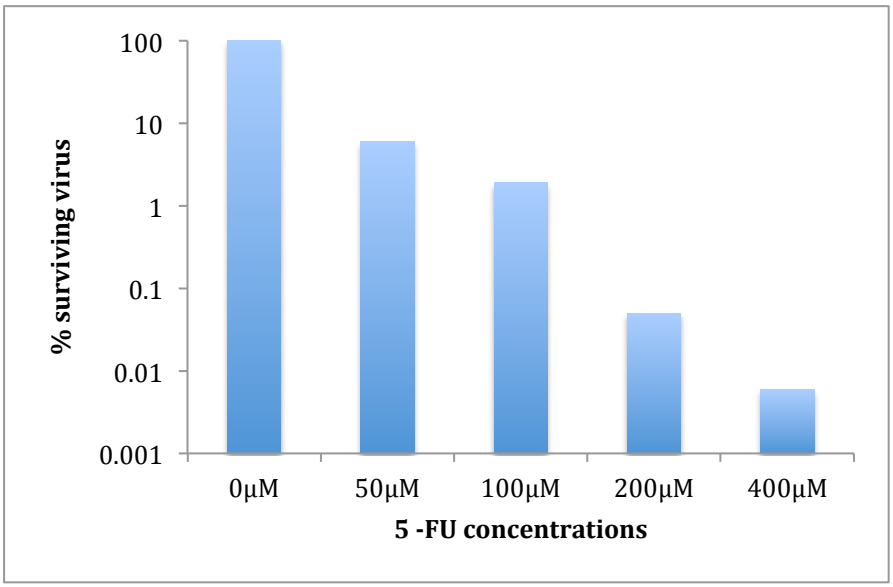
100
10
1
0.1
0.01
0.001
% surviving virus
0μM
50μM
100μM
200μM
400μM
5 -FU concentrations

B

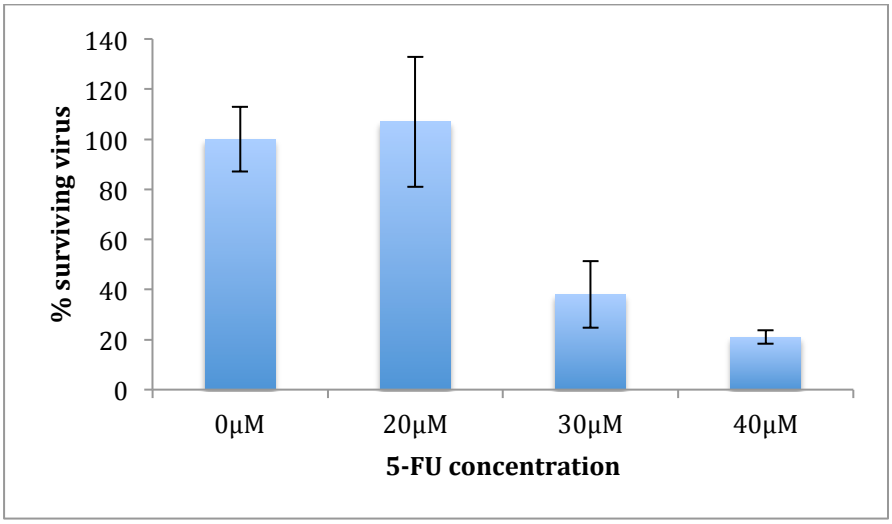
140
120
100
80
60
40
20
0
% surviving virus
0μM
20μM
30μM
40μM
5-FU concentration

C

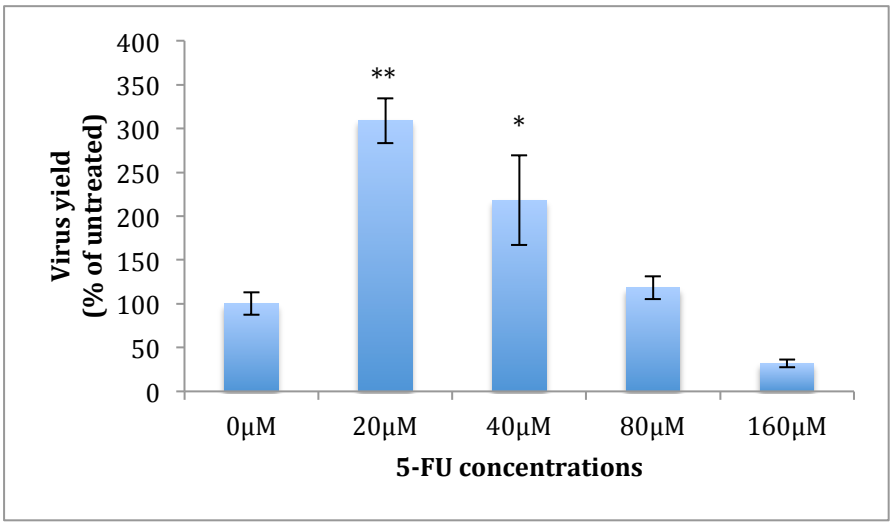

D

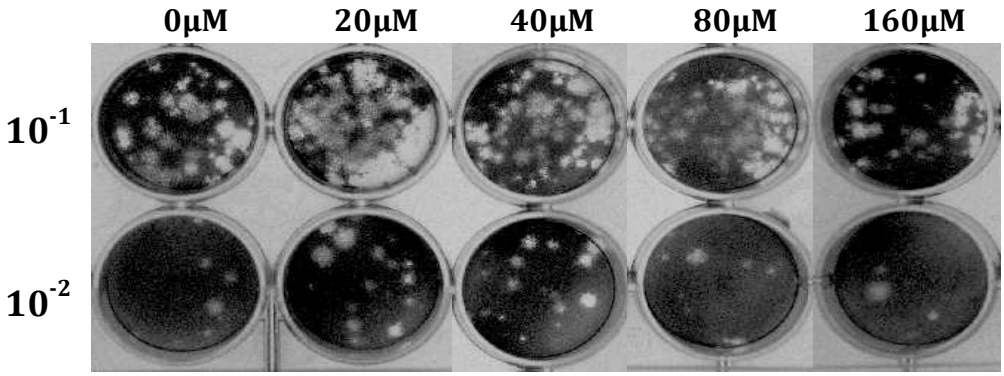

Figure 4.10: Intratypic recombination in the presence of varying levels of 5-FU

(A) + (B) HeLa cells were treated 2 hours prior and post infection with 5-FU (concentrations as indicated). Cells were then infected at an MOI of 0.01 with PV3. Media supernatant was harvested following an incubation period of 48 hrs and a plaque assay was used to quantify viable virus. Percentage of viable virus is shown in relation to an untreated sample. Error bars (B only) indicate standard deviation of three independent experiments **(C)** Intratypic recombinants recovered from co-transfections of Rep3-L and SL3 in L929 cells seeded in the presence of varying 5-FU concentrations. Figures show the effect of varying concentrations of 5-FU. The data are means from three separate experiments. Error bars indicate standard deviation. Asterisk; *$P < 0.05$, **P<0.01 by one tailed T-test with the 5-FU treated samples compared to the untreated sample **(D)** Representative plaque assay. Co-transfection supernatant was inoculated in a dilution series, as indicated, onto a fresh RD cell monolayer and overlaid with plaque overlay medium. Cells were stained 60 hours post-inoculation with crystal violet. Viable recombinant virus is evident by the presence of plaques.

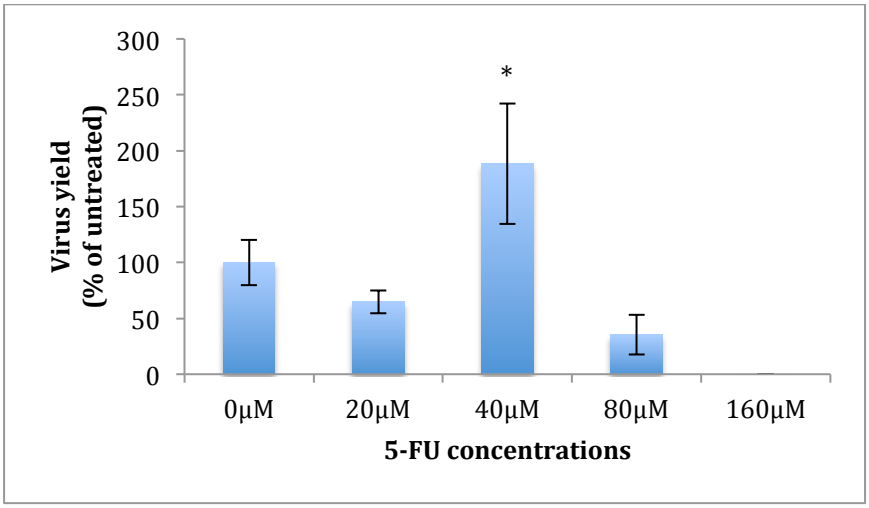

Figure 4.11: PV3/1 recombination in the presence of varying levels of 5-FU

Intertypic recombinants recovered from co-transfections of RLucWT and SL3 in L929 cells seeded in the presence of varying 5-FU concentrations. Figures show the effect of varying concentrations of 5-FU. The data are means from three separate experiments. Error bars indicate standard deviation. Asterisk; $*P < 0.05$, by one tailed T-test with the 5-FU treated samples compared to the untreated sample.

4.7 The influence of higher ribavirin concentrations on the high fidelity variant (G64S) in the CRE-REP assay

The high fidelity variant (G64S), as previously mentioned, was selected via serial passage of virus in the presence of the mutagen ribavirin. However, the ribavirin resistance phenotype that the G64S mutation provides is not complete. Ribavirin doses in the range of 400 μM to 800 μM increase mutation rates in a population of viruses carrying this high fidelity variant, in a similar fashion previously outlined (Pfeiffer and Kirkegaard, 2003).

It was therefore decided to test the G64S high fidelity RdRp with a higher dose of ribavirin. Perhaps the reduction in recombination frequency due to increased fidelity could be reversed if a higher dose was used? An intertypic CRE-REP assay was set up that used the high fidelity PV1 replicon RLuc-G64S along with the PV3 CRE mutant (SL3). A dose of 600 μM ribavirin was deemed appropriate as it was at the mid-point of doses used in a previous study that were shown to have a mutagenic effect (Pfeiffer and Kirkegaard, 2003). At these levels the mutagen does not affect translation and replication of a sub-genomic replicon bearing a G64S mutation, but does reduce RdRp fidelity (Vignuzzi et al., 2006). This was an important fact to consider, as any alteration in recombination frequency would therefore be directly related to fidelity only. L929 cells in a 12-well plate were incubated with the mutagen 2 hrs prior to transfection and following, with no obvious toxic affect to the cells observed. Five hundred nanograms of RNA in a 1:1 ratio (replicon: CRE mutant) was transfected in triplicate wells and incubated for 48 hrs. Dilutions of harvested media supernatant were then used to inoculate HeLa cell monolayers for plaque assays. Cells were incubated for 60 hrs, stained with crystal violet and photographed (figure 4.12). Quantification of recombinant progeny indicated that treatment with a higher dose of ribavirin led to a significant increase in recombination frequency of around 3-fold when compared to mock treated controls (determined by student T-Test). Although, ribavirin treatment led to a smaller plaque phenotype - this was presumably due to additional mutations that were present in the recombinant genome. This result further supports a direct role for the RdRp in recombination. It also strongly suggests that fidelity is a key characteristic that determines recombination frequency.

A

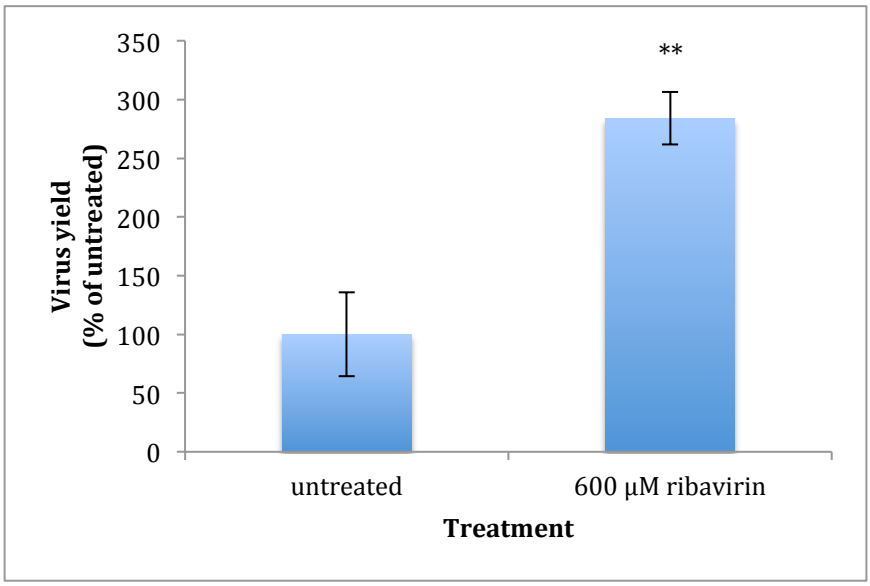

B

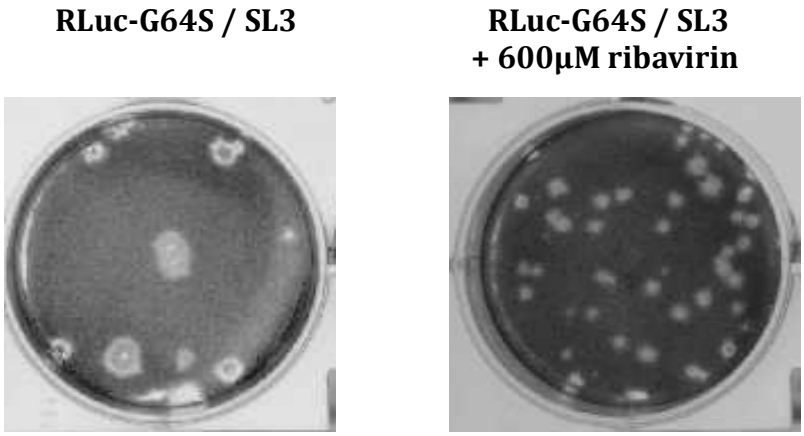

Figure 4.12: Influence of a high fidelity polymerase (G64S) upon intertypic recombination in the presence of 600µM ribavirin

PV1 sub-genomic replicon (RLucWT) bearing a G64S high fidelity polymerase mutation co-transfected with SL3 +/- 600µM ribavirin. **(A)** The figures represent the mean from three independent samples. Error bars indicate standard deviation. Asterisk; $^{**}P < 0.01$ by Student's T-test test **(B)** Representative crystal violet stained HeLa cell monolayers inoculated with undiluted transfection supernatant and overlayed with plaque assay overlay medium. RNA partners and conditions as indicated. Control wells containing only one RNA partner were free of plaques (not shown)

4.8 Characterisation of PV3/1 recombinant clones produced in the presence of ribavirin

The direct interaction of ribavirin with viral RdRp's has already been outlined in section 4.2. The increase in recombination frequency observed when CRE-REP partners were co-transfected in the presence of ribavirin suggested that its incorporation, or attempted incorporation, might have been sufficient to induce an increase in template switching. It would be reasonable to suggest that if ribavirin were incorporated into the RNA that a transition mutation may be observable. It was decided to isolate and sequence a number of intertypic recombinant biological clones, which had arisen from a co-transfection in the presence of ribavirin. If ribavirin were having a direct influence upon template switching then perhaps sequence analysis of a number of junctions would highlight a potential sequence motif, or indeed mutation that could be linked to the nucleoside analogue. Intertypic isolates were obtained by a limiting dilution approach. It was deemed most suitable to use one of the 100 - 200 μM ribavirin transfection supernatants, which were isolated from the intertypic CRE-REP assay (figure 4.8). These samples had shown a 2-3-fold increase in recombination compared to untreated controls.

Biological cloning was done by a limiting dilution approach, and the 1.058 Kb zone of recombination amplified by RT-PCR using the primers PV1/3-3280F and GEN-4615R. A total of nine unique PV3/1 recombinant junctions were characterised (figure 4.13A). Four of the characterised recombinant junctions fell within cluster one (VP1/2A boundary), and all of the isolates in this region were imprecise and carried additional sequence when compared to wild type poliovirus genome length (figure 4.13B). Two of the recombinants had junctions that suggested template switching had occurred at or just before an 'A' dinucleotide upon the donor template. One isolate had a junction that spanned a 'U' dinucleotide with the final imprecise junction at a 'UA' sequence upon the donor template. Two of the characterised recombinant junctions fell within cluster two, a region that spans the 2A/2B boundary (figure 4.13C). One was imprecise, and carried additional sequence. This isolate had a junction that suggested template switching had occurred at a 'UU' dinucleotide upon the donor template. The final

A

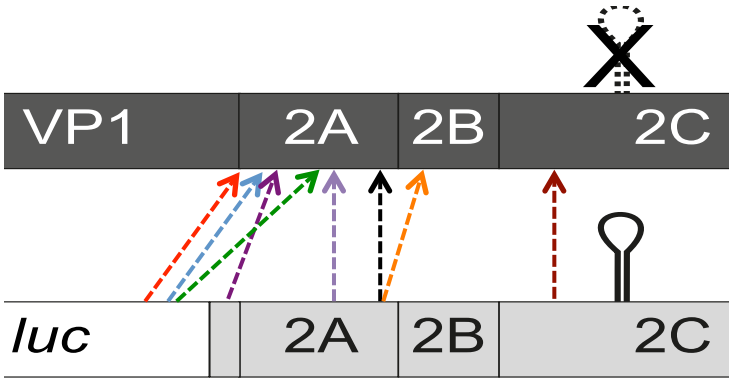

B

PV3 (1-3507) Luc (26) PV1 - A tail

```
PV3: GGTTGTTGAATCAAAAGCTCAAGGTAC
LUC: CA-AAAG-CCAAG--G-GCGG-AAGT-
REC: ------------G--G-GCGG-AAGT-
```

PV3 (1-3391/2) Luc (134/5) - PV1 - A tail

```
PV3: GGCTTTGGGCATCAGAATAAAGCTGTGTA
LUC: -T-GCCA-T--AGTA-CA-CC--GAAAA-
REC: ---------------CA-CC--GAAAA-
```

PV3 (1-3422/3) Luc (89/90) - PV1 - A tail

```
PV3: GCTGGTTACAAGATCTGCAACTACCATC
LUC: TT--TGG--G-AG-ACCG--AGGT-T-A
REC: -------------ACCG--AGGT-T-A
```

PV3 (1-3434) PV1 (3390-A tail)

```
PV3: TCTGCAACTACCATCTCGCCACTAAGG
PV1: C-ACAT-TGGATTCGGACA-CAA--CA
REC: ------------TCGGACA-CAA--CA
```

C

PV3 (1-3830/31) PV1 (3773/74- A tail)

```
PV3: GAGCAGGGCATTTCAAACTATATTGAG
PV1: -GTGGC-AAGGGTTGGTTGCAT--TCA
REC: ----------TTGGTTGCAT--TCA
```

PV3 (1-3756) PV1 (3754-A tail)

```
PV3: GACAGCTGGTGGAGAGGGATTAG
PV1: --T--GGATCATTACT-CTGGA-
REC: ----------TACT-CTGGT-
```

D

PV3 (1-3610/12) - PV1 - A tail

```
PV3: GTCGTTTGTGGGACCCACCTTCCAATACAT
PV1: A--C--C--T--C--A--G-----G-----
REC: ----------------G-----G-----
```

PV3 (1- 4147/64) - PV1 - A tail

```
PV3: TGAGGCGTGCAACGCAGCTAAGGGGTTGGAA
PV1: ---A--A-----------------AC----G
REC: -------------------------AC----G
```

Figure 4.13: Biologically cloned PV3/1 recombinants obtained from co-transfection of RNA partners in the presence of 100 - 200 µM ribavirin

(A) Dashed arrows indicate points of crossover from donor (replicon) to acceptor template (CRE mutant) in all of the isolates. Colour codes same as nomenclature of recombinants. PV3 = Leon strain, PV1 = Mahoney strain (GenBank accession numbers X00925 and V01149 respectively), LUC = Luciferase sequence carried by the PV1 replicon. REC = recombinant sequence. Red boxes indicate sequence homology in the region of template switching. **(B)** Genome sequences of four biologically cloned intertypic recombinant viruses with junctions that fall within cluster one **(C)** Genome sequences of two biologically cloned intertypic recombinant virus that fall within cluster two **(D)** Genome sequences of two biologically cloned intertypic recombinants that fall outside of the cluster one and cluster two regions.

recombinant in this area was precise with no additional sequence when compared to wild type poliovirus length. Similarly, its junction mapped to a 'UU' dinucleotide upon the donor template.

Two final isolates were characterised that had recombinant junctions that were precise with no additional sequence present (figure 4.13D). In both examples the exact location of recombination could not be found due to sequence identity between parental genomes. The two isolates fell outside of the characterised cluster one and cluster two regions that span protein cleavage boundaries. Both had sequences that encoded chimeric protein, something rarely observed in the genomes of imprecise intertypic recombinants isolated from the CRE-REP assay. Although, precise recombination within the 2C region is something that has been seen before and seems to be tolerated (Lowry et al., 2014). The isolation of a recombinant genome with a junction within this region was therefore not surprising. It was surprising to see an isolate that had a recombination junction midway through the 2A coding region. However, this recombinant genome may not necessarily represent the product of the initial crossover event. The Lowry study found imprecise isolates where the recombination site upon the acceptor template was in a similar position. Potentially, this isolate had already gone through the secondary resolution events characterised in section 3.6. This would explain why it is precise with no additional sequence.

A final intertypic recombinant junction was characterised that had sequence that suggested two recombination events had occurred (figure 4.14AB). An initial template switch from the luciferase-coding region on the donor template (RLucWT) to a region within the capsid coding area of the acceptor template (SL3) was identified. This would be considered a *trans* event. Sequence analysis suggested that a second recombination event occurred where the RdRp left at a point in the capsid coding region and replication begins adjacent to the VP1/2A boundary upon the SL3 template. In principle, this could have occurred *in cis* upon the same acceptor template or, by a template switch to another acceptor template. A double recombination event like this has been observed before in an isolate known as 25A (Lowry et al., 2014). No obvious dinucleotide or sequence motif was identified with the double recombinant isolate.

A

PV3 (1-3402) PV3 (2966-2986/88) Luc (164/66) PV1 -A tail

```
PV3:  AAAGCTGTGTACACTGCTGGTTACAAGATCTGCAACTA
CAP:  GGGCACCCACCA-AGTCAT-GG--G-CTACACTTGGC-
Luc:  TGTTG-T-TGGAGAACGGAAAG--G-TGACGATCGTGG
REC:  --------ACCA-AGTCAT-GG--G-CTACGATCGTGG
```

B

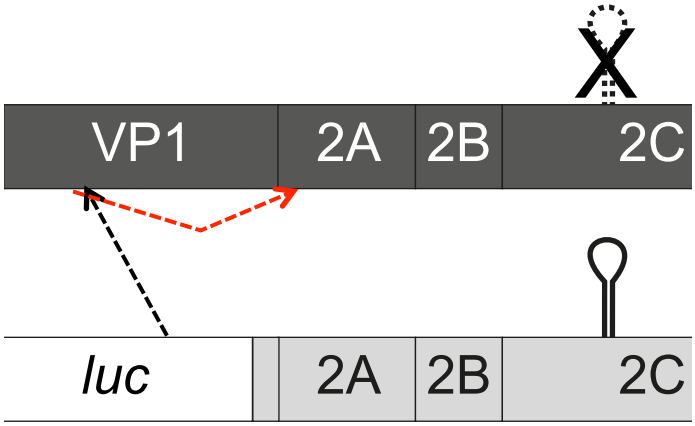

Figure 4.14: Intertypic recombinant isolate with a double template switch

(A) Genome sequence of a biologically cloned intertypic recombinant that has two-recombination junctions. PV3 = Leon strain, LUC = Luciferase sequence carried by the PV1 replicon (GenBank accession numbers X00925 and V01149 respectively). CAP = Capsid sequence of PV3, REC = recombinant sequence. Red-boxed dinucleotide indicates sequence identity in the region of the first template switch. Yellow box indicates capsid-coding sequence followed by a secondary recombination event. Dashes indicate nt identity with PV3, any differences in sequence are indicated **(B)** Dashed arrow **(Black)** indicates the first point of crossover from donor (replicon) to acceptor template (CRE mutant). Dashed arrow **(Red)** indicates second positional switch upon the acceptor template only.

4.9 Impact of fidelity on the resolution process

The biphasic nature of recombination in enteroviruses has been discussed in section 3.10, where a molecular clone known as JC105B was shown to go through the same 'resolution' stages as a biological clone of the same sequence (#105B, section 3.6). Potentially, the loss of additional sequence could have been due to secondary recombination events. If this were replicative, like 'copy-choice', then RdRp fidelity may impact the resolution process in a similar fashion to the recombination events observed in the CRE-REP assay. To answer this question, the high fidelity G64S mutation was sub-cloned into the JC105B cDNA from the pRLuc-G64S cDNA using the unique restriction enzymes *BglII and ApaI.* The construct was then linearised with *ApaI* and used as a template to transcribe RNA using T7 polymerase. A similar experimental approach to that outlined in section 3.8 was used, where 250 ng of JC105B and JC105B-G64S RNA were transfected individually into L929 cells and allowed to incubate for 48 hrs. The transfection supernatant was then isolated and then subjected to a further ten serial passages in HeLa cells. Viral RNA was isolated from each passage and subjected to RT-PCR analysis. The JC105B material was amplified using the primers PV1/3-3280F and GEN-4615R and the G64S variant was amplified using the primers PV3-3249F and PV1-3679R. The JC105B molecular clone that carried a wild-type sequence RdRp went through a similar 'resolution event' observed in chapter three (figure 4.15A). This was included as a control to compare to the G64S variant. The appearance of a smaller PCR product can be seen by passage 4, which seems to migrating as far as the SL3 control (wild type length). The pattern of resolution in the JC105B-G64S variant differed dramatically to the JC105B molecular clone (figure 4.15B). The appearance of a smaller PCR product does not appear until passage 8, and a mixed population can still be seen at passage 10. This observation strongly suggests that the resolution event may indeed be due to replicative recombination and is affected by RdRp fidelity. To further support this interpretation, it was decided to passage the JC105B-G64S variant in the presence of ribavirin. As shown previously, recombination frequency in the CRE-REP assay with the G64S variant increased when ribavirin was present. In this experiment 400 μM was added to HeLa cells at each passage. Products of RT-PCR indicated that the presence of ribavirin has led to the

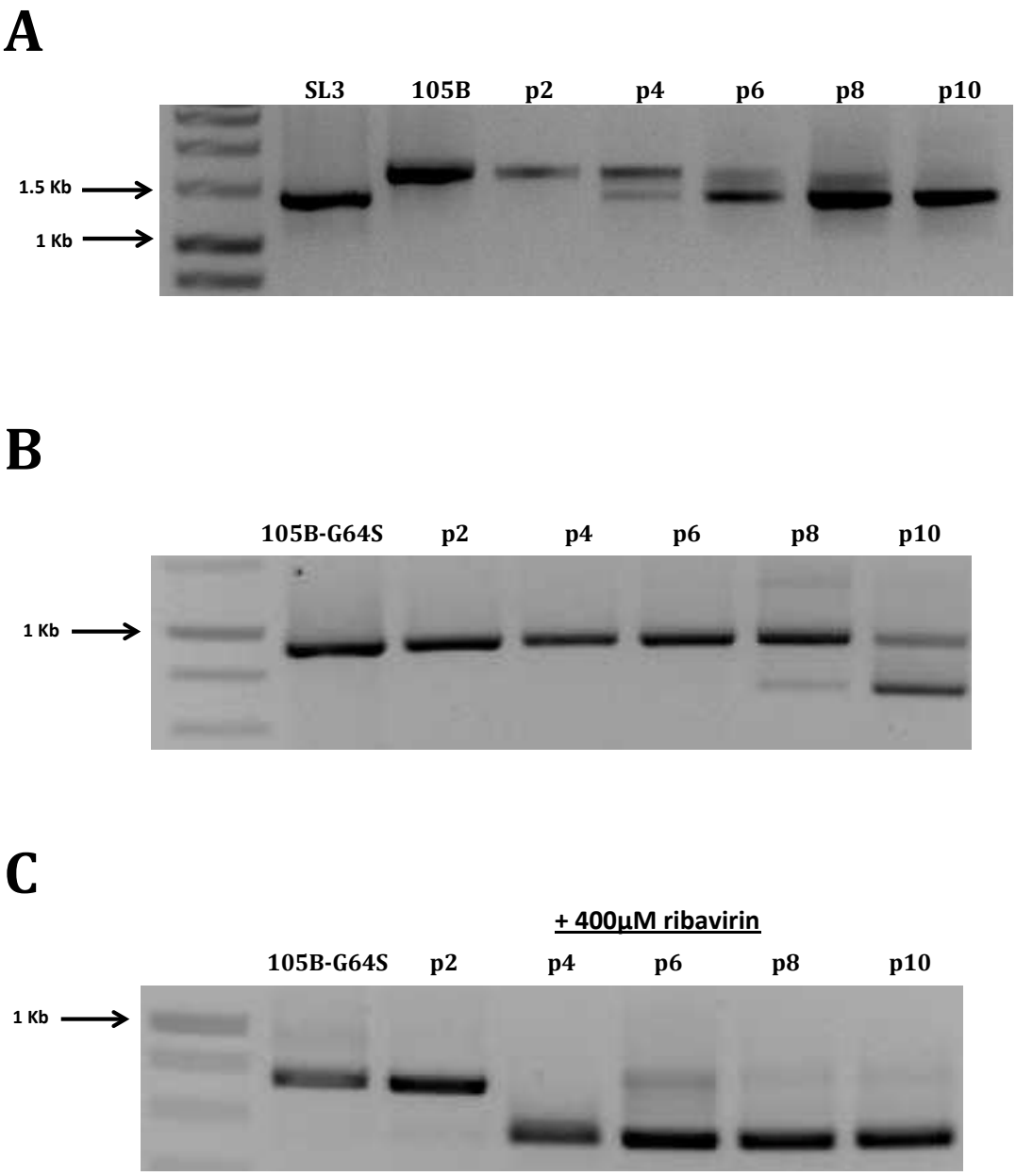

Figure 4.15: Resolution of a molecular clone with a high fidelity polymerase +/- ribavirin

(A) RT-PCR product of the amplified region in the JC105B recombinant virus was run on 1% agarose gel and stained with ethidium bromide following serial passaging in HeLa cells. Passages as indicated. SL3 = wild-type product size **(B)** RT-PCR product of JC105B-G64S following serial passage **(C)** As (B), except passaging in the presence of 400 µM ribavirin.

loss of additional sequence by passage 4, four passages earlier than without the mutagen (figure 4.15C).

4.10 Influence of nocodazole treatment on the CRE-REP assay

For genetic re-arrangements to occur, like recombination, genomes must be closely juxtaposed, presumably in the same membrane associated replication complex. As described in chapter one, replication of the viral RNA occurs in replication complexes (RCs), which are rosette like vesicles derived from the host endoplasmic reticulum. A technique known as fluorescent *in situ* hybridisation (FISH) showed that individual replication complexes initially form on the endoplasmic reticulum where synthesis of negative strand RNA begins. The individual complexes then move in a microtubule (MT) dependent fashion to a peri-nuclear location where positive strand RNA synthesis follows (Egger and Bienz, 2005). The movement of RCs to a similar location within the cell leads to a coalescence, so mixing their RNA contents. Indeed, by use of strain specific riboprobes mixing of replication complexes occurs following RC migration which may contribute to the recombination process (Egger and Bienz, 2002).

Nocodazole is an anti-neoplastic agent that exerts its effect in cells by interfering with the polymerisation of microtubules. The treatment of cells with nanomolar concentrations of the drug has been shown to lead to microtubule instability (Vasquez et al., 1997). The migration pattern of poliovirus replication complexes can also be affected by nocodazole treatment. Transient chilling of host cells disrupts the MTs; re-polymerization is then blocked by addition of the drug. This has profound effects on the localisation pattern of poliovirus replication complexes, with a more diffuse localisation pattern following treatment (Egger and Bienz, 2005). Indeed, the altered pattern of RC movement reduces co-localisation of different PV serotypes by up 50% when compared to untreated cells, whilst having no impact on replication *per se* (Egger and Bienz, 2005). The results in this chapter so far have indicated that recombination frequency can be affected when fidelity of the RdRp is manipulated. This implies that the templates involved in the genetic re-arrangements are in close proximity, presumably within the same replication complex. The flexibility of the CRE-REP and NON-REP assays

allowed the introduction of nocodazole into the experiment. If co-localisation of viral RNA could be affected then perhaps recombination frequency would be reduced?

As a control, it was deemed prudent to analyse the effect of the drug on replication of a PV3 full-length clone to assess whether the drug treatment would affect replication levels and therefore bias any interpretation of recombination frequency. L929 cells in a 12-well plate were transiently chilled to disrupt the MTs then treated with 5mM nocodazole. Control cells were not chilled and were treated with 5mM of the carrier DMSO (section 2.1.9). Following a brief incubation period post drug treatment, cells were transfected with 250 ng of PV3 full-length clone RNA and left to incubate for 48 hrs. A dilution series of harvested media supernatant was used to inoculate HeLa cell monolayers for plaque assays. Cells were incubated for 60 hrs, stained with crystal violet and photographed (figure 4.16). Quantification of virus yield showed that the drug nocodazole did not significantly affect replication of PV3 following transfection, in agreement with results from a previous study (Egger and Bienz, 2005).

A similar experimental approach to the CRE-REP assays described in section 4.3 involving the intertypic partners (RLucWT and SL3) and the intratypic partners (Rep3-L and SL3) was then carried out. The experiment also incorporated the nocodazole and control DMSO treatment prior and post transfection. Following an incubation of 48 hrs post transfection, media supernatant was harvested and used diluted and undiluted to inoculate HeLa cell monolayers for plaque assays. Cells were incubated for 60 hrs and stained with crystal violet. In both combinations, disruption of the MTs followed by nocodazole treatment significantly reduced recombination frequencies (figure 4.17). Indeed, intratypic recombination was reduced to around 30% compared to the DMSO treated control while intertypic recombination frequency was reduced to less than 10% of the DMSO treated control.

A

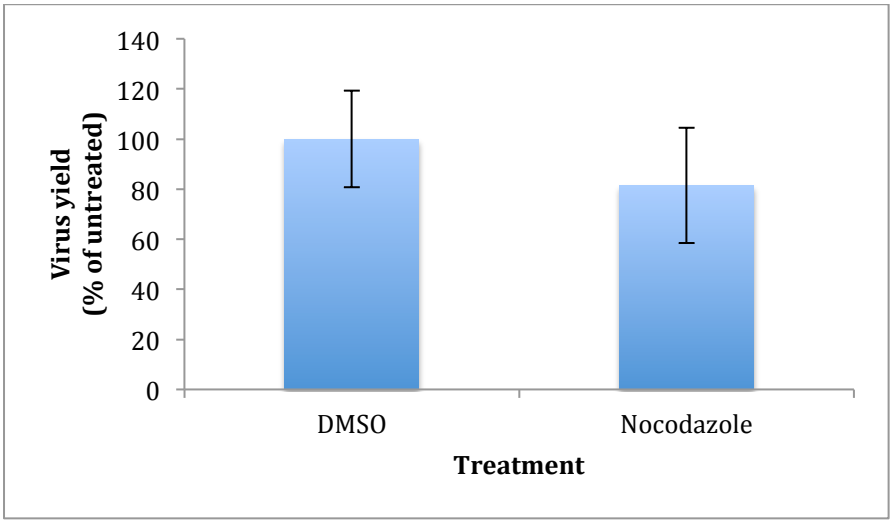

B

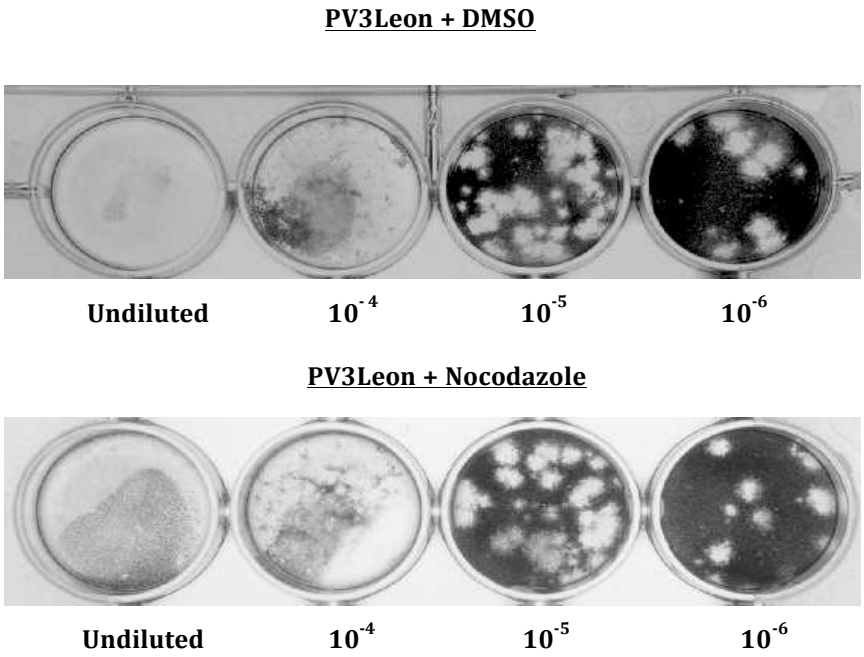

Figure 4.16: Nocodazole treatment does not affect PV3 replication

(A) Figures represent PV3 virus yield from three independent samples. Transfection treatments with either nocodazole or the carrier DMSO are indicated. Error bars indicate standard deviation **(B)** Representative crystal violet stained HeLa cell monolayers inoculated with diluted transfection supernatant (dilutions as indicated) and overlayed with plaque assay overlay medium. Transfection treatment conditions as indicated.

A

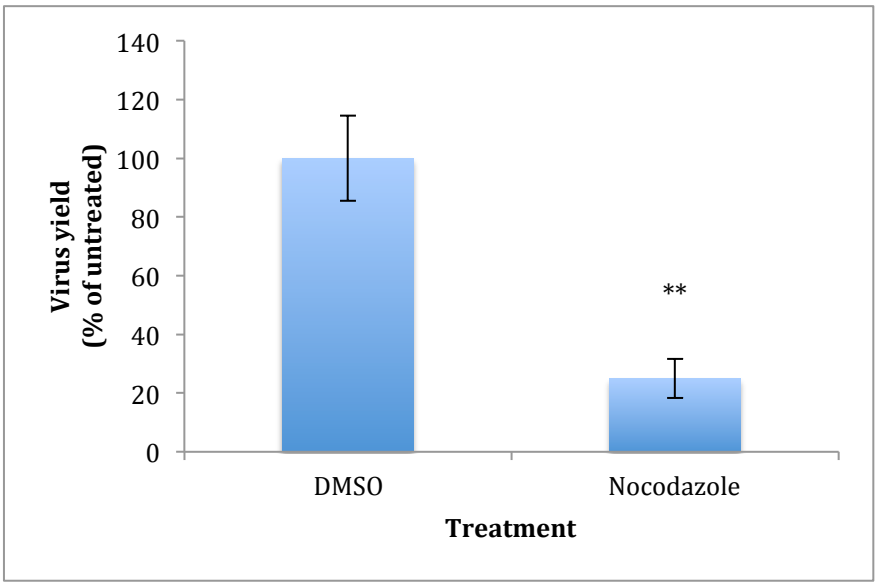
140
120
100
80
60
40
20
0
Virus yield
(% of untreated)
**
DMSO
Nocodazole
Treatment

B

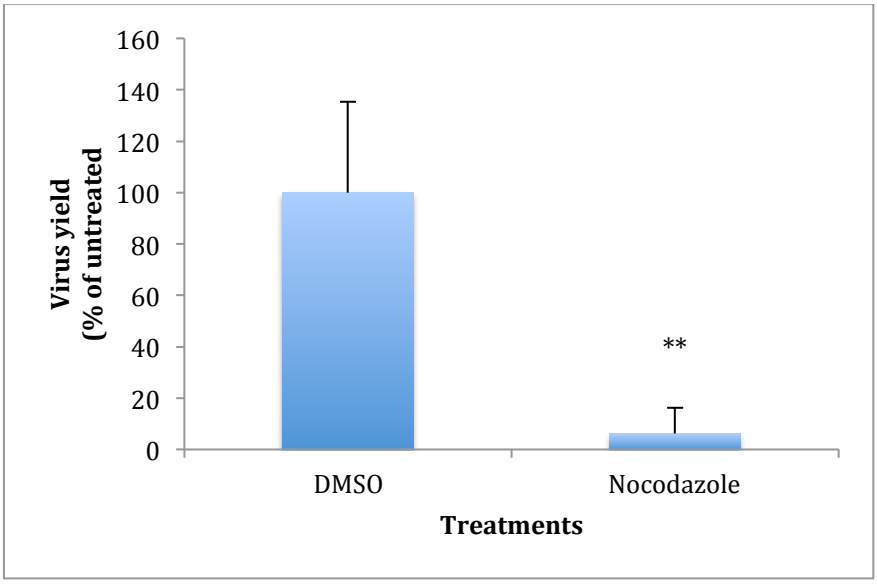
160
140
120
100
80
60
40
20
0
Virus yield
(% of untreated
**
DMSO
Nocodazole
Treatments

C

Rep3-L / SL3 + DMSO
10^{-1} Dilution

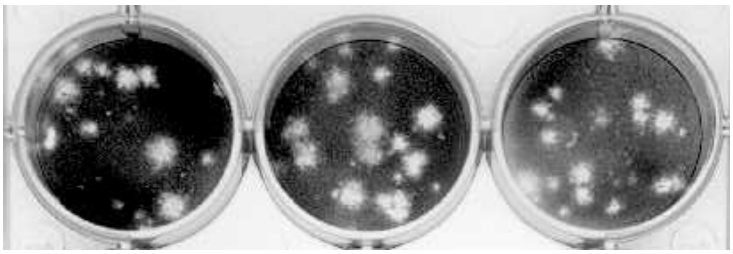

Rep3-L / SL3 + Nocodazole
10^{-1} Dilution

Figure 4.17: Nocodazole treatment inhibits replicative recombination

(A) Figures represent intratypic recombinant virus yield from three independent samples using RNA generated *in vitro* from pT7rep3-L and pT7FLC/SL3. Transfection treatments with either nocodazole or the carrier DMSO are indicated. Error bars indicate standard deviation. Asterisk; $^{**}P < 0.005$ by Student's T-test test **(B)** Figures represent intertypic recombinant virus yield from three independent samples using RNA generated *in vitro* from pRLucWT and pT7FLC/SL3. Transfection treatments with either nocodazole or the carrier DMSO are indicated. Error bars indicate standard deviation. Asterisk; $^{**}P < 0.005$ by Student's T-test test **(C)** Representative crystal violet stained HeLa cell monolayers infected with diluted transfection supernatant (dilutions as indicated) and overlayed with plaque assay overlay medium. RNA partners as indicated. Transfection treatment conditions as indicated.

Results strongly suggested that recombination was primarily a replicative process that was reliant upon co-localisation of replication complexes. In principle, MT disruption and subsequent nocodazole treatment should have had little affect upon non-replicative recombination. To ensure that nocodazole treatment was solely affecting replicative recombination a final experiment was considered necessary. The treatments outlined in this section were incorporated into the NON-REP assay described in section 3.9 using the non-replicative intratypic partners only. Recombinant progeny counts under both conditions (nocodazole and DMSO) were low, as expected, with no significant difference between the two (figure 4.18).

4.11 Discussion

The 'copy-choice' mechanism of recombination is a replicative process (Kirkegaard and Baltimore, 1986b). The results in this study have showed that the recombinant progeny produced from the CRE-REP assay was primarily due to replicative recombination that is biphasic in nature. The aim in this area of the investigation was to identify characteristics of the viral RdRp that were important in recombination. The results in section 4.2 showed that manipulation of RdRp fidelity did not affect recombinant progeny yield from the NON-REP assay. This result was important because it showed that this recombination process is via a mechanism that is independent of the viral polymerase. Presumably the recombinant RNA produced in the NON-REP assay is via an unknown cellular ligase or via a trans-esterification reaction that has been postulated in previous studies (Gmyl et al., 1999, Gmyl et al., 2003). In contrast, results showed that RdRp fidelity influenced recombination frequency in the replicative CRE-REP assay. The use of a well-characterised high fidelity RdRp variant (Pfeiffer and Kirkegaard, 2003, Vignuzzi et al., 2005) that carried a G64S mutation within the RdRp coding region (3D), inhibited intratypic and intertypic recombination frequencies by 10 and 20-fold respectively. Importantly, the luciferase assays conducted in section 4.3 showed that this mutation does not significantly affect the replication kinetics of the virus, a result that is supported by a previous study (Vignuzzi et al., 2006). This ensured that any difference in

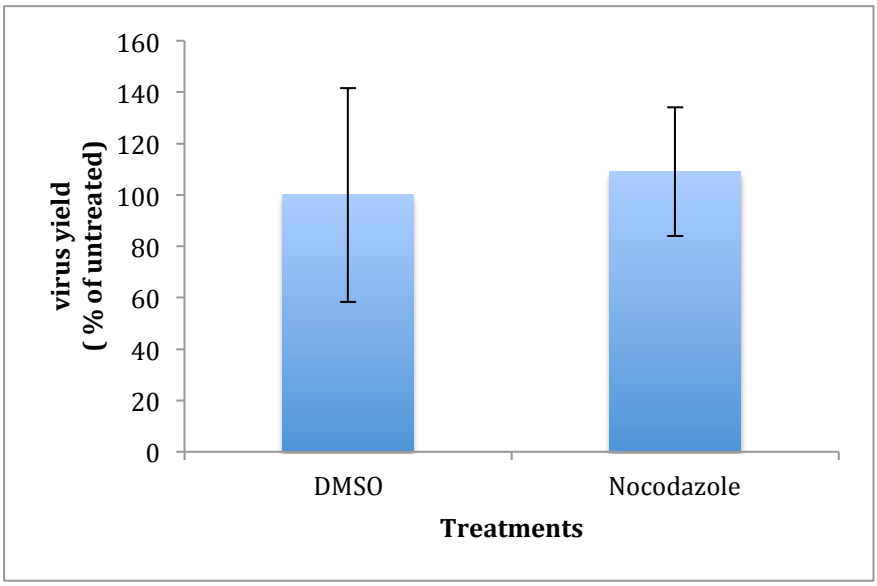

Figure 4.18: Nocodazole does not inhibit non-replicative recombination

Figures represent non-replicative intratypic recombinant virus yield from three independent samples co-transfected with RNA templates ΔRep3-L and SL3Δ. Treatments with either nocodazole or the carrier DMSO are indicated. Error bars indicate standard deviation.

recombination frequency was due to fidelity of the viral RdRp alone. In contrast, the use of the nucleoside analogue mutagen ribavirin, that is known to decrease RdRp fidelity (Vignuzzi et al., 2005), led to a significant increase in recombination frequency whilst having no impact upon transfection efficiency. The levels of ribavirin required to increase recombination were between 100-200 μM in the intertypic CRE-REP assay and 50 μM in the intratypic CRE-REP assay. The differences in the dosage that led to a significant increase in recombination may indicate an underlying difference between the two serotypes at the RdRp level. Further experiments in this area will be required. Ribavirin treatment at the 100-200 μM levels was shown to reduce viability of a full length PV3 virus by up 80% (figure 4.19A). If the level of recombination increases with higher concentrations of ribavirin then why wasn't there an increase at levels above 200 μM? Poliovirus lives on the edge of 'error catastrophe' (Crotty and Andino, 2002). In all probability the mutagenic load carried by the recombinant genomes that were produced at the higher doses of ribavirin made them non-viable. As the CRE-REP assay measures viable recombinant virus only and not the generation of hybrid RNA, these would not have been detected. It seems there is a critical 'tipping-point' between increased recombination frequency and general mutation rates, above which genomes become non-viable. This hypothesis fits well with the 'error-catastrophe' theory. To further support the role of RdRp fidelity, a similar nucleoside analogue called 5-FU was used. This was considered an appropriate mutagen to use because it has a similar mode of action as ribavirin. An infectivity assay showed that levels of 100 μM and above reduced virus yield by over two $\log_{10}$. A lower range was subsequently used, and it was shown that treatment of cells prior and post infection with 40 μM was enough to lower virus viability by 80%. At this same level recombination from the intertypic and intratypic CRE-REP assays was significantly increased (figure 4.19B). This result correlates with the ribavirin results and indicates that lowering fidelity leads to an increase in template switching.

A number of biologically cloned isolates were characterised in sections 4.3 and 4.8. The presence of a high fidelity RdRp had little effect upon the location of the recombination junctions characterised in figure 4.5. All were at or spanned the previously observed cluster 1 and cluster 2 protein cleavage boundaries, and the majority were imprecise with additional

A

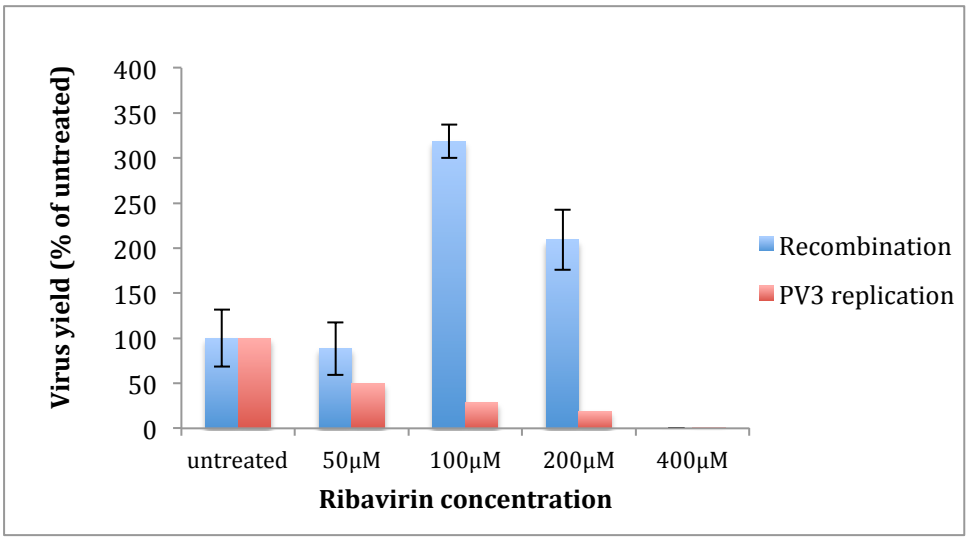

B

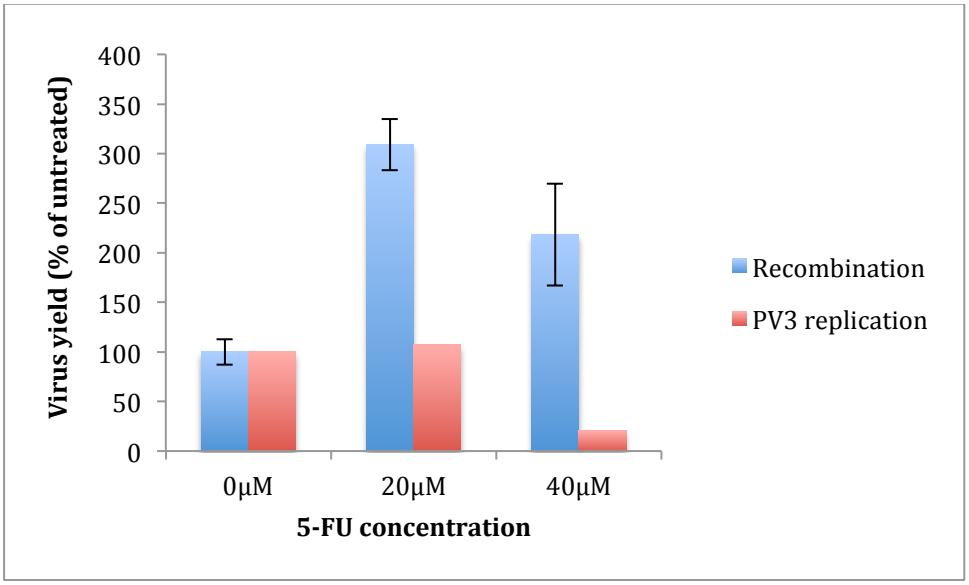

Figure 4.19: Comparison of recombination frequency and virus viability

(A) Intertypic recombination frequency and PV3 viability comparison following ribavirin treatment. Mutagen doses as indicated. All figures normalised to an untreated control **(B)** Intratypic recombination frequency and PV3 viability comparison following 5-FU treatment. Mutagen doses as indicated. All figures normalised to an untreated control.

sequence (Lowry et al., 2014). This further supports the hypothesis that the overriding criteria in selection of an early recombinant are based upon a genome that doesn't encode chimeric proteins; this ensures correct protein-protein interactions during subsequent replication. Unlike the Lowry et al., 2014 study, the majority of intertypic biologically cloned recombinant genomes in this chapter have recombination junctions that are associated to U/A dinucleotide motifs, a similar finding to a previous study (King, 1988b). This suggests that use of a high fidelity RdRp or mutagen have biased the location of template switch upon the donor template. Perhaps the high fidelity RdRp will leave a donor template but only at regions of the lowest stability. The two hydrogen bonds between A:U during RNA replication represent the most unstable interaction. When interpreting the data caution is required. The sequenced junctions may not represent the initial crossover event, even though the experimental approach isolates the products as early as possible.

As described in sections 4.2 and 4.6, ribavirin and 5-FU are nucleoside analogues that have been shown to interact directly with the viral RdRp mimicking the kinetics of incorrect nucleotides. If the mutagen had been inserted into the nascent RNA and been a factor in template switching then transition mutations would be expected at the site of recombination. No mutations were observed in the recombinant junctions analysed following ribavirin treatment (figure 4.13 and 4.14). Potentially, the interaction of the mutagen with the viral RdRp alone during replication could have been enough to de-stabilise the elongation complex and induce template switching. Indeed, 66% of recombinant junctions characterised in figures 4.13 and 4.14 are associated with a 'UU' or 'UA' dinucleotide motif upon the donor template. In principle, the attempt to incorporate ribavirin opposite the template base 'U' could have been enough to de-stabilise the elongation complex inducing a template switch. Alternatively, the mutagen could be having an indirect role within the host cell. Ribavirin monophosphate (RMP) has been shown to inhibit a host enzyme, *Inosine Monophosphate Dehydrogenase* (IMPDH). This causes a decrease in the intracellular concentration of GTP (Crotty et al., 2000). The subsequent effect upon nucleotide homeostasis may be a trigger for stalling events that increases the opportunity for template switching to occur. A study involving a larger data set is required; this may provide insights into

the possible mechanisms of recombination that these nucleoside mutagens induce. At present, the limited sequences identified only allow a hypothesis.

The resolution phenomenon, where additional sequence is lost has provided data to suggest that sequence identity may play a role in this stage of recombination (section 3.10). The results in section 4.9 strongly suggest that the mechanisms of 'resolution' are replicative. By using a molecular clone (JC105B) with a high fidelity RdRp it was shown that the process of resolution where additional sequence is lost was inhibited, or 'slowed' down when compared to a wild type RdRp control. In contrast, passaging the same high fidelity clone in the presence of the mutagen ribavirin sped up the process, with loss of sequence occurring four passages earlier. These observations strongly suggest that the resolution event is RdRp dependent and that fidelity is important. This could be due to a copy-choice recombination event where the RdRp leaves one template and associates to another, a jumping event that leads to loss of sequence. Alternatively, the resolution events that have been observed could be *in cis*. Potentially, a 'looping' out event within the same RNA template has occurred, where additional sequence is eventually lost. The two models of resolution may not be mutually exclusive and could both be happening. Perhaps the resolution event is M.O.I. dependent? By lowering the multiplicity of infection a distinction between the two may be found. What these results do show is that by increasing and decreasing RdRp fidelity this process was affected in a similar fashion to that shown in the CRE-REP assays under the same conditions. This emphasises the role of the viral RdRp in both stages of recombination.

Mixing of replication complexes with both parental RNA would seem to be a key prerequisite for replicative recombination to occur. Transiently disrupting the host cell microtubules using a cold-shock approach and then preventing their re-polymerisation by using nocodazole inhibits poliovirus RNA co-localisation (Egger and Bienz, 2005). Similar treatments in this study showed that this does not affect replication of the virus. This key control experiment allowed an interpretation of the results obtained from the CRE-REP assay under the same conditions. Subsequent CRE-REP assays carried out in the presence of nocodazole showed that this treatment did have an inhibitory affect upon recombination. These results support the

hypothesis that co-occupancy of the same replication complex is necessary for 'copy-choice' recombination to occur. This is further supported by the fact that similar nocodazole treatment had no affect upon the NON-REP assay.

In summary, the observations in this chapter strongly suggest that fidelity of the viral RdRp is a key determinant of recombination in enteroviruses. The impact upon recombination frequency following treatment with a chemical that inhibits viral RNA co-localisation also strongly supports the replicative 'copy-choice' model. Additionally, the influence of fidelity upon the resolution stage suggests that the RdRp is involved in additional template switching *in cis* or *trans*, which aids the subsequent selection of recombinant progeny where additional sequence is lost. Taken together, these observations strongly support the replicative 'copy-choice' model of recombination. Poliovirus has evolved a low fidelity polymerase and exist as a quasi-species (Crotty et al., 2001). This diversity allows the population to adapt and evolve to new and changing environments. The results in this study show that low fidelity also allows a basal level of recombination. This process leads to vast changes in the viral genome, leading to far greater diversity, an obvious advantageous characteristic.

CHAPTER FIVE: RNA Dependent RNA Polymerase Variants That Influence Recombination and the Development of an Expanded CRE-REP Assay

5.1 Introduction

The results in chapter four showed that the yield of recombinant progeny from the CRE-REP assay was influenced when viral RdRp fidelity was manipulated. Additionally, co-localisation of viral RNA was shown to be important in the replicative assay. Taken together, these findings supported the 'copy-choice' replicative model of recombination.

Previous studies have looked at RdRp fidelity as a way of generating new attenuated vaccine strains (Vignuzzi et al., 2006, Weeks et al., 2012, Vignuzzi et al., 2008). These studies have shown that high fidelity variants, like G64S, produce populations of viruses that are not as diverse as wild-type populations and this is the basis of their attenuation. The 'quasi-species' are considered as a cloud of viruses that contain potentially beneficial mutations that allow the population to evolve and adapt to new environments (Vignuzzi et al., 2006, Vignuzzi et al., 2008). The lack of diversity in the high fidelity population is thought to limit viral pathogenesis, as this population is unable to adapt to adverse growth conditions (Korboukh et al., 2014). The G64S mutation considered in chapter four had an additional benefit that may be relevant to future vaccine development. The high fidelity RdRp dramatically reduced recombination frequency, which is a problem with the current live attenuated strains (section 1.3).

There are other well-characterised RdRp variants that have altered fidelity phenotypes (Korboukh et al., 2014, Weeks et al., 2012). Due to the results with the high fidelity variant, G64S, the next step in this study was to introduce another well-characterised RdRp fidelity variant into the CRE-REP assay and observe its effect upon recombination frequency. Additionally, during the course of this study other interesting mutations to the poliovirus RdRp that may affect recombination frequency were made available and were also introduced into the assay (Raul Andino, personal communication). Currently, the CRE-REP assay is limited to an

area of 1.058 Kb, as previously outlined. Development of a new recombination assay that has a region of recombination that spans the entire non-structural region of the poliovirus genome was undertaken. This was deemed important, as it would allow a larger scale study on recombination frequency and location of recombination junctions.

Aims

The aim was to introduce additional RdRp variants into the RNA partners that are currently used in the CRE-REP assay and characterise their influence on recombination frequency. Additionally, development of an altered CRE-REP assay was undertaken. Potentially, recombination can occur outside of the current 1.058 Kb window which is a limitation of the current CRE-REP assay. Manipulation of viral RNA elements was considered as an approach that would expand this window to the entire non-structural region - an area of around 4.1 Kb.

5.2 RdRp variant K359R

All positive stranded RNA viruses share a conserved amino acid triplet motif at their active site that consist of a glycine and two aspartic acids (GDD) (Jablonski and Morrow, 1995). These amino acid residues in the active site of polymerases are thought to contribute only indirectly to catalysis by serving as ligands for the two divalent cations required for activity or substrate binding (Castro et al., 2009). Two proton transfer reactions are necessary for polymerase-catalyzed nucleotidyl transfer. The first is de-protonation of the terminal 3′-hydroxyl group of the nascent RNA (or primer). This leads to nucleophilic attack of the triphosphate moiety upon the incoming base. The subsequent pyrophosphate-leaving group is protonated in the second reaction by a general acid found within an area known as motif D (Castro et al., 2007, Castro et al., 2009, Weeks et al., 2012). Indeed, studies that have used model enzymes representing all four classes of nucleic acid polymerases show that the proton donor to pyrophosphate is an active site amino acid residue (figure 5.1). A conserved lysine at position 359 of the 3D coding region serves as the general acid in the poliovirus RdRp (Castro et al., 2009).

Functional studies that have mutated the lysine residue to an arginine (K359R) show that this polymerase is still active, but turns over nucleotides at a rate between 10-20 fold slower than wild-type RdRp at physiological pH (Castro et al., 2009). This study also suggested that replication speed might be directly linked to fidelity. A later study showed that the K359R mutation did indeed produce a viral RdRp that replicated slower and with a high fidelity phenotype when compared to wild type RdRp. A poliovirus population that carried the K359R variation was genetically stable, replicated well in cell culture, and was attenuated whilst eliciting a highly protective immune response in a murine model (Weeks et al., 2012). Due to the conservation of this residue in viral polymerases, this study suggested that a universal, mechanism-based strategy might exist for viral attenuation and vaccine development. The results in chapter four strongly suggested that fidelity also influences recombination frequency. The K359R mutation was therefore considered an important poliovirus RdRp variant that required investigating in this study.

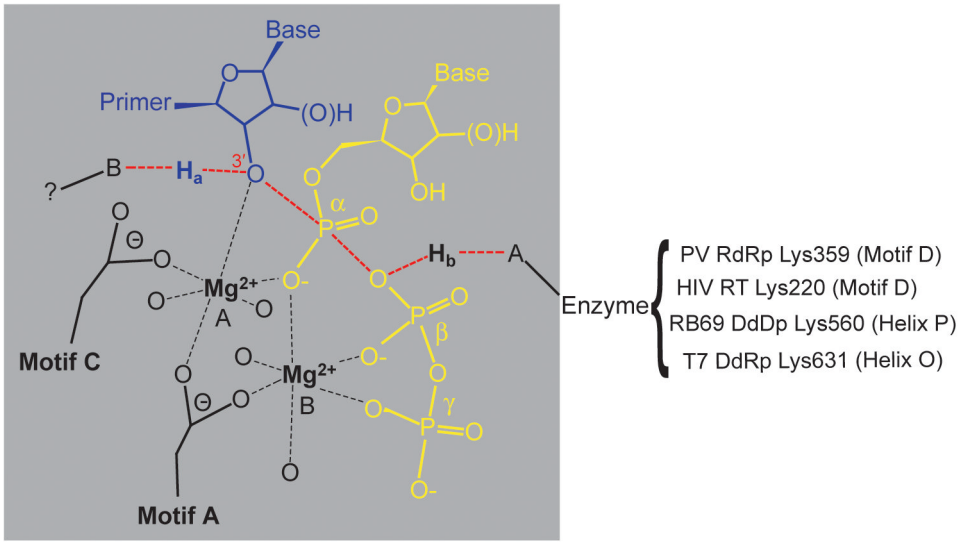

Figure 5.1: The general acid employed in RNA catalysis

Nucleoside triphosphate (yellow) enters the active site with a divalent cation (Mg^{2+}, metal B). This metal ion is coordinated by the phosphates of the nucleotide, an Asp residue located in structural motif A of all polymerases. Metal B orientates the triphosphate in the active site. A second divalent cation binds (Mg^{2+}, metal A) that is coordinated by the 3′-OH of the nascent RNA (blue), the nucleotide α-phosphate, as well as Asp residues of structural motifs A and C. Metal A lowers the pKa of the 3′-OH facilitating de-protonation and subsequent nucleophilic attack at physiological pH. As the transition state of nucleotidyl transfer is approached (indicated by dashed red lines), the nascent RNA 3′-OH proton, Ha, is transferred to an unidentified base (B). The model suggests that the pyrophosphate-leaving group is protonated (Hb) by a basic amino acid on the enzyme. The positions of the candidate general acids of the model polymerases are shown. DdDp = DNA dependent DNA polymerases. RT = reverse transcriptases. DdRp = DNA dependent RNA polymerases. Adapted with permission from Castro et al., 2009.

The K359R mutation was introduced into the PV1 and PV3 replicon cDNA (pRLucWT and pT7rep3-L) along with the mutated CRE acceptor template (pT7FLC/SL3) by overlap extension PCR. All constructs were sequenced to verify the presence of the mutation and used to transcribe RNA using T7 polymerase. An initial luciferase assay was undertaken to look at the replication kinetics of the K359R variant compared to its wild type counterpart using both PV1 and PV3 replicons. HeLa cells in 24 well plates were transfected in duplicate wells with 250 ng of wild type RdRp replicon or replicon carrying the K359R mutation. Additional controls were also used, including a mock transfection and transfection in the presence of guanidine hydrochloride (an inhibitor of RNA replication). Samples were harvested at the time points indicated and luciferase activity was measured and normalised using a mock transfection control (figure 5.2AB).

The luciferase signal of the K359R RdRp variant replicons indicated that the K359R mutation was inhibiting replication when compared to the luciferase signal from a replicon with an unmodified RdRp. This was not surprising given that previous studies have shown this RdRp variant replicates at a speed around 10-fold slower than wild type (Weeks et al., 2012, Castro et al., 2009). After 14 hrs in both experiments the luciferase signal is ~30% of the unmodified replicons, consistent with a previous study (Weeks et al., 2012). It has to be noted that there was a definite 'stalling' in replication with both mutant replicons between 2-6 hrs when compared to unmodified replicon. The signals were however higher than the guanidine hydrochloride control that produced a luciferase signal based upon translation only, as replication was inhibited. This showed that the modified replicons were replicating, albeit at a lower level than the unmodified replicon.

Both intratypic and intertypic combinations were then used in a CRE-REP assay with the yield of recombinant virus produced when the K359R mutation is present compared to a wild type RdRp combination control. L929 cells were seeded in 12 well plates and co-transfected in triplicate wells with 0.5 μg of total RNA in a 1:1 ratio (replicon: CRE mutant), RNA pairings as shown in figure 5.2CD. Cells were incubated for 48 hrs and then the transfection supernatant was used to inoculate HeLa cell monolayers for plaque assays. Following 60 hrs incubation, cells

were stained with crystal violet and virus titre was quantified. In both intratypic and intertypic CRE-REP assays no recombinant virus was produced when the K359R mutation was present in the replicon (donor template) or in both templates (donor and acceptor). At the same time recombinant progeny was produced when wild-type RdRp partners were present. This positive control indicated that the assay was functional. Many additional experiments were subsequently carried out that used an alternate rodent cell line (BsrT7) and various donor to acceptor RNA ratios. In all experiments no recombinant virus was identified when the K359R mutation was present.

It was considered that the production of recombinant virus may have occurred but was below the level of detection. If any recombinant were produced it would have carried the K359R mutation, which slows replication and may not have been detectable in a plaque assay (Craig Cameron, personal communication). In order to answer this, additional controls were done. Transfection supernatant was also used in $TCID_{50}$ assays (section 2.1.5) as a method to quantify recombinant virus. The control CRE-REP assays (wild type RdRp partners) produced plaque assay, and $TCID_{50}$ results that correlated well (data not shown). In contrast, no recombinant virus was found in any $TCID_{50}$ assay when the K359R mutation was present.

The K359R mutation in a full length poliovirus construct produces a titre of virus that is normally around one log_{10} lower than wild type (Weeks et al., 2012). Potentially, this defect in replication alone could have accounted for the lack of recombinant virus seen in the intertypic CRE-REP assay, which usually yields between 80-140 pfu/ml. However, this fall in replication does not account for the lack of intratypic recombination that was observed. Intratypic yields in the CRE-REP assay are typically over 1000 pfu/ml, we would therefore have expected to see recombinant virus even if replication were inhibited. Potentially, the K359R mutation that has a high fidelity phenotype that is linked to its slower replication rate is non-recombinogenic.

In order to compensate for any replication defect that the K359R mutation provides, and to consider recombination outside the current 1.058 Kb window a new approach to expand the region within which recombination could occur was developed.

A

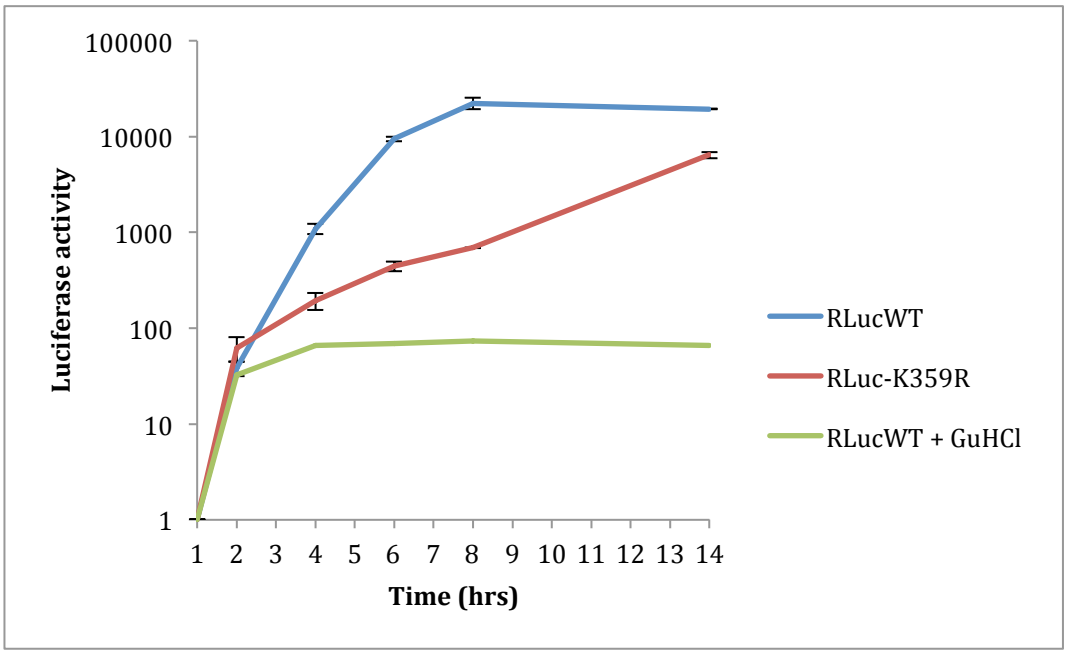
100000
10000
1000
100
10
1
Luciferase activity
1 2 3 4 5 6 7 8 9 10 11 12 13 14
Time (hrs)
RLucWT
RLuc-K359R
RLucWT + GuHCl

B

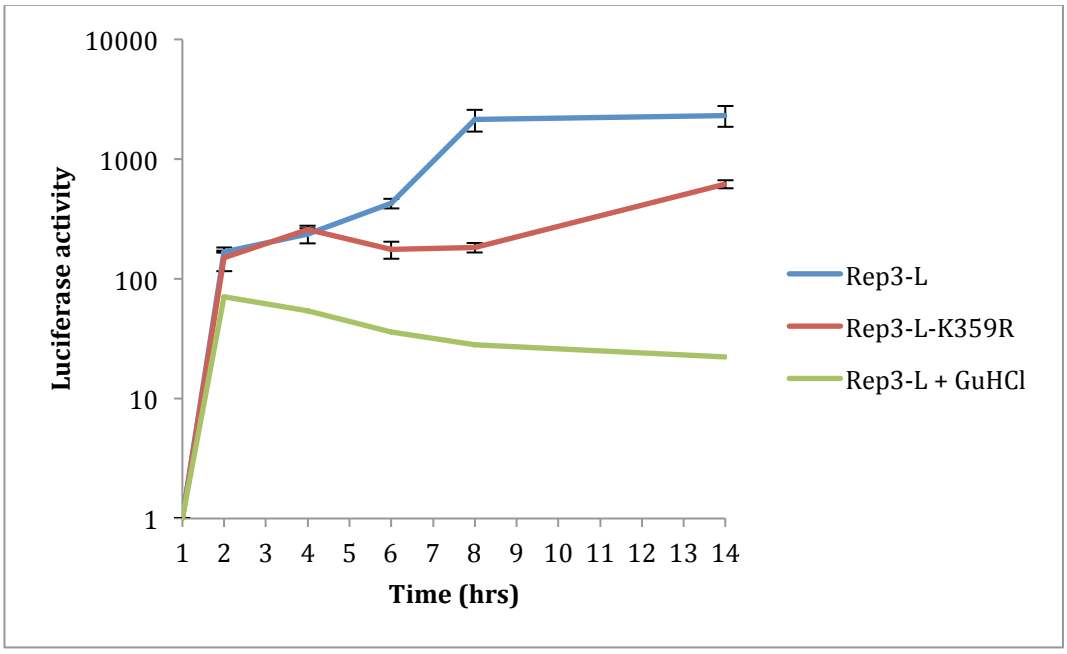
10000
1000
100
10
1
Luciferase activity
1 2 3 4 5 6 7 8 9 10 11 12 13 14
Time (hrs)
Rep3-L
Rep3-L-K359R
Rep3-L + GuHCl

C

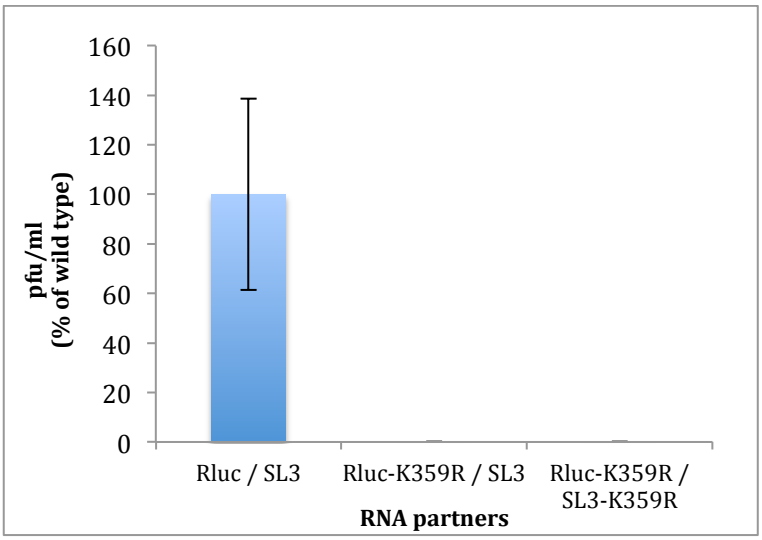

D

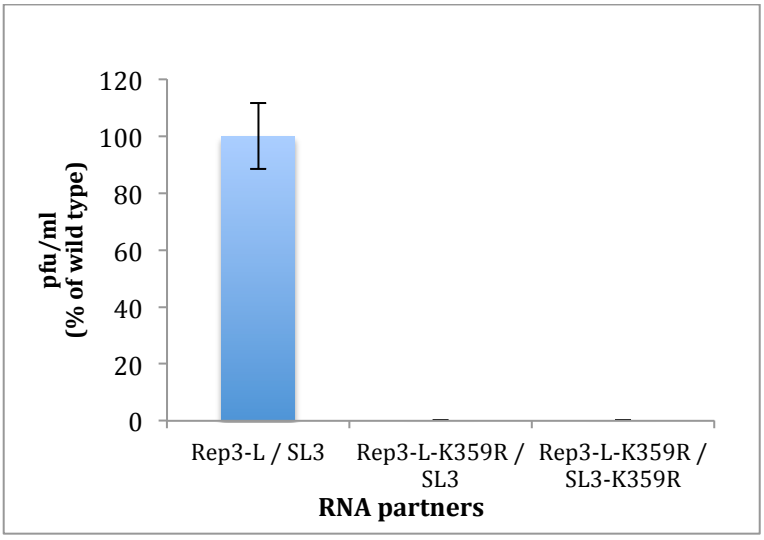

Figure 5.2: Replication kinetics and recombination frequency of the RdRp K359R variant

(A) + (B) Replication kinetics of a PV1 sub-genomic replicon (RLucWT) and PV3 sub-genomic replicon (Rep3-L) bearing a K359R high fidelity polymerase mutation. 250ng of RNA was transfected into HeLa cells. Samples were taken at the times indicated and luciferase activity was measured and normalised using a mock transfected control. Error bars indicate standard deviation of two independent samples. Guanidine hydrochloride control as indicated **(C) + (D)** Influence of a K359R high fidelity polymerase upon the frequency of intertypic and intratypic recombination. The data represents the mean from three independent samples. Error bars indicate standard deviation. RNA partners as indicated.

5.3 An expanded *in vitro* recombination assay

The CRE-REP assay has a region of recombination of 1.058 Kb that is determined by the lesions that are present in the donor and acceptor templates (described in section 3.1). The function of the 2C CRE in poliovirus is not location specific. A previous study has shown that positioning of a synthetic CRE into the hyper-variable region of the 5'NTR of the CRE mutated genome SL3 rescues replication (Goodfellow et al., 2003a). Additionally, the positioning of a native CRE within the 3'NTR of FMDV (normally found within the 5'NTR) rescues replication of a CRE defective virus (Mason et al., 2002).

Mutation of the native CRE and positioning of a synthetic CRE into the 3'NTR of PV1

By manipulating the position of the CRE in the PV1 replicon (pRLucWT) a new intertypic recombination assay was developed. Eight synonymous mutations, similar to the ones put into the pT7FLC/SL3 template (Goodfellow et al., 2000) were incorporated into pRLucWT by a process of overlap extension PCR (figure 5.3A). This ensured that the amino-acid coding region of 2C was maintained, but the secondary structure of the RNA in this area was affected. The presence of the desired mutations was verified by sequencing, with the predicted affect upon secondary RNA structure of the critical CRE stem-loop shown in figure 5.3B. This was called pRLucΔCRE. A unique restriction enzyme site, *BssHII*, was then introduced into the 3'NTR of the pRLucΔCRE directly after the termination codon by overlap extension PCR. A 34 nt synthetic CRE shown to restore replication in poliovirus (Goodfellow et al., 2003a) was then cloned into the cDNA by use of the *BssHII* restriction enzyme site (figure 5.4). Two complementary oligonucleotides carrying the required sequences with complementary 'sticky' ends of a cleaved *BssHII* restriction enzyme site were annealed and used as templates (see table 2.4). The decision to use a synthetic CRE that is smaller and different in sequence to the native CRE was done to avoid duplicated sequences in the virus genome. Importantly, the design of the 3'NTR CRE replicon was predicted not to alter the native 3'NTR structure, including the important X and Y stems (Rohll et al., 1995). The cDNA was verified by sequencing and was called pRLucΔCRE_3'CRE. To ensure that this modification did not compromise replication, a luciferase time-course assay was carried out (figure 5.5). Oligonucleotides that were used

A

```
          4449                                                  4499
PV1         *                                                     *
CRE:TATTAACAACTACATACAGTTCAAGAGCAAACACCGTATTGAACCAGTATGTTTGCTAGTA
MUT:TATTAACAACTATATCCAATTTAAATCCAAACACCGTATCGAACCAGTATGTTTGCTAGTA
```

B

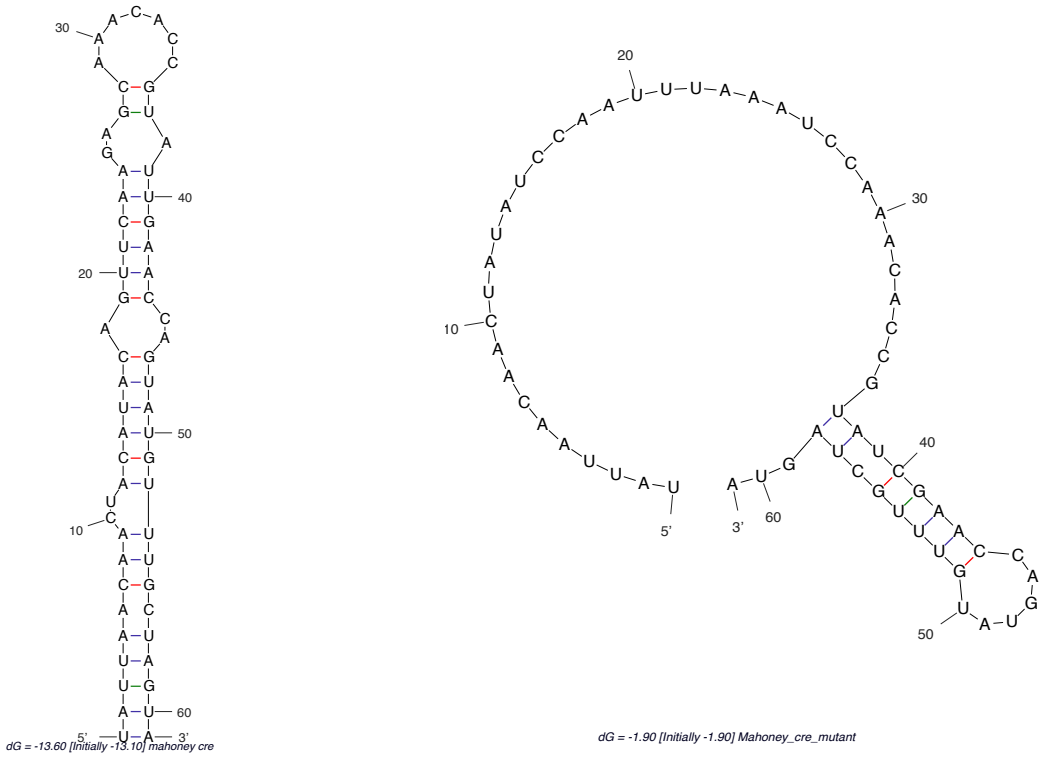

Figure 5.3: Sequence alignment and predicted secondary structure of wild type and mutagenized PV1 CRE stem loop

(A) Alignment of native PV1 2C CRE and mutated PV1 2C CRE bearing 8 synonymous mutations, shown in red. Stars and numbering indicate position within the PV1 Mahoney genome. The CAAACA motive that is required for CRE dependent VPg uridylylation is shown underlined. **(B)** Wild-type PV1 CRE structure (left) and the predicted mutated PV1 CRE structure (right) created by MFold (Zuker and Stiegler, 1981). Numbering from 1-61 based upon first and final nt in the stem-loop structure.

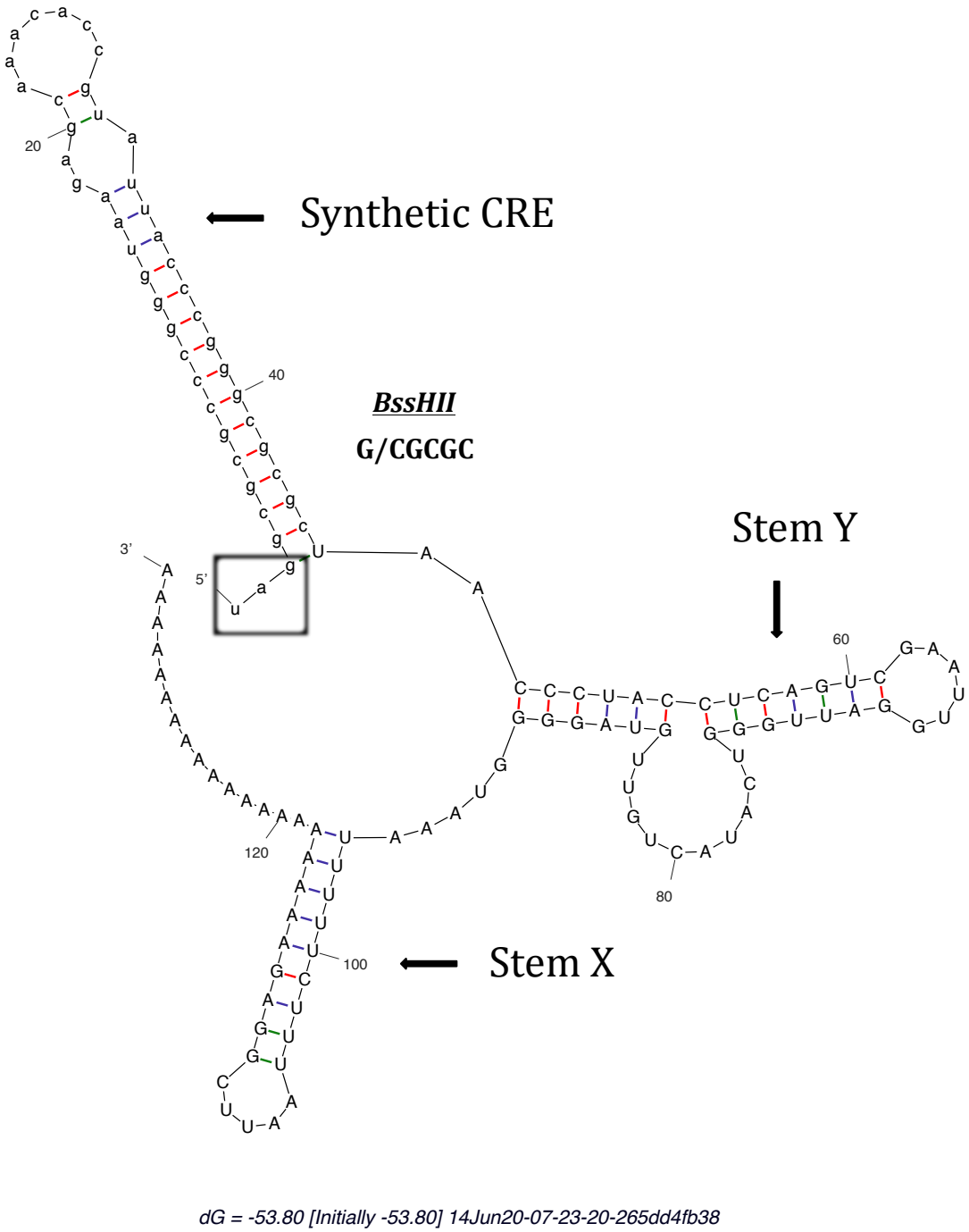

Figure 5.4: Predicted secondary structure of the 3'NTR of FLCΔCRE_3'CRE and pRLucΔCRE_3'CRE following insertion of a synthetic CRE.

MFold predicted structure of the CRE modified 3'NTR. Numbering from 1-133, beginning from the termination codon UAG (boxed). A synthetic CRE known as Synth3 (Goodfellow et al., 2003a) along with a unique *BssHII* restriction enzyme site are located after the termination codon. *BssHII* restriction sequence as indicated. Predicted structures of stem X and Y are also indicated (Rohll et al., 1995).

in all of the constructs can be found in section 2.9. L929 cells in 12 well plates were transfected with RNA as indicated. Samples were harvested at various time-points and luciferase activity was measured and normalised using a mock transfection control. The RLucΔCRE template produced a luciferase signal over time that was very similar to the controls, which had been incubated with guanidine hydrochloride indicating that this was from translation only. This chemical, as previously described, is a reversible inhibitor of RNA replication (Pfister and Wimmer, 1999). As expected, this result indicated that the synonymous mutations introduced into the 2C CRE had indeed inhibited RNA replication. The RNA generated from pRLucΔCRE_3'CRE in contrast, produced a luciferase signal over time that was slightly higher than the RLucWT, indicating that it was replication competent. This demonstrated that the positioning of a synthetic CRE into the 3'NTR does not significantly influence replication.

To further validate the results obtained in the luciferase assay it was decided to introduce the same modifications into a PV1 full-length clone to characterise their effect. This was felt important, as the luciferase assay is an indirect way to measure RNA replication only. Potentially, the positioning of a synthetic CRE into the 3'NTR could have had an effect on packaging of the viral RNA. This was done in a similar process to the PV1 replicon. Briefly, overlap extension PCR was used to introduce the 8 synonymous mutations into a PCR product. The PCR product was then sub-cloned into the PV1 Mahoney full-length clone background using the unique restriction enzyme sites *NheI* and *BglII*. This produced an intermediate known as pPV1FLCΔCRE, analogous to pT7FLC/SL3. The 3'NTR region of the pRLucΔCRE_3'CRE was then sub-cloned into the intermediate pPV1FLCΔCRE by use of the unique restriction enzyme sites *ApaI* and *BglII*. This produced the final pFLCΔCRE_3'CRE construct which was verified by sequencing and restriction enzyme digestion. An experiment was carried out that compared virus yields from a wild type virus and a CRE modified version. The PV1 full-length clone, pPV1FLCΔCRE and pFLCΔCRE_3'CRE were linearised with the restriction enzyme *ApaI* and used as templates to transcribe RNA using T7 polymerase. L929 cells in a 12 well plate were transfected individually with 250 ng RNA in triplicate wells and left to incubate for 48 hrs. Dilutions of transfection supernatant were then used to inoculate HeLa cell monolayers for

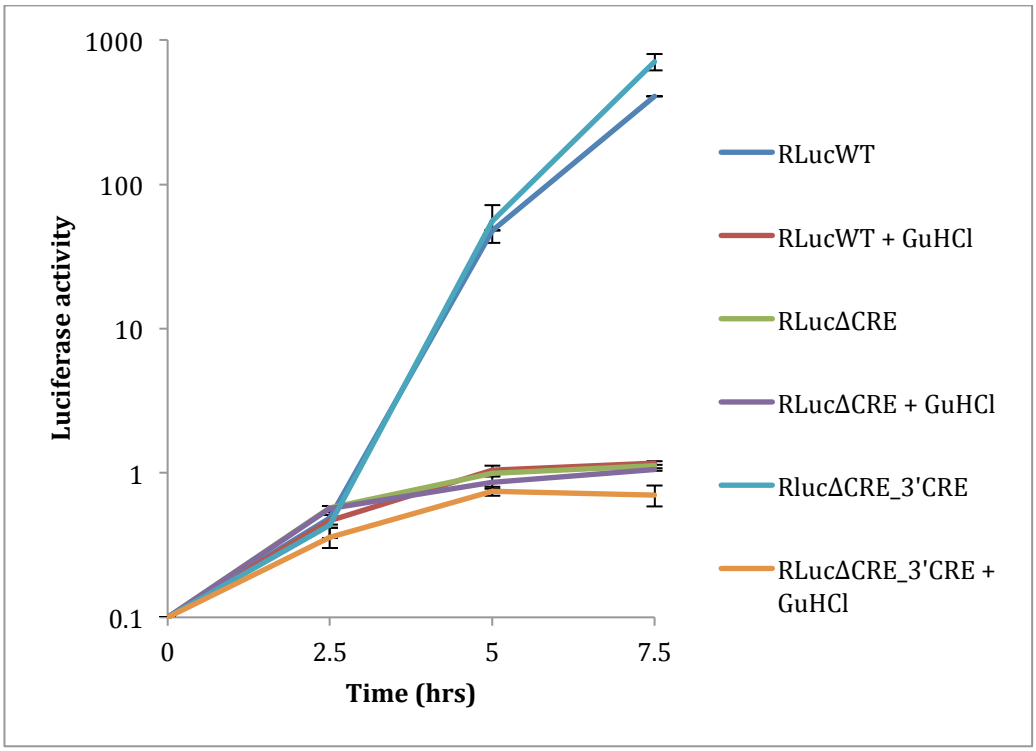

Figure 5.5: PV1 sub-genomic replicon bearing a 3'UTR CRE luciferase time-course

250ng of RNA generated *in vitro* was transfected into L929 in triplicate. RNA as indicated. Samples were harvested at 2.5hr time-points and measured for luciferase activity and normalized using a mock transfected control. GuHCl indicates guanidine hydrochloride, a reversible inhibitor of poliovirus RNA replication.

A

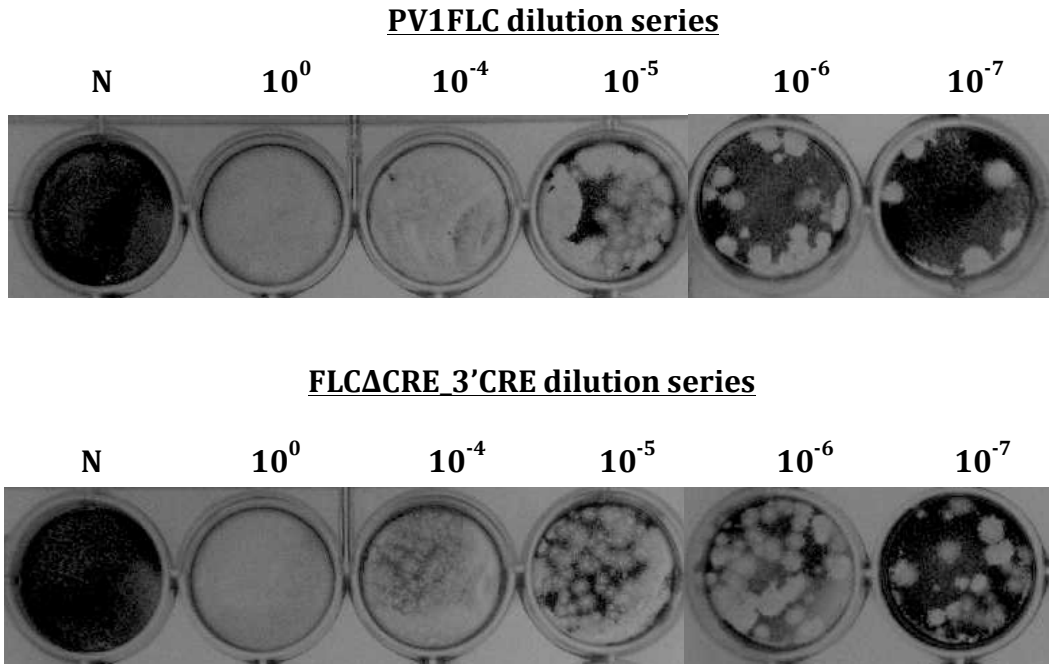

B

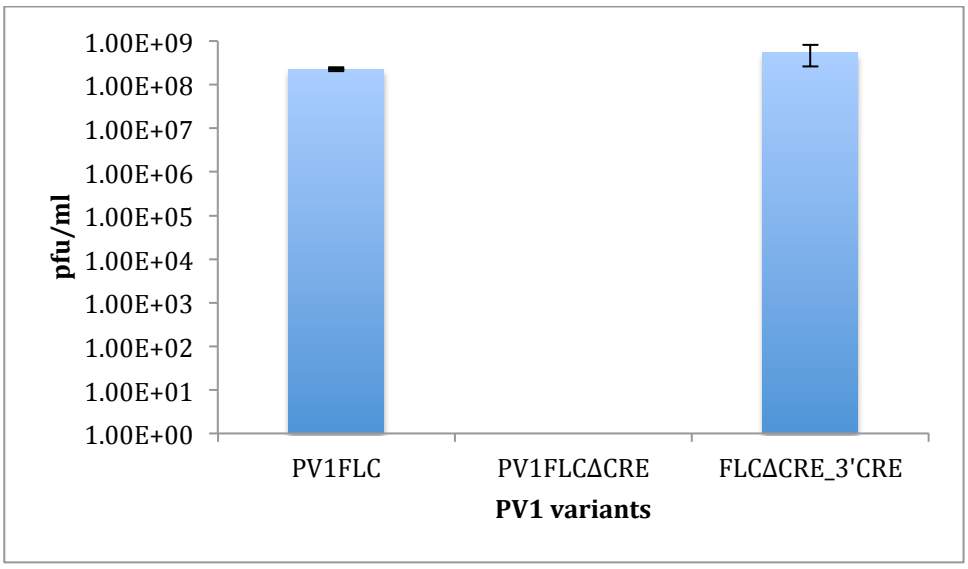

Figure 5.6: Synthetic CRE in the 3'NTR of PV1FLCΔCRE restores replication

(A) Representative crystal violet stained Hela cell monolayers inoculated with transfection supernatant and overlaid with plaque assay overlay medium. Dilutions as indicated. RNA as indicated (N) indicates negative control **(B)** Figures show virus yield from three independent samples. Error bars indicate standard deviation.

plaque assays. Cells were incubated for 60 hrs, stained with crystal violet and photographed (figure 5.6). As expected the PV1FLCΔCRE transfection supernatant produced no plaques, which indicated no virus was present (data not shown), in agreement with the same mutations that were introduced into a PV3 virus (Goodfellow et al., 2000). This supported the luciferase assay produced from the replicon containing the same 2C CRE mutations. Blind passage of the supernatant was subsequently done five times, and no virus was found. The positioning of a synthetic CRE into the 3'NTR of the PV1FLCΔCRE rescued replication, as indicated by the formation of plaques. The RNA generated from pFLCΔCRE _3'CRE produced a yield of virus that was almost identical to the yield from the PV1 wild type RNA. In addition, there was no discernable difference in plaque phenotype. This result fully supported the luciferase time-course assay and indicated that the CRE can be positioned into the 3'NTR without affecting viability and yield of the virus from a single transfection.

However, it remained to be determined if re-positioning of the CRE had any affect in a mixed infection environment. It was therefore deemed necessary to carry out a competition assay, which included wild-type virus and the re-positioned CRE variant. If there were any subtle differences in replication capability then this type of assay would highlight it. HeLa cells in T20 flasks were infected at an M.O.I of 10 at a ratio of 1:1, 10:1 and 1:10 (PV1 wild type virus: FLCΔCRE_3'CRE virus). Each was serially passaged five times. RNA was extracted from passage 1 and 5 respectively and a region that covered the native 2C CRE region was amplified by RT-PCR using the forward primer PV1/3-3280F and reverse primer PV1-5440R. An equal mass of PCR product was then run on a 1% agarose gel (figure 5.7A). The PCR products from each sample, as well as the controls, migrated to a similar position on the gel, as expected. The introduction of the 8 synonymous mutations into the native CRE also introduced a unique *SwaI* restriction enzyme site (Goodfellow et al., 2000). This site was used to screen the relative proportion of wild type virus to CRE modified virus in a mixed population infection. An equal mass of each PCR product was incubated with the *SwaI* restriction enzyme then run on a 1% agarose gel (figure 5.7B). The controls indicated that this restriction enzyme is unique to the FLCΔCRE_3'CRE virus as this PCR product was cut to produce two bands and the wild type virus PCR product did not.

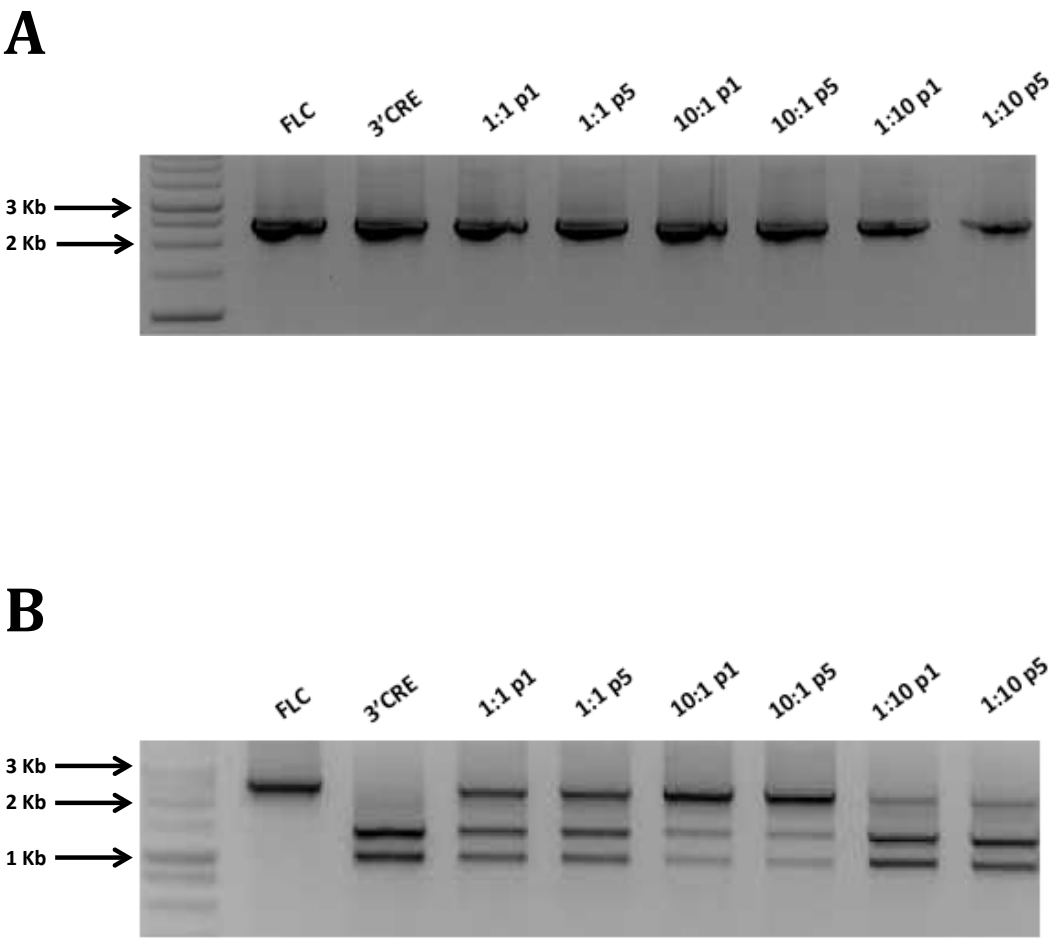

Figure 5.7: PV1FLC and FLCΔCRE_3'CRE competition assay

(A) Gel electrophoresis of RT-PCR product of the 2C CRE region of PV1FLC and FLCΔCRE_3'CRE. Run on a 1% agarose gel and stained with ethidium bromide. HeLa cells were infected at an M.O.I of 10 either individually or at a 1:1, 10:1 and 1:10 ratio of PV1FLC to FLCΔCRE_3'CRE and passaged 5 times. Ratios and passages as indicated **(B)** The same RT-PCR products were then subjected to restriction enzyme digestion by *SwaI*, a unique site to the FLCΔCRE_3'CRE genome.

Additionally, the controls show that sufficient enzyme was present to cut all available restriction sites. The 1:1 ratio infection PCR product following restriction enzyme screening produced banding with no visual difference in density from passage 1 and passage 5. This indicated that the modified virus (FLCΔCRE_3'CRE) was present and competed well with the wild type virus. The 1:10 and 10:1 ratio infections also produced banding patterns that inferred that the FLCΔCRE_3'CRE virus competed well in a mixed infection environment. Taken together, these results show that positioning of a synthetic CRE into the 3'NTR of poliovirus does not affect replication and the virus's ability to compete.

By positioning a synthetic CRE sequence within the 3'NTR of the RLucΔCRE replication was rescued and this modification was shown to have no affect upon the overall replication of a full-length clone carrying the same alterations. The new replicon RLucΔCRE_3'CRE could therefore be used as a donor template that allowed for an expanded intertypic CRE-REP assay hereafter termed 3'-CRE-REP. The acceptor template remained the same as in the CRE-REP assay (SL3). The functional synthetic CRE sequence in the 3'NTR of the replicon would be incorporated after initiation of anti-sense RNA synthesis, any template exchange to SL3 past this point would potentially produce a viable recombinant genome (figure 5.8). This increased the potential region of recombination from 1.058 Kb (CRE-REP) to 4.1 Kb, incorporating the entire P2 and P3 non-structural coding region.

An assay was carried out to determine if the 3'-CRE-REP approach increased recombinant progeny yield when compared to the control CRE-REP assay. Expectations were that the 3'-CRE-REP assay would produce more recombinant progeny than the CRE-REP, and this would correlate with the increased region of recombination. L929 cells in 12 well plates were co-transfected in triplicate wells with intertypic partners (CRE-REP and 3'-CRE-REP). An additional co-transfection control involving the RNA partners RLucΔCRE and SL3 was also done. Total RNA was 0.5 μg in a 1:1 ratio (replicon: CRE mutant genome). Cells were incubated for 48 hrs and the transfection supernatant was used to inoculate HeLa cell monolayers for plaque assays. Following 60 hrs incubation, cells were stained with crystal violet and photographed (figure 5.9). Additional single transfection controls were also carried out (data not shown).

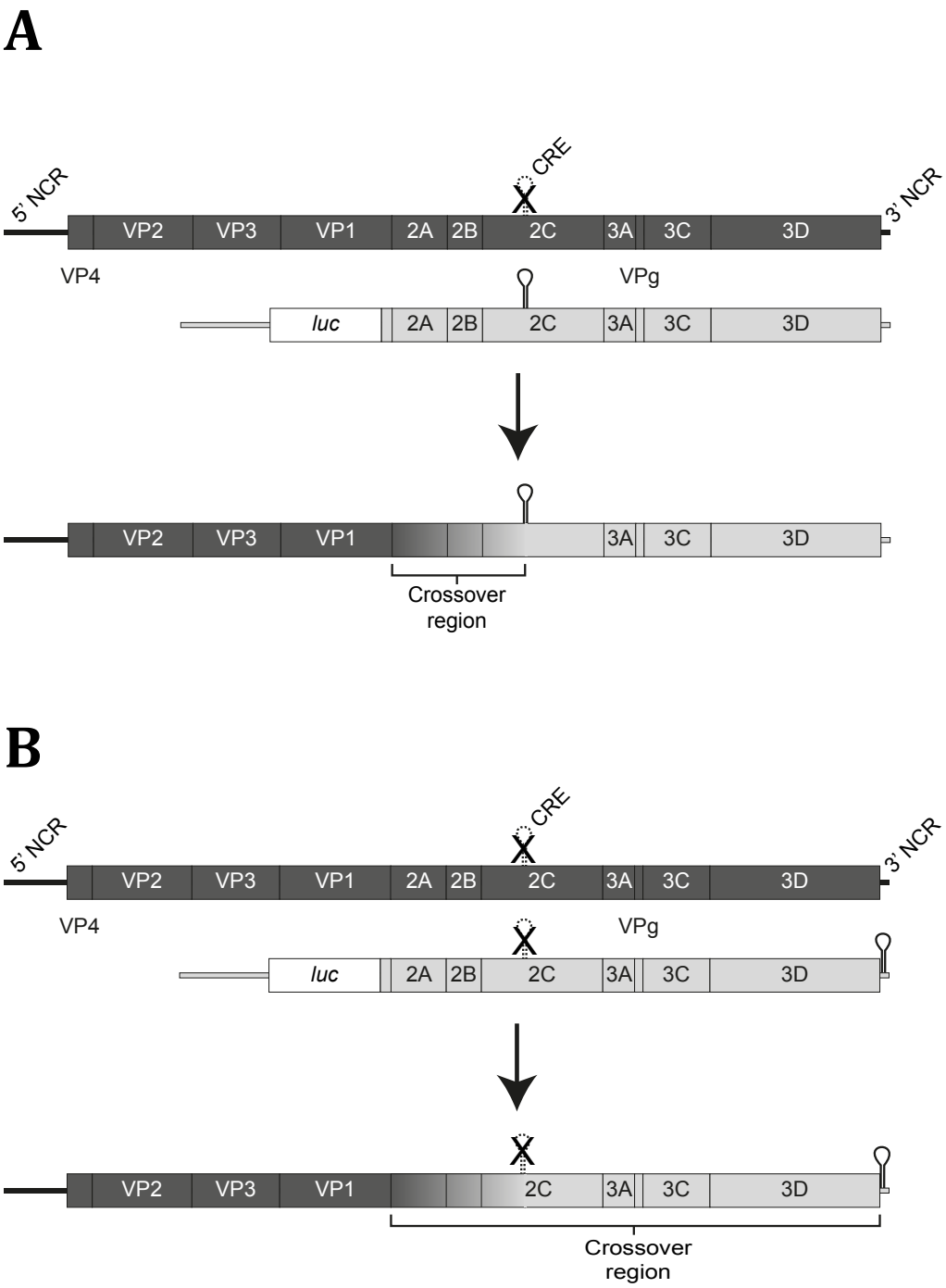

Figure 5.8: Expansion of the original CRE-REP assay

(A) Original CRE-REP assay, see chapter 3 for description **(B)** Expanded CRE-REP assay known as 3'-CRE-REP. The upper genome (dark shading) bearing a defective CRE indicated as a broken line with a superimposed X in the 2C-coding region and a luciferase-encoding replicon (light shading) that also bears a defective 2C CRE. The sub-genomic replicon has a 3'NTR CRE as indicated by an intact stem. Following co-transfection into permissive cells (indicated by an arrow), a replication competent recombinant genome may be recovered of the generic structure shown, consisting of the 5' part of the genome derived from the CRE-defective parent (the acceptor) and the 3' part of the genome from the luciferase-encoding replicon (the donor). This modification increases the potential 'zone' of recombination from 1.058Kb to 4.1Kb.

A

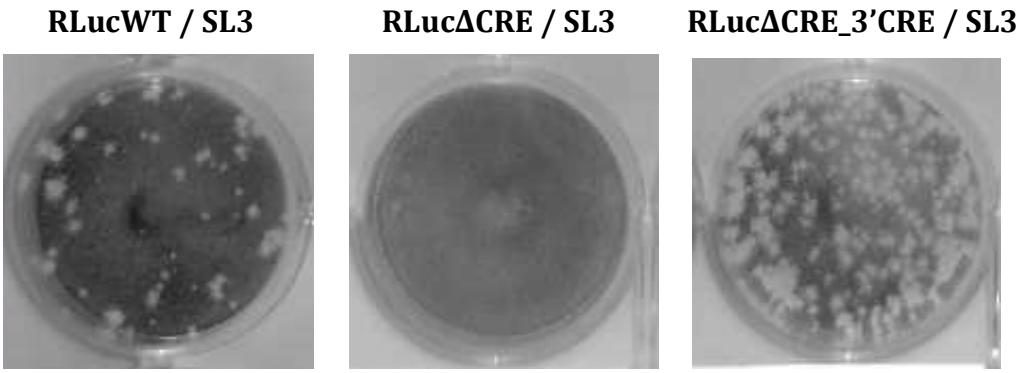

B

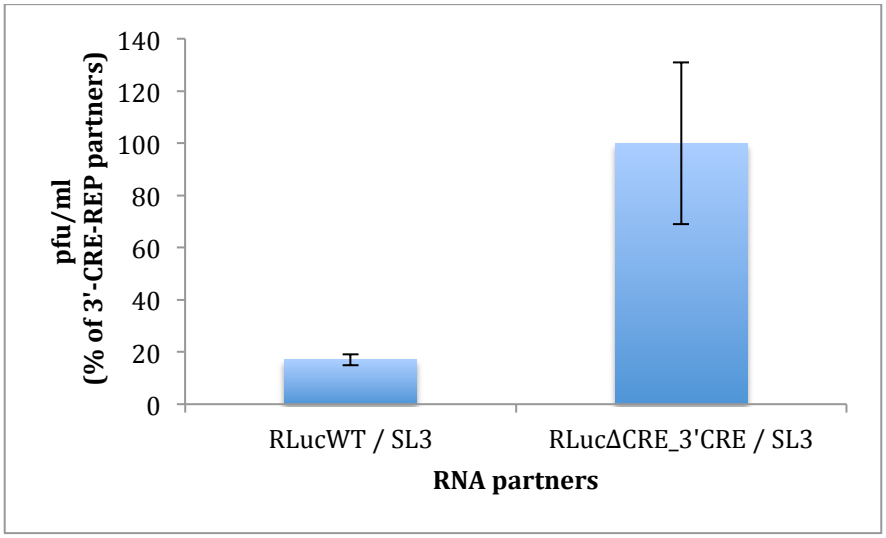

Figure 5.9: 3'-CRE-REP intertypic *in vitro* recombination assay

(A) Representative crystal violet stained Hela cell monolayers inoculated with transfection supernatant and overlaid with plaque assay overlay medium. Transfected RNA partners as indicated. Individual transfections yielded no virus (not shown) **(B)** Quantification of recombinant virus yield. Error bars indicate standard deviation of three independent samples.

As expected the co-transfection with RLucΔCRE and SL3 yielded no recombinant virus, showing that the presence of a functional CRE from one parental genome is required. The yield of recombinant progeny from the intertypic CRE-REP assay was broadly in line with previous results averaging at 157 pfu/ml. This control showed that the conditions for any recombination assay were satisfactory. In contrast the intertypic 3'-CRE-REP assay produced a yield of recombinant progeny that averaged at 920 pfu/ml, a 5.85 fold increase when compared to the CRE-REP assay, larger than expected. Subsequent repeated experiments found the increase in yield to be reproducible and consistent (data not shown). A large in-depth study upon the type of intertypic recombinant virus isolated from the 3'-CRE-REP is being conducted in collaboration with a colleague, Fadi Alnaji. The aim of this work is to identify and characterise the recombinant junctions across the 4.1 Kb window. This in principle will identify any link between RNA sequence and structure that may determine the location of recombination.

5.4 K359R high fidelity RdRp variant in the 3'-CRE-REP assay

As described in section 5.2, the K359R RdRp variant typically reduces replication rates by around 1 $\log_{10}$ when compared to wild type (Weeks et al., 2012). This could have explained why no intertypic recombinant was isolated from the CRE-REP assay when the mutation was present in the donor and acceptor templates. It was hoped that the near six-fold increase in recombinant progeny observed in the 3'-CRE-REP would overcome any replication defect that the K359R variant provides. The K359R mutation was therefore introduced into the pRLucΔCRE_3'CRE by overlap extension PCR using the unique restriction enzyme sites *BglII* and *ApaI*. The construct was verified by sequencing the entire sub-cloned region. The cDNA carrying the K359R mutation was then linearised with *ApaI* and the template was used to transcribe RNA using T7 polymerase. An experiment was carried out that measured the yield of intertypic recombinant virus produced when the K359R mutation was present compared to a wild type RdRp combination control. L929 cells in a 12 well plate were co-transfected in triplicate wells with 3'-CRE-REP partners. An additional co-transfection involving 3'-CRE-REP partners carrying the K359R mutation was also done. Total RNA was 0.5 μg in a 1:1 ratio (replicon: CRE mutant genome). Cells were incubated for 48 hrs and then the transfection supernatant was

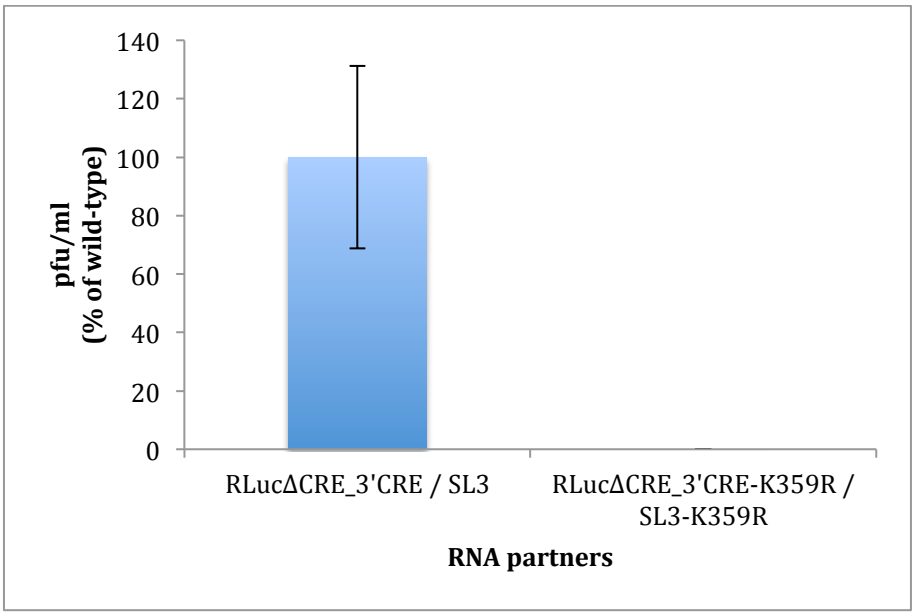

Figure 5.10: 3'-CRE-REP RdRp variant K359R

Quantification of intertypic recombinant yield from co-transfected L929 cells. RNA partners as indicated. The data represents the mean from three independent samples. Error bars indicate standard deviation.

used to inoculate HeLa cell monolayers for plaque assays. Following 60 hrs incubation, cells were stained with crystal violet and recombinant progeny quantified (figure 5.10). The control co-transfection produced a yield of recombinant virus broadly in line with previous results and averaged 1200 pfu/ml. This indicated that the conditions for the assay were satisfactory. No recombinant virus was identified from the K359R variant co-transfection supernatant. The supernatant from this experiment was further analysed by $TCID_{50}$. The results of the control $TCID_{50}$ correlated well with the plaque assay results. No virus was identified with the K359R samples. This experiment was repeated and produced similar results (data not shown).

5.5 RdRp variant D79H-Y275H

During the course of this investigation additional RdRp mutations that were considered important in poliovirus recombination were made available. The Raul Andino research group at the University of California, San Francisco, U.S.A. isolated poliovirus variants from an assay that were unable to recombine. The Andino group identified mutations within the RdRp coding sequence that were considered important. Selection of the RdRp variants was done by a *green fluorescent protein* (GFP) retention assay. In the assay, a poliovirus construct, which has the GFP reporter gene inserted between the VP1 and 2A genes, is used to infect HeLa cells. Normally, the GFP reporter gene is rapidly lost following serial passage in HeLa cells in a process that is analogous to the 'resolution' stage of recombination outlined in chapter three. Using a process of fluorescence-activated cell sorting (FACS), cells that retain expression of the GFP were isolated (infected with virus that has not lost the GFP coding gene). Subsequent isolation and characterisation of the poliovirus RNA identified two mutations that were present in the RdRp coding region, D79H and Y275H respectively. These mutations were considered important because they were the only ones found in the RdRp consensus sequence produced (Raul Andino, personal communication). The mutations were isolated from a PV1 Mahoney background, but the residues identified are conserved in all poliovirus strains. It was therefore considered important to characterise these mutations in the CRE-REP assay and also in the molecular clone JC105B, which was used in this study to look at the resolution stage of recombination. The mutations were introduced into the PV1 replicon (pRLucWT) individually

and dually by overlap extension PCR using the unique restriction enzymes *BglII* and *ApaI*. This produced the replicons pRLuc-D79H, pRLuc-Y275H and pRLuc-D79H-Y275H. The presence of all mutations was verified by sequencing of the constructs. All three were linearised with the restriction enzyme *ApaI* and templates were used to transcribe RNA using T7 polymerase. A luciferase assay was carried out to characterise the effect of the mutations on replication. L929 cells in 12 well plates were transfected with 250 ng of replicon RNA in duplicate wells. Luciferase activity was measured and normalised using a mock transfection control (figure 5.11). The D79H mutation reduced luciferase signal to 56% of wild type and the Y275H mutation reduced luciferase signal to 36% of wild type at 7.5 hrs post transfection. When both mutations are present, overall replication at 7.5 hrs was reduced to 31% of wild type.

The replicons used in the luciferase assay were then introduced into a CRE-REP assay, with the wild type intertypic partners considered as the control. L929 cells in 12 well plates were co-transfected in triplicate wells with 0.5 µg of total RNA in a 1:1 ratio (replicon: CRE mutant), RNA partners as indicated (figure 5.12A). Cells were incubated for 48 hrs and then the transfection supernatant was used to inoculate HeLa cell monolayers for plaque assays. Following 60 hrs incubation, cells were stained with crystal violet and recombinant yield was quantified. When the D79H mutation was present in the donor replicon template recombination progeny yield fell to 57% of wild type, in line with the fall in replication that was characterised in the luciferase assay. When the Y275H mutation was present alone or in combination with the D79H mutation in the donor replicon template no recombinant progeny was recovered. The supernatant was additionally subjected to a $TCID_{50}$ assay, which produced results in line with the plaque assay (data not shown). This result suggested that the presence of the Y275H mutation in the donor template alone might have been enough to inhibit recombination.

For completeness the D79H and Y275H mutations were also introduced into the acceptor template pT7FLC/SL3 by overlap extension PCR using the unique restriction enzyme sites *XhoI* and *SalI*. The presence of the mutations was confirmed by sequencing. This template was also

A

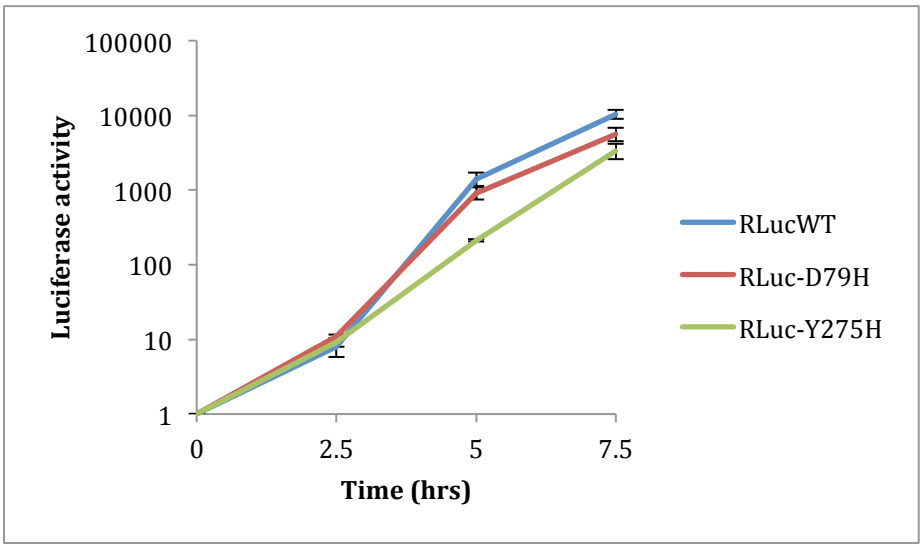

B

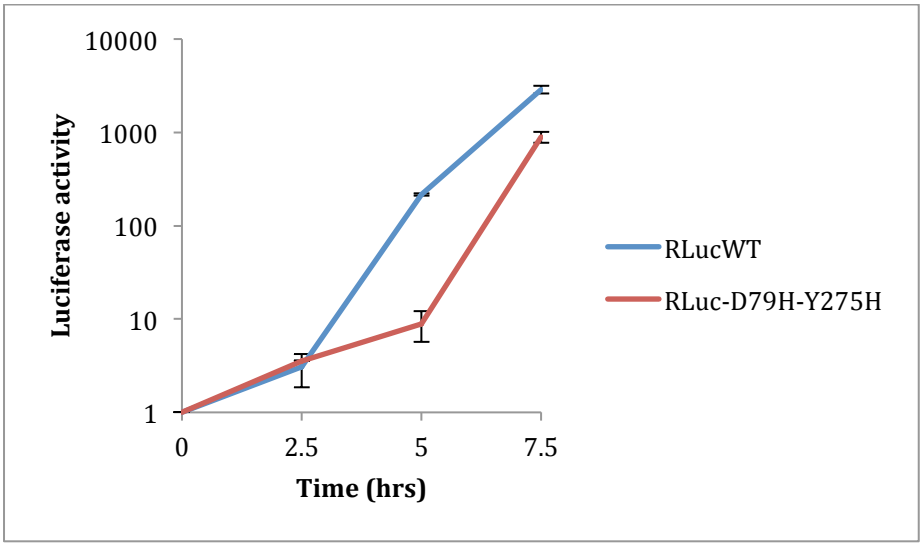

Figure 5.11: pRLucWT replicon bearing a D79H and/or Y275H RdRp luciferase time-course

(A) Replication kinetics of a PV1 sub-genomic replicon (RLucWT) bearing either a D79H or Y275H polymerase mutation. 250ng of RNA was transfected into L929 cells. Samples were taken at the times indicated and luciferase activity was measured and normalised using a mock transfected control. Error bars indicate standard deviation of two independent samples **(B)** Replication kinetics of a PV1 sub-genomic replicon (RLucWT) bearing a dual D79H - Y275H polymerase mutation. All other aspects remain the same as (A)

A

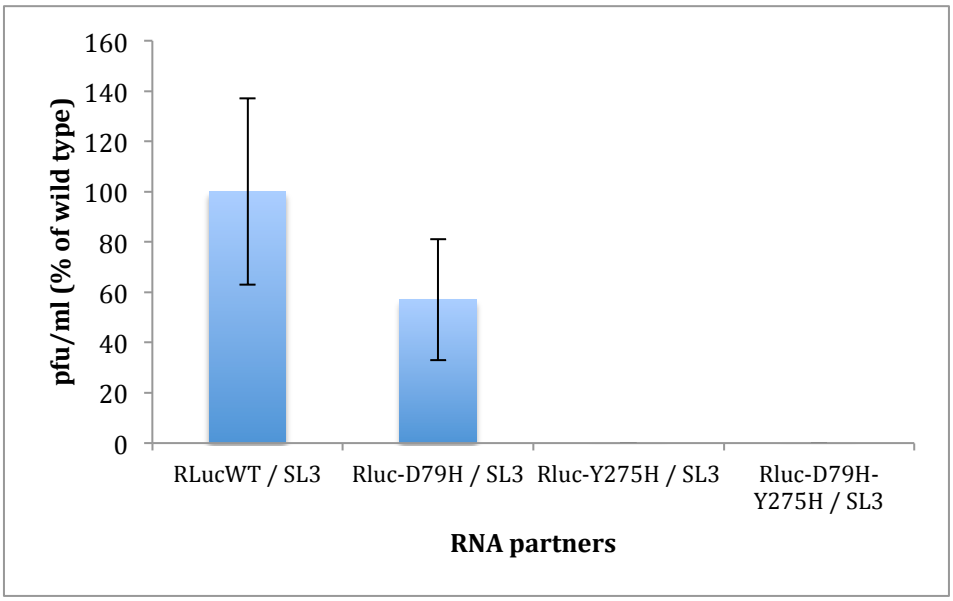

B

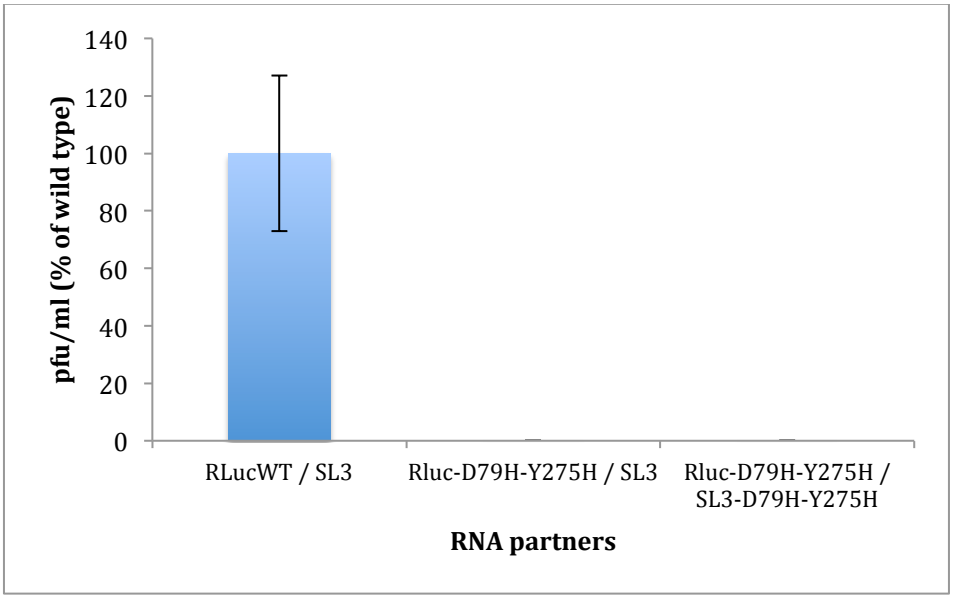

Figure 5.12: Intertypic CRE-REP assay with D79H and Y275H RdRp variants

(A) Quantification of an intertypic CRE-REP assay from co-transfected L929 cells. RNA partners as indicated. Mutations are present in the replicon (donor) template only. The data represents the mean from three independent samples. Error bars indicate standard deviation **(B)** As (A) except dual mutations are present in either donor or both templates.

introduced into the CRE-REP assay using a similar protocol outlined previously in this section. As expected no recombinant virus was isolated from co-transection supernatant when both mutations were in the donor and recipient templates (figure 5.12B).

5.6 Y275H variant in the intratypic CRE-REP assay

The results from the intertypic CRE-REP assay suggested that the Y275H mutation in the donor template was sufficient to inhibit recombination. The Y275H mutation was subsequently introduced into the PV3 replicon donor cDNA (pT7rep3-L) and acceptor cDNA (pT7FLC/SL3) by overlap extension PCR using the unique restriction enzyme sites *XhoI* and *SalI*. All constructs were verified by sequencing. Plasmids were linearised with the restriction enzyme *SalI* and used as templates to transcribe RNA using T7 polymerase. The replication kinetics of the Y275H replicon variant was compared to the wild type RdRp replicon in a luciferase time course assay. L929 cells in 12 well plates were transfected with 250 ng of Rep3-L or the Y275H variant in duplicate with samples taken at the times indicated. Luciferase activity was measured and normalised using a mock transfection control (figure 5.13A). The Y275H mutation had a similar inhibitory effect upon replication as the K359R mutation characterised in section 5.2. The luciferase activity of the Y275H replicon at 7.5 hrs was one $\log_{10}$ lower than the wild type RdRp replicon, a larger decrease in replication than that observed in a PV1 replicon background. However, the replication defect that the Y275H provides would have been overcome, as recombinant progeny yields from the intratypic CRE-REP assay are typically 1-2 $\log_{10}$ higher than the intertypic CRE-REP. A subsequent CRE-REP assay was therefore carried out. It was reasoned that if replication were inhibited by one $\log_{10}$ then recombination frequency would fall by a similar amount if the mutation had no effect upon template switching. Three separate co-transfections were carried out in triplicate. The control co-transfection consisted of RNA from the wild type intratypic CRE-REP partners (Rep3-L and SL3). The remaining two conditions had the Y275H mutation present in the donor template only or in both donor and acceptor templates. L929 cells in 12 well plates were co-transfected with 0.5 µg of total RNA in a 1:1 ratio (replicon: CRE mutant). Cells were incubated for 48 hrs and then the transfection supernatant was used to inoculate HeLa cell monolayers for plaque assays.

A

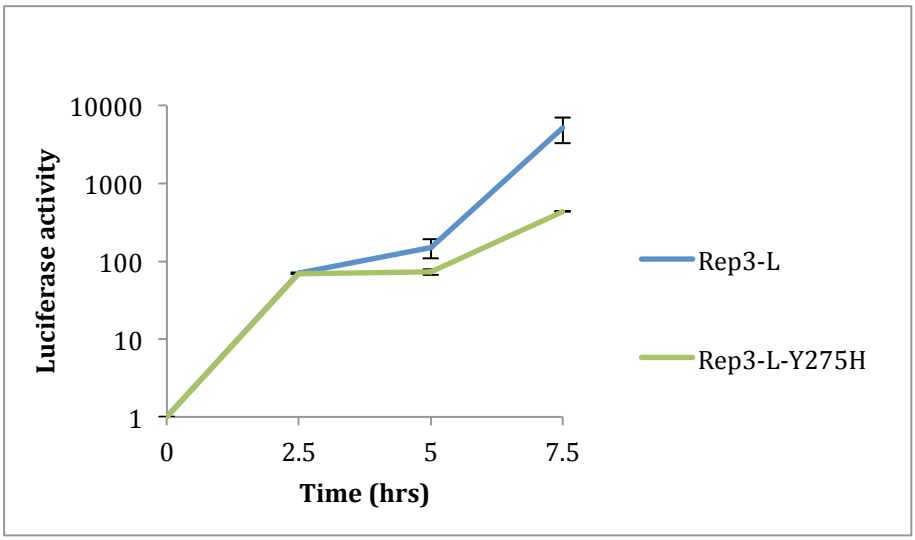

B

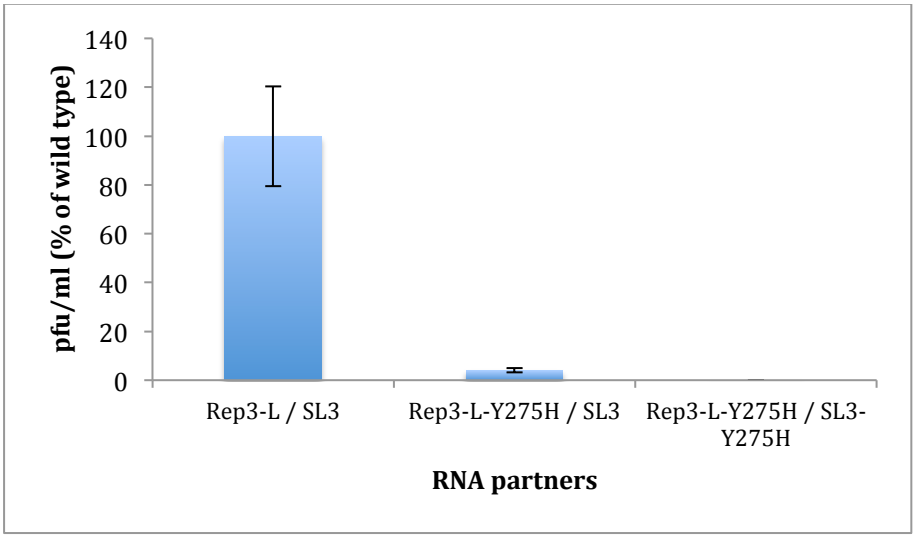

Figure 5.13: Luciferase and intratypic CRE-REP assay with Y275H RdRp variant

(A) Replication kinetics of a PV3 sub-genomic replicon (Rep3-L) bearing either a Y275H polymerase mutation. 250ng of RNA as indicated were transfected into L929 cells. Samples were taken at the times indicated and luciferase activity was measured and normalised using a mock transfected control. Error bars indicate standard deviation of two independent samples **(B)** Quantification of an Intratypic CRE-REP assay from co-transfected L929 cells. RNA partners as indicated. The data represents the mean from three independent samples. Error bars indicate standard deviation.

Following 60 hrs incubation, cells were stained with crystal violet and recombinant progeny was quantified (figure 5.13B). The control transfection yielded an average of 1300 pfu/ml, in line with previous results. Recombinant progeny was produced when the Y275H mutation was present in the donor template alone. The yield was only 4.1% of the control co-transfection (average of 53 pfu/ml). No recombinant virus was identified when the mutation was present in both donor and acceptor templates.

5.7 D79H - Y275H RdRp variant and the resolution event

The results outlined in section 4.3 showed that a high fidelity variant (G64S) significantly reduced the yield of recombinant progeny in the CRE-REP assay. The G64S RdRp variant also affected the rate of resolution of the molecular clone JC105B. In section 5.6, the dual mutation (D79H-Y275H) had been shown to affect the yield of recombinant progeny from the CRE-REP assay. The discovery of the D79H and Y275H dual mutation was from a GFP retention assay, described previously. This approach was used to identify RdRp variants based upon the ability of the construct to retain additional non-viral sequences. The JC105B construct in contrast is a natural recombinant intermediate; it was therefore considered that the role of D79H and Y275H deserved investigation in a true resolution assay. A similar approach to the one outlined in section 4.9 was done to validate whether these mutations did indeed affect the resolution stage of recombination. The RdRp coding region of pRLuc-D79H-Y275H was sub-cloned into JC105B cDNA using the unique restriction enzyme sites *XhoI* and *ApaI*. The new construct pJC105B-D79H-Y275H was verified by sequencing the entire region that was sub-cloned. The cDNA was then linearised with *ApaI* and used as a template to transcribe RNA using T7 polymerase. L929 cells in a 12 well plate were transfected with 250 ng of JC105B or the D79H-Y275H variant. Cells were incubated for 48 hrs and then the transfection supernatant was used to inoculate HeLa cells in T20 flasks. Media was isolated at 24 hr periods and passaged a total of 10 times. RNA was extracted from various passages and subjected to RT-PCR analysis. The primers used to amplify the specific region where resolution occurred were PV1/3-3280F and GEN-4615R (figure 5.14). The molecular clone JC105B that had a wild type RdRp went through the

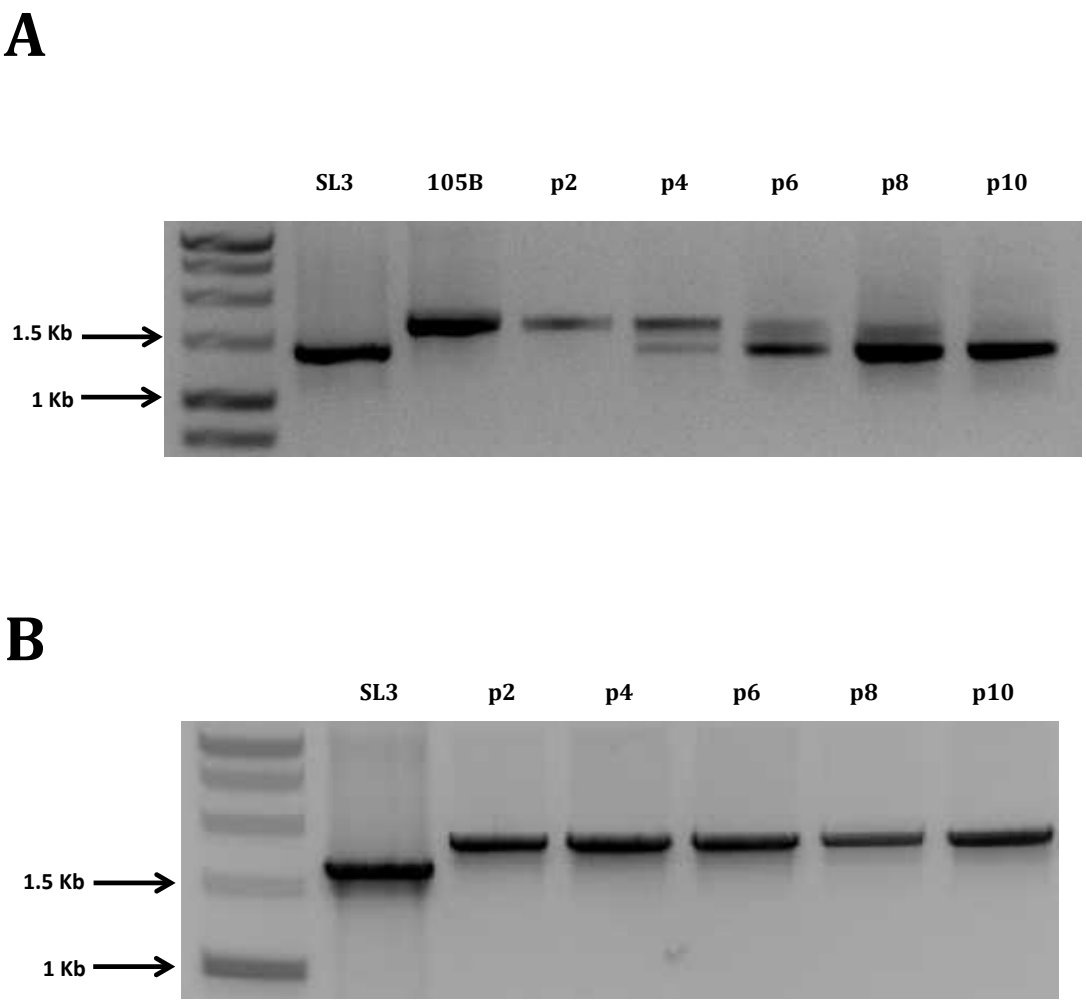

Figure 5.14: Resolution of an imprecise molecular clone - JC105B containing an RdRp with the D79H and Y275H mutations

(A) RT-PCR product of the amplified region of the JC105B molecular clone recombinant virus was run on 1% agarose gel and stained with ethidium bromide following serial passaging in HeLa cells. SL3 indicates wild-type length without insert. Passages as indicated **(B)** As (A), except passaged virus has an RdRp containing a D79H and Y275H mutation.

previously characterised resolution process where additional sequences within the zone of recombination were rapidly lost, as indicated by the PCR products migrating as far as the wild type control template (SL3) from passage 6 onwards. In contrast, the molecular clone that carried the D79H-Y275H RdRp variation produced a homogenous PCR product at each passage that was larger than the control (SL3). No obvious changes in the migration pattern of this band were observed. This suggested that the additional sequence within the region of recombination was still present. The PCR product from passage 10 was sequenced and all of the additional sequence was present and identical to the original cDNA. Additionally, to confirm the sequence of the viral RdRp, the 3D coding region was also amplified by PCR and sequenced. The D79H and Y275H mutations were present at passage 10 and no other secondary site mutations were observed in the RdRp coding region.

5.8 Discussion

The results in this study have supported the 'copy-choice' replicative model of recombination and have shown that fidelity of the viral RdRp is a key determinant that affects recombinant progeny yield. The experiments outlined in this chapter have introduced another characterised high fidelity RdRp variant, K359R, into the CRE-REP assay. In all of the CRE-REP assays conducted no intratypic or intertypic recombinants could be isolated when the K359R mutation was present in either the donor template (replicon) alone or when the mutation was present in both templates (donor and acceptor). The K359R polymerase variant has a higher fidelity than wild type (Weeks et al., 2012). One interpretation is that the high fidelity of this variant alone is sufficient to inhibit recombination, in a similar fashion to the G64S mutation, perhaps by reduced template transfer due to increased affinity of the enzyme for the RNA template. However, the fidelity of the K359R variant is lower than the G64S RdRp variant (Weeks et al., 2012). Results in chapter four showed that recombination still occurred, albeit at a significantly lower level, when the G64S mutation was in both templates. Therefore increased fidelity alone cannot explain why no recombinant virus was observed when the K359R mutation was present.

The substitution of the lysine for an arginine at position 359 of the RdRp has been well characterised, and this modification reduces RNA replication rates by around 10 fold compared to wild type (Castro et al., 2009). This result was supported by the luciferase assays carried out in this study. As previously stated, this approach allows RNA synthesis to be evaluated indirectly by monitoring luciferase activity (Barclay et al., 1998). The replication defect of K359R could explain why no intertypic recombinant progeny from the CRE-REP assay was observed. Potentially, the fall in replication rates by one $\log_{10}$ would have been enough to reduce recombination to below the levels of detection. The plaque and $TCID_{50}$ assays do not use all of the transfection supernatant that is isolated. In principle, a very low level of recombinant may have been missed. This however does not explain the lack of recombinant progeny observed in the intratypic CRE-REP assay when the K359R mutation was present. Yields of recombinant in the wild type RdRp control were above 1000 pfu/ml. If replication rates were inhibited by one $\log_{10}$, then detection of recombinant virus would still be possible, if they were present. This result suggests that the K359R mutation not only inhibits replication rates but also inhibits recombination frequency.

To overcome the replication rate deficiencies of the K359R variant in the intertypic CRE-REP assay and to allow a wider study on recombination frequency and type, a new intertypic recombination assay called 3'-CRE-REP was developed. By mutating the native CRE in the PV1 replicon (pRLucWT) in a similar fashion to a previous study (Goodfellow et al., 2000) it was shown that replication was completely ablated. Insertion of a synthetic CRE used in a previous study (Goodfellow et al., 2003a) into the 3'NTR directly after the termination codon had no obvious impact on replication. The positioning of a CRE in the 3'NTR of poliovirus has never been characterised before and the result supports previous observations that the function of the CRE is not location specific (Mason et al., 2002, Goodfellow et al., 2003a). Indeed, this study and the study by Goodfellow et al., 2003, have moved the CRE in poliovirus by a combined length of 6.8 Kb. The flexibility in location with regard to the CRE begs the question as to why it is located within the 2C region and not elsewhere? One reason could be that the 2C region is predicted to be highly unstructured (Goodfellow et al., 2000). This may prevent competing RNA interactions

that affect its function. Alternatively, being centrally positioned may protect it from host exoribonuclease digestion.

The positional manipulation of the CRE stem loop allowed a larger potential region of recombination. The new assay, 3'-CRE-REP, increased recombination yields by 5.85 fold compared to the CRE-REP assay. This was higher than expected. The potential region of recombination in the 3'-CRE-REP was four-fold larger, a similar four-fold increase in recombination frequency would therefore have correlated. The increased recombination frequency observed above what was expected may be linked to a number of factors. The 3'-CRE-REP incorporates an additional four protein cleavage boundaries (seven in total compared to three in the CRE-REP). Observations in this study and that by Lowry et al., 2014, have shown a clustering of recombinant junctions to cleavage sites. In principle, the availability of more boundaries could provide an increased opportunity to produce a viable genome that is determined by correct protein-to-protein interactions during subsequent replication. Alternatively, the increased yield could be due to the processivity of the RdRp. If the rate of RdRp disassociation were constant then the opportunity for recombination would be proportionally larger over a longer region than compared to a shorter one. Sequence identity may also be a factor to consider. The 3D coding region as well as the 3'NTR of PV1 and PV3 shares high sequence similarity. If recombination is in fact influenced by sequence identity then this may account for the increased frequency above that expected. Detailed analysis of a large sample of recombinant junctions from this type of assay will provide data to answer some of these hypotheses.

In respect to this study, it was hoped that the increased intertypic recombinant yield observed in the intertypic 3'-CRE-REP assay would overcome the replication defect that the K359R mutation provides. No recombinant virus was observed in the 3'-CRE-REP assay when the K359R mutation was present in the donor and acceptor templates. This suggested that this mutation provided a non-recombinogenic phenotype. The striking difference between the G64S mutation and the K359R variant is its replication rates. Potentially, the lack of recombination observed may be in fact due to the reduced nucleotide incorporation speed of the K359R

polymerase as well as the higher fidelity phenotype. As a side note, the Sabin I vaccine strain contains a T362I mutation within motif D (Georgescu et al., 1995, Bouchard et al., 1995). This substitution has been shown to produce a 'mutator' phenotype in cell culture by disrupting the function of the lysine residue at position 359 (Liu et al., 2013). This indicates the importance of this residue in replication.

An additional observation with the K359R variant needs to be discussed. The luciferase assay results outlined in figure 5.2AB and in a previous study (Weeks et al., 2012) show that replication 'stalls' from around 2-6 hrs, with luciferase signal being only slightly higher than the guanidine hydrochloride control. This showed that replication was occurring, but at a vastly reduced rate. Viable virus is produced when this mutation is present but at yield that is generally one $\log_{10}$ lower than wild-type (Weeks et al., 2012). During this time, as outlined in chapter one, negative strand RNA production is at its peak. If 'copy-choice' recombination occurs during negative sense RNA synthesis then perhaps a certain basal level of replication is required. Potentially, the stalling in replication is enough at this early stage to inhibit recombination. Alternatively, the opportunity for recombination may not be available. Recombination via copy-choice would require mixing and co-occupancy of replication complexes. If RNA synthesis is temporally affected then perhaps mixing of replication complexes is also affected. A previous study that stalled RNA replication within the replication complex by use of the reversible inhibitor guanidine hydrochloride showed that the migration pattern of the RCs is affected (Egger and Bienz, 2005), perhaps something similar is occurring with the K359R variant?

The mutations kindly provided by the Andino research group were introduced into the transcripts used in the intertypic CRE-REP assay, and had an effect on intertypic recombination frequency. When both mutations were present in the donor template no viable recombinant virus was identified. Of the two mutations, Y275H was the most important. When D79H was present in the donor template (RLuc-D79H) alone recombination occurred at a rate lower than the wild type RdRp partner control. The fall in recombination frequency did however correlate with the reduction in replication, as shown in the luciferase time-course assay. The reduction in

the recombination frequency observed with the D79H mutation may have therefore been due to an overall reduction in replication rates. In contrast, the Y275H mutation in the donor template (RLuc-Y275H) alone was enough to completely inhibit recombination, at least that detectable in the intertypic CRE-REP assay, which detects viable recombinant virus only and not the generation of hybrid RNA. The absence of recombination cannot be completely attributed to any replication defects that this mutation confers, as this variant was still able to replicate at a level that should have been detectable if any recombinants were present. This result was further supported by the intratypic CRE-REP assay that concentrated solely upon the Y275H mutation. When the mutation was present in the donor template alone a small amount of recombination was observed. In principle, this may have been due to the low levels of wild type RdRp produced from translation of the SL3 template. It is known that the RdRp forms higher order lattices in the replication complex consisting of multiple RdRps (Tellez et al., 2011). Potentially, a small amount of the wild type RdRp complemented the process of recombination *in trans*. When the mutations were present in both donor and acceptor templates no recombination was identified. In principle, this could have been due to a replication defect. The replication of a PV3 sub-genomic replicon bearing the Y275H mutation was therefore characterised in a luciferase time-course assay. In a PV3 background this mutation has a more profound effect upon replication than when in a PV1 genome, reducing luciferase signal by around one $\log_{10}$ when compared to wild type. This however cannot account for the lack of recombinant progeny, as the control intratypic CRE-REP partners produced recombinant yields of 1-2 $\log_{10}$ higher than intertypic partners. If this mutation had no effect upon recombination, progeny should have been detected.

The dual mutations provided by the Andino research group were identified in a GFP retention assay, analogous to the resolution assay used in this study. The CRE-REP assay and the resolution assay, that used the molecular clone JC105B, produced results that in part validated the Andino groups approach. Resolution was completely inhibited when both mutations were present. The results in section 4.9 showed that fidelity affected this stage of recombination as well, indicating that secondary recombination events may be important. However, the mechanisms by which these mutants inhibit the loss of the GFP coding insert remain to be

determined. Potentially, this event can occur *in cis* or *in trans*. By characterising the mutations in the CRE-REP assay it was shown that only one of the mutations inhibited recombination in a fashion unrelated to any replication defect. The results indicated that the Y275H mutation and not the D79H mutation were likely to be the determinant of the non-recombinogenic phenotype.

The K359 residue is located within the characterised motif D of the poliovirus RdRp, a region that plays a direct role in RNA synthesis (Castro et al., 2009). The G64S mutation is believed to indirectly induce conformational changes to the RdRp active site (Arnold et al., 2005). The location of the D79 and Y275 residues upon the RdRp was therefore of particular interest, and provided information that requires discussion. The D79 amino acid residue is located in a region known as interface II, an area known to be important in the higher order structure lattices formed by multiple RdRps (Tellez et al., 2011). The D79H mutation may be sufficient to disrupt the higher order RdRp structures, thus affecting other protein-protein interactions that may be important. Potentially, this could affect the secondary resolution stage of recombination and not the initial template switch. The Y275 residue in contrast, is located in the RNA channel very near to the active site of the RdRp, and is considered a high processivity mutant (Raul Andino, personal communication). It is particularly interesting to note that all of the mutations that have affected recombination yields in the CRE-REP assays are associated with regions that directly (or indirectly with G64S) interact with the RNA template and nucleotide. This suggests that the poliovirus RdRp alone may be responsible for template switching. Modifications that increase fidelity, processivity or reduce replication speed inhibit this process.

Although, the results outlined in this chapter and in the previous chapter provide interesting observations in relation to the poliovirus RdRp, they are by no means definitive. The replication defects that the K359R and Y275H mutations provide may have had some unknown temporal affect that inhibits recombination (discussed above). The next step of this investigation was to develop an *in vitro* biochemical assay that measured the kinetics of recombination using the RdRp variants outlined in this study so far.

CHAPTER 6: Biochemical and Genetic Support for the Role of the RNA Dependent RNA Polymerase and Sequence Identity in Recombination

6.1 Introduction

The poliovirus RdRp has a glycine as its first amino acid as a consequence of 3C cleavage that occurs *in trans* at a Gln/Gly amino acid pair (Semler et al., 1981a). Expression and purification of 'authentic' poliovirus RdRp that has a glycine at its N-terminus has exploited the observation that proteins fused to the carboxyl terminus of ubiquitin can be processed in *E. coli* to produce proteins with any amino acid as the first residue when expressed in the presence of a ubiquitin-specific, carboxy-terminal protease (Gohara et al., 1999). This approach allowed subsequent studies that characterised the mechanistic properties of the native poliovirus RdRp (Gohara et al., 2000, Arnold et al., 1999, Freistadt et al., 2007). Indeed, the ability to purify the poliovirus RdRp, has also allowed two of the poliovirus RdRp variants used in this study, G64S and K359R to be extensively studied and characterised (Pfeiffer and Kirkegaard, 2003, Arnold et al., 2005, Vignuzzi et al., 2006, Castro et al., 2009, Weeks et al., 2012).

This investigation has provided evidence to support the 'copy-choice' replicative model of recombination in enteroviruses. Manipulations of the poliovirus RdRp by use of nucleoside analogue mutagens or by well-characterised mutations have shown that fidelity and replication speed are important in recombination frequency. However, the evidence provided with the fidelity variants G64S and K359R (chapters four and five) was reliant upon observations gained from a cell-based assay approach only (CRE-REP and 3'-CRE-REP). It was reasoned that an alternate approach was required to validate the observations outlined in this investigation so far. A previous study that used homo-polymeric RNA templates and primers along with purified poliovirus RdRp showed that the poliovirus RdRp alone was sufficient for template switching (Arnold and Cameron, 1999). This study indicated that this might be the primary determinant of recombination. Many of the historic biochemical studies on the poliovirus RdRp have been carried out in the laboratory of Professor Craig Cameron at Penn State University, Pennsylvania,

U.S.A. The Cameron research group kindly agreed to collaborate in this study with the aim of developing a biochemical recombination assay. This allowed the RdRp fidelity variants, identified in this study to be important in recombination frequency, to be characterised in a cell-free system. Additionally, the characterisation of the Y275H mutation provided by the Raul Andino research group was further validated using this biochemical approach.

Section 1.3 discussed the role of RNA sequence and structure as being key determinants of recombination. However, the sequence analysis of over 100 intertypic recombinant viruses characterised in a previous study could find no obvious link to RNA sequence, and only limited influence of RNA structure (Lowry et al., 2014). Although, the resolution assay described in sections 3.6 and 3.8 provided evidence to suggest that sequence identity may play a role in the secondary events of recombination. By manipulating sequence identity in the acceptor templates used in the biochemical assay (described later), minimal regions of RNA identity were identified. Additionally, modification of the donor templates in the CRE-REP assay was also considered. Quantitative biological data was obtained by manipulating sequence identity and RNA structure at a known region of recombination.

Aims

The aim was to develop an *in vitro* biochemical assay, in collaboration with the Craig Cameron research group and characterise the role played by poliovirus RdRp fidelity variants in recombination. The importance of sequence homology and recombination frequency was also investigated using a similar biochemical approach. An additional aim was to manipulate RNA sequence identity within the donor template at a known recombination 'hot-spot' and characterise its influence upon recombination location and frequency in the CRE-REP assay.

6.2 Biochemical assay Sym-subU

Detailed studies of the kinetics of nucleotide incorporation by the poliovirus RdRp have been aided by the development of a biochemical assay known as 'Sym-subU'. The heteropolymeric RNA primer-template substrate (figure 6.1A) is a 10-nt, self-complementary radiolabelled RNA that forms a 6-base pair duplex flanked by two, 4-nt 5'-overhangs (Arnold and Cameron, 2000). The complementary RNA is symmetrical and the first templating base is a 'U', hence the name 'Sym-subU'. This design allowed the evaluation of single and multiple cycles of nucleotide incorporation following addition of purified polio RdRp along with the appropriate co-factors and nucleotides (Arnold and Cameron, 2000). The observations in a previous study that showed the poliovirus RdRp alone was sufficient for template switching *in vitro* (Arnold and Cameron, 1999) inspired a modification of the original Sym-subU assay. The introduction of a potential acceptor template into the assay (figure 6.1A) that contains two regions of sequence identity to the fully extended Sym-subU (UACG) would provide the opportunity for a template-switching event to occur. The products of any template switching would be quantified by running samples from the Sym-subU assay on an appropriate denaturing polyacrylamide gel. The complete assay is described in full in section 2.3. For clarity, as shown in figure 6.1BCD, the reaction assay mix 1 (containing radiolabelled Sym-subU, buffers, co-factors and ATP) are incubated at 30°C for 5 mins. The addition of the poliovirus RdRp (3Dpol) allows the elongation complex to be formed by incorporation of the first templated base (figure 6.1D). The second reaction mix is then added (containing the remaining nucleotides along with acceptor template). Samples are then taken at timed intervals and quenched for RdRp activity by the use of a divalent cation chelator (EDTA).

6.3 Sym-subU optimisation

Initial experiments were carried out with the aim to optimise the original assay in light of its modification. Firstly, historical Sym-subU assays have typically used $ZnCl_2$ in the first assay mix. It was believed that that the RdRp didn't use the divalent cation as a cofactor, but it's inclusion might aid the overall reaction, potentially by increasing RNA-RNA interactions (Craig Cameron, personal communication).

A

Sym-subU

^{32}**P**-5′GCAUGGGCCC3′
3′CCCGGGUACG5′-^{32}**P**

Acceptor RNA

3′GGUACGUACGAACG5′

B

Reaction:
<u>Assay Mix 1</u>
50 mM HEPES pH 7.5
5 mM $MgCl_2$
10 mM BME
60 µM $ZnCl_2$
1 µM s/s-U
500 µM ATP

<u>Assay Mix 2</u>
500 µM CTP, GTP, UTP
60 µM RNA Acceptor
1 mM $MgCl_2$
Temp = 30°C

3Dpol (RdRp) concentration = 5 µM

C

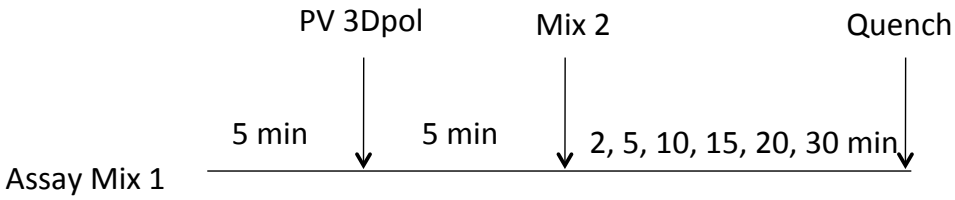

D

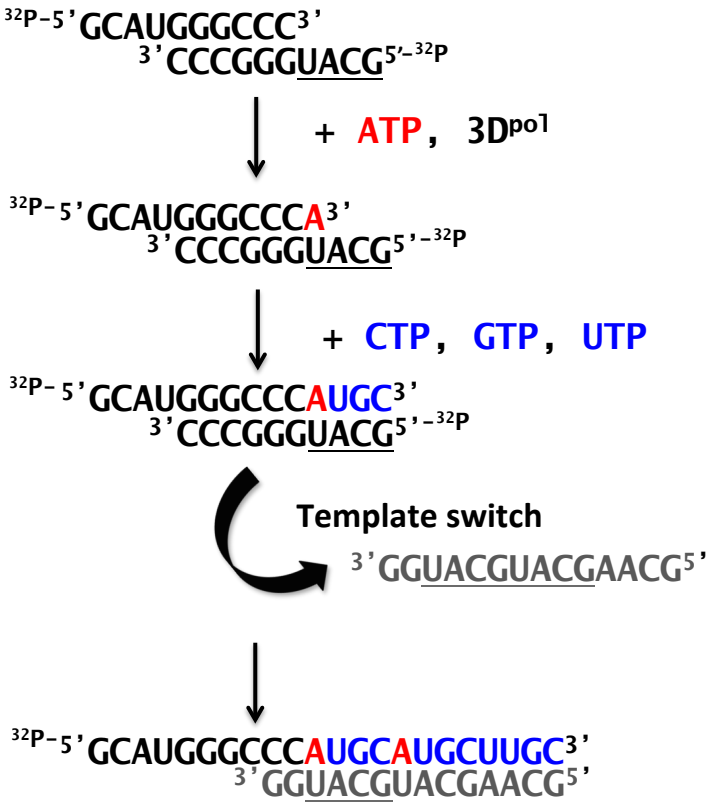

Figure 6.1: Sym-subU assay overview

(A) Substrates. A radiolabelled primer substrate pair known as Sym-subU (symmetrical substrate; 'U' for the first template base). Acceptor RNA contains two 4-nt regions (UACG) that can base pair with the last 4-nt from the 3'-end of a fully extended Sym-subU RNA **(B)** Overview of the contents of assay mix 1 and 2 **(C)** Brief layout of the Sym-subU assay. Assay mix 1 is incubated for 5 mins at 30 °C, followed by addition of 3Dpol (RdRp). Assay mix 2 is then introduced after additional 5 mins incubation, with samples taken and quenched (EDTA) to stop the reaction at the times specified **(D)** First base is incorporated into Sym-subU (ATP), followed by complete extension of Sym-subU. Template switching indicated by arrow. Acceptor template is shown (grey) with sequences of identity underlined. Sym-subU is then extended further using the acceptor template. For convenience extension and template switching is only shown at one end of the Sym-subU template.

A Sym-subU assay was carried out with and without 60 μM $ZnCl_2$. Additionally, two types of RdRp were used in the initial optimisation assay, wild-type and the Interface I mutant L446D-R455D. The two mutations (L446D-R455D) within the 3D coding region are known to disrupt the higher order structures formed by RdRp monomers (section 1.2) and are lethal in cell culture (Thompson and Peersen, 2004, Hobson et al., 2001). However, the mutations have little or no impact on the molecular dynamics of the RdRp in biochemical assays (Moustafa et al., 2014). The poliovirus RdRp can become insoluble at higher concentrations due to its tendency to form higher order structures (Hobson et al., 2001). Using the Interface I variant allowed higher concentrations of RdRp to be purified following expression in *E. coli,* thus allowing increased flexibility in experimental design. It was reasoned that a comparison of wild-type and Interface I mutant may also highlight the potential role played by higher order RdRp structure in the template switching event. Samples were taken at various time-points and then run on a denaturing 20% polyacrylamide gel. The gels were then visualised by using a PhosphorImager (figure 6.2). The controls in this assay were Sym-subU without extension and Sym-subU following addition of the first templated base only (n+1). The n+1 control indicated that the first templated base (ATP) had been incorporated in the absence of assay mix 2. This showed formation of the elongation complex was successful, which is typically a slow reaction (Arnold and Cameron, 2000). The assay generated extended Sym-subU product as indicated by the banding of >n+1 shown in figure 6.2A. The band of n+4 in the presence of assay mix 2 indicated a fully extended Sym-subU template. Banding above this area was likely due to un-templated nucleotide addition at the blunt end of the primer-template (Arnold et al., 1999). Initial analysis also indicated a product following template switching (black arrow). An over exposed image of the gel (figure 6.2B) clearly showed (arrow) a product that had arisen from extension following template switching. The ImageQuant software (Molecular Dynamics) was used as a tool to accurately measure the amount of extended Sym-subU and the relative proportion that was as a result of template switching. The calculation of the RNA transfer product as a percentage of total RNA products is described in section 2.3.3. The quantitative data showed that the addition of $ZnCl_2$ in the assay mix was beneficial to the overall yield of RNA product with both RdRps (figure 6.3A). As a consequence of the increased yield, the amount of transfer product was also proportionally higher when $ZnCl_2$ was included (figure 6.3B). At 30 mins the transfer product in

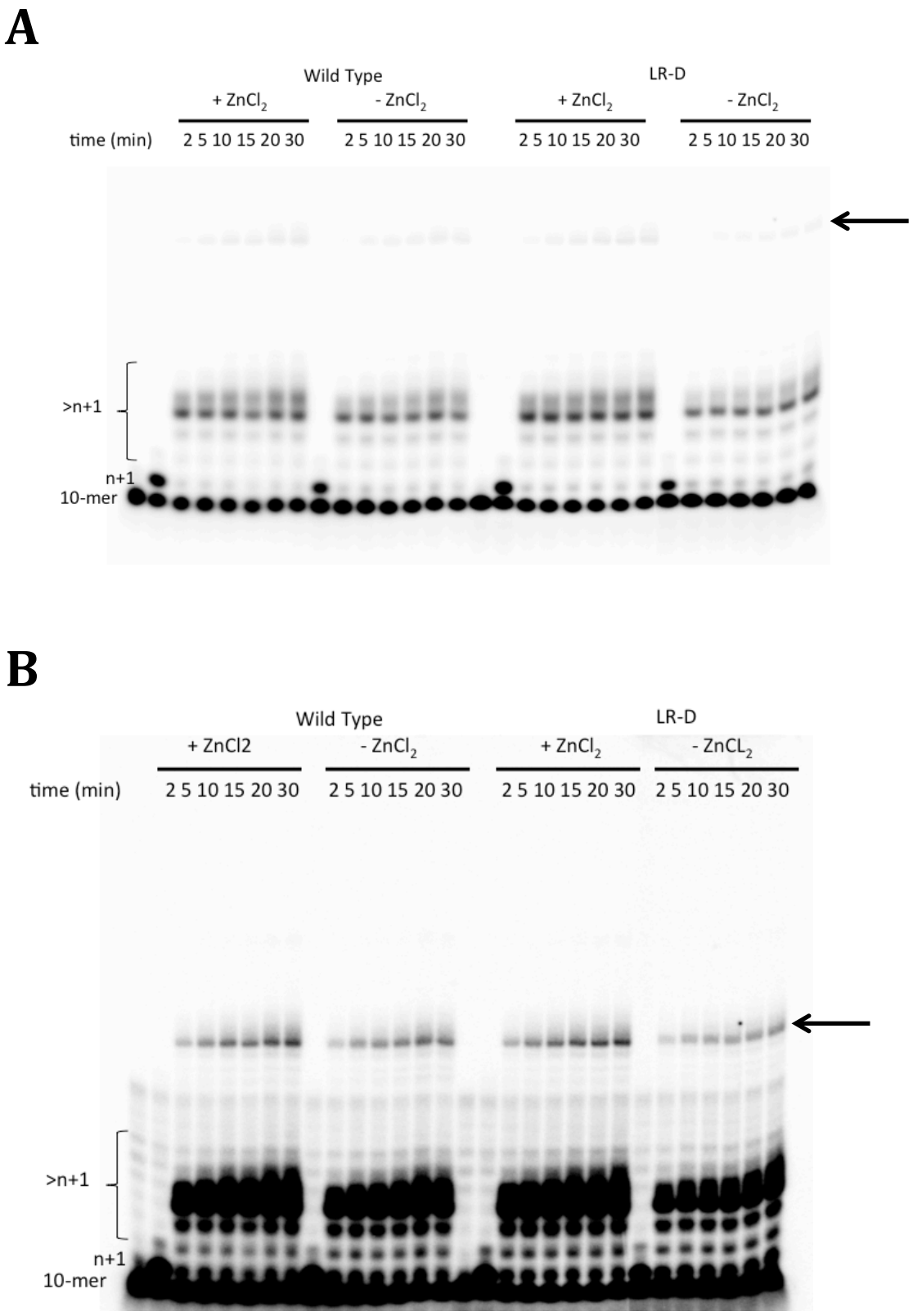

Figure 6.2: Sym-subU $ZnCl_2$ optimisation assay - Gel images

(A) Template transfer +/- 60μM $ZnCl_2$. Two polymerase variants were used - wild type and an Interface I mutant variant LR-D = L446D - R455D. 10-mer indicates Sym-subU, n+1 indicates the product following first nucleotide incorporation, >n+1 indicates extended Sym-subU. The arrow highlights the product from template transfer. Sample times as indicated **(B)** An over exposed image, highlighting the difference in template transfer.

A

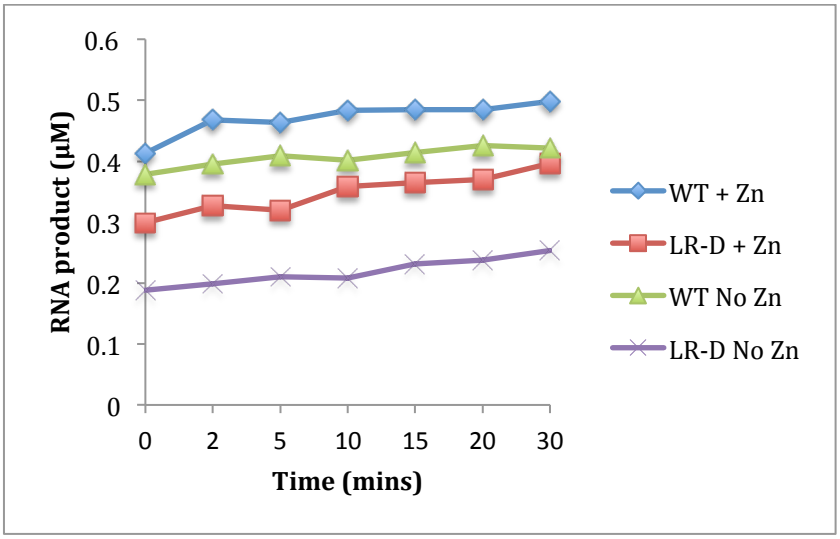

B

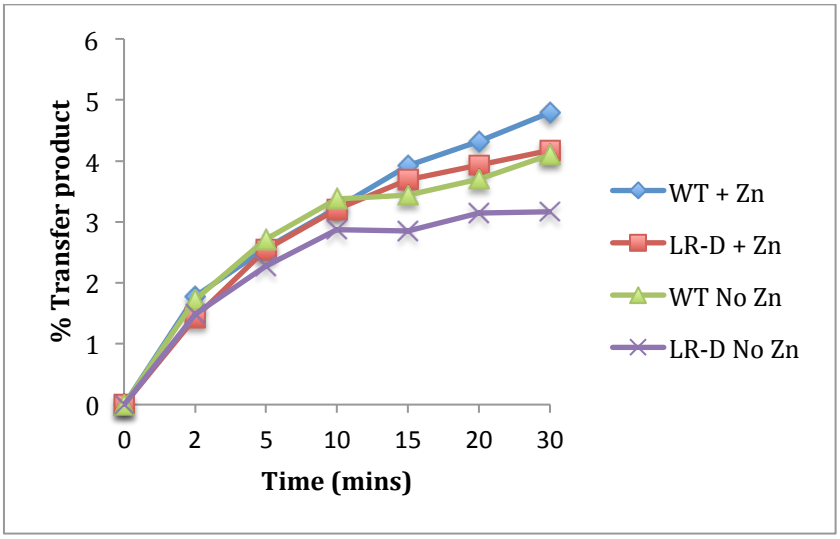

Figure 6.3: $ZnCl_2$ optimisation quantification of RNA product and transfer product

(A) Figure represents the total RNA product [(n+1) + (>n+1) + (transfer product)] from the Sym-subU assay over time +/- $ZnCl_2$ **(B)** Figure represents the total % of transfer product over time +/- $ZnCl_2$. WT = wild-type polymerase. LR-D = Interface I mutant virus L446D - R455D.

both RdRp conditions represented 4.7 % of overall product (wild-type RdRp) and 4.1 % of overall product (Interface I mutant RdRp) respectively. Conclusions from this experiment were that the poliovirus RdRp alone is sufficient for template switching and that $ZnCl_2$ should be included in the assay mix. Additionally, the results showed that the Interface I mutations did not significantly inhibit the ability of the RdRp to switch to the acceptor template. This implied that higher-order RdRp complexes were not an absolute requirement for the template transfer event.

Historical studies that have used the Sym-subU assay to measure the kinetics of nucleotide incorporation have used a standard 5 μM of poliovirus RdRp (Arnold and Cameron, 2000, Arnold et al., 2005). The results in this study so far have indicated a central role for the RdRp in recombination. Potentially, the template-switching event can be affected by the concentration of RdRp. It was therefore reasoned that optimisation of RdRp concentration was required. Similar assay mixes and experimental approaches were used to those indicated in figure 6.1BC. The only difference to the experiment was the use of various concentrations of wild type RdRp (0.5μM - 20μM). Two separate experiments were carried out that overlapped with regard to the concentration of RdRp used, with the product of temple switching shown (figure 6.4). The overall RNA product was quantitated (figure 6.5), and results indicated a dose response relationship between RNA product and RdRp concentration. Although, the increase in RNA yield did not correlate with the increased concentration of RdRp when it was at 10 μM and above. This result indicated that higher concentrations were sub-optimal. This was more evident when the percentage of product transfer was calculated. RdRp concentrations of 10 μM and above inhibited the template transfer event by up to 30% when compared to 5 μM concentrations (figure 6.6B).

The results from figures 6.5A and 6.6A indicated some variability, which may be attributed to the low concentrations of RdRp being used, or experimental error. The results in figures 6.5B and 6.6B showed limited variability, with a 5 μM concentration of RdRp producing the highest percentage of transfer product as a proportion of overall yield. As a result, it was decided that

A

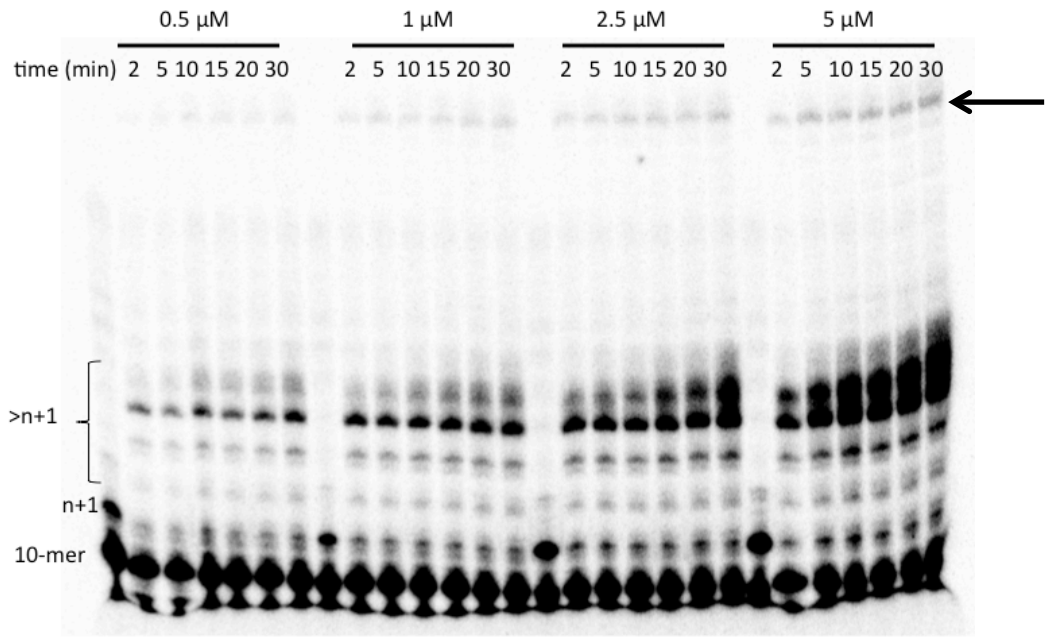

B

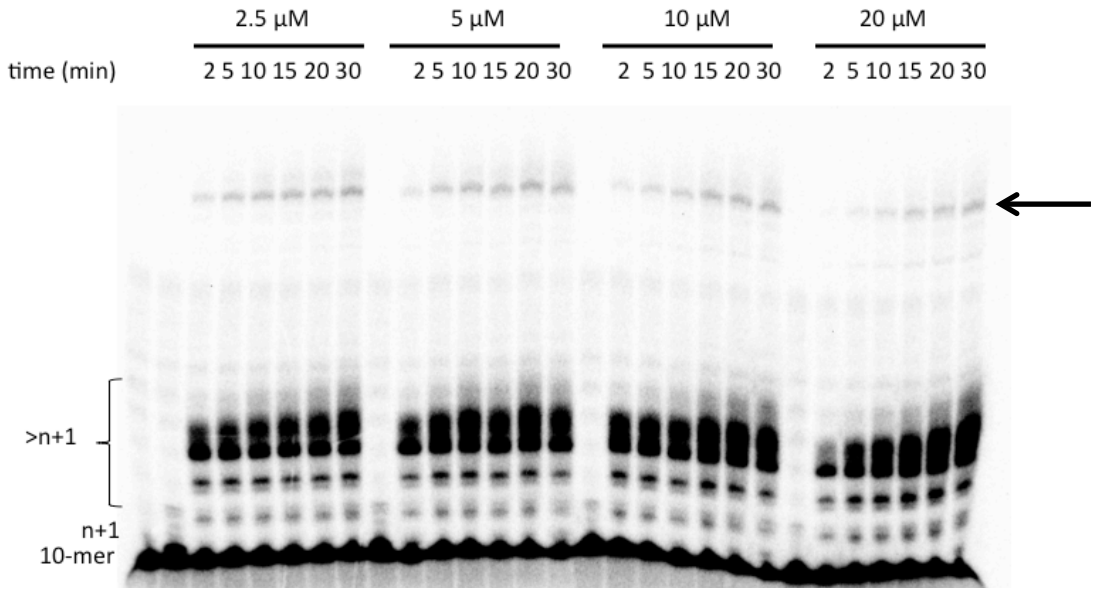

Figure 6.4: Sym-subU 3Dpol optimisation assay - Gel images

(A) Template transfer assay using various concentrations of RdRp (concentrations as indicated) 10-mer indicates Sym-subU, n+1 indicates the product following first nucleotide incorporation, >n+1 indicates extended Sym-subU. The arrow highlights the product from template transfer. Sample times as indicated **(B)** A second experiment with concentrations of RdRp as indicated.

A

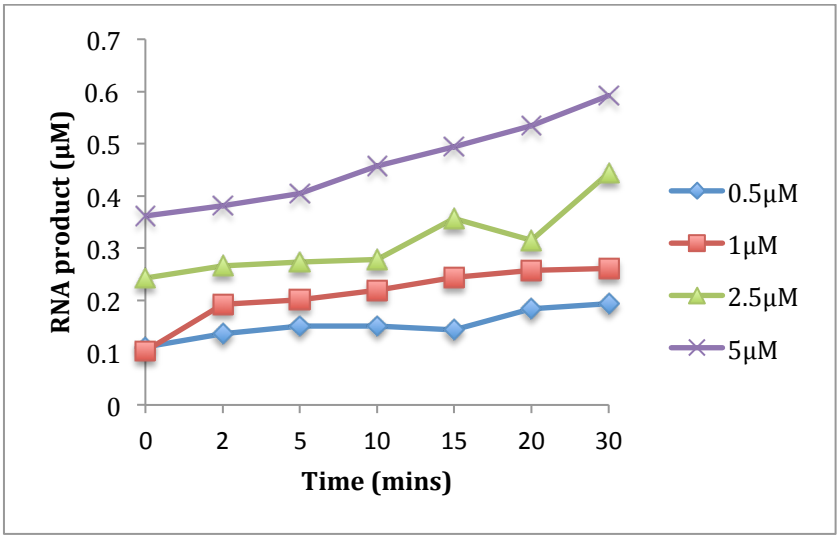

B

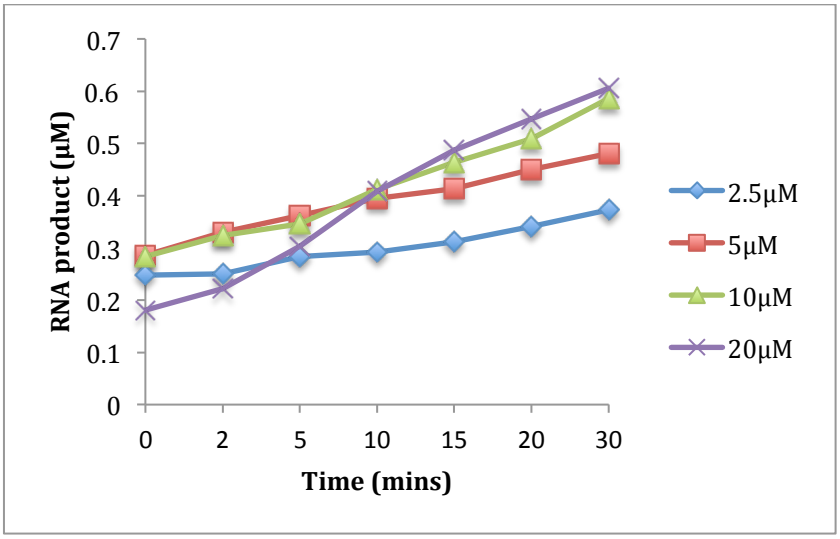

Figure 6.5: 3Dpol (RdRp) optimisation - quantification of RNA product

(A) + (B) Figures represent the total RNA product [(n+1) + (>n+1) + (transfer product)] from the Sym-subU assay over time. Concentrations of RdRp as indicated in the figure legends.

A

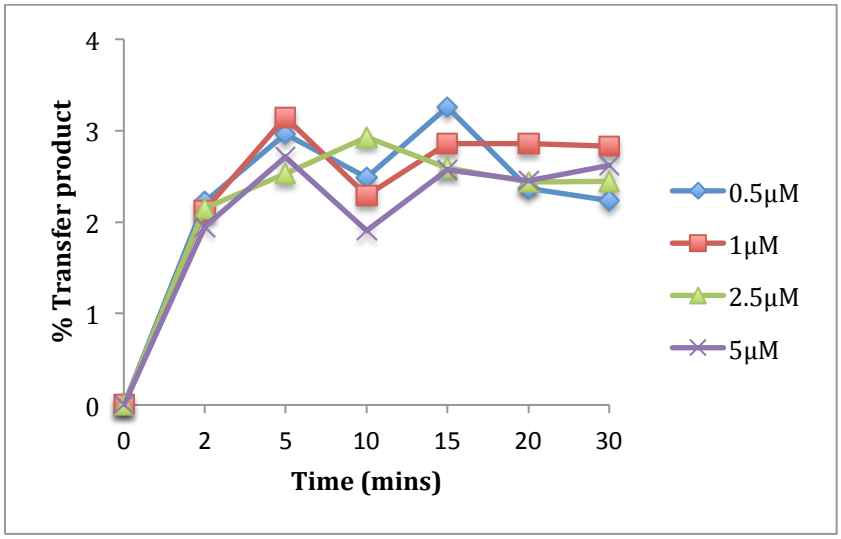

B

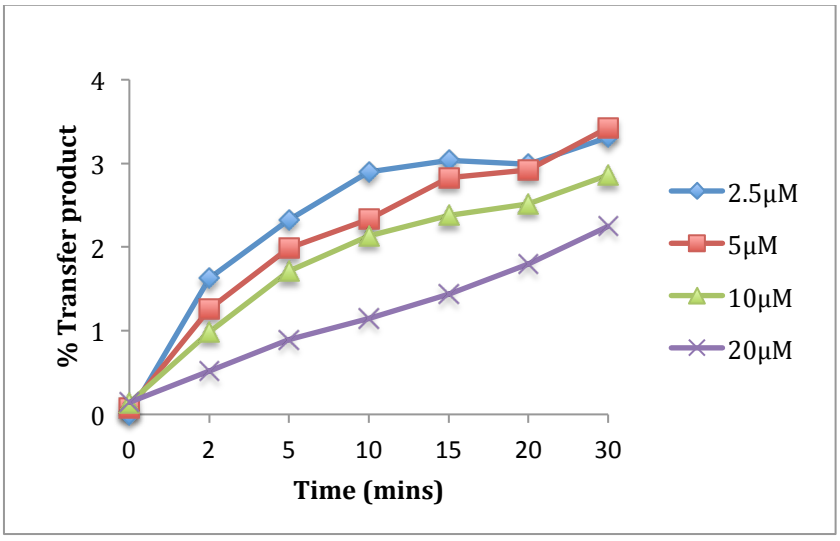

Figure 6.6: 3Dpol (RdRp) optimisation - quantification of transfer product

(A) + (B) Figure represents the total transfer product from the Sym-subU assay over time. Concentrations of 3D (RdRp) as indicated in the figure legend.

all subsequent experiments would use a concentration of 5 μM RdRp, in line with previous studies involving Sym-subU (Arnold and Cameron, 2000). A final experiment that involved determining the optimal concentration of acceptor template was considered necessary. Preliminary experiments that were conducted prior to the collaborative studies described in this chapter had used an arbitrary amount of acceptor template (60 μM). This was deemed appropriate during initial experimental development because it would be greatly in excess of the Sym-subU template (1 μM), and would therefore provide a good opportunity for template switching (Jamie Arnold, personal communication). However, no verification that this level was optimal was available. In principle, a rate-limiting step in any template switching recombination experiment would be the availability of an acceptor RNA strand. A series of Sym-subU assays was carried out that used the previously optimised $ZnCl_2$ (60 μM) and RdRp (5 μM) concentrations, along with various concentrations of acceptor templates (2.5 - 60μM).

The products of the Sym-subU assays were run on a denaturing 20% polyacrylamide gel and visualised using a PhosphorImager (figure 6.7). The product of template switching is barely visible when lower concentrations of acceptor template were used (2.5 and 5 μM), even after over-exposure. As the concentration of acceptor template increases so does the product of template switching (indicated by the arrow). This suggested that the availability of acceptor template was a limiting factor in the Sym-subU assay. Quantification of the gels using ImageQuant software indicated that the higher concentrations of acceptor template impacted negatively on the overall RNA product yield (figure 6.8A). Potentially, the excess of acceptor template may have been enough to recruit free RdRp and therefore inhibit potential extension of the Sym-subU template. The transfer product however, increased as a percentage of overall products when acceptor template concentrations increased (figure 6.8B). This showed that the amount of template switching in the Sym-subU assay could be affected by the concentration of acceptor template.

There was potential to use an even higher concentration of acceptor template, but due to time restraints it was considered that 60 μM would be sufficient in all future experiments. The three

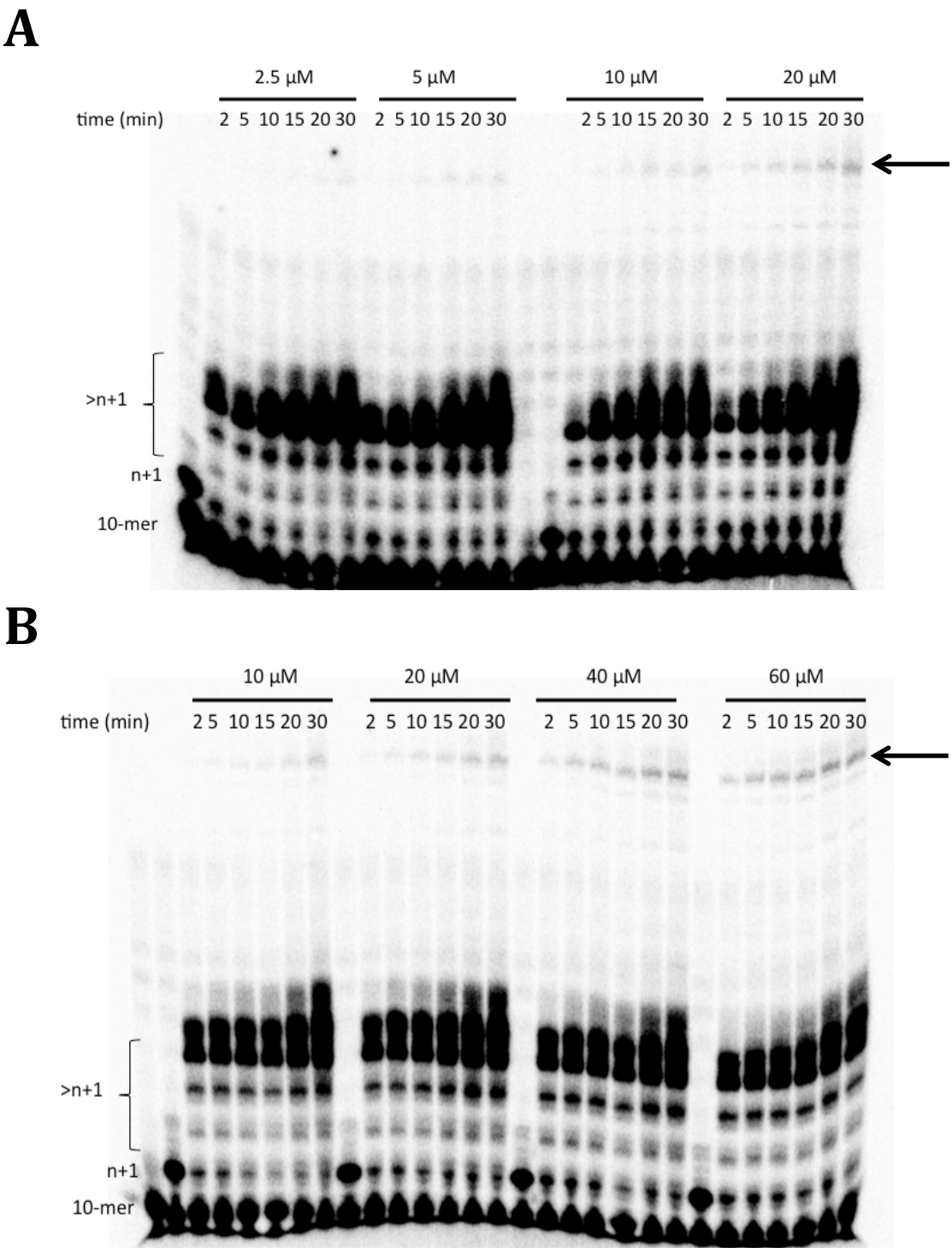

Figure 6.7: Sym-subU acceptor template optimisation assay - Gel images

(A) Template transfer assay using various concentrations of acceptor template (concentrations as indicated) 10-mer indicates Sym-subU, n+1 indicates the product following first nucleotide incorporation, >n+1 indicates extended Sym-subU. The arrow highlights the product from template transfer **(B)** A second experiment with concentrations of acceptor template as indicated.

A

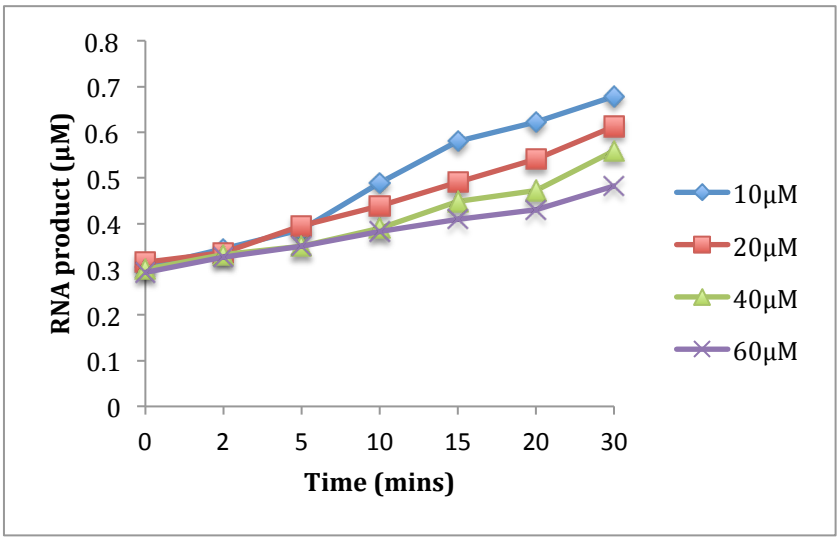

B

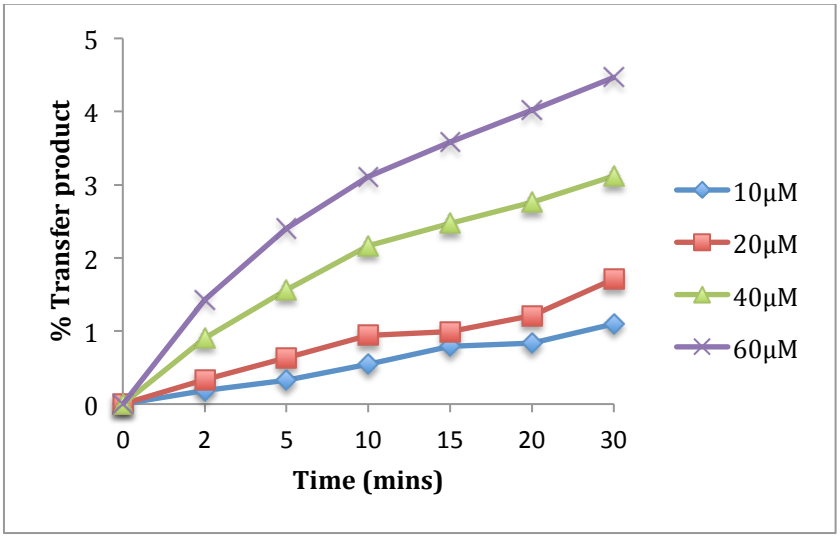

Figure 6.8: Acceptor template optimisation - quantification of RNA and transfer product

(A) Figure represents the total RNA product [(n+1) + (>n+1) + (transfer product)] from the Sym-subU assay over time. Concentrations of acceptor template as indicated **(B)** Figure represents the total % of transfer product over time. 10, 20, 30 and 60 µM represent acceptor template concentrations.

conditions that were optimised in this section ($ZnCl_2$, RdRp and acceptor template) allowed for the introduction of poliovirus RdRp fidelity variants into the assay.

6.4 Biochemical analysis of poliovirus RdRp fidelity variants

The high fidelity RdRp variants, G64S and K359R have been shown to be important in reducing recombination frequency in the CRE-REP and 3'-CRE-REP cell based assays (chapter four and five). However, it remained to be determined if fidelity really was the significant determining factor. The development of a biochemical recombination assay, based upon an already successful assay (Sym-subU) provided a quantitative mechanism to directly measure the template-switching propensity of the high fidelity variants when compared to a wild type RdRp control.

Results in sections 4.5 and 4.6 showed that lower RdRp fidelity (induced by mutagen treatment) increased recombination frequency in the CRE-REP assay. A recent study identified a 'mutator' poliovirus RdRp that had a H273R substitution. Biochemical studies have shown that this mutation leads to a two to three-fold increase in GMP misincorporation. Additionally, sequencing of a virus population carrying this mutation exhibit a similar increase in diversity (Korboukh et al., 2014). It was reasoned that use of this low fidelity RdRp would contrast well with the high fidelity variants. If fidelity were a key determinant in recombination frequency then perhaps this low fidelity variant would show an increase in template switching.

Using the optimised conditions described in section 6.3, three RdRp fidelity variants (G64S, K359R and H273R) were introduced into the biochemical recombination assay and were compared to a wild type RdRp control. The products of the recombination assay were run on a denaturing 20% polyacrylamide gel and visualised using a PhosphorImager (figure 6.9AB). A black arrow indicates the products of template switching. The product of template switching with the K359R variant is undetectable in figure 6.9A and only barely detectable following gross overexposure. In contrast, under similar experimental conditions, the wild type RdRp control produced an easily identifiable band as a result of template switching (figure 6.9AB). This strongly suggested that template switching in the biochemical recombination assay is greatly

inhibited when the RdRp carried a K359R substitution. This result correlated with the CRE-REP and 3'-CRE-REP cell based assays described in chapter 5. To verify these observations the gel image was quantitated using ImageQuant software. The product of template switching was calculated as a percentage of overall RNA products over time and was plotted (figure 6.9C).

The data in figure 6.9C clearly shows that template switching was dramatically inhibited with the K359R variant, with a maximum of 0.17% of total RNA product as a result of template switching (compared to 4.27% with wild type). This represented a 25-fold reduction in recombination frequency between the two, a result that fully supported the cell-based assays. The G64S variant also showed a reduction in template switching when compared to wild type, with a maximum of 2.4% of total RNA product resulting from template switching. This represented a near 1.8 fold reduction when compared to the wild type control. Potentially, this fall in recombination frequency may account for the reduced yield from the cell-based assays conducted with the G64S RdRp variants described in chapter four. Although, the enzymatic ability of the purified G64S RdRp looked to be lower than the wild type RdRp control, as indicated by the overall RNA yield which was ~ 50% lower than the control (data not shown). The RNA product from template switching with the low fidelity variant (H273R) reached a maximum of 5.82% of total product, a 1.4-fold increase compared to wild type RdRp. This result was of particular interest because it indicated that a decrease in fidelity led to an increase in template switching, a result that contrasts well with the higher fidelity variants. This result also supports the cell-based assays conducted in the presence of mutagen (sections 4.5 and 4.6) that are known to lower fidelity. Taken together, the results in figure 6.9 show that RdRp fidelity is a key determinant of template switching.

To further verify the results presented in figure 6.9, and to incorporate another RdRp variant (Y275H) that was shown to reduce recombination frequency in the cell-based CRE-REP assay, it was decided to carry out an additional Sym-subU biochemical recombination assay. Three RdRp variants were used (G64S, K359R and Y275H) with the control being a wild type RdRp. The products of the biochemical recombination assay were run on a denaturing 20%

A

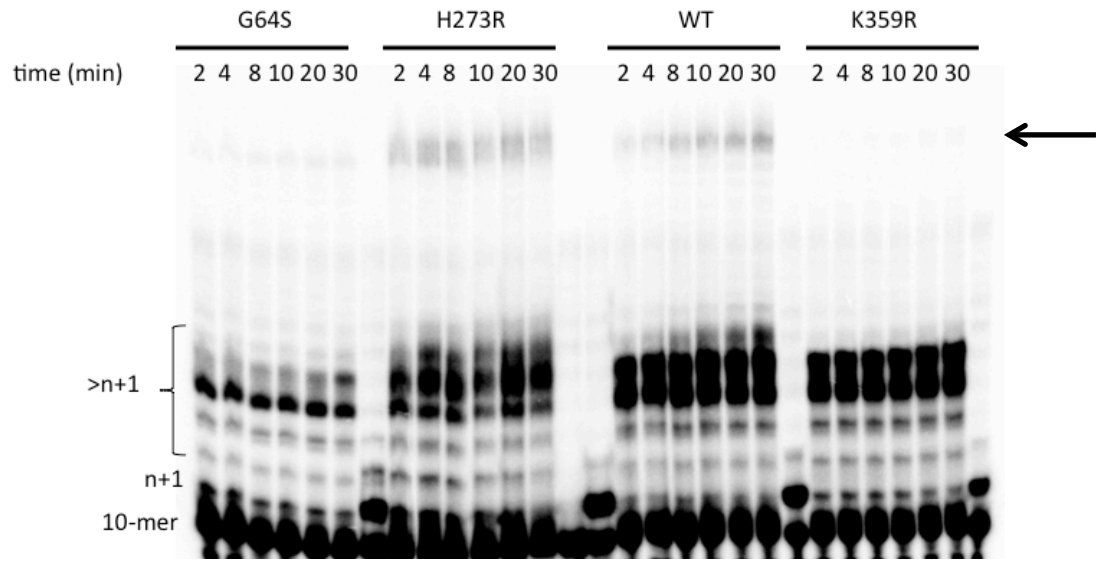
G64S
H273R
WT
K359R
time (min)
2 4 8 10 20 30
2 4 8 10 20 30
2 4 8 10 20 30
2 4 8 10 20 30
>n+1
n+1
10-mer

B

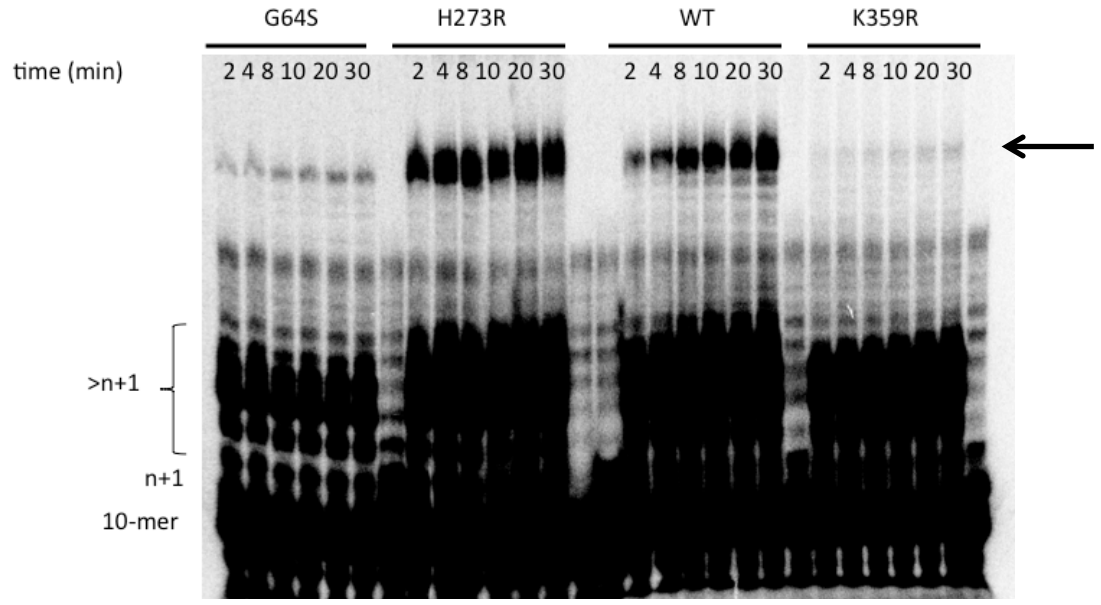
G64S
H273R
WT
K359R
time (min)
2 4 8 10 20 30
2 4 8 10 20 30
2 4 8 10 20 30
2 4 8 10 20 30
>n+1
n+1
10-mer

C

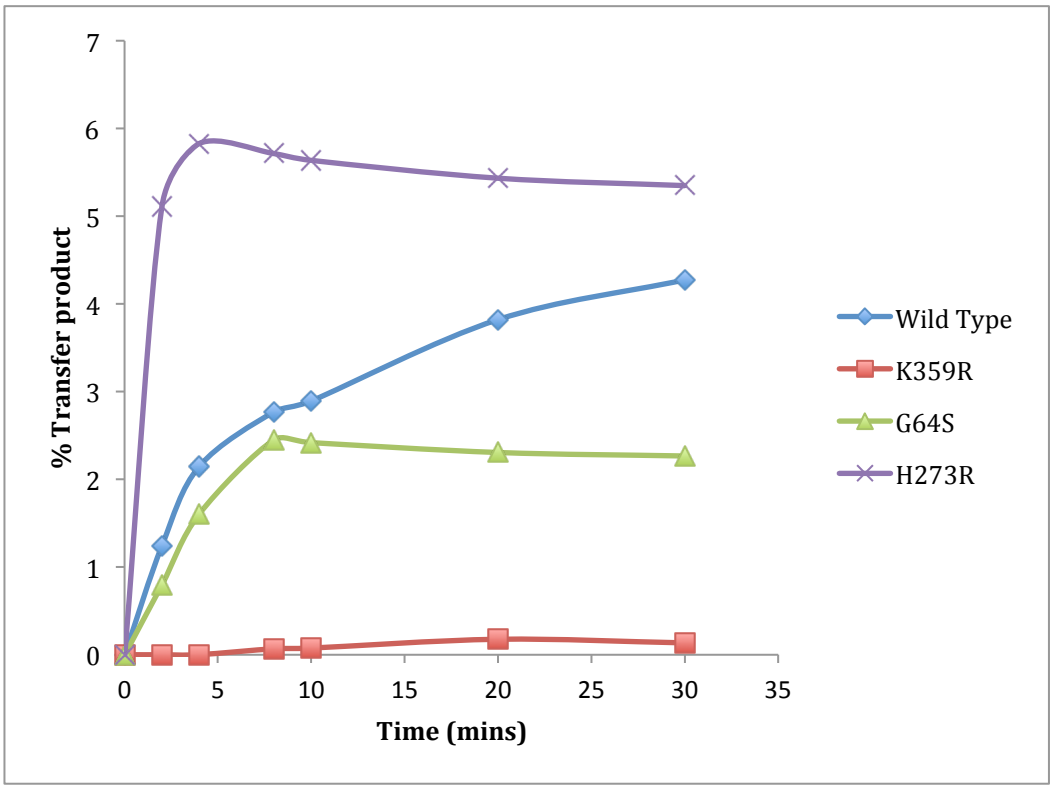

Figure 6.9: Sym-subU recombination assay: RdRp variants assay (1)

(A) Strand transfer assay after optimisation using fidelity variants as indicated (G64S, H273R, wild type and K359R) 10-mer indicates Sym-subU, n+1 indicates the product following first nucleotide incorporation, >n+1 indicates extended Sym-subU. The arrow highlights the product from strand transfer **(B)** Overexposure of image (A) **(C)** Quantification of template transfer product, taken as a % of overall RNA product.

polyacrylamide gel and visualised using a PhosphorImager. A black arrow indicates the product of template switching (figure 6.10A). Early interpretations suggested that an error was made during the experiment. The G64S samples at the 4 and 8-minute time-points looked as if they were incorrectly loaded. The gel image was quantitated using ImageQuant software. To overcome any issues with the G64S sample, all data points from 4 and 8 minutes were removed in the subsequent analysis. The product of template switching was calculated as a percentage of overall RNA products over time and was plotted (figure 6.10B).

Even after removal of some of the data points, the results in figure 6.10B do provide interpretable data. The Y275H and K359R showed a similar non-recombinogenic phenotype, with each exhibiting on average a 16-fold and 22-fold reduction in template switching respectively when compared to the wild type control at the 30-minute time point. The G64S data is more difficult to interpret given the potential error with the samples. Although, from ten minutes onward the G64S variant exhibited a consistent near 2-fold reduction in template switching when compared to the wild type control. This result correlated with the previous Sym-subU recombination assay shown in figure 6.9C. The repeated experiment provided additional data to support the observations that fidelity directly influences recombination frequency and also showed that the Y275H has a similar phenotype as K359R with regard to recombination. The Y275H data supports the CRE-REP assay results in section 5.5, and also provides further validation to the GFP-retention assay carried out by the Andino research group. However, due to the time-restraints involved during this area of investigation, caution must be used when considering these results. The biochemical recombination assay does show reproducibility. For example, the product of template switching with the wild type RdRp in all of the assays conducted ranged from 4.17 % to a maximum of 4.7%. Similarly, the reduction in template switching with the high fidelity RdRp variants (G64S and K359R) in two separate experiments was consistent. However, to completely validate this approach multiple samples at each time point will be required i.e. repeat each experiment in triplicate.

A

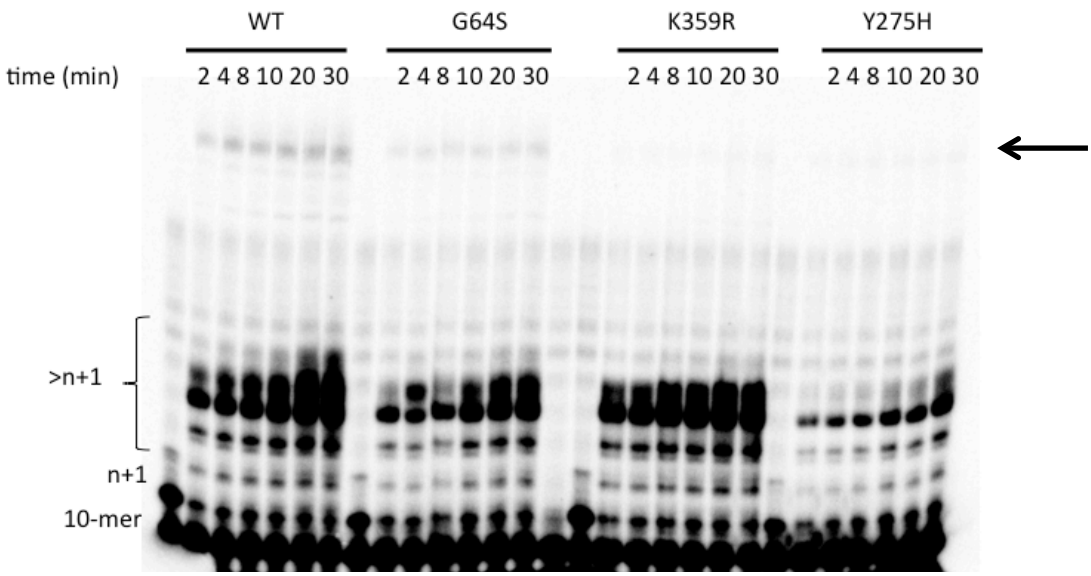

B

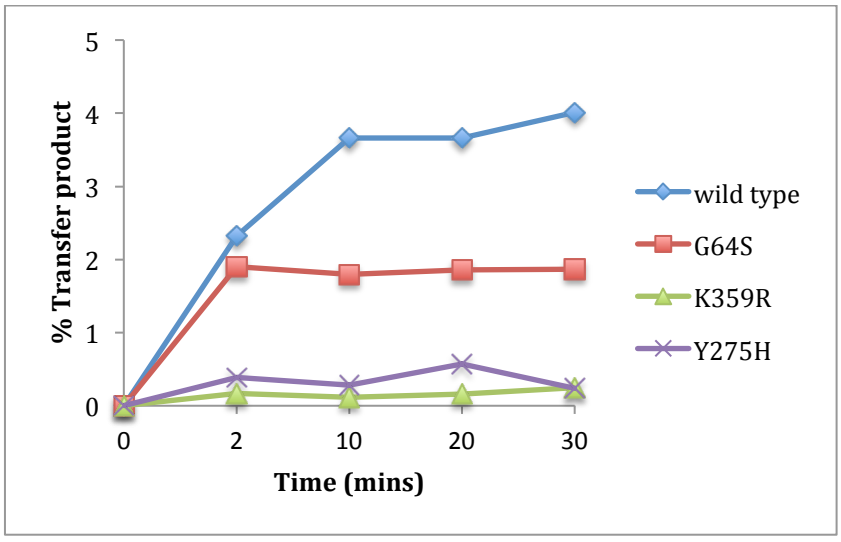

Figure 6.10: Sym-subU recombination assay: RdRp variants assay (2)

(A) Template transfer assay using fidelity variants as indicated (wild type, G64S, K359R and Y275H) 10-mer indicates Sym-subU, n+1 indicates the product following first nucleotide incorporation, >n+1 indicates extended Sym-subU. The arrow highlights the product from strand transfer **(B)** Scatterplot quantification of template transfer product, taken as a % of overall RNA product.

6.5 Minimal sequence requirements for the biochemical recombination assay

The Sym-subU recombination assay was designed to have two direct repeats of UACG in the acceptor template (figure 6.11A). These regions were thought to provide two potential areas where the extended Sym-subU template could anneal, thus allowing continued RNA synthesis. The single product seen in figure 6.4 and 6.7 suggested that only one of these, if used at all, was involved. The characterisation of intertypic recombinants isolated from the CRE-REP assay previously, has found no obvious link to sequence identity and location of the recombination junction (Lowry et al., 2014). Although, the resolution assays described in section 3.8 suggested that sequence identity might be a factor during subsequent recombination events. Due to the 'promiscuous' nature of recombination in the CRE-REP assay, it was reasoned that a study upon the minimal sequence requirements of the Sym-subU recombination assay might shed light on the template-switching event. In order to investigate this phenomenon a series of acceptor templates were designed that would enable: - (1) identification of minimal sequence required for template switching, and (2) identify the preferred site upon the acceptor template for this switch. Acceptor templates #1 and #2 have a single UACG motif (figure 6.11B), at the 3' end or internally. It was reasoned that use of these acceptor templates would identify the primary site upon the acceptor template where the template-switching event occurs. It was also decided that modification of the original acceptor template might aid the identification of the primary site of template switching. To accomplish this, a 4-nt sequence that shared no identity to the Sym-subU template was positioned between the two postulated acceptor sites (acceptor #3, figure 6.11B). This modified acceptor template was considered the control template in all subsequent reduced complementarity experiments. To carry out these assays a series of acceptor templates were designed and manufactured by Dharmacon™. Acceptor templates #3 to #6 have reduced complementarity from the 3' end of the Sym-subU template or primer (sequences underlined). To contrast these templates, acceptors #7, #8 and #11 have reduced complementarity from the 5' end of the Sym-subU template or primer (sequences underlined). By reducing this complementarity, in either direction, it was expected that a reduction in template switching

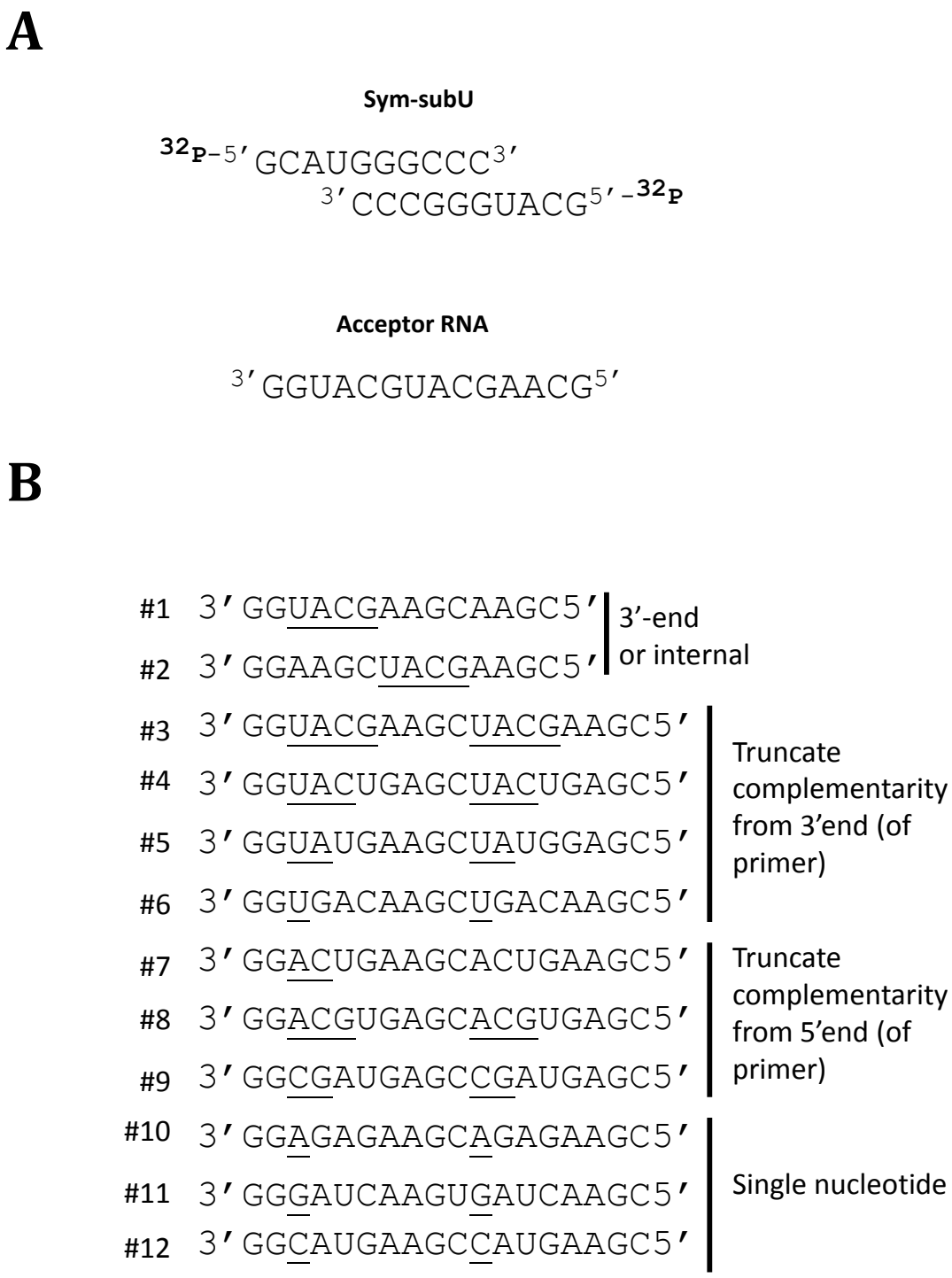

Figure 6.11: Alternate acceptor templates with reduced complementarity

(A) Sym-subU and the original acceptor RNA with two (UACG) regions of identity **(B)** New acceptor templates. # 1 and #2 have a single UACG sequence at 3' end or internal. #3 (new acceptor) #4 to #6 have reduced complementarity (underlined sequence) from the 3' end of the primer. #7, #8 and #11 have reduced complementarity (underlined sequence) from the 5' end of the primer. Remaining templates (#10 and #12) have single nucleotide complementarity to the Sym-subU template.

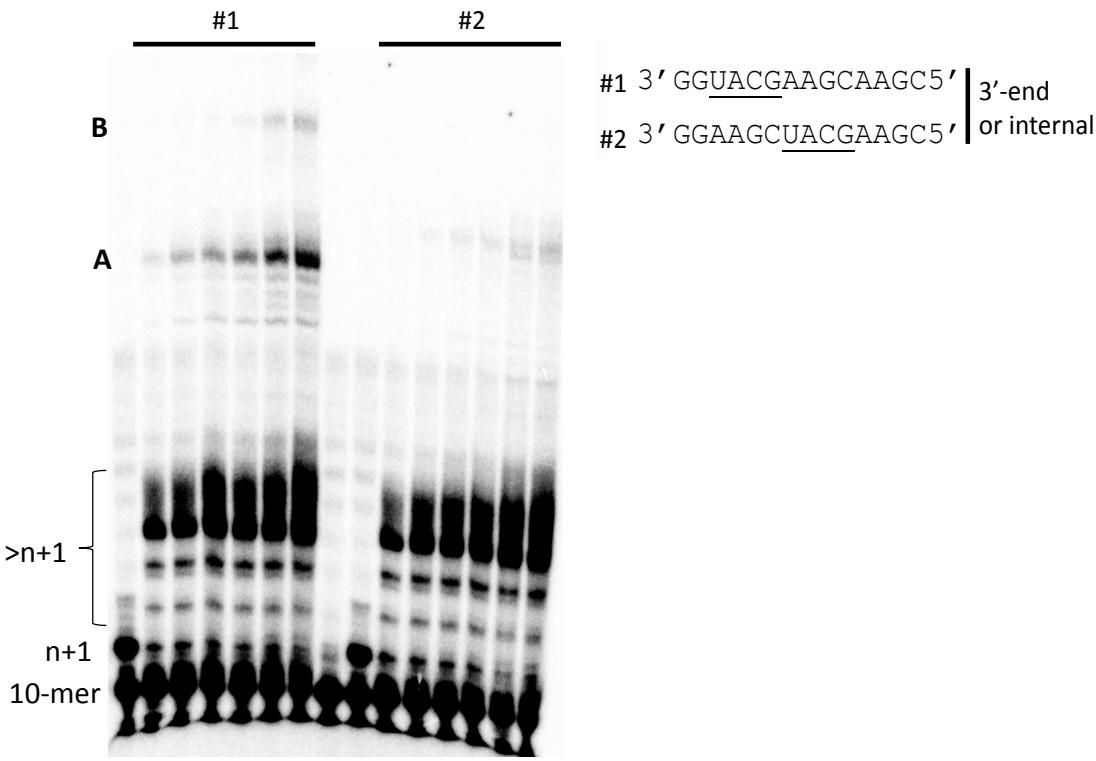

Figure 6.12: Sym-subU recombination assay - preferred site of template switch

Template transfer assay using modified acceptor templates #1 and #2 with either 3' end or internal complementarity (underlined). 10-mer indicates Sym-subU, n+1 indicates the product following first nucleotide incorporation, >n+1 indicates extended Sym-subU **(A)** Indicates the product from template transfer **(B)** Product from secondary template switching.

might be observed (if this was important in the template switching event) in an interpretable manner. Additional single nucleotide templates are also shown. An initial Sym-subU assay was carried out that used the acceptor templates #1 and #2. A similar optimised protocol to that used in section 6.3 was used. Samples were taken at 2, 4, 8, 10, 20 and 30 mins intervals, quenched for RdRp activity, and were run on a denaturing 20% polyacrylamide gel and visualised using a PhosphorImager (figure 6.12). The product of template switching was clearly visible (band A) when the #1 template was used, indicating that template switching had occurred. Additional bands can be seen beneath the major A band, and these can be potentially attributed to template switching that have not fully extended on the acceptor template. The presence of a higher molecular weight band (B) suggested that products from template switching had been involved in secondary template switching. In contrast, only a barely detectable band with a higher molecular weight than band A was observed when the #2 template was used. In principle, if the internal UACG site had been used with this template then the expected product of template switching would have been shorter so should have migrated further on the gel. This higher molecular weight band is therefore hard to interpret. Perhaps this was a product from a promiscuous, sequence independent template switch? The strong signal obtained from the #1 template (band A) that had a UACG motif at its 3' end suggested that this was the primary site upon the acceptor where template switching was occurring.

By using the acceptor templates #4, 5 and 6 with reduced complementarity from the 3'end of the Sym-subU primer it was expected that products from template switching in the biochemical recombination assay would reduce in line with the gradual reduction in sequence identity. A Sym-subU recombination assay was carried out using the aforementioned templates along with the #3 template, which was considered the control. Samples were taken at timed intervals (2, 4, 8, 10, 20 and 30 mins) and quenched for RdRp activity. The products of the assay were then run on a denaturing 20% polyacrylamide gel and visualised using a PhosphorImager (figure 6.13A). The control template (#3) produced a band that was believed to be the product from template switching (black arrow). A banding pattern beneath the indicated product of template switching was also observed (lowest molecular weight band indicated by red arrow). Like the result outlined in figure 6.12, these can be potentially attributed to template switching products that

A

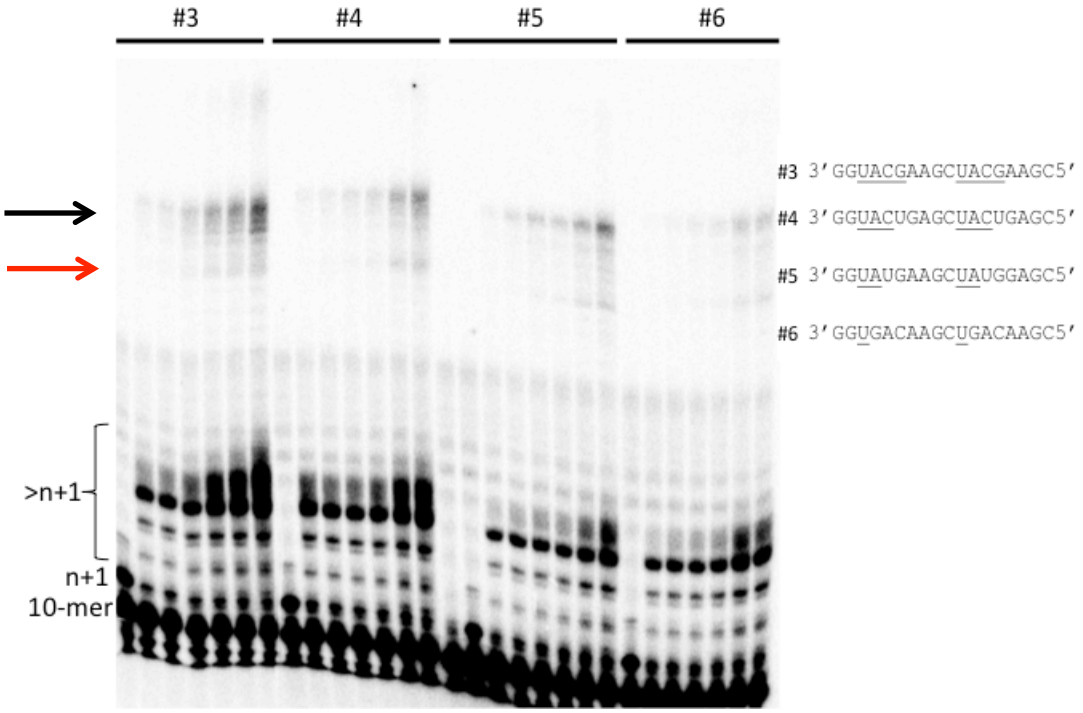
#3
#4
#5
#6
#3 3′GGUACGAAGCUACGAAGC5′
#4 3′GGUACUGAGCUACUGAGC5′
#5 3′GGUAUGAAGCUAUGGAGC5′
#6 3′GGUGACAAGCUGACAAGC5′
>n+1
n+1
10-mer

B

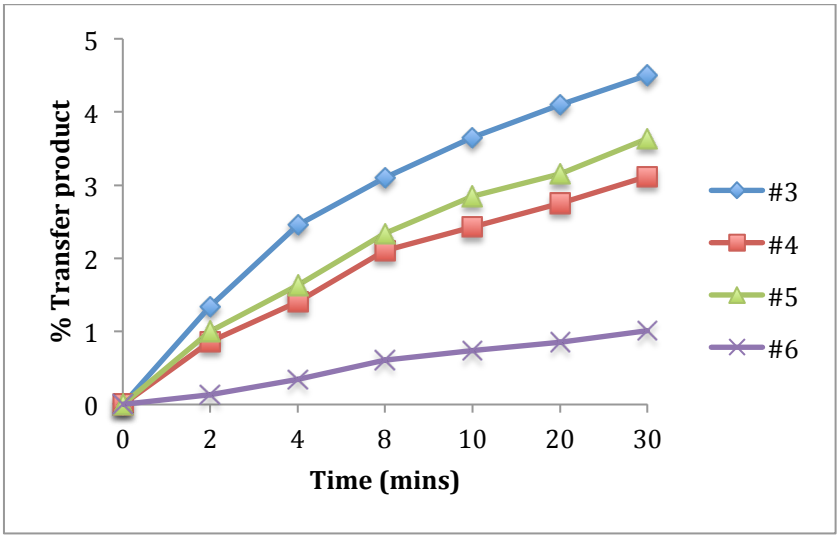
% Transfer product
0
1
2
3
4
5
0
2
4
8
10
20
30
Time (mins)
#3
#4
#5
#6

C

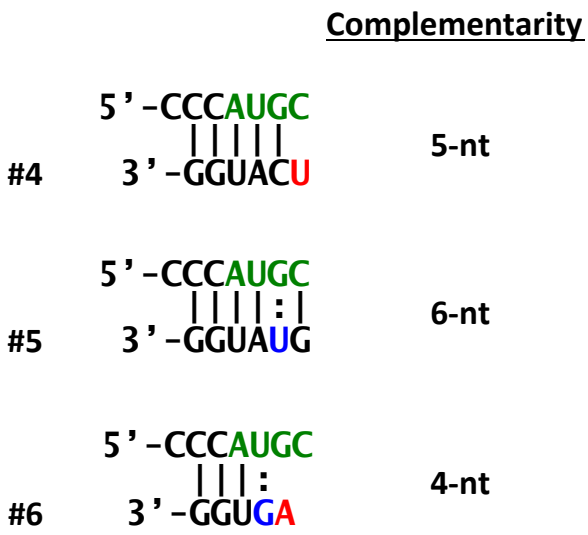

Figure 6.13: Sym-subU reduced acceptor complementarity assay (1)

(A) Template transfer assay using modified acceptor templates #3, 4, 5 and 6 with reduced complementarity (underlined) from the 3' end of the Sym-subU primer. 10-mer indicates Sym-subU, n+1 indicates the product following first nucleotide incorporation, >n+1 indicates extended Sym-subU. The black arrow highlights the product from template transfer. Red arrow indicates the lowest molecular weight product from template switching **(B)** Scatterplot quantification of template transfer product, taken as a % of overall RNA product. Acceptor templates as indicated. **(C)** Potential complementarity following template switching. **Green** indicates fully extended Sym-subU. Acceptor templates as indicated. **Black** upon acceptor indicates regions of complementarity. **Blue** indicates potential base pairing. **Red** indicates incorrect base pairing. Length of potential complementarity as indicated.

have not fully extended. The image was quantitated using ImageQuant software and the product of template switching was calculated as a percentage of overall RNA products over time and was plotted (figure 6.13B). The reduction in template switching was confirmed, with acceptor #4 exhibiting 1.44-fold reduction in products from template switching than acceptor #3. However, the assay carried out using acceptor #5 produced more products from template switching than acceptor #4, a result that was unexpected, given that complementarity was reduced. This result might be explained by closer inspection of the potential regions of identity between the Sym-subU template and the acceptor templates (figure 6.13C). Acceptor #4 has a maximum of 5-nt of sequence complementarity with the Sym-subU template, whereas acceptor #5 has a potential 6-nt of sequence complementarity with the Sym-subU template due to a G:U wobble base pairing. The product of template switching with acceptor #6 was reduced by around 4-fold when compared to the control. This template has a region of complementarity that was at least 3-nt in length and could potentially be as much as 4-nt given the G:U wobble base pairing that may be possible. Conclusions from this assay were that a region of complementarity that was at least 3-nt in length was sufficient for template switching in the Sym-subU recombination assay. It remained to be determined if complementarity could be reduced further. To answer this question, acceptor templates #8, 9 and 11 were used in a Sym-subU recombination assay using the same protocol. The control acceptor #3 remained the same. In principle, by reducing complementarity from the 5' end of the Sym-subU template using these alternate acceptor templates would reduce complementarity to only two bases (GG). Alignment of potential primer - acceptor interactions showed this to be the case (figure 6.14B). The samples from the experiment were run on a denaturing 20% polyacrylamide gel and visualised using a PhosphorImager (figure 6.14A). As expected the control acceptor (#3) produced banding that indicated template switching. In contrast, it was clearly evident that reducing complementarity to only two bases had almost completely inhibited template switching. This experiment was not quantitated given the clear reduction in template switching. Conclusions from both experiments showed that a minimal 3-nt sequence of complementarity is required for detectable template switching in the Sym-subU recombination assay.

A

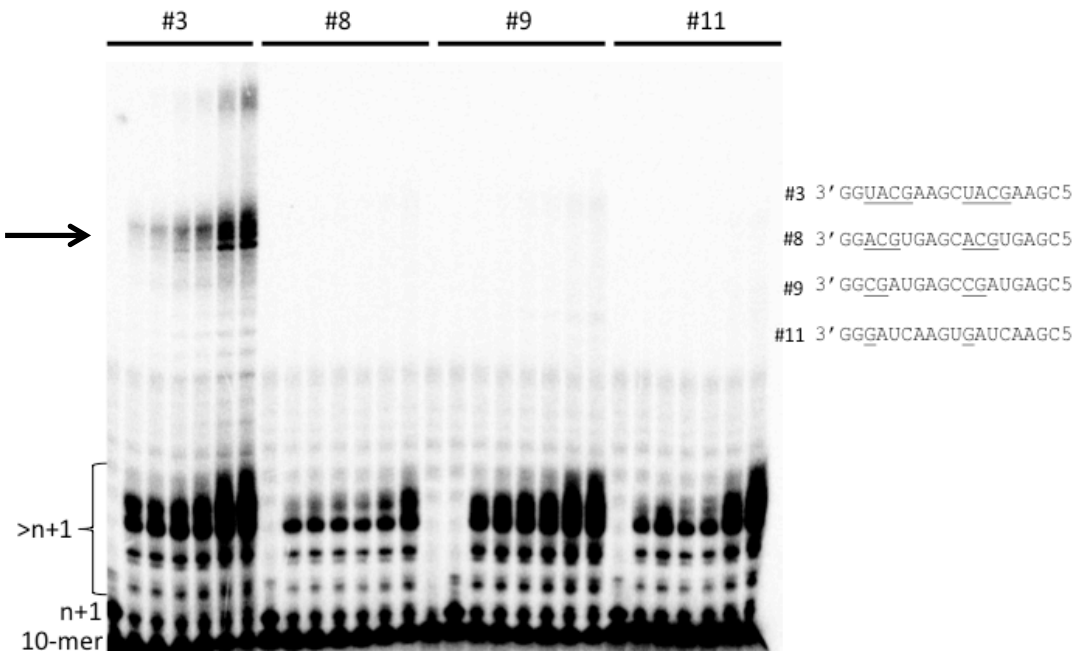

B

Complementarity

#8	5'-CCCAUGC || 3'-GGACG	2-nt
#9	5'-CCCAUGC || : 3'-GGCGA	2-nt
#11	5'-CCCAUGC || |: 3'-GGGAU	2-nt

Figure 6.14: Sym-subU reduced acceptor complementarity assay (2)

(A) Template transfer assay using modified acceptor templates #3, 8, 9 and 11 with reduced complementarity (underlined) from the 5' end of the Sym-subU primer. 10-mer indicates Sym-subU, n+1 indicates the product following first nucleotide incorporation, >n+1 indicates extended Sym-subU. The arrow highlights the product from template transfer **(B)** Potential complementarity following template switching. **Green** indicates fully extended Sym-subU. Acceptor templates as indicated. **Black** upon acceptor indicates regions of complementarity. **Blue** indicates potential base pairing. **Red** indicates incorrect base pairing. Length of identity as indicated.

6.6 Sequence modifications in the intertypic CRE-REP assay

The results in the Sym-subU recombination assay suggested that minimal sequence identity was required for a detectable level of template switching. Additionally, the resolution assays described in chapter three suggested that sequence homology might be important for this phase of recombination.

The CRE-REP assay, by nature of the lesions carried by the parental RNA templates, has a potential region of recombination of 1.058 Kb. Sequencing of over 100 intertypic recombinants isolated from this assay had shown that recombination clusters to regions encoding two protein-protein cleavage boundaries (section 3.3). The analysis of the primary products of recombination could find no obvious link to RNA sequence at the site of template switching. This might imply that protein-protein compatibility is the overriding requirement in the selection of the primary intertypic recombinant. However, intratypic recombination in the CRE-REP assay was primarily precise in nature with no additional sequence (unlike intertypic), suggesting that sequence identity between parental RNA might be important. Alternatively, the primary product of intratypic recombination might have a fitness advantage (due to the optimal protein content of its genome) and therefore goes through the resolution stage at a faster rate than its intertypic counterpart. Due to the sequence identity of the parental genomes it would be impossible to identify the sites of recombination, other than imprecise junctions. Poliovirus type 1 has an RNA sequence that is 21% divergent to PV3 within the CRE-REP recombination region. Which results in a 4-9% divergence at the amino acid level between type 1 and type 3 proteins 2A, 2B and 2C (Lowry et al., 2014). The observation that the primary products of intertypic recombination fall primarily into two main cluster groups allowed development of a modified donor template. The manipulation of sequence identity at a known region of recombination allowed an investigation into sequence identity between donor and recipient template to be carried out. It was reasoned that the cluster one region (luciferase / 2A) would be the internal control and would therefore remain unaltered. A region of 450-nt that precisely spans the 2A/2B cleavage boundary (cluster 2) within the PV1 replicon (pRLucWT) template was targeted for modification. The objective of this alteration was to produce a donor template

that was as similar to the acceptor template in RNA sequence as possible. The 450-nt sized region was chosen because it spanned all of the characterised imprecise intertypic recombinant isolated to date in this region. This area of PV1 has a divergence of 22.4% in RNA sequence when compared to the same region of the PV3 acceptor template (figure 6.15A). However, this only represents a divergence of 5.3% at the amino-acid level (figure 6.15B). This discrepancy is due to the majority of nucleotide differences being located at the 'wobble' base position of the amino acid codon. A modified sequence was designed (PV3-LIKE) that was as similar to the RNA sequence of the acceptor template (SL3) as possible, whilst still maintaining the amino acid code of the native PV1 sequence (figure 6.16). It was reasoned that if recombination frequency or location was influenced by sequence identity then the modified donor (that was only 2.2% divergent in RNA sequence to the acceptor) might provide the best opportunity for this to be highlighted. Eurofins™ manufactured the modified sequence as cDNA, which was subsequently PCR amplified. The PCR product (carrying the modified sequence) was then used to produce a larger cDNA fragment by two steps of overlap extension PCR (oligonucleotides that were used can be found in section 2.9). The subsequent 2.4 Kb fragment was then sub-cloned into pRLucWT by use of the unique restriction enzyme sites *PacI* and *BglII*. The final construct was called pPV3-LIKE and the entire modified region was sequence verified. The cDNA was linearised using the restriction enzyme *ApaI* and RNA was transcribed using T7 polymerase. A luciferase time course assay was carried out to examine the replication kinetics of the replicon encoded by the modified donor template (figure 6.17A). This was considered an important control, as any effect on replication would affect interpretation of any CRE-REP assay results. The luciferase signal produced by the PV3-LIKE donor template was around ~30% of the wild type PV1 replicon control. This indicated that modification of the 450-nt region had an adverse affect upon replication. This was unexpected given the controls used in the design of the sequence. A subsequent intertypic CRE-REP assay was carried out that would compare the yield of recombinant virus from the PV3/PV3-LIKE and control PV3/1 partners. L929 cells in a 12-well plate were co-transfected in triplicate wells with RLucWT and SL3 or PV3-LIKE and SL3. Total RNA was 0.5 μg in a 1:1 ratio (replicon: CRE mutant genome). Cells were incubated for 48 hrs post transfection and media supernatant was then harvested and used to inoculate HeLa cell monolayers for plaque assays. Following sixty hours incubation, cells were stained with crystal

A

```
PV1             TTCGTTGGCCCAACGTTCCAGTACATGGAGGCTAATAACTATTACCCAGCTAGGTACCAG 60
PV3             TTTGTGGGACCCACCTTCCAATACATGGAGGCTAATGACTACTACCCAGCTAGATACCAA 60
                ** ** **.**.** *****.***************.**** ***********.*****.

PV1             TCCCATATGCTCATTGGCCATGGATTCGCATCTCCAGGGGATTGTGGTGGCATACTCAGA 120
PV3             TCCCACATGTTAATCGGGCACGGCTTTGCCTCACCAGGTGACTGTGGTGGTATCCTTAGG 120
                ***** *** *.** ** ** **.** **.**:***** ** ******** **.** **.

PV1             TGTCACCACGGGGTGATAGGGATCATTACTGCTGGTGGCGAAGGGTTGGTTGCATTTTCA 180
PV3             TGTCAACATGGCGTCATCGGAATCGTGACAGCTGGTGGAGAGGGATTAGTCGCATTCTCT 180
                *****.** ** ** **.**.***.* **:********.**.**.**.** ***** **:

PV1             GACATTAGAGACTTGTATGCCTACGAAGAAGAAGCCATGGAACAAGGCATCACCAATTAC 240
PV3             GACATAAGGGACTTGTATGCTTACGAGGAAGAGGCCATGGAGCAGGGCATTTCAAACTAT 240
                *****:**.********** *****.*****.********.**.***** :*.** **

PV1             ATAGAGTCACTTGGGGCCGCATTTGGAAGTGGATTTACTCAGCAGATTAGCGACAAAATA 300
PV3             ATTGAGTCACTCGGTGCTGCGTTCGGTAGTGGGTTCACTCAGCAAATAGGGGATAAGATA 300
                **:******** ** ** **.** **:*****.** ********.**:.* ** **.***

PV1             ACAGAGTTGACCAATATGGTGACCAGTACCATCACTGAAAAGCTACTTAAGAACTTGATC 360
PV3             TCAGAACTAACCAGCATGGTGACCAGCACGATTACAGAGAAGCTACTTAAAAACCTAATC 360
                :****. *.****. ********** ** ** **:**.**********.*** *.***

PV1             AAGATCATATCCTCACTAGTTATTATAACTAGGAACTATGAAGACACCACAACAGTGCTC 420
PV3             AAAATTATTTCATCTCTGGTGATTATCACTAGAAATTACGAAGATACCACCACAGTGCTC 420
                **.** **:**.**:**.** *****.*****.** ** ***** *****.*********

PV1             GCTACCCTGGCCCTTCTTGGGTGTGATGCT 450
PV3             GCCACTCTAGCTCTTCTTGGGTGTGATGTT 450
                ** ** **.** *************** *
```

B

```
PV1             FVGPTFQYMEANNYYPARYQSHMLIGHGFASPGDCGGILRCHHGVIGIITAGGEGLVAFS 60
PV3             FVGPTFQYMEANDYYPARYQSHMLIGHGFASPGDCGGILRCQHGVIGIVTAGGEGLVAFS 60
                ***********:**************************:******:**********

PV1             DIRDLYAYEEEAMEQGITNYIESLGAAFGSGFTQQISDKITELTNMVTSTITEKLLKNLI 120
PV3             DIRDLYAYEEEAMEQGISNYIESLGAAFGSGFTQQIGDKISELTSMVTSTITEKLLKNLI 120
                ****************:******************.***:***.***************

PV1             KIISSLVIITRNYEDTTTVLATLALLGCDA 150
PV3             KIISSLVIITRNYEDTTTVLATLALLGCDV 150
                ****************************.
```

Figure 6.15: Sequence alignments of PV1 and PV3 across the 2A/2B boundary

(A) RNA sequence alignment of a 450-nt region that precisely spans the 2A/2B cleavage boundary of PV1 and PV3. Glutamine and glycine codons underlined (cleavage boundary) **(B)** Amino acid sequence of the same region of PV3 and PV1. Glutamine and glycine residues underlined.

Figure 6.16: Sequence alignments of PV3 and the modified PV1 replicon (PV3-LIKE)

(A) RNA sequence alignment of a 450-nt region that precisely spans the 2A/2B cleavage boundary of PV3 and PV3-LIKE. Glutamine and glycine codons underlined (cleavage boundary).

A

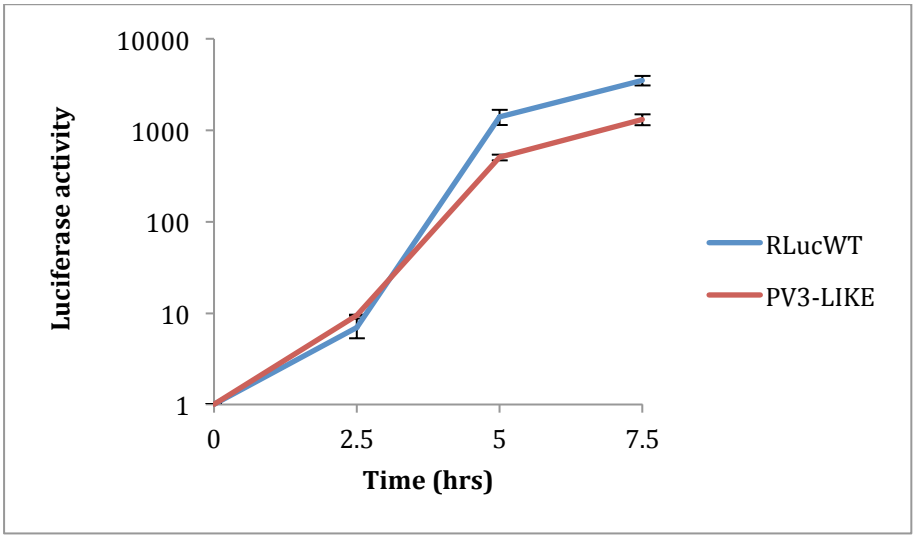

B

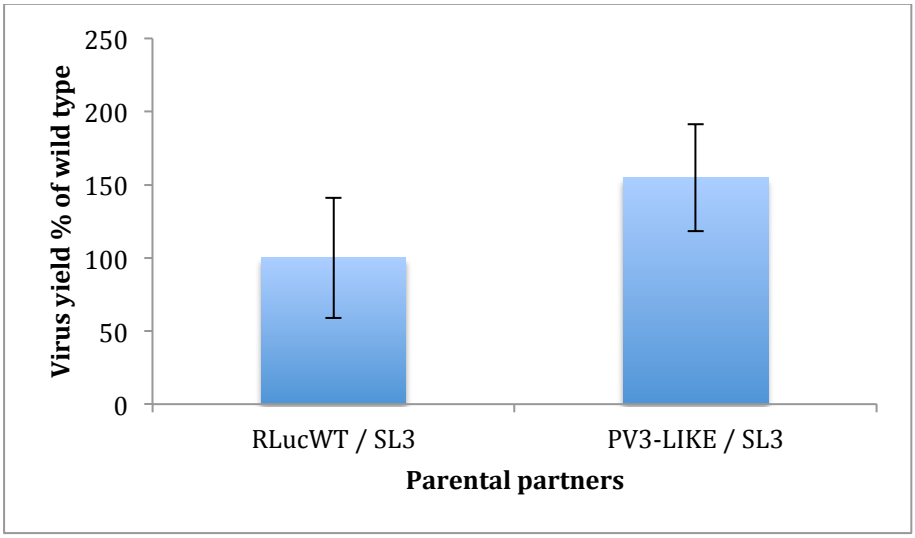

Figure 6.17: Replication kinetics and recombination frequency of PV3-LIKE pRLuc replicon

(A) Replication kinetics of a PV1 sub-genomic replicon (pRLucWT) and PV3-Like sub-genomic replicon. 250ng of RNA was transfected into HeLa cells in duplicate. Samples were taken at the times indicated and luciferase activity was measured and normalised using a mock transfected control. Error bars indicate standard deviation of two independent samples **(B)** Intertypic CRE-REP assay involving the modified PV1 replicon (PV3-LIKE). The data represents the mean from three independent samples. Error bars indicate standard deviation. RNA partners as indicated.

violet and plaques quantified (figure 6.17B). Results indicated that the modified donor template led to an increase in recombination frequency (average of 96 pfu/ml) when compared to the wild type intertypic partner control (average of 62 pfu/ml). The data was analysed by Students T-test. A two-tailed test found no significant difference. A one-tailed test did find significance with the *P* value at 0.035. The increase in recombination frequency might have been due to a bias in recombination to the cluster two boundary. It was therefore decided to investigate the location of recombination in a pool of PV3/PV3-LIKE intertypic recombinant isolates.

In order to characterise a pool of intertypic recombinants it was decided to carry out six separate co-transfections in L929 cells using the same intertypic partners shown in figure 6.17B. It was reasoned that pooling of the media supernatant would avoid any bias in recombinant that may be due to any 'founder-effect'. In principle, a recombinant genome that is produced at a very early stage may be subsequently used as a template for further replication in the same cell, which may bias any down-stream characterisation. This phenomenon can probably account for the numerous similar sequences obtained in a previous study (Lowry et al., 2014). All separate transfections produced similar yields of viable intertypic recombinant virus (data not shown). The transfection supernatant (carrying viable recombinant virus) was used in a limiting dilution approach to biologically clone individual recombinants. Thirty biologically cloned recombinants from the wild type intertypic partners (RLucWT / SL3) and thirty recombinants from the modified partners (PV3-LIKE / SL3) were isolated and their RNA was extracted and reverse transcribed. The region of recombination in all samples was then amplified by PCR using the primers PV3-2995F and PV1-4470R (figure 6.18A). This produced a PCR product that covered the entire 1.058 Kb region of recombination. In order to screen a large pool of recombinants in a timely and cost-effective manner, a restriction fragment length polymorphism (RFLP) approach was deemed most appropriate. The donor templates (RLucWT and PV3-LIKE) have a unique *PstI* restriction enzyme site located immediately adjacent to the luciferase/2A boundary. It was reasoned that the unique restriction enzyme site would be present in the recombinant genome if the recombination junction were located within cluster one. Similarly, if the recombination junction were within the characterised cluster two-region

A

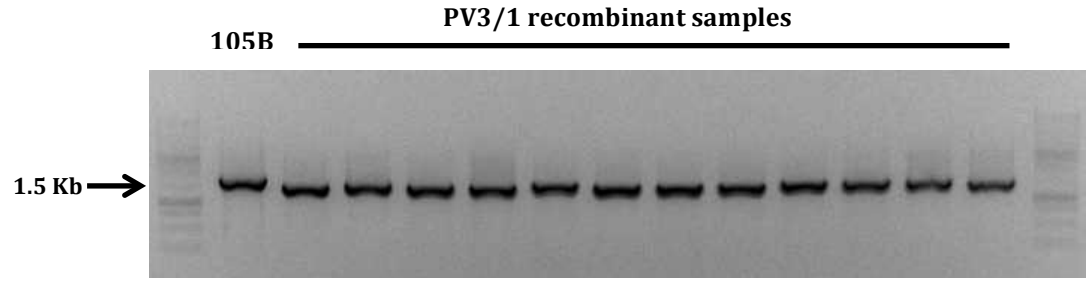
PV3/1 recombinant samples
105B
1.5 Kb

B

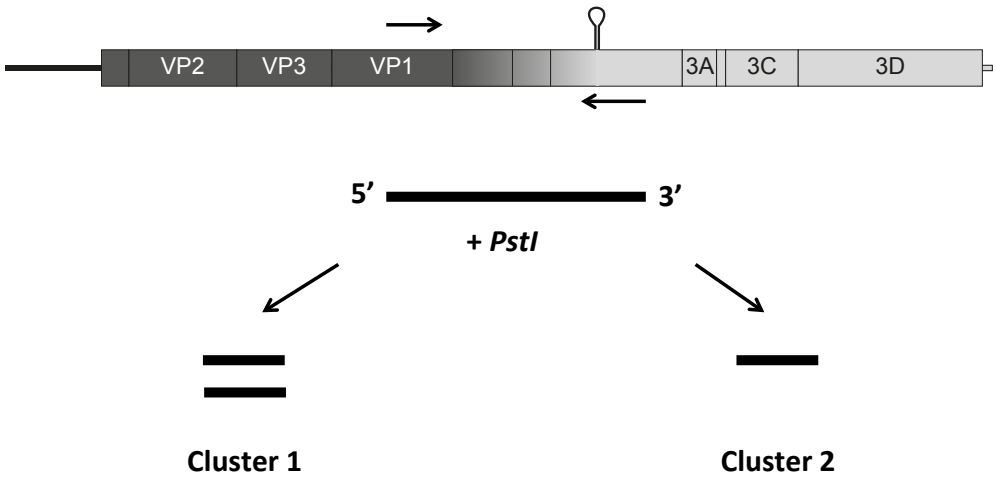
VP2
VP3
VP1
3A
3C
3D
5'
3'
+ PstI
Cluster 1
Cluster 2

C

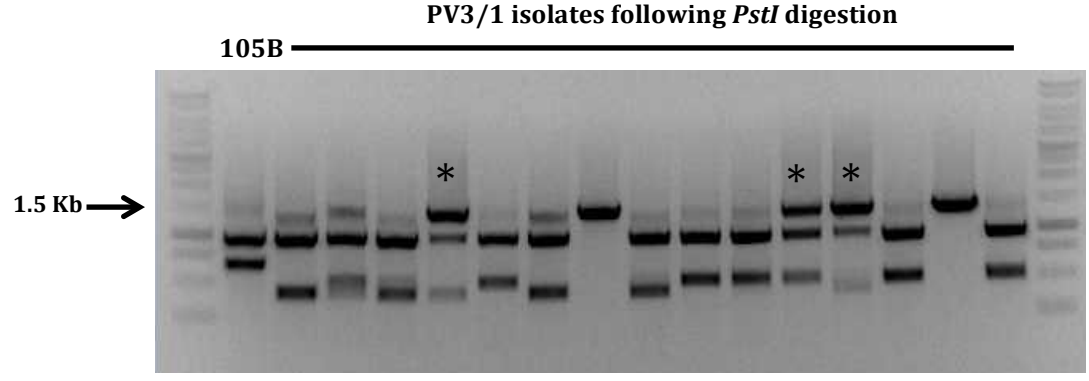
PV3/1 isolates following PstI digestion
105B
1.5 Kb
*
*
*

D

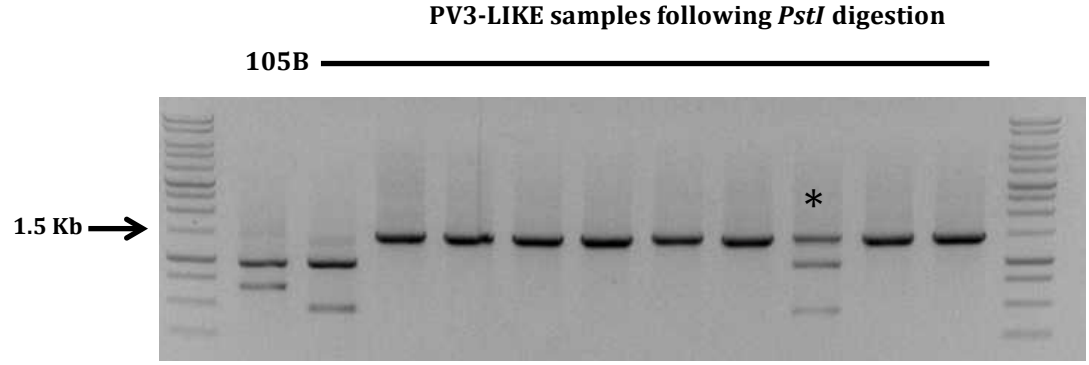

Figure 6.18: Comparison of recombination junctions by restriction fragment polymorphism (RFLP)

(A) Representative ethidium bromide stained 1% agarose gel showing the products of RT-PCR amplification from biologically cloned PV3/1 recombinants. Molecular clone 105B control as indicated. **(B)** Recombinant genome. Forward and reverse arrows indicate primers used to amplify the region of recombination from VP1 to the 2C CRE. Beneath is a black 5' to 3' line representing the PCR product. Subsequent digestion with the restriction enzyme *PstI* should produce two bands if the recombinant has a junction within cluster 1, no digestion occurs in the PCR product if the recombinant has a junction within cluster 2 **(C)** Representative ethidium bromide stained 1% agarose gel showing the products of RT-PCR amplification from biologically cloned PV3/1 recombinants following *PstI* restriction enzyme digestion. * Indicates a potential mixed population **(D)** Representative ethidium bromide stained 1% agarose gel showing the products of RT-PCR amplification from biologically cloned PV3/PV3-Like recombinants following *PstI* restriction enzyme digestion. * Indicates a potential mixed population.

the restriction enzyme site would not be present (detailed in figure 6.18B). The control samples in this assay were the recombinant clones isolated from the co-transfections using the intertypic partners RLucWT and SL3. To further validate the approach, a molecular clone carrying a cluster one junction (JC105B) was also assayed. All PCR products that were amplified from the viral cDNA were incubated with the restriction enzyme *PstI* and the samples were then run on a 1% agarose gel (figure 6.18C). A single band would indicate that the isolate falls outside of the cluster one region. A double band (as a result of digestion) would indicate the presence of the restriction enzyme site and indicate that the recombinant had a junction that falls within cluster one. The digestion of the control PCR product (JC105B) indicated that the approach was valid. A mixed banding pattern indicated a mixed population (highlighted with asterisk). These samples were removed from the subsequent statistical analysis, with values being normalised to the overall sample size. In total, 71% of the control PV3/1 recombinant isolates had a cluster-one recombination junction, with the remaining junctions falling outside of this area. A similar approach was used to screen the products of PCR amplification from the PV3/PV3-LIKE isolates (figure 6.18D). The products following restriction enzyme incubation looked largely un-digested. The additional control (105B) indicated that the restriction enzyme was working correctly. This result suggested that the majority of recombinants in the PV3-LIKE isolates had recombination junctions that were not within cluster one, and presumably within cluster 2. In total, only 10% of these isolates had a cluster one junction. Statistical analysis of the data was carried using a *Chi* square test for association. The wild type PV3/1 samples were considered the expected values and the PV3/PV3-LIKE were considered the observed. The null hypothesis was that there would be no significant difference between the two samples. The results in table 6.1 show that there was a significant difference between the two groups, as expected. This suggested that sequence identity does influence the location of recombination in the CRE-REP assay.

Junction	Observed (O)	Expected (E)	O-E	$(O-E)^2$	$(O-E)^2/E$
Cluster 1	3.1	21.25	-18.15	329.42	15.5
Non-cluster 1	26.9	8.75	18.15	329.42	37.65
				χ^2 =	**53.15

Table 6.1: Statistical test upon the PV3/1 and PV3/PV3-LIKE recombination junctions

Degrees of freedom = n-1. One degree of freedom at the 0.01 confidence level = 6.63. ** Asterisk; $P < 0.01$ by *Chi* square test for association.

6.7 Discussion

The major aim in this area of the investigation was to develop a biochemical *in vitro* recombination assay that would assist in characterising the influence of RdRp fidelity upon recombination frequency. The collaboration with the Cameron research group at Penn State University, using their Sym-subU experimental approach (Arnold and Cameron, 2000) was successful in producing a fully defined cell free assay that would recapitulate the template switching event. The optimisation experiments shown in section 6.3 provided a standardised protocol that allowed comparison of template switching frequency between RdRp variants. In principle, the concentration of acceptor template in the assay could have been optimised further given that the results suggested that saturation point was not reached. Due to time limitations the conditions that were used in subsequent experiments was considered sufficient. Section 6.4 described the analysis of a range of poliovirus RdRps in the Sym-subU recombination assay. The experiments were not repeated sufficiently to allow robust statistical analysis, so caution must be used when interpreting the results. However, the experiments that were carried out did show reproducibility. The G64S high fidelity variant did switch templates in the Sym-subU recombination assays, but at a frequency that was nearly two-fold lower than wild type RdRp and this was consistent in the two assays carried out. The reduction in template switching ability may account for the reduced recombination frequency observed in the CRE-REP assays described in chapter four. Although, the overall activity of the enzyme sample that was used seemed to be sub-optimal, given the reduction in extension of the Sym-subU template when compared to the wild type RdRp. This experiment would need to be repeated with a sample of RdRp that was more enzymatically active to be assured of the results obtained to date. What was clearly evident is that the K359R substitution significantly inhibited template switching, and this was also consistent in the two assays carried out. This was an important finding that validated the results from the cell-based CRE-REP and 3'-CRE-REP assays described in chapter five that used the same RdRp variant. The non-recombinogenic phenotype observed in the biochemical assay can explain why no recombinant virus was obtained from any cell-based assays conducted in this study. One point of discussion provided in section 5.8 suggested that a K359R substitution in the poliovirus RdRp led to a temporal or basal disruption in replication

that might account for the lack of recombinant. In principle, this theory can now be dismissed. The results with the K359R variant should also be considered in a wider context. All viral RNA dependent RNA polymerases have a conserved element known as motif D (Liu et al., 2013). As shown in figure 5.1, nucleic acid polymerases employ a general acid for nucleotidyl transfer (Castro et al., 2009), and in many examples this is a lysine residue within the conserved motif D (Castro et al., 2007, Liu et al., 2013). The attenuation that a K359R substitution elicits has been described in section 5.2, the additional benefit that this mutation provides is to inhibit template switching frequency. The live-attenuated poliovirus vaccine strains have been hugely successful in limiting the outbreak of poliomyelitis, but they are prone to recombination events, which can lead to severe illness (Kew et al., 2002, Zhang et al., 2010, Kew et al., 2005). Perhaps the K359R variant could be considered as a suitable vaccine candidate that will aid poliovirus eradication? Vaccines are successful in preventing the onset of severe disease symptoms. Potentially, the development of this cell-free biochemical assay might provide a suitable system that will allow the characterisation of other viral RdRps and their propensity to recombine.

The role of high RdRp fidelity in reducing recombination frequency has now been shown in two distinct, separate assays in this study. In contrast, the use of mutagen (that decreases RdRp fidelity) was shown to increase recombinant yield in the CRE-REP assay. The well characterised H273R low fidelity RdRp (Korboukh et al., 2014) was used in the Sym-subU recombination assay in order to investigate the role of low fidelity and recombination frequency. Initial experimental design considered the use of ribavirin triphosphate as a potential analogue to investigate fidelity in the cell free biochemical assay. However, the optimisation steps that would have been required were not permissible given the timeframe involved. The increase in template switching observed with the H273R variant in the Sym-subU recombination assay lends support to the previous results outlined in section 4.4 that used ribavirin as a mechanism to reduce fidelity. The sharper incline and higher amount in template switching when compared to the wild type RdRp control (figure 6.9) provided direct evidence to show that low fidelity leads to an increase in template switching. However, the products from template switching seemed to plateau from 8 minutes onwards. This could be attributed to lack of acceptor template at this point. Although, the acceptor template was in 60-fold excess, so this seems

unlikely. Potentially, the plateau observed could be due to the concentration of enzymatically active RdRp. Previous studies that have used a similar experimental approach have shown that only 1% of the elongation complexes are enzymatically active (Arnold and Cameron, 2000). This would limit any recycling of active RdRp following a template switch. Perhaps a repeated experiment with a higher concentration of RdRp would provide better conditions to characterise this RdRp variant completely. In contrast, the wild type RdRp didn't seem to reach any saturation point, indicating a reduced template switching phenotype. The recombinogenic phenotype observed with the H273R variant may provide some answers to why a population with this variation can replicate successfully in cell culture. The increase in mutation rates (2-3 fold) observed with this variant (Korboukh et al., 2014) would suggest that this population would be lost rapidly due to 'error-catastrophe' (Crotty and Andino, 2002). The higher template switching phenotype observed with this variant maybe a characteristic that aids the population as a whole. If a genome carried a lethal mutation due to low RdRp fidelity, then in principle this mutation could be removed by a recombination event to an acceptor template that carries a non-lethal allele. As discussed in section 5.8, there seems to be fine-line between fidelity and a viable recombinant virus. As recombination rates increase due to low fidelity so do the potential lethal mutations that the genome carries as a whole.

The Y275H variant provided by the Andino research group was further validated in this study. The high processivity RdRp variant (Raul Andino, personal communication) had a similar non-recombinogenic phenotype as the K359R variant. Their individual mechanisms of reducing recombination frequency still remain to be fully characterised. The Y275H has a stronger affinity for the RNA template, and this is the basis of its high processivity (Jamie Arnold, personal communication). Potentially, the RdRp interaction is strong enough on its own to prevent any template switch.

The results in the optimisation assays, described in section 6.3, showed that the interface mutant I (L446D - R455D) RdRp could template switch at a level only slightly lower than that of the wild type RdRp. This RdRp variant is lethal in a full-length virus, but has no affect on the dynamics of the RdRp in biochemical assays (Moustafa et al., 2014, Hobson et al., 2001). Initial

interpretations would therefore suggest that the interaction of RdRp monomers within interface I are not an absolute requirement for recombination. This is an important finding given the Andino research group have identified a pool of RdRp variants that have mutations within the interface II region from their GFP-retention assay (discussed in chapter seven). Like the Y275H variant, these were isolated under conditions that assumed that the virus was non-recombinogenic. Perhaps RdRp interactions at interface II and not interface I are important in recombination? However, caution must be used with this interpretation. Disruption of residues at known protein-protein interaction sites may have a gross impact on interactions with other viral proteins that are involved in replication (i.e. P3 precursor proteins).

The results in section 6.5 suggested that the template-switching event occurred at the 3' end of the acceptor template and that a 3/4-nt identity was required for detectable template switching. This suggests that minimal regions of identity are required for recombination to occur. A finding that does not support the characterised intertypic recombinants isolated previously, which were more promiscuous in nature with limited identity at the recombination junction (Lowry et al., 2014). The identification of sequence identity at the recombination junction of three resolved intertypic recombinants described in section 3.6, suggests that the Sym-subU recombination assay recapitulates the resolution stage only. However, these observations highlight a potential flaw in the Sym-subU recombination assay in its current format. The assay does not include additional poliovirus proteins that are known to interact with the RNA and RdRp within the replication complex. One example is the precursor 3AB that is known to have chaperone activity that influence RNA-RNA interactions (DeStefano and Titilope, 2006, Gangaramani et al., 2010). Perhaps template switching in a more 'promiscuous' manner would be observed if this precursor protein were added into the assay? A further potential limitation of the Sym-subU recombination assay is the length of the templates involved. Can the results from a duplex RNA template that is only 10-nt in length be representative of what is happening *in vivo*? Perhaps this accounts for the need of sequence identity for efficient template switching in this assay? A further modification could be the inclusion of longer templates into the approach, then an investigation into the influence of size of template and recombination frequency could be undertaken.

The modification of the donor template (RLuc) in the CRE-REP assay provided some results that strongly suggested that sequence identity was influencing the yield and location of recombination. The sequence of a 450-nt stretch that precisely spanned the 2A/2B boundary (cluster two) was modified to be as like the acceptor template (SL3) as possible. The change in sequence reduced the 22.4% divergence in this region to only 2.2%. Importantly, protein coding was maintained. The fall in replication that was observed in the luciferase assay when compared to the control was therefore unexpected. The dinucleotide frequency in the genome of enteroviruses has recently been shown to be a key modulator of replication efficiency (Atkinson et al., 2014). This cannot account for the fall in replication, as the dinucleotide frequency of the modified donor remained the same. Perhaps there is an unknown *cis*-acting element within the modified sequence that has been disrupted? However, this region is highly unstructured (Goodfellow et al., 2000). This remains to be explained. Perhaps, sub-cloning the modified region into a full-length virus followed by transfection, virus isolation and subsequent sequencing may allow identification of the key sequences that have impacted upon replication (if reversions were observed). The fall in replication that was observed with the PV3-LIKE replicon made it impossible to accurately interpret the output from the CRE-REP assay. The increase in yield observed with the modified replicon when compared to the original might have been greater if they replicated in a similar fashion. However, the yield of recombinant virus was higher than the control when the PV3-LIKE replicon was used. This suggested that there might have been a bias in where the recombination event had occurred. By carrying out a simple RFLP assay on biologically cloned recombinant isolates it was clear to see that there was a difference between the control group and the modified donor group, even when the mixed population isolates were removed. This difference was significant. An interpretation of this result would suggest that sequence identity is a key regulator of recombination frequency and type. In preliminary studies, modification of structure in the same region does not significantly alter the location of recombination (data not shown). This is surprising given that a recent study showed that structure was a key determinant in recombination junction location (Runckel et al., 2013). The sequences of the primary products of intertypic recombination in the CRE-REP assay suggested that protein-protein compatibility was key in selection. The sequence that was modified in section 6.6 covered a natural protein cleavage site (2A/2B). In principle, the key

selection criteria with protein compatibility were still paramount. The modified sequences just increased the opportunity of recombination to occur in this region, presumably by potential base pairing during replication. If it is RNA sequence and not protein compatibility of the recombinant genome that are important in frequency and location, then regions away from the protein boundaries need to be modified in a similar fashion. If recombination then occurs and produces chimeric proteins, then sequence identity can be then deemed as the key factor. Alternatively, the availability of additional protein cleavage boundaries in the 3'-CRE-REP assay provides for an expansion on this area of investigation. Similar sequence modifications can be introduced across the entire non-structural region. This would provide the best opportunity to link sequence identity and location of recombination.

In summary, the results outlined in this chapter shows that recombination frequency is affected by fidelity of the viral RdRp. These results support the previous cell based data that have concentrated on the same RdRp fidelity variants. The new Sym-subU recombination assay also shows that the RdRp alone is sufficient for template switching. Modifications and further optimisation may be required. In principle, this new biochemical approach can be used with other viral RdRps. This will allow the characterisation of RdRp variants that may be important in recombination in other viral species. There is also potential to include other non-RdRp viral proteins that are involved in genome replication. Sequence identity also seems to be important in recombination location. However, additional studies will be required to confirm this.

CHAPTER SEVEN: General Discussion

7.1 Current understanding

Members of the *Picornaviridae* have error prone polymerases, short replication cycles and high yields that together generate genetic diversity. The high mutation rates create virus populations that contain potentially beneficial mutations that allow the population to evolve and adapt to new environments. However, far greater genetic variation is achieved by chance recombination events than is possible in a single round of genome replication. The implications of such genomic re-arrangements can be the onset of disease that is associated, for example the outbreak of poliomyelitis due to chance recombination events between the live attenuated poliovirus oral vaccine and unknown circulating enterovirus C members.

This study has benefited from using novel cell based assays, which have provided insights into the potential mechanisms of recombination. To support the cell-based data, a new cell-free biochemical recombination assay has been developed (in collaboration with the Cameron research group) that provided additional insights into the template-switching event. The biological relevance of this assay remains to be determined, but initial calculations can be done. The amount of donor template used in the cell-based assays was 250 ng on average, which equates to 10^{10} templates of RNA. This would produce 6 x 10^{10} templates, assuming 100% uptake of RNA and that each is replicated six times on average (Stern et al., 2014). The biochemical recombination assay showed that the products from template switching were ~4-5% of total RNA product. This suggests that ~ 2.4 x10^{9} hybrid templates from recombination might be produced in the CRE-REP assay if the biochemical assay is correct. At face value this seems a very high amount. However, to produce a viable recombinant virus additional considerations are needed: - the genome must be in-frame, can contain no deletions, cannot contain large insertions that may adversely affect packaging, preferably outside the capsid coding region, cannot contain mutations that affect viability, must fall between the end of VP1 and 2C CRE on the donor and acceptor and can only be localised to certain regions within the

1.058 Kb region of recombination (protein cleavage boundaries). In order to fulfill all of the criteria set out (without even considering host responses) suggests that template switching is common and that the biochemical assay may indeed be biologically relevant. The work presented in this thesis has advanced the understanding of recombination in enteroviruses and is broadly summarised below:

- Recombination is primarily a replicative process.
- Co-localisation of parental RNA within the host cell is a key determinant.
- Intertypic recombination is typically biphasic in nature; a promiscuous template-switching event is then followed by a resolution stage where all additional sequence is removed from the genome.
- A number of single stranded positive sense RNA viruses have genomes that have 'evolved by duplication'. The identification of duplicated sequences in this study suggests that imprecise recombination is a likely mechanism by which they could be produced.
- Clustering of intertypic recombination junctions to cleavage boundaries indicates that selection of the early viable recombinant is influenced by protein-protein complementarity of the hybrid genome.
- The location of fully resolved intertypic recombination junctions are influenced by RNA sequence identity.
- The fidelity of the RdRp is a key determinant of recombination frequency. Lowering fidelity leads to an increase in recombination frequency whereas increasing fidelity lowers recombination frequency in the cell-based assays.
- The function of the 2C CRE is not location specific. Positioning a synthetic CRE into the 3'NTR of poliovirus does not significantly affect replication.
- By manipulating the position of the CRE in a PV1 sub-genomic replicon an expanded intertypic cell-based assay, termed 3'-CRE-REP was developed. This produced an experimental approach where the opportunity for recombination across the whole non-structural coding region was present.
- The development of a novel cell free biochemical recombination assay showed that the

RdRp alone was sufficient for template switching. High fidelity and low fidelity RdRp variants reduced and increased recombination frequency in a manner that supported the cell-based data.

- Reducing complementarity of the acceptor template in the biochemical recombination showed that a minimal 3-4-nt sequence of identity is required for detectable template switching.
- Sequence manipulation of a known recombination region within the replicon donor template showed that the frequency and location of recombination could be manipulated.

7.2 Replicative models of recombination

The role of the viral RdRp in enterovirus recombination has clearly been shown in this study, indicating that this process is primarily replicative. However, the precise mechanisms of template switching remain to be determined. At present, the results show that RdRp fidelity is a key characteristic that influences the recombination process. Previous studies have suggested that the low fidelity characteristics of the viral RdRp might be important in recombination frequency (Agol, 1997, Freistadt et al., 2007). A nucleotide misincorporation event that is thermodynamically unfavourable might be sufficient to affect the stability of the elongation complex, leading to a template-switching event. However, no mutations were found at the recombination junctions characterised in this study and in a previous study that used the same experimental approach (Lowry et al., 2014). These observations don't necessarily mean that the hypothesis is incorrect. Potentially, the attempt to incorporate the incorrect nucleotide (or mutagen, if ribavirin and 5-FU are considered) is sufficient to de-stabilise the elongation complex, leading to template switching. The lack of sequence identity at the recombination junctions observed with the primary products of intertypic recombination showed that sequence identity is not a key prerequisite. Taken together, this suggests a non-processive 'copy-choice' mechanism, where the RdRp disassociates from the template RNA but retains the nascent RNA produced (Jarvis and Kirkegaard, 1991). The RdRp then recruits an acceptor template (in a sequence independent manner) and replication can continue, forming a hybrid

RNA sequence. If the selection criteria set out in section 7.1 are fulfilled then a viable recombinant may be produced. The lack of sequence identity between nascent RNA and acceptor template during template switching could potentially be overcome by the RNA chaperone activity of 3AB (DeStefano and Titilope, 2006, Gangaramani et al., 2010), a virus protein that is within the replication complex (Cameron et al., 2010, Pathak et al., 2007, Pathak et al., 2008). The role of P3 precursor proteins, and chaperone activity, has been considered in pilot studies that have used the biochemical recombination assay (Craig Cameron, personal communication) and this model is described in figure 7.1 (pathway A).

Alternatively, the misincorporation event could lead to stalling of the RdRp on the RNA template. Indeed, recent observations using an elegant approach that studied the elongation rate of individual poliovirus RdRps showed that the polymerase pauses or dwells at certain points during replication and may even slip on the RNA template (Dulin et al., 2015). The pausing events themselves had the signature of a misincorporation event (Dulin et al., 2015). It is well known that DNA and RNA can form triplex conformations via hoogstein-base pairing, where the third strand occupies the major groove of the double stranded helix whilst having no impact on structural dimensions. Perhaps, the stalling in replication due to nucleotide misincorporation (or attempt to incorporate) would provide the best opportunity for a third RNA template that is present in the RNA channel and active site of the RdRp, to displace the original RNA template by a form of 'strand invasion' (pathway B, figure 7.1). This model would therefore suggest that sequence identity might contribute to the location of template switching. In this study, the precise intratypic recombinants isolated would indicate that sequence identity is important in template switching. Additionally, the modification of a 450-nt region that precisely spanned the 2A/2B cleavage boundary of the PV1 replicon had a significant affect upon the site of template switching in the intertypic CRE-REP assay, indicating that sequence identity is a major factor to consider (section 6.6). The location of the recombination junctions of the fully resolved intertypic isolates was also linked to regions of sequence identity.

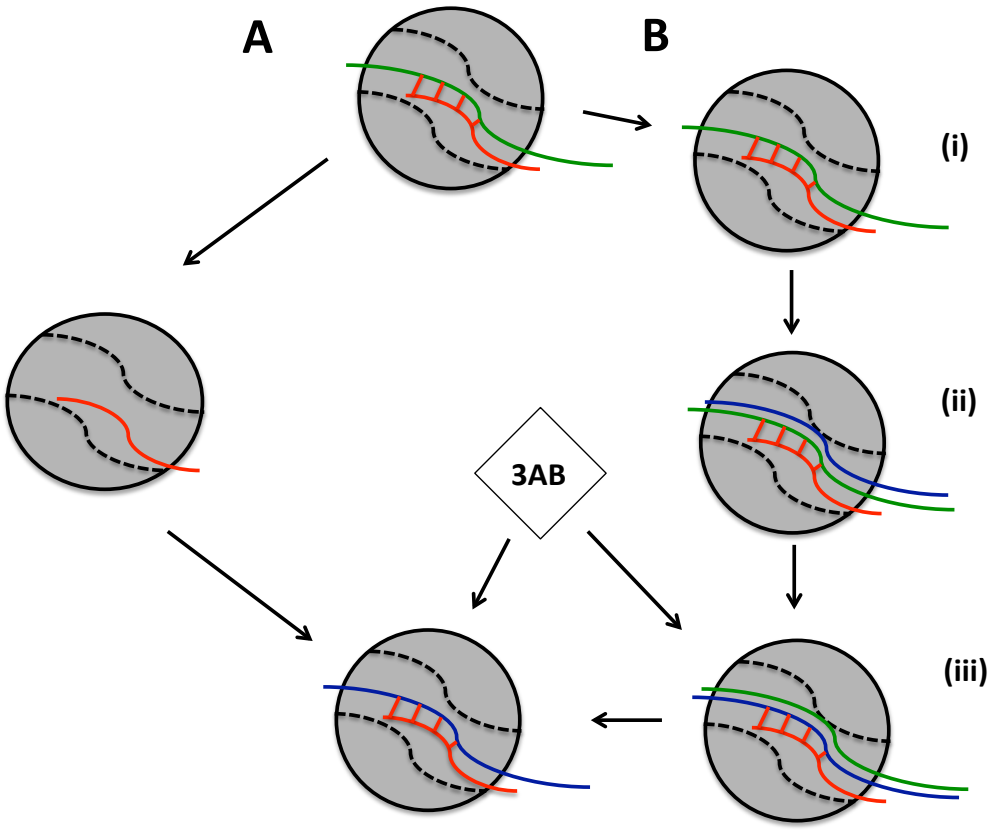

Figure 7.1: Two alternative mechanisms of 'copy-choice' recombination

Both models of recombination begin with normal synthesis. RdRp is shown as a grey circle with RNA channel and active site depicted as dashed lines. The nascent RNA is depicted in **red** base paired with the donor template in **green**. **Pathway A**, de-stabilised elongation complex disassociates with the donor template but retains the nascent RNA (red). Acceptor template (**blue**) enters the RNA channel and interacts with the nascent RNA, potentially mediated by the chaperone activity of 3AB. Template switch complete, elongation continues. **Pathway B**, **(i)** RdRp stalls during elongation (due to misincorporation event) increasing the opportunity for triplex strand formation and 'strand-invasion' **(ii)** Triplex strand formation **(iii)** Template switch that also may be mediated by 3AB, followed by complete displacement of original template by the new acceptor template (blue) followed by elongation. Both pathways lead to the same final event. Adapted from (Jarvis and Kirkegaard, 1991).

Although, the mechanism of template switch in the latter example could be either *in cis* or *in trans*. In principle, the mechanism of 'strand invasion' by a third template would be applicable to either form (*cis* or *trans*), three strands of RNA would be present in the active site at anyone time. The conformation of the acceptor template if it were *in cis* would be comparable to the lariat formation that occurs during mRNA splicing.

The two models described in figure 7.1 are not necessarily mutually exclusive. The results in this study suggest both may be occurring. The lack of sequence identity in the intertypic recombinants suggests that these are derived from pathway A. Where there is sequence identity, pathway B may be more applicable. However, the results also show that the overriding criteria for selection of viable recombinant virus in the cell based CRE-REP assay is dependent on the protein coding content of the hybrid genome. The genome must be able to establish a productive infection in HeLa cells. The clustering to cleavage boundaries observed in this and a previous study (Lowry et al., 2014) ensured that the intertypic recombinants isolated have either a complete 2A and 2B or a complete 2B from one parental genome, thus no chimeric proteins are produced following the initial recombination event. This suggested that correct protein-protein interactions are important in establishing foci of replication. This point can be related to the asymmetry in reciprocal recombinants in the P2 region of poliovirus and related species C coxsackie A viruses which may reflect important protein-protein interactions required for genome replication and particle assembly (Jiang et al., 2007).

7.3 Future experiments

The results in section 3.3 suggested that intratypic recombination was primarily precise in nature whereas intertypic recombination was primarily imprecise. There still remains some ambiguity in this area. Potentially, an imprecise intratypic recombinant could have a growth advantage over any intertypic counterpart, due to the optimal protein coding content of its genome. This may result in a swifter resolution stage. Indeed, this may occur during subsequent rounds of replication within the same cell following the initial recombination event. Construction of an imprecise intratypic molecular clone, similar to the JC105B molecular clone

used in this study may allow a comparison of relative resolution rates. A similar serial passaging regime that was used in section 3.8 should be used and the JC105B molecular clone could be used for comparison.

It remains to be determined if the resolution stage observed in this study is due to template switching *in cis* or *in trans.* In principle, it could be a combination of both. If it were primarily *in trans* then the availability of acceptor template would be a limiting factor. There is potential to test this experimentally. Treatment of HeLa cells with nocodazole prior to passaging would limit the co-localisation of RNA during replication. If resolution of the JC105B molecular clone were inhibited compared to an untreated control then it might suggest that resolution is via additional template switching *in trans.*

The manipulation of sequence at a known recombination hotspot, described in section 6.6, showed that sequence identity had an influence on the location of recombination in the CRE-REP assay. The development of the 3'-CRE-REP assay, described in section 5.3, allows for this type of approach to be expanded to other regions of the replicon template. Similar sequence manipulations at all of the protein cleavage boundaries within the P2 and P3 regions could be employed to enable investigation of sequence identity on recombination frequency and location. This methodology can be expanded even further, preliminary studies have suggested that modification of the donor template that affect RNA structure have little influence on recombination frequency or location (data not shown). This approach was slightly flawed. Only the donor template was considered for modification. Lowry et al., showed that the location of recombination on the acceptor template was primarily biased to unstructured regions. To completely characterise the influence of RNA structure and recombination frequency / location structural alterations to the donor and acceptor template would be required.

Furthermore, a combination of modifications to RNA sequence and structure could be introduced into donor and acceptor templates. Exhaustive studies involving Turnip Crinkle virus indicated a central role for RNA structure and specific sequence motifs in the generation of satellite RNAs. A hairpin structure known as '*motif1'* along with regions of sequence

homology specifically influenced the non-random distribution of RNA recombination (Nagy and Simon, 1998a, Nagy and Simon, 1998b). Indeed, these studies supported a central role for the viral RdRp in replicative recombination.

Replicative recombination involving the viral RdRp via a copy-choice mechanism requires close proximity of the parental RNA, presumably within the same replication complex. In this study, repeated attempts were made to identify interspecies recombinant virus in the cell based CRE-REP assays using enterovirus species C and species B partners (PV and echovirus pairings). The lack of viable recombinant may be due to protein incompatibility following translation that may affect replication or packaging. Alternatively, the rarity of interspecies recombination may reflect the lack of opportunity, perhaps due to occupancy of distinct replication complexes. Historical studies that have used serotype specific riboprobes have shown that two different serotypes of poliovirus co-localise during replication following a co-infection of HeLa cells at similar peri-nuclear locations, thus providing the opportunity for recombination (Egger et al., 1999, Egger and Bienz, 2002). During the course of this investigation a pilot study was conducted that used a fluorescent *in situ* hybridisation (FISH) approach. A series of Stellaris™ serotype specific riboprobes were designed and ordered from Biosearch Technologies™. This approach was chosen due to the reported single molecule sensitivity of the probes in recent studies involving influenza virus (Chou et al., 2013) and other cell based mRNA (Shaffer et al., 2013). A set of riboprobes consisted of up to forty-eight individual serotype specific 20-mer sequences, each containing a 3' fluorophore. It was reasoned that antisense viral RNA would be targeted given that recombination reportedly occurs during antisense RNA synthesis (Kirkegaard and Baltimore, 1986b). Riboprobes specific for poliovirus type 3 positive-sense RNA and antisense RNA were ordered along with probes for echovirus 7 (E7) antisense RNA. The protocol that was used is described in section 2.4. Optimisation experiments were carried out with initial results suggesting that species B and species C partners (E7 and PV3) localise to similar regions during replication following a co-infection (appendix i). Further quantifiable experiments will be required to confirm these observations. This approach, in principle, can be expanded to other virus serotypes and species groups in order to ascertain whether the opportunity for recombination exists (i.e. similar localisation patterns during replication).

The identification of recombinant virus in the CRE-REP and 3'-CRE-REP assays are based upon the viability of the hybrid genome that is produced. This could be considered a limitation. The identification of unviable genomes is not available in the current approach. If co-localisation of different species group partners is confirmed by the use of species-specific riboprobes then there is the potential for recombinant genome to be produced as well. The use of fluorophore labeled primers that are specific to recombinant genome in an emulsion PCR approach (Runckel et al., 2013) might provide the best chance to identify recombinant genome in a mixed population following RNA extraction. Sorting of the individual emulsions based upon their fluorescent intensities (akin to FACS) could highlight the type and amount of recombination.

The recent investigation that showed the poliovirus RdRp pausing during replication, potentially due to a misincorporation event (Dulin et al., 2015) allows for further studies on the RdRp fidelity variants identified in this study as being important in recombination. Do the G64S and K359R variants pause in a similar fashion to wild type RdRp? Can templates carrying cold or hot spots of pausing be related to recombinant sequences obtained in this study or from field isolates? The Dulin et al., study suggested that the type of co-factor might influence the level of pausing during replication, with an increase observed with Mn^{2+} when compared to Mg^{2+}. This observation has been shown in a biochemical assay, where the error rate of the poliovirus RdRp increased when Mn^{2+} was used as a co-factor (Crotty et al., 2003). Manipulation of the co-factor pool by use of a divalent cation chelator like EDTA followed by spiking of the media with various concentrations of co-factor may add to the already strong data that shows fidelity as being important in the cell based CRE-REP assay. This can be expanded further by carrying out similar modifications to the biochemical recombination assay described in section 6.2.

The biochemical recombination assay developed during this investigation provides the basis for further expansion. The RdRp alone was shown to be sufficient for template switching in this assay. To suggest that characteristics of the viral RdRp alone drive recombination would be too simplistic. Many other viral and host proteins are located in close proximity to the RdRp within

the replication complex (Andino et al., 1990, Cameron et al., 2010). In particular, the role of P3 precursor proteins needs to be investigated. The chaperone activity of 3AB has been previously characterised (DeStefano and Titilope, 2006, Gangaramani et al., 2010). Inclusion of 3AB and /or other viral (and host) proteins into the cell free assay may elucidate their role in template switching. Additionally, known mutations that ablate the chaperone activity of 3AB (Gangaramani et al., 2010) can be incorporated into the CRE-REP assay partners. This type of approach will show if chaperone activity is important in the non-processive sequence independent copy-choice pathway described in figure 7.1. Modifications to the templates used in the biochemical recombination assay may highlight the role of triplex RNA formation and its contribution to the recombination process (described in figure 7.1, pathway B). In principle, the use of triplex forming oligonucleotide RNA templates would increase the amount of template transfer if this were an important factor.

The K359R RdRp has been well characterised (Castro et al., 2009). The non-recombinogenic phenotype observed with this variant in the CRE-REP and biochemical recombination assays could be due to either fidelity or speed of replication (or both). The K359H variant that has also been previously characterised (Castro et al., 2009) has a similar phenotype to the K359R variant. However, the serial passage of a virus population that has carries this RdRp variation has previously selected two separate second site RdRp substitutions (Jamie Arnold, personal communication). One of the second site substitutions returns the replication speed of the RdRp to wild type whilst the other lowers the fidelity of the K359H back to wild type levels. Introduction of the second site RdRp variations into both experimental approaches (cell based and biochemical) may tease out the relative contribution of replication speed and fidelity in the recombination process.

The Y275H variant kindly provided by the Raul Andino research group was characterised in the CRE-REP assay, resolution assay and biochemical assay during this investigation. The use of the interface I RdRp mutant (L446D - R455D) suggested that the higher order structures formed by RdRp monomers at interface I are not important in template switching in the biochemical recombination assay. However, substitutions in amino acid residues found at the interface II

region (Tellez et al., 2011) have been postulated to be important in recombination (Ashley Acevedo, personal communication). These were identified in the same GFP-retention assay that identified the high processivity Y275H RdRp variant. Inclusion of the substitutions into the donor and acceptor templates in the CRE-REP assay in a logical manner may elucidate their contribution to recombination frequency. Additionally, the RdRp variants can also be included into the biochemical recombination assay. However, caution may be required when characterising the interface II variants in any subsequent investigation. The interface II region is not known to interact directly with viral RNA, unlike the K359R and Y275H variants characterised in this study. Potentially, the substitution of residues within this region may de-stabilise important protein-protein interactions between the RdRp and other accessory proteins (viral or host) that might influence recombination.

Genome-wide screens representing ~95% of host genes have been performed with Tomato bushy stunt virus (TBSV) in a yeast model, in the attempt to identify host genes affecting RNA recombination (Serviene et al., 2005, Serviene et al., 2006). In one study, it was reported that inactivation of yeast host Pmr1p, an ion pump that controls Ca2+/Mn2+ movement into the Golgi from the cytosol, led to an ~160-fold increase in TBSV recombination in yeast (Jaag et al., 2010, Jaag and Nagy, 2010). Potentially, this finding may relate the type of co-factor used by the viral RdRp and recombination frequency. In this study, an attempt to knockdown a murine equivalent known as ATP2CI with shRNA was carried out with limited success (data not shown). Revisiting this area of investigation would seem logical given the observations with RdRp fidelity and recombination frequency. In another study, it was demonstrated that the *MET22/Xrn1* pathway (5' exoribonuclease) regulated the frequency of TBSV RNA recombination and efficiency of virus replication in a yeast system (Jaag and Nagy, 2010). In this investigation knockdown of murine *XrnI* expression by shRNA was successful (data not shown). Initial results show that knockdown of XrnI does not affect replication of full-length poliovirus or recombination yield via the CRE-REP assay. This is not surprising given that cytoplasmic XrnI is rapidly degraded during poliovirus infection (Dinh, 2013). However, preliminary data suggests that XrnI knockdown does inhibit the yield from the non-replicative (NON-REP) assay. This indicates that the non-replicative partners need to be processed by the host exo and

endonucleases in order to produce compatible RNA fragments for the postulated subsequent ligation events that are required. To further validate these findings an additional mechanism to minimise the processing ability of the XrnI exoribonuclease could be employed. A recent study has shown that a noncoding RNA from an arthropod-borne flavivirus inhibits XrnI function (Moon et al., 2012). Constructs expressing the flavivirus RNA could be used in combination with the enterovirus RNA partners in a NON-REP assay in a dose response manner. More recently, a DDX3-like helicase has also been shown to affect recombination and RNA stability using TBSV as a model virus (Chuang et al., 2015). Whether this is a replicative or non-replicative mechanism of recombination is still open to debate, but knockdown of the host factor by siRNA or shRNA may be applicable to either CRE-REP or NON-REP cell based approaches.

7.4 Final summary

Experimental evidence has shown that the error-prone nature of the RdRp leads to a virus population that is mostly composed of lethal or deleterious mutations (Stern et al., 2014, Acevedo et al., 2014). How does the virus population tolerate this high mutational rate? Recombination provides a mechanism that can remove a deleterious mutation and also provides an opportunity to break the link between mutations that are lethal and those that are beneficial in the same genome. In this study, the role of RdRp fidelity in recombination frequency has been clearly shown. The error rate of the viral RdRp not only creates a diverse population that can respond to a changing environment, it also provides a mechanism (recombination) that ensures mutational robustness of the population is maintained. The global effort to eradicate poliovirus may fall short using the current vaccination regime, due in part, to recombination (Zhang et al., 2010). From a host's perspective, the K359R non-recombinogenic phenotype that was observed in this study provides an interesting opportunity. This variant is attenuated and elicits a suitable immune response in a murine model (Weeks et al., 2012). The potential of the K359R variant as a suitable mechanism-based poliovirus vaccine shouldn't be underestimated.

Bibliography:

Acevedo, A., Brodsky, L. & Andino, R. 2014. Mutational and fitness landscapes of an RNA virus revealed through population sequencing. *Nature,* 505**,** 686-+.

Agol, V. I. 1997. Recombination and other genomic rearrangements in picornaviruses. *Seminars in Virology,* 8**,** 77-84.

Agudo, R., Arias, A. & Domingo, E. 2009. 5-fluorouracil in lethal mutagenesis of foot-and-mouth disease virus. *Future Medicinal Chemistry,* 1**,** 529-539.

Ambros, V., Pettersson, R. F. & Baltimore, D. 1978. ENZYMATIC-ACTIVITY IN UNINFECTED CELLS THAT CLEAVES THE LINKAGE BETWEEN POLIO-VIRION RNA AND THE 5' TERMINAL PROTEIN. *Cell,* 15**,** 1439-1446.

Andino, R., Rieckhof, G. E. & Baltimore, D. 1990. A FUNCTIONAL RIBONUCLEOPROTEIN COMPLEX FORMS AROUND THE 5' END OF POLIOVIRUS RNA. *Cell,* 63**,** 369-380.

Arden, K. E. & Mackay, I. M. 2009. Human rhinoviruses: coming in from the cold. *Genome Medicine,* 1.

Arnold, J. J. & Cameron, C. E. 1999. Poliovirus RNA-dependent RNA polymerase (3D(pol)) is sufficient for template switching in vitro. *Journal of Biological Chemistry,* 274**,** 2706-2716.

Arnold, J. J. & Cameron, C. E. 2000. Poliovirus RNA-dependent RNA polymerase (3D(pol)) - Assembly of stable, elongation-competent complexes by using a symmetrical primer-template substrate (sym/sub). *Journal of Biological Chemistry,* 275**,** 5329-5336.

Arnold, J. J., Ghosh, S. K. B. & Cameron, C. E. 1999. Poliovirus RNA-dependent RNA polymerase (3D(pol)) - Divalent cation modulation of primer, template, and nucleotide selection. *Journal of Biological Chemistry,* 274**,** 37060-37069.

Arnold, J. J., Vignuzzi, M., Stone, J. K., Andino, R. & Cameron, C. E. 2005. Remote site control of an active site fidelity checkpoint in a viral RNA-dependent RNA polymerase. *Journal of Biological Chemistry,* 280**,** 25706-25716.

Atkinson, N. J., Witteveldt, J., Evans, D. J. & Simmonds, P. 2014. The influence of CpG and UpA dinucleotide frequencies on RNA virus replication and characterization of the innate cellular pathways underlying virus attenuation and enhanced replication. *Nucleic Acids Research,* 42**,** 4527-4545.

Bachrach, H. L. 1968. Foot-and-mouth disease. *Annual review of microbiology,* 22**,** 201-44.

Barclay, W., Li, Q. Y., Hutchinson, G., Moon, D., Richardson, A., Percy, N., Almond, J. W. & Evans, D. J. 1998. Encapsidation studies of poliovirus subgenomic replicons. *Journal of General Virology,* 79**,** 1725-1734.

Barton, D. J. & Flanegan, J. B. 1997. Synchronous replication of poliovirus RNA: Initiation of negative-strand RNA synthesis requires the guanidine-inhibited activity of protein 2C. *Journal of Virology,* 71**,** 8482-8489.

Belov, G. A. & Ehrenfeld, E. 2007. Involvement of cellular membrane traffic proteins in poliovirus replication. *Cell Cycle,* 6**,** 36-38.

Belov, G. A., Feng, Q., Nikovics, K., Jackson, C. L. & Ehrenfeld, E. 2008. A Critical Role of a Cellular Membrane Traffic Protein in Poliovirus RNA Replication. *Plos Pathogens,* 4.

Belov, G. A., Nair, V., Hansen, B. T., Hoyt, F. H., Fischer, E. R. & Ehrenfeld, E. 2012. Complex Dynamic Development of Poliovirus Membranous Replication Complexes. *Journal of Virology,* 86**,** 302-312.

Bernhardt, G., Bibb, J. A., Bradley, J. & Wimmer, E. 1994. Molecular characterization of the cellular receptor for poliovirus. *Virology,* 199**,** 105-113.

Bird, S. W., Maynard, N. D., Covert, M. W. & Kirkegaard, K. 2014. Nonlytic viral spread enhanced by autophagy components. *Proceedings of the National Academy of Sciences of the United States of America,* 111**,** 13081-13086.

Bouchard, M. J., Lam, D. H. & Racaniello, V. R. 1995. DETERMINANTS OF ATTENUATION AND TEMPERATURE SENSITIVITY IN THE TYPE-1 POLIOVIRUS SABIN VACCINE. *Journal of Virology,* 69**,** 4972-4978.

Buchholz, U. J., Finke, S. & Conzelmann, K. K. 1999. Generation of bovine respiratory syncytial virus (BRSV) from cDNA: BRSV NS2 is not essential for virus replication in tissue culture, and the human RSV leader region acts as a functional BRSV genome promoter. *Journal of Virology,* 73**,** 251-259.

Cameron, C. E. & Castro, C. 2001. The mechanism of action of ribavirin: lethal mutagenesis of RNA virus genomes mediated by the viral RNA-dependent RNA polymerase. *Current Opinion in Infectious Diseases,* 14**,** 757-764.

Cameron, C. E., Oh, H. S. & Moustafa, I. M. 2010. Expanding knowledge of P3 proteins in the poliovirus lifecycle. *Future Microbiology,* 5**,** 867-881.

Cammack, N., Phillips, A., Dunn, G., Patel, V. & Minor, P. D. 1988. Intertypic genomic rearrangements of poliovirus strains in vaccinees. *Virology,* 167**,** 507-14.

Caro, V., Guillot, S., Delpeyroux, F. & Crainic, R. 2001. Molecular strategy for 'serotyping' of human enteroviruses. *J Gen Virol,* 82**,** 79-91.

Castro, C., Smidansky, E., Maksimchuk, K. R., Arnold, J. J., Korneeva, V. S., Gotte, M., Konigsberg, W. & Cameron, C. E. 2007. Two proton transfers in the transition state for nucleotidyl transfer catalyzed by RNA- and DNA-dependent RNA and DNA polyrnerases. *Proceedings of the National Academy of Sciences of the United States of America,* 104**,** 4267-4272.

Castro, C., Smidansky, E. D., Arnold, J. J., Maksimchuk, K. R., Moustafa, I., Uchida, A., Gotte, M., Konigsberg, W. & Cameron, C. E. 2009. Nucleic acid polymerases use a general acid for nucleotidyl transfer. *Nature Structural & Molecular Biology,* 16**,** 212-218.

Chetverin, A. B., Chetverina, H. V., Demidenko, A. A. & Ugarov, V. I. 1997. Nonhomologous RNA recombination in a cell-free system: Evidence for a transesterification mechanism guided by secondary structure. *Cell,* 88**,** 503-513.

Chou, Y.-y., Heaton, N. S., Gao, Q., Palese, P., Singer, R. & Lionnet, T. 2013. Colocalization of Different Influenza Viral RNA Segments in the Cytoplasm before Viral Budding as Shown by Single-molecule Sensitivity FISH Analysis. *Plos Pathogens,* 9.

Chuang, C., Prasanth, K. R. & Nagy, P. D. 2015. Coordinated Function of Cellular DEAD-Box Helicases in Suppression of Viral RNA Recombination and Maintenance of Viral Genome Integrity. *PLoS pathogens,* 11**,** e1004680-e1004680.

Coffin, J. M. 1979. STRUCTURE, REPLICATION, AND RECOMBINATION OF RETROVIRUS GENOMES - SOME UNIFYING HYPOTHESES. *Journal of General Virology,* 42**,** 1-26.

Cole, C. N., Smoler, D., Wimmer, E. & Baltimor.D 1971. DEFECTIVE INTERFERING PARTICLES OF POLIOVIRUS .1. ISOLATION AND PHYSICAL PROPERTIES. *Journal of Virology,* 7**,** 478-&.

Colonno, R. J., Condra, J. H., Mizutani, S., Callahan, P. L., Davies, M. E. & Murcko, M. A. 1988. EVIDENCE FOR THE DIRECT INVOLVEMENT OF THE RHINOVIRUS CANYON IN RECEPTOR-BINDING. *Proceedings of the National Academy of Sciences of the United States of America,* 85**,** 5449-5453.

Combelas, N., Holmblat, B., Joffret, M.-L., Colbere-Garapin, F. & Delpeyroux, F. 2011. Recombination between Poliovirus and Coxsackie A Viruses of Species C: A Model of Viral Genetic Plasticity and Emergence. *Viruses-Basel,* 3**,** 1460-1484.

Contreras, A. M., Hiasa, Y., He, W. P., Terella, A., Schmidt, E. V. & Chung, R. T. 2002. Viral RNA mutations are region specific and increased by ribavirin in a full-length hepatitis C virus replication system. *Journal of Virology,* 76**,** 8505-8517.

Coyne, C. B. & Bergelson, J. M. 2005. CAR: A virus receptor within the tight junction. *Advanced Drug Delivery Reviews,* 57**,** 869-882.

Crotty, S. & Andino, R. 2002. Implications of high RNA virus mutation rates: lethal mutagenesis and the antiviral drug ribavirin. *Microbes and Infection,* 4**,** 1301-1307.

Crotty, S., Cameron, C. E. & Andino, R. 2001. RNA virus error catastrophe: Direct molecular test by using ribavirin. *Proceedings of the National Academy of Sciences of the United States of America,* 98**,** 6895-6900.

Crotty, S., Gohara, D., Gilligan, D. K., Karelsky, S., Cameron, C. E. & Andino, R. 2003. Manganese-dependent polioviruses caused by mutations within the viral polymerase. *Journal of Virology,* 77**,** 5378-5388.

Crotty, S., Maag, D., Arnold, J. J., Zhong, W. D., Lau, J. Y. N., Hong, Z., Andino, R. & Cameron, C. E. 2000. The broad-spectrum antiviral ribonucleoside ribavirin is an RNA virus mutagen. *Nature Medicine,* 6**,** 1375-1379.

Cuervo, N. S., Guillot, S., Romanenkova, N., Combiescu, M., Aubert-Combiescu, A., Seghier, M., Caro, V., Crainic, R. & Delpeyroux, F. 2001. Genomic features of intertypic recombinant sabin poliovirus strains excreted by primary vaccinees. *J Virol,* 75**,** 5740-51.

Dedepsidis, E., Kyriakopoulou, Z., Pliaka, V. & Markoulatos, P. 2010. Correlation between recombination junctions and RNA secondary structure elements in poliovirus Sabin strains. *Virus Genes,* 41**,** 181-191.

DeStefano, J. J. & Titilope, O. 2006. Poliovirus protein 3AB displays nucleic acid chaperone and helix-destabilizing activities. *Journal of Virology,* 80**,** 1662-1671.

Deterding, K., Gruner, N., Buggisch, P., Wiegand, J., Gale, P. R., Spengler, U., Hinrichsen, H., Berg, T., Potthoff, A., Malek, N., Groshennig, A., Koch, A.,

Diepolder, H., Luth, S., Feyerabend, S., Jung, M. C., Rogalska-Taranta, M., Schlaphoff, V., Comberg, M., Manns, M. P. & Wedemeyer, H. 2013. Delayed versus immediate treatment for patients with acute hepatitis C: a randomised controlled non-inferiority trial. *Lancet Infectious Diseases,* 13**,** 497-506.

Dinh, P. X. 2013. Manipulation of Cellular Processing Bodies and Their Constituents by Viruses. *DNA and Cell Biology,* 32**,** 286-291.

Domingo, E., Baranowski, E., Escarmis, C., Sobrino, F. & Holland, J. J. 2002. Error frequencies of picornavirus RNA polymerases: Evolutionary implications for virus populations. *Molecular biology of picornaviruses***,** 285-298.

Domingo, E. & Holland, J. J. 1997. RNA virus mutations and fitness for survival. *Annual Review of Microbiology,* 51**,** 151-178.

Dulin, D., Vilfan, I. D., Berghuis, B. A., Hage, S., Bamford, D. H., Poranen, M. M., Depken, M. & Dekker, N. H. 2015. Elongation-Competent Pauses Govern the Fidelity of a Viral RNA-Dependent RNA Polymerase. *Cell Reports,* 10**,** 983-992.

Dunn, G., Begg, N. T., Cammack, N. & Minor, P. D. 1990. VIRUS EXCRETION AND MUTATION BY INFANTS FOLLOWING PRIMARY VACCINATION WITH LIVE ORAL POLIOVACCINE FROM 2 SOURCES. *Journal of Medical Virology,* 32**,** 92-95.

Egger, D. & Bienz, K. 2002. Recombination of poliovirus RNA proceeds in mixed replication complexes originating from distinct replication start sites. *Journal of Virology,* 76**,** 10960-10971.

Egger, D. & Bienz, K. 2005. Intracellular location and translocation of silent and active poliovirus replication complexes. *Journal of General Virology,* 86**,** 707-718.

Egger, D., Bolten, R., Rahner, C. & Bienz, K. 1999. Fluorochrome-labeled RNA as a sensitive, strand-specific probe for direct fluorescence in situ hybridization. *Histochemistry and Cell Biology,* 111**,** 319-324.

Egger, D., Gosert, R. & Bienz, K. 2002. *Role of cellular structures in viral RNA replication*.

Egger, D., Teterina, N., Ehrenfeld, E. & Bienz, K. 2000. Formation of the poliovirus replication complex requires coupled viral translation, vesicle production, and viral RNA synthesis. *Journal of Virology,* 74**,** 6570-6580.

Eggers, H. J. 2002. History of poliomyelitis and poliomyelitis research. *Molecular biology of picornaviruses***,** 3-14.

Eigen, M. 1996. On the nature of virus quasispecies. *Trends in Microbiology,* 4**,** 216-218.

Etchison, D., Milburn, S. C., Edery, I., Sonenberg, N. & Hershey, J. W. B. 1982. INHIBITION OF HELA-CELL PROTEIN-SYNTHESIS FOLLOWING POLIOVIRUS INFECTION CORRELATES WITH THE PROTEOLYSIS OF A 220,000-DALTON POLYPEPTIDE ASSOCIATED WITH EUKARYOTIC INITIATION FACTOR-III AND A CAP BINDING-PROTEIN COMPLEX. *Journal of Biological Chemistry,* 257**,** 4806-4810.

Evans, D. J. & Almond, J. W. 1998. Cell receptors for picornaviruses as determinants of cell tropism and pathogenesis. *Trends in Microbiology,* 6**,** 198-202.

Forss, S. & Schaller, H. 1982. A tandem repeat gene in a picornavirus. *Nucleic Acids Res,* 10**,** 6441-50.

Freistadt, M. S., Vaccaro, J. A. & Eberle, K. E. 2007. Biochemical characterization of the fidelity of poliovirus RNA-dependent RNA polymerase. *Virology Journal,* 4.

Fricks, C. E. & Hogle, J. M. 1990. CELL-INDUCED CONFORMATIONAL CHANGE IN POLIOVIRUS - EXTERNALIZATION OF THE AMINO TERMINUS OF VP1 IS RESPONSIBLE FOR LIPOSOME BINDING. *Journal of Virology,* 64**,** 1934-1945.

Gallei, A., Pankraz, A., Thiel, H. J. & Becher, P. 2004. RNA recombination in vivo in the absence of viral replication. *Journal of Virology,* 78**,** 6271-6281.

Galli, A. & Bukh, J. 2014. Comparative analysis of the molecular mechanisms of recombination in hepatitis C virus. *Trends in Microbiology,* 22**,** 354-364.

Gamarnik, A. V. & Andino, R. 1998. Switch from translation to RNA replication in a positive-stranded RNA virus. *Genes & Development,* 12**,** 2293-2304.

Gangaramani, D. R., Eden, E. L., Shah, M. & DeStefano, J. J. 2010. The twenty-nine amino acid C-terminal cytoplasmic domain of poliovirus 3AB is critical for nucleic acid chaperone activity. *Rna Biology,* 7**,** 820-829.

Georgescu, M. M., Tardypanit, M., Guillot, S., Crainic, R. & Delpeyroux, F. 1995. MAPPING OF MUTATIONS CONTRIBUTING TO THE TEMPERATURE SENSITIVITY OF THE SABIN-1 VACCINE STRAIN OF POLIOVIRUS. *Journal of Virology,* 69**,** 5278-5286.

Gmyl, A. P., Belousov, E. V., Maslova, S. V., Khitrina, E. V., Chetverin, A. B. & Agol, V. I. 1999. Nonreplicative RNA recombination in poliovirus. *Journal of Virology,* 73**,** 8958-8965.

Gmyl, A. P., Korshenko, S. A., Belousov, E. V., Khitrina, E. V. & Agol, V. I. 2003. Nonreplicative homologous RNA recombination: Promiscuous joining of RNA pieces? *Rna-a Publication of the Rna Society,* 9**,** 1221-1231.

Gnanashanmugam, D., Falkovitz-Halpern, M. S., Dodge, A., Fang, M., Wong, L. J., Esparza, M., Hammon, R., Rivas-Merelles, E. E., Santos, J. I. & Maldonado, Y. 2007. Shedding and reversion of oral polio vaccine type 3 in Mexican vaccinees: Comparison of mutant analysis by PCR and enzyme cleavage to a real-time PCR assay. *Journal of Clinical Microbiology,* 45**,** 2419-2425.

Gohara, D. W., Crotty, S., Arnold, J. J., Yoder, J. D., Andino, R. & Cameron, C. E. 2000. Poliovirus RNA-dependent RNA polymerase (3D(pol)) - Structural, biochemical, and biological analysis of conserved structural motifs A and B. *Journal of Biological Chemistry,* 275**,** 25523-25532.

Gohara, D. W., Ha, C. S., Ghosh, S. K. B., Arnold, J. J., Wisniewski, T. J. & Cameron, C. E. 1999. Production of "authentic" poliovirus RNA-dependent RNA polymerase (3D(pol)) by ubiquitin-protease-mediated cleavage in Escherichia coli. *Protein Expression and Purification,* 17**,** 128-138.

Goodfellow, I., Chaudhry, Y., Richardson, A., Meredith, J., Almond, J. W., Barclay, W. & Evans, D. J. 2000. Identification of a cis-acting replication element within the poliovirus coding region. *Journal of Virology,* 74**,** 4590-4600.

Goodfellow, I. G., Kerrigan, D. & Evans, D. J. 2003a. Structure and function analysis of the poliovirus cis-acting replication element (CRE). *Rna-a Publication of the Rna Society,* 9**,** 124-137.

Goodfellow, I. G., Polacek, C., Andino, R. & Evans, D. J. 2003b. The poliovirus 2C cis-acting replication element-mediated uridylylation of VPg is not required for synthesis of negative-sense genomes. *Journal of General Virology,* 84**,** 2359-2363.

Gorbalenya, A. E., Pringle, F. M., Zeddam, J. L., Luke, B. T., Cameron, C. E., Kalmakoff, J., Hanzlik, T. N., Gordon, K. H. & Ward, V. K. 2002. The palm subdomain-based active site is internally permuted in viral RNA-dependent RNA polymerases of an ancient lineage. *J Mol Biol,* 324**,** 47-62.

Greve, J. M., Davis, G., Meyer, A. M., Forte, C. P., Yost, S. C., Marior, C. W., Kamarck, M. E. & McClelland, A. 1989. THE MAJOR HUMAN RHINOVIRUS RECEPTOR IS ICAM-1. *Cell,* 56**,** 839-847.

Grist, N. R., Bell, E. J. & Assaad, F. 1978. Enteroviruses in human disease. *Prog Med Virol,* 24**,** 114-57.

Guillot, S., Caro, V., Cuervo, N., Korotkova, E., Combiescu, M., Persu, A., Aubert-Combiescu, A., Delpeyroux, F. & Crainic, R. 2000. Natural genetic exchanges between vaccine and wild poliovirus strains in humans. *Journal of Virology,* 74**,** 8434-8443.

Herold, J. & Andino, R. 2001. Poliovirus RNA replication requires genome circularization through a protein-protein bridge. *Molecular Cell,* 7**,** 581-591.

Herremans, T., Reimerink, J. H. J., Kimman, T. G., van der Avoort, H. & Koopmans, M. P. G. 2000. Antibody responses to antigenic sites 1 and 3 of serotype 3 poliovirus after vaccination with oral live attenuated or inactivated poliovirus vaccine and after natural exposure. *Clinical and Diagnostic Laboratory Immunology,* 7**,** 40-44.

Hirst, G. K. 1962. Genetic recombination with Newcastle disease virus, polioviruses, and influenza. *Cold Spring Harbor symposia on quantitative biology,* 27**,** 303-9.

Hobson, S. D., Rosenblum, E. S., Richards, O. C., Richmond, K., Kirkegaard, K. & Schultz, S. C. 2001. Oligomeric structures of poliovirus polymerase are important for function. *Embo Journal,* 20**,** 1153-1163.

Hogle, J. M., Chow, M. & Filman, D. J. 1985. 3-DIMENSIONAL STRUCTURE OF POLIOVIRUS AT 2.9 A RESOLUTION. *Science,* 229**,** 1358-1365.

Hyypia, T., Hovi, T., Knowles, N. J. & Stanway, G. 1997. Classification of enteroviruses based on molecular and biological properties. *Journal of General Virology,* 78**,** 1-11.

Jaag, H. M. & Nagy, P. D. 2010. The combined effect of environmental and host factors on the emergence of viral RNA recombinants. *PLoS pathogens,* 6**,** e1001156-e1001156.

Jaag, H. M., Pogany, J. & Nagy, P. D. 2010. A Host Ca2+/Mn2+ Ion Pump Is a Factor in the Emergence of Viral RNA Recombinants. *Cell Host & Microbe,* 7**,** 74-81.

Jablonski, S. A. & Morrow, C. D. 1995. MUTATION OF THE ASPARTIC-ACID RESIDUES OF THE GDD SEQUENCE MOTIF OF POLIOVIRUS RNA-DEPENDENT RNA-POLYMERASE RESULTS IN ENZYMES WITH ALTERED METAL-ION REQUIREMENTS FOR ACTIVITY. *Journal of Virology,* 69**,** 1532-1539.

Jacobs, S. E., Lamson, D. M., St George, K. & Walsh, T. J. 2013. Human Rhinoviruses. *Clinical Microbiology Reviews,* 26**,** 135-162.

Jarvis, T. C. & Kirkegaard, K. 1991. THE POLYMERASE IN ITS LABYRINTH - MECHANISMS AND IMPLICATIONS OF RNA RECOMBINATION. *Trends in Genetics,* 7**,** 186-191.

Jarvis, T. C. & Kirkegaard, K. 1992. POLIOVIRUS RNA RECOMBINATION - MECHANISTIC STUDIES IN THE ABSENCE OF SELECTION. *Embo Journal,* 11**,** 3135-3145.

Jiang, P., Faase, J. A., Toyoda, H., Paul, A., Wimmer, E. & Gorbalenya, A. E. 2007. Evidence for emergence of diverse polioviruses from C-cluster coxsackie A viruses and implications for global poliovirus eradication. *Proc Natl Acad Sci U S A,* 104**,** 9457-62.

Kew, O., Morris-Glasgow, V., Landaverde, M., Burns, C., Shaw, J., Garib, Z., Andre, J., Blackman, E., Freeman, C. J., Jorba, J., Sutter, R., Tambini, G., Venczel, L., Pedreira, C., Laender, F., Shimizu, H., Yoneyama, T., Miyamura, T., van der Avoort, H., Oberste, M. S., Kilpatrick, D., Cochi, S., Pallansch, M. & de Quadros, C. 2002. Outbreak of poliomyelitis in Hispaniola associated with circulating type 1 vaccine-derived poliovirus. *Science,* 296**,** 356-359.

Kew, O. M., Sutter, R. W., de Gourville, E. M., Dowdle, W. R. & Pallansch, M. A. 2005. Vaccine-derived polioviruses and the endgame strategy for global polio eradication. *Annual Review of Microbiology,* 59**,** 587-635.

King, A. M. 1988a. Preferred sites of recombination in poliovirus RNA: an analysis of 40 intertypic cross-over sequences. *Nucleic Acids Res,* 16**,** 11705-23.

King, A. M. Q. 1988b. PREFERRED SITES OF RECOMBINATION IN POLIOVIRUS RNA - AN ANALYSIS OF 40 INTERTYPIC CROSSOVER SEQUENCES. *Nucleic Acids Research,* 16**,** 11705-11723.

Kirkegaard, K. & Baltimore, D. 1986a. RNA RECOMBINATION IN POLIOVIRUS. *Journal of Cellular Biochemistry***,** 289-289.

Kirkegaard, K. & Baltimore, D. 1986b. THE MECHANISM OF RNA RECOMBINATION IN POLIOVIRUS. *Cell,* 47**,** 433-443.

Korboukh, V. K., Lee, C. A., Acevedo, A., Vignuzzi, M., Xiao, Y., Arnold, J. J., Hemperly, S., Graci, J. D., August, A., Andino, R. & Cameron, C. E. 2014. RNA Virus Population Diversity, an Optimum for Maximal Fitness and Virulence. *Journal of Biological Chemistry,* 289**,** 29531-29544.

Krausslich, H. G., Faecke, M., Lee, C. K., Hellen, C. & Wimmer, E. 1989. SITE DIRECTED MUTAGENESIS OF THE POLIOVIRUS PROTEINASE 2A ACTIVE CENTER AND A CLEAVAGE SITE. *Journal of Cellular Biochemistry Supplement***,** 73-73.

Kroon, F. P., Weiland, H. T., Vanloon, A. M. & Vanfurth, R. 1995. ABORTIVE AND SUBCLINICAL POLIOMYELITIS IN A FAMILY DURING THE 1992 EPIDEMIC IN THE NETHERLANDS. *Clinical Infectious Diseases,* 20**,** 454-456.

Kuge, S., Saito, I. & Nomoto, A. 1986. PRIMARY STRUCTURE OF POLIOVIRUS DEFECTIVE-INTERFERING PARTICLE GENOMES AND POSSIBLE GENERATION MECHANISMS OF THE PARTICLES. *Journal of Molecular Biology,* 192**,** 473-487.

Lai, M. M. C. 1992a. GENETIC-RECOMBINATION IN RNA VIRUSES. *Current Topics in Microbiology and Immunology,* 176**,** 21-32.

Lai, M. M. C. 1992b. RNA RECOMBINATION IN ANIMAL AND PLANT-VIRUSES. *Microbiological Reviews,* 56**,** 61-79.

Lauring, A. S. & Andino, R. 2010. Quasispecies Theory and the Behavior of RNA Viruses. *Plos Pathogens,* 6.

Lawson, M. A. & Semler, B. L. 1992. ALTERNATE POLIOVIRUS NONSTRUCTURAL PROTEIN PROCESSING CASCADES GENERATED BY PRIMARY SITES OF 3C-PROTEINASE CLEAVAGE. *Virology,* 191**,** 309-320.
Ledinko, N. 1963. Genetic recombination with poliovirus type 1. Studies of crosses between a normal horse serum-resistant mutant and several guanidine-resistant mutants of the same strain. *Virology,* 20**,** 107-19.
Leitch, E. C. M., Bendig, J., Cabrerizo, M., Cardosa, J., Hyypia, T., Ivanova, O. E., Kelly, A., Kroes, A. C. M., Lukashev, A., MacAdam, A., McMinn, P., Roivainen, M., Trallero, G., Evans, D. J. & Simmonds, P. 2009. Transmission Networks and Population Turnover of Echovirus 30. *Journal of Virology,* 83**,** 2109-2118.
Levy, H. C., Bostina, M., Filman, D. J. & Hogle, J. M. 2010. Catching a Virus in the Act of RNA Release: a Novel Poliovirus Uncoating Intermediate Characterized by Cryo-Electron Microscopy. *Journal of Virology,* 84**,** 4426-4441.
Liu, X., Yang, X., Lee, C. A., Moustafa, I. M., Smidansky, E. D., Lum, D., Arnold, J. J., Cameron, C. E. & Boehr, D. D. 2013. Vaccine-derived Mutation in Motif D of Poliovirus RNA-dependent RNA Polymerase Lowers Nucleotide Incorporation Fidelity. *Journal of Biological Chemistry,* 288**,** 32753-32765.
Liu, Y., Wang, C., Mueller, S., Paul, A. V., Wimmer, E. & Jiang, P. 2010. Direct Interaction between Two Viral Proteins, the Nonstructural Protein 2C(ATPase) and the Capsid Protein VP3, Is Required for Enterovirus Morphogenesis. *Plos Pathogens,* 6.
Lowry, K., Woodman, A., Cook, J. & Evans, D. J. 2014. Recombination in Enteroviruses Is a Biphasic Replicative Process Involving the Generation of Greater-than Genome Length 'Imprecise' Intermediates. *Plos Pathogens,* 10.
Lukashev, A. N. 2010. Recombination among picornaviruses. *Reviews in Medical Virology,* 20**,** 327-337.
Mason, P. W., Bezborodova, S. V. & Henry, T. M. 2002. Identification and characterization of a cis-acting replication element (cre) adjacent to the internal ribosome entry site of foot-and-mouth disease virus. *Journal of Virology,* 76**,** 9686-9694.
McIntyre, C. L., Knowles, N. J. & Simmonds, P. 2013. Proposals for the classification of human rhinovirus species A, B and C into genotypically assigned types. *Journal of General Virology,* 94**,** 1791-1806.
McMinn, P., Stratov, I., Nagarajan, L. & Davis, S. 2001. Neurological manifestations of enterovirus 71 infection in children during an outbreak of hand, foot, and mouth disease in Western Australia. *Clinical Infectious Diseases,* 32**,** 236-242.
McWilliam Leitch, E. C., Cabrerizo, M., Cardosa, J., Harvala, H., Ivanova, O. E., Koike, S., Kroes, A. C., Lukashev, A., Perera, D., Roivainen, M., Susi, P., Trallero, G., Evans, D. J. & Simmonds, P. 2012. The association of recombination events in the founding and emergence of subgenogroup evolutionary lineages of human enterovirus 71. *J Virol,* 86**,** 2676-85.
Mellits, K. H., Meredith, J. M., Rohll, J. B., Evans, D. J. & Almond, J. W. 1998. Binding of a cellular factor to the 3 ' untranslated region of the RNA

genomes of entero- and rhinoviruses plays a role in virus replication. *Journal of General Virology,* 79**,** 1715-1723.
Mendelsohn, C. L., Wimmer, E. & Racaniello, V. R. 1989. Cellular receptor for poliovirus: molecular cloning, nucleotide sequence, and expression of a new member of the immunoglobulin superfamily. *Cell,* 56**,** 855-865.
Moon, S. L., Anderson, J. R., Kumagai, Y., Wilusz, C. J., Akira, S., Khromykh, A. A. & Wilusz, J. 2012. A noncoding RNA produced by arthropod-borne flaviviruses inhibits the cellular exoribonuclease XRN1 and alters host mRNA stability. *Rna,* 18**,** 2029-40.
Moustafa, I. M., Korboukh, V. K., Arnold, J. J., Smidansky, E. D., Marcotte, L. L., Gohara, D. W., Yang, X., Antonieta Sanchez-Farran, M., Filman, D., Maranas, J. K., Boehr, D. D., Hogle, J. M., Colina, C. M. & Cameron, C. E. 2014. Structural Dynamics as a Contributor to Error-prone Replication by an RNA-dependent RNA Polymerase. *Journal of Biological Chemistry,* 289**,** 36229-36248.
Murray, K. E. & Barton, D. J. 2003. Poliovirus CRE-dependent VPg uridylylation is required for positive-strand RNA synthesis but not for negative-strand RNA synthesis. *Journal of Virology,* 77**,** 4739-4750.
Nagy, P. D. & Bujarski, J. J. 1997. Engineering of homologous recombination hotspots with AU-rich sequences in brome mosaic virus. *Journal of Virology,* 71**,** 3799-3810.
Nagy, P. D. & Simon, A. E. 1997. New insights into the mechanisms of RNA recombination. *Virology,* 235**,** 1-9.
Nagy, P. D. & Simon, A. E. 1998a. In vitro characterization of late steps of RNA recombination in turnip crinkle virus. I. Role of motif1-hairpin structure. *Virology,* 249**,** 379-92.
Nagy, P. D. & Simon, A. E. 1998b. In vitro characterization of late steps of RNA recombination in turnip crinkle virus.II. The role of the priming stem and flanking sequences. *Virology,* 249**,** 393-405.
Nakashima, N. & Shibuya, N. 2006. Multiple coding sequences for the genome-linked virus protein (VPg) in dicistroviruses. *J Invertebr Pathol,* 92**,** 100-4.
Nathanson, N. & Fine, P. 2002. Virology: Poliomyelitis eradication - a dangerous endgame. *Science,* 296**,** 269-270.
Nathanson, N. & Kew, O. M. 2010. From Emergence to Eradication: The Epidemiology of Poliomyelitis Deconstructed. *American Journal of Epidemiology,* 172**,** 1213-1229.
Nishimura, Y. & Shimizu, H. 2009. Identification of P-selectin glycoprotein ligand-1 as one of the cellular receptors for enterovirus 71. *Uirusu,* 59**,** 195-203.
Nomoto, A., Kitamura, N., Golini, F. & Wimmer, E. 1977. GENOME-LINKED PROTEIN OF PICORNAVIRUSES .3. 5'-TERMINAL STRUCTURES OF POLIO-VIRION RNA AND POLIOVIRUS MESSENGER-RNA DIFFER ONLY IN GEOME-LINKED PROTEIN VPG. *Proceedings of the National Academy of Sciences of the United States of America,* 74**,** 5345-5349.
Novak, J. E. & Kirkegaard, K. 1991. IMPROVED METHOD FOR DETECTING POLIOVIRUS NEGATIVE STRANDS USED TO DEMONSTRATE SPECIFICITY OF POSITIVE-STRAND ENCAPSIDATION AND THE RATIO

OF POSITIVE TO NEGATIVE STRANDS IN INFECTED-CELLS. *Journal of Virology,* 65**,** 3384-3387.
Oberste, M. S., Maher, K., Flemister, M. R., Marchetti, G., Kilpatrick, D. R. & Pallansch, M. A. 2000. Comparison of classic and molecular approaches for the identification of untypeable enteroviruses. *J Clin Microbiol,* 38**,** 1170-4.
Oberste, M. S., Maher, K., Kilpatrick, D. R. & Pallansch, M. A. 1999. Molecular evolution of the human enteroviruses: correlation of serotype with VP1 sequence and application to picornavirus classification. *J Virol,* 73**,** 1941-8.
Oberste, M. S., Maher, K. & Pallansch, M. A. 2004a. Evidence for frequent recombination within species Human enterovirus B based on complete genomic sequences of all thirty-seven serotypes. *Journal of Virology,* 78**,** 855-867.
Oberste, M. S., Maher, K., Schnurr, D., Flemister, M. R., Lovchik, J. C., Peters, H., Sessions, W., Kirk, C., Chatterjee, N., Fuller, S., Hanauer, J. M. & Pallansch, M. A. 2004b. Enterovirus 68 is associated with respiratory illness and shares biological features with both the enteroviruses and the rhinoviruses. *Journal of General Virology,* 85**,** 2577-2584.
Oh, H. S., Pathak, H. B., Goodfellow, I. G., Arnold, J. J. & Cameron, C. E. 2009. Insight into Poliovirus Genome Replication and Encapsidation Obtained from Studies of 3B-3C Cleavage Site Mutants. *Journal of Virology,* 83**,** 9370-9387.
Pathak, H. B., Arnold, J. J., Wiegand, P. N., Hargittai, M. R. S. & Cameron, C. E. 2007. Picornavirus genome replication - Assembly and organization of the VPg uridylylation ribonucleoprotein (initiaion) complex. *Journal of Biological Chemistry,* 282**,** 16202-16213.
Pathak, H. B., Oh, H. S., Goodfellow, I. G., Arnold, J. J. & Cameron, C. E. 2008. Picornavirus genome replication: roles of precursor proteins and rate-limiting steps in oriI-dependent VPg uridylylation. *The Journal of biological chemistry,* 283**,** 30677-88.
Paul, A. V., Rieder, E., Kim, D. W., van Boom, J. H. & Wimmer, E. 2000. Identification of an RNA hairpin in poliovirus RNA that serves as the primary template in the in vitro uridylylation of VPg. *J Virol,* 74**,** 10359-70.
Paul, A. V., vanBoom, J. H., Filippov, D. & Wimmer, E. 1998. Protein-primed RNA synthesis by purified poliovirus RNA polymerase. *Nature,* 393**,** 280-284.
Pelletier, J., Kaplan, G., Racaniello, V. R. & Sonenberg, N. 1988. CAP-INDEPENDENT TRANSLATION OF POLIOVIRUS MESSENGER-RNA IS CONFERRED BY SEQUENCE ELEMENTS WITHIN THE 5' NONCODING REGION. *Molecular and Cellular Biology,* 8**,** 1103-1112.
Pelletier, J. & Sonenberg, N. 1988. INTERNAL INITIATION OF TRANSLATION OF EUKARYOTIC MESSENGER-RNA DIRECTED BY A SEQUENCE DERIVED FROM POLIOVIRUS RNA. *Nature,* 334**,** 320-325.
Peng, C. W., Peremyslov, V. V., Mushegian, A. R., Dawson, W. O. & Dolja, V. V. 2001. Functional specialization and evolution of leader proteinases in the family Closteroviridae. *J Virol,* 75**,** 12153-60.

Perales, C., Agudo, R. & Domingo, E. 2009. Counteracting Quasispecies Adaptability: Extinction of a Ribavirin-Resistant Virus Mutant by an Alternative Mutagenic Treatment. *Plos One,* 4.

Percy, N., Barclay, W. S., Sullivan, M. & Almond, J. W. 1992. A POLIOVIRUS REPLICON CONTAINING THE CHLORAMPHENICOL ACETYLTRANSFERASE GENE CAN BE USED TO STUDY THE REPLICATION AND ENCAPSIDATION OF POLIOVIRUS RNA. *Journal of Virology,* 66**,** 5040-5046.

Pfeiffer, J. K. & Kirkegaard, K. 2003. A single mutation in poliovirus RNA-dependent RNA polymerase confers resistance to mutagenic nucleotide analogs via increased fidelity. *Proceedings of the National Academy of Sciences of the United States of America,* 100**,** 7289-7294.

Pfister, T. & Wimmer, E. 1999. Characterization of the nucleoside triphosphatase activity of poliovirus protein 2C reveals a mechanism by which guanidine inhibits poliovirus replication. *J Biol Chem,* 274**,** 6992-7001.

Racaniello, V. R. & Baltimore, D. 1981. Cloned poliovirus complementary DNA is infectious in mammalian cells. *Science,* 214**,** 916-9.

Rajtar, B., Majek, M., Polanski, L. & Polz-Dacewicz, M. 2008. ENTEROVIRUSES IN WATER ENVIRONMENT - A POTENTIAL THREAT TO PUBLIC HEALTH. *Annals of Agricultural and Environmental Medicine,* 15**,** 199-203.

Rhoades, R. E., Tabor-Godwin, J. M., Tsueng, G. & Feuer, R. 2011. Enterovirus infections of the central nervous system. *Virology,* 411**,** 288-305.

Rohll, J. B., Moon, D. H., Evans, D. J. & Almond, J. W. 1995. THE 3'-UNTRANSLATED REGION OF PICORNAVIRUS RNA - FEATURES REQUIRED FOR EFFICIENT GENOME REPLICATION. *Journal of Virology,* 69**,** 7835-7844.

Romanova, L. I., Blinov, V. M., Tolskaya, E. A., Viktorova, E. G., Kolesnikova, M. S., Guseva, E. A. & Agol, V. I. 1986. THE PRIMARY STRUCTURE OF CROSSOVER REGIONS OF INTERTYPIC POLIOVIRUS RECOMBINANTS - A MODEL OF RECOMBINATION BETWEEN RNA GENOMES. *Virology,* 155**,** 202-213.

Rossmann, M. G., Arnold, E., Erickson, J. W., Frankenberger, E. A., Griffith, J. P., Hecht, H. J., Johnson, J. E., Kamer, G., Luo, M., Mosser, A. G., Rueckert, R. R., Sherry, B. & Vriend, G. 1985. STRUCTURE OF A HUMAN COMMON COLD VIRUS AND FUNCTIONAL-RELATIONSHIP TO OTHER PICORNAVIRUSES. *Nature,* 317**,** 145-153.

Runckel, C., Westesson, O., Andino, R. & DeRisi, J. L. 2013. Identification and Manipulation of the Molecular Determinants Influencing Poliovirus Recombination. *Plos Pathogens,* 9.

Rust, R. C., Landmann, L., Gosert, R., Tang, B. L., Hong, W. J., Hauri, H. P., Egger, D. & Bienz, K. 2001. Cellular COPII proteins are involved in production of the vesicles that form the poliovirus replication complex. *Journal of Virology,* 75**,** 9808-9818.

Salk, J. E. 1954. Studies in Human Subjects on Active Immunization Against Poliomyelitis. *American Journal of Public Health and the Nations Health,* 44**,** 994-1009.

Sambrook, J. & Russell, D. W. 2001. Molecular cloning: A laboratory manual. *Molecular cloning: A laboratory manual*.

Scheel, T. K. H., Galli, A., Li, Y.-P., Mikkelsen, L. S., Gottwein, J. M. & Bukh, J. 2013. Productive Homologous and Non-homologous Recombination of Hepatitis C Virus in Cell Culture. *Plos Pathogens,* 9.

Schulte, M. B., Draghi, J. A., Plotkin, J. B. & Andino, R. 2015. Experimentally guided models reveal replication principles that shape the mutation distribution of RNA viruses. *Elife,* 4.

Semler, B. L., Anderson, C. W., Hanecak, R., Dorner, L. F. & Wimmer, E. 1982. A membrane-associated precursor to poliovirus VPg identified by immunoprecipitation with antibodies directed against a synthetic heptapeptide. *Cell,* 28**,** 405-412.

Semler, B. L., Anderson, C. W., Kitamura, N., Rothberg, P. G., Wishart, W. L. & Wimmer, E. 1981a. Poliovirus replication proteins:RNA sequence encoding P3-1b and the sites of proteolytic processing. *Proceedings of the National Academy of Sciences of the United States of America,* 78**,** 3464-3468.

Semler, B. L., Hanecak, R., Anderson, C. W. & Wimmer, E. 1981b. Cleavage sites in the polypeptide precursors of poliovirus protein P2-X. *Virology,* 114**,** 589-594.

Serviene, E., Jiang, Y., Cheng, C. P., Baker, J. & Nagy, P. D. 2006. Screening of the yeast yTHC collection identifies essential host factors affecting tombusvirus RNA recombination. *Journal of Virology,* 80**,** 1231-1241.

Serviene, E., Shapka, N., Cheng, C. P., Panavas, T., Phuangrat, B., Baker, J. & Nagy, P. D. 2005. Genome-wide screen identifies host genes affecting viral RNA recombination. *Proceedings of the National Academy of Sciences of the United States of America,* 102**,** 10545-10550.

Shaffer, S. M., Wu, M.-T., Levesque, M. J. & Raj, A. 2013. Turbo FISH: A Method for Rapid Single Molecule RNA FISH. *Plos One,* 8.

Simon-Loriere, E. & Holmes, E. C. 2011. Why do RNA viruses recombine? *Nat Rev Microbiol,* 9**,** 617-26.

Simon-Loriere, E. & Holmes, E. C. 2013. Gene duplication is infrequent in the recent evolutionary history of RNA viruses. *Mol Biol Evol,* 30**,** 1263-9.

Sonenberg, N. & Pelletier, J. 1989. POLIOVIRUS TRANSLATION - A PARADIGM FOR A NOVEL INITIATION MECHANISM. *Bioessays,* 11**,** 128-132.

Steil, B. P. & Barton, D. J. 2009. Cis-active RNA elements (CREs) and picornavirus RNA replication. *Virus Research,* 139**,** 240-252.

Stern, A., Bianco, S., Yeh, M. T., Wright, C., Butcher, K., Tang, C., Nielsen, R. & Andino, R. 2014. Costs and Benefits of Mutational Robustness in RNA Viruses. *Cell Reports,* 8**,** 1026-1036.

Tellez, A. B., Wang, J., Tanner, E. J., Spagnolo, J. F., Kirkegaard, K. & Bullitt, E. 2011. Interstitial Contacts in an RNA-Dependent RNA Polymerase Lattice. *Journal of Molecular Biology,* 412**,** 737-750.

Thompson, A. A. & Peersen, O. B. 2004. Structural basis for proteolysis-dependent activation of the poliovirus RNA-dependent RNA polymerase. *Embo Journal,* 23**,** 3462-3471.

Tolskaya, E. A., Romanova, L. A., Kolesnikova, M. S. & Agol, V. I. 1983. INTERTYPIC RECOMBINATION IN POLIOVIRUS - GENETIC AND BIOCHEMICAL-STUDIES. *Virology,* 124**,** 121-132.

Tolskaya, E. A., Romanova, L. I., Blinov, V. M., Viktorova, E. G., Sinyakov, A. N., Kolesnikova, M. S. & Agol, V. I. 1987. STUDIES ON THE RECOMBINATION

BETWEEN RNA GENOMES OF POLIOVIRUS - THE PRIMARY STRUCTURE AND NONRANDOM DISTRIBUTION OF CROSSOVER REGIONS IN THE GENOMES OF INTERTYPIC POLIOVIRUS RECOMBINANTS. *Virology,* 161**,** 54-61.

Towner, J. S., Ho, T. V. & Semler, B. L. 1996. Determinants of membrane association for poliovirus protein RAB. *Journal of Biological Chemistry,* 271**,** 26810-26818.

Tuthill, T. J., Groppelli, E., Hogle, J. M. & Rowlands, D. J. 2010. Picornaviruses. *Cell Entry by Non-Enveloped Viruses,* 343**,** 43-89.

Vasquez, R. J., Howell, B., Yvon, A. M. C., Wadsworth, P. & Cassimeris, L. 1997. Nanomolar concentrations of nocodazole alter microtubule dynamic instability in vivo and in vitro. *Molecular Biology of the Cell,* 8**,** 973-985.

Ventoso, I., MacMillan, S. E., Hershey, J. W. B. & Carrasco, L. 1998. Poliovirus 2A proteinase cleaves directly the eIF-4G subunit of eIF-4F complex. *Febs Letters,* 435**,** 79-83.

Vignuzzi, M., Stone, J. K. & Andino, R. 2005. Ribavirin and lethal mutagenesis of poliovirus: molecular mechanisms, resistance and biological implications. *Virus Research,* 107**,** 173-181.

Vignuzzi, M., Stone, J. K., Arnold, J. J., Cameron, C. E. & Andino, R. 2006. Quasispecies diversity determines pathogenesis through cooperative interactions in a viral population. *Nature,* 439**,** 344-348.

Vignuzzi, M., Wendt, E. & Andino, R. 2008. Engineering attenuated virus vaccines by controlling replication fidelity. *Nature Medicine,* 14**,** 154-161.

Wang, Z. R., Day, N., Trifillis, P. & Kiledjian, M. 1999. An mRNA stability complex functions with poly(A)-binding protein to stabilize mRNA in vitro. *Molecular and Cellular Biology,* 19**,** 4552-4560.

Weeks, S. A., Lee, C. A., Zhao, Y., Smidansky, E. D., August, A., Arnold, J. J. & Cameron, C. E. 2012. A Polymerase Mechanism-based Strategy for Viral Attenuation and Vaccine Development. *Journal of Biological Chemistry,* 287**,** 31618-31622.

Weidman, M. K., Yalamanchili, P., Ng, B., Tsai, W. & Dasgupta, A. 2001. Poliovirus 3C protease-mediated degradation of transcriptional activator p53 requires a cellular activity. *Virology,* 291**,** 260-271.

Zhang, Y., Zhu, S., Yan, D., Liu, G., Bai, R., Wang, D., Chen, L., Zhu, H., An, H., Kew, O. & Xu, W. 2010. Natural Type 3/Type 2 Intertypic Vaccine-Related Poliovirus Recombinants with the First Crossover Sites within the VP1 Capsid Coding Region. *Plos One,* 5.

A

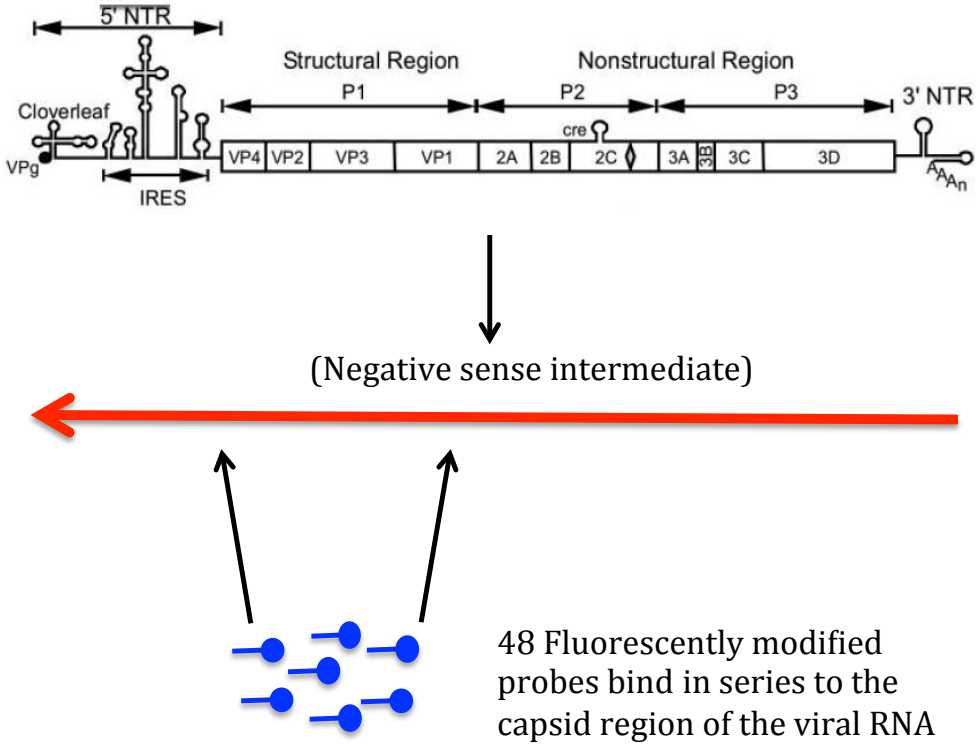

B

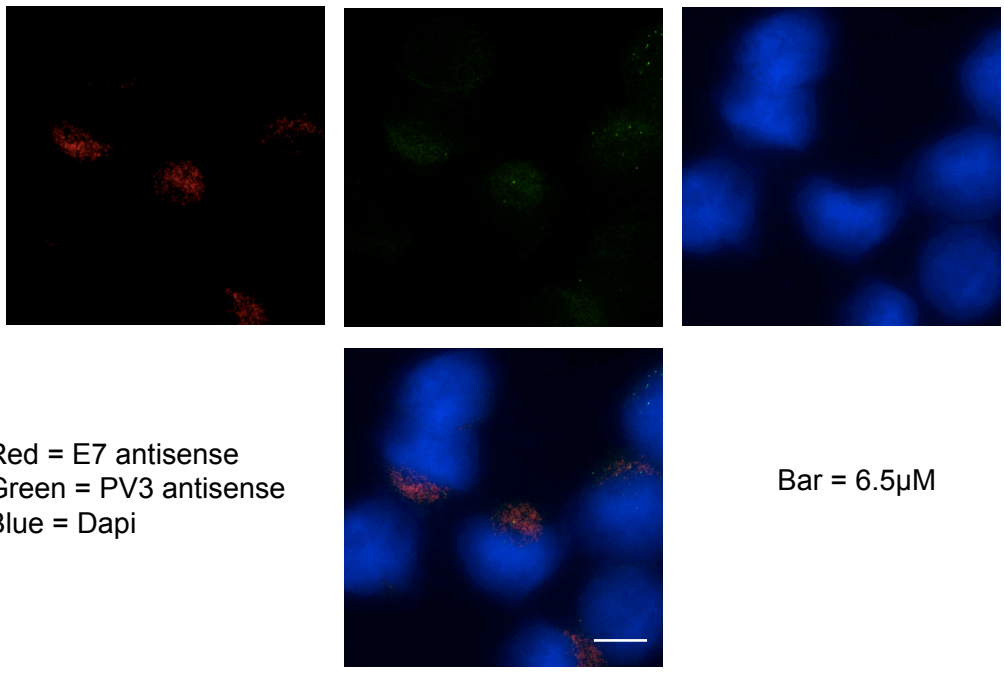

Red = E7 antisense
Green = PV3 antisense
Blue = Dapi

Bar = 6.5μM

C

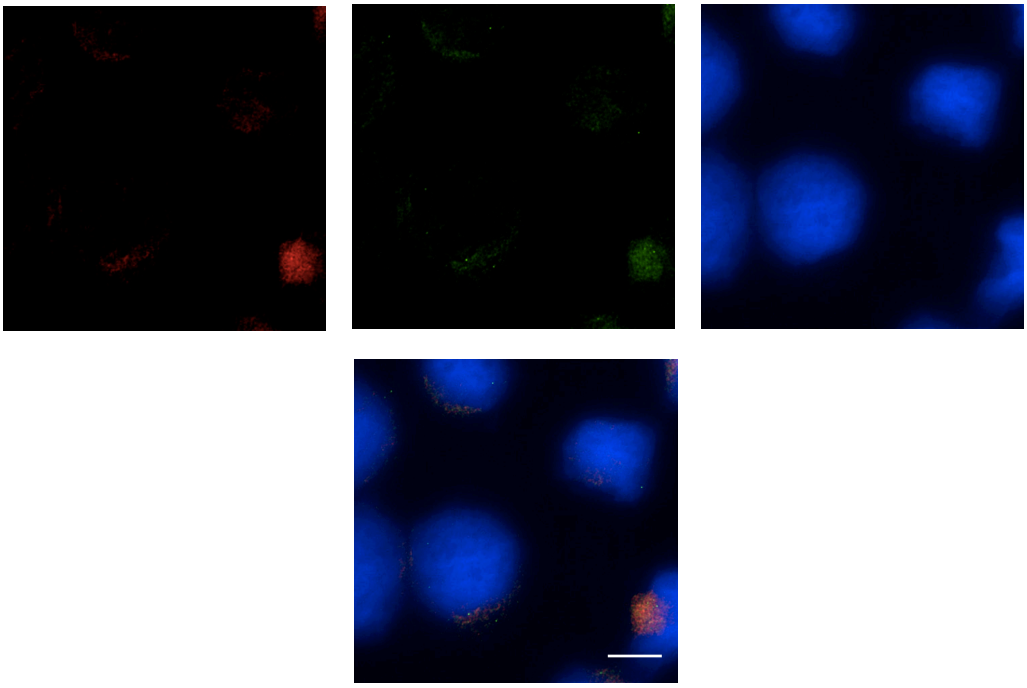

Appendix i: Fluorescent in situ hybridisation (FISH) Stellaris probes

(A) Enterovirus genome layout. Red line indicates antisense RNA intermediate produced during replication. Blue lollipops represent 48 individual 20mer oligonucleotides carrying a 3' fluorescent modification. Each bind to separate unique sequences with the capsid-coding region of the antisense RNA intermediate template **(B)** Example images obtained from a wide-field microscope. Red indicates fluorescent signal obtained from the echovirus 7 specific probes. Green indicates fluorescent signal obtained from the Poliovirus type 3 specific probes. Blue indicates nuclear staining (Dapi). Individual fluorescent images from each wavelength followed with a final overlaid image with all fluorescent wavelengths. White bar = 6.5 μM **(C)** Repeated experiment. All images de-convoluted and processed with ImageJ.